Pervaporation using modified polysiloxanes: Removal of priority organic contaminants from aqueous streams

Bennett, Matthew

Award date:
1996

Awarding institution:
University of Bath

Pervaporation Using Modified Polysiloxanes: Removal of Priority Organic Contaminants from Aqueous Streams

Submitted by Matthew Bennett
for the degree of Ph.D.
of the University of Bath
1996

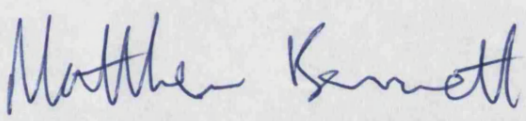

ProQuest LLC
789 East Eisenhower Parkway
P.O. Box 1346
Ann Arbor, MI 48106-1346

To the fond memory of

Peter Matus

(1969 - 1994)

who to the end displayed great dignity and courage

Acknowledgements

The financial backing of the EPSRC for this project (research grant GR/H78177) is gratefully acknowledged.

I would like to thank my three supervisors, Dr Robert Field, Dr Brian Brisdon and Dr Richard England for their excellent input throughout the past three years and for being probably the most easy going supervisors in the world.

Thanks are also due to my grandfather, Harold Bennett, for all the encouragement and to my grandmother, Ida Bennett, for cooking me all of those pasties!

Most of all I would like to thank my parents, Ken and Muriel Bennett, for both their encouragement and financial support over the past twenty five years.

Table of Contents

Summary

Modified polysiloxane membranes containing different organofunctional side chains are produced and tested for the recovery of various organic contaminants from aqueous streams, using the process of pervaporation. Four separate organic components, each representative of an industrially significant family of chemicals, are chosen for evaluation, phenol, chloroform, pyridine and methylisobutylketone (MIBK).

In each case significant performance enhancements, over that achieved with an unfunctionalised polydimethylsiloxane membrane, are realised. Phenol transport is significantly facilitated by the incorporation of basic groups, such as amines, into the membrane structure. This is thought to be due to a weak acid-base interaction, increasing phenol sorption into the membrane. For pyridine, chloroform and MIBK separations from water, selectivity towards the organic component is greatly enhanced by the incorporation of long chained alkyl groups. A dual effect of the increased organic content leading to increased organic component sorption and reduced water sorption is thought to be responsible.

A comprehensive review of mass transfer mechanisms within pervaporation systems is undertaken. Models based upon the solution/diffusion mechanism and using Ficks first law to describe transport are developed. These models are verified with experimental data and used to theoretically examine the effect of varying process conditions within practical systems. The possibility of enhancing the performance of pervaporation systems through the incorporation of permeate phase separation is discussed.

Differential mass and energy balance equations are developed and numerically solved in order to determine membrane area and energy requirements for model separation problems. Substantial savings may be realised by the use of functionalised membranes, provided that feed side boundary layer resistance (concentration polarisation) does not control organic component transport. If boundary layer resistance is dominant it is shown that much greater performance enhancements may be realised by optimising feed side hydrodynamics as opposed to improving membrane materials.

Chapter 1
Introduction

Scope of Chapter 1

The aim of this chapter is to introduce the process of pervaporation, discuss the classes of membrane materials generally employed and to place the work undertaken within this project into context with existing literature.

The various applications of pervaporation technology are discussed, with particular emphasis being placed upon the removal of dilute organics from aqueous streams. A review of previous work with the membrane material polydimethylsiloxane (PDMS), the base material utilised within this study, is presented. The nature of the organic species chosen for study and the commercial significance of the separation of each species from aqueous streams is discussed.

1.1 Project Objectives

The project was undertaken in order to achieve the following pre-determined objectives:-

1. To determine fluxes and separation factors for various organic compounds at low concentrations, including (a) phenolic and (b) halogenated compounds, in water, through a range of modified polysiloxane membranes.
2. To investigate the relationship between the organofunctionality and structure of the membranes and their performance, for each class of solute.
3. To undertake predictive studies, using data from 1 and 2, which will permit the construction of improved membranes.
4. To consider the engineering implications of Pervaporation.
5. To examine the economic feasibility of using organophilic membranes.

1.2 Background

Liquid mixtures can be separated by partial vaporisation through a non-porous, permselective membrane. This technique, which was originally termed liquid permeation, has subsequently been termed pervaporation, in order to emphasise the fact that the permeate undergoes a phase change, from liquid to vapour, during its transport through the barrier. The driving force for mass transfer can be expressed in terms of a concentration or activity gradient across the membrane.

The liquid feed mixture, generally at atmospheric pressure, is in direct contact with one side of the membrane. On the other side the partial pressure of the permeants is lowered, generally by lowering the total pressure. In this case a vacuum pump is employed and the permeate is collected after being condensed. An alternative is to sweep the permeate vapour space with an inert gas.

Pervaporation systems are generally regarded as being very flexible and easy to maintain *(Barber and Miller, 1994)*. The modular design of membrane systems allows for easy expansion and contraction of configurations as required. In 1986 pervaporation was ranked as being the third most promising of 31 technologies considered for energy saving fluid separation *(Feng and Huang, 1992)*.

The transport of the permeate through the pore free, permselective membrane involves three successive steps *(Neel, 1991)*:-

1. Upstream partitioning of the feed components between the liquid mixture and the, generally swollen, upstream layer of the membrane
2. Diffusion of the penetrants through the, generally unevenly swollen, permselective barrier
3. Permeate desorption, which takes place at the downstream surface of the film

This multistage process is evidently more complex than a single vaporisation step and it is easily understandable that the composition of the permeate may widely differ from that of the mixed vapour evolved after the establishment of a free liquid-vapour equilibrium. The

use of an appropriate membrane makes it possible to efficiently separate a number of azeotropic mixtures *(Neel, 1991)*.

1.3 Applications of Pervaporation

Four potential industrial applications for pervaporation technology have so far been identified:-

1. Dehydration of organic solvents
2. Removal of dilute organics from aqueous streams
3. Continuous extraction of product and inhibitory byproduct in biological and food processes
4. Separation of organic mixtures

To date the only two areas of techno-economical success have been identified *(Rautenbach, Klatt and Vier, 1992)*:-

- The separation of water or a highly polar organic component, such as methanol, from complex organic-aqueous and organic mixtures in cases where the feed concentration of water/methanol is relatively low
- The separation of traces of halogenated hydrocarbons or other organic solvents from water

World-wide intensive research continues into all four potential applications and each is described briefly below.

1.3.1 Organic Dehydration

The dehydration of organic solvents is the only application in which pervaporation technology has so far been employed successfully on a full industrial scale. Currently more than 90 industrial units are in operation world-wide *(Rautenbach et al, 1992)* for the dehydration of ethanol, isopropanol, ethylacetate and multipurpose applications. Most applications employ the hydrophilic PVA composite membrane manufactured by GFT (also known as Deutchse Carbonne).

The dehydration of ethanol has become the classic example of successful membrane pervaporation *(Fleming, 1990)* and indeed the largest pervaporation units are employed for this purpose. As mass transport through the membrane determines permeate composition, the water/ethanol azeotrope can readily be broken, producing ethanol product of much higher purity than is possible through simple distillation. At high water levels, distillation can be shown to be more thermodynamically efficient than pervaporation and it is usual for the pervaporation unit to be incorporated within a hybrid separation process, the first step of which being the concentration of ethanol to the azeotropic composition by distillation.

Besides the dehydration of binary systems, pervaporation is especially successful for the dehydration of solvent mixtures, containing both high and low boilers, where numerous individual azeotropes can be formed. Pervaporation has also proved particularly economical where a variety of solvents have to be treated batchwise *(Rautenbach et al, 1992)*. The main reason for this is that it is impossible to compensate for the higher specific energy requirements of azeotropic distillation by heat integration, as may take place in continuous processes.

The US Department of Energy ranked the development of membranes for the dehydration of acids and bases as fifteenth in the priority order of topics worth studying in membrane science *(Xie, Ping, Nguyen and Neel, 1992)*.

1.3.2 Removal of Dilute Organics from Aqueous Streams

Drinking and ground water are vulnerable to contamination by volatile chemicals, especially phenolic, benzenic and halogenated compounds, which are widely used for household, agricultural and industrial purposes *(Beaumelle, Marin and Gibert, 1993)*. Owing to the considerable pressure applied within recent years to reduce pollution of the environment, the permissible levels of volatile organic compounds allowable within discharged water have been dramatically lowered. It has also proved necessary to develop technologies capable of cleaning industrially contaminated soil and one of the best ways of achieving this is by washing the soil with water and then treating the resultant contaminated ground water. These factors make the development of cheap, efficient

recovery processes a priority. Significant raw material cost savings may also be realised by the efficient recovery of valuable solvent.

Pervaporation appears a potentially attractive process for this application, to compete with the more traditionally used technologies of air stripping, liquid extraction and adsorption. A major advantage of pervaporation over these technologies is that further separation of the pollutant from the gaseous or liquid solvent, or solid phase is not required.

To date only pilot scale units are in operation *(Rautenbach et al, 1992)* and the standard membrane for this application is hydrophobic PDMS, which is now available commercially, usually cast upon a polysulphone microporous support.

In order to make pervaporation a more economically attractive process for this application, it has been suggested *(Beaumelle et al, 1993)* that more efficient membranes are required. Membranes displaying higher selectivities would reduce the specific energy requirement for organic recovery since less water would have to be evaporated and condensed. Membranes with higher organic flux would reduce membrane area and investment cost.

As solute flux is roughly proportional to feed concentration, reducing solvent concentration to very low levels would require very large membrane areas. For this reason the possibility of combining pervaporation in a hybrid process with reverse osmosis *(Rautenbach and Klatt, 1991)* or adsorption *(Schofield, McCray, Ray and Newbold, 1991)* has been investigated. In order to meet discharge limits, the maximum allowable organic component concentrations are generally of the order of < 100 ppb for drinking and ground waters, < 10 ppm for CHC- and aromatic contaminated wastewaters and > 100 ppm for oxygenated solvent contaminated wastewaters *(Schofield et al, 1991)*.

1.3.3 Biological and Food Processes

In biotechnology the valuable product is generally very dilute in aqueous broths and recovery is often difficult and expensive. Pervaporation is well suited for the treatment of biological matter for the following reasons *(Beaumelle et al, 1993)*:-

- Operating temperatures need not be high
- No additional solvent or chemical is required
- Micro-organisms do not undergo mechanical stress as high pressure or cross flow velocity is not required
- The use of a non porous membrane almost eliminates the problem of membrane fouling
- The evaporation enthalpy is taken from the broth, contributing to the regulation of temperature control

By selecting an appropriate hydrophobic (organophilic) membrane, valuable volatile biosolvents can be removed continuously from fermentation broths. As well as providing a concentrated product stream, removing potentially inhibitory product continuously can dramatically increase fermentation efficiency.

Apart from the production of ethanol, fermentation processes to produce biosolvents are not much developed on an industrial scale. In the future, however, fermentation may become an economically attractive way of producing fuels and solvents, when traditional fossil fuels become scarce and their associated processes expensive. For example the recovery of product from the ABE (acetone-butanol-ethanol) fermentation process, using PDMS membranes, has been investigated *(Bengtson, Pingel and Boddeker, 1991)*.

Pervaporation is a suitable process for the treatment of food matter, for the same reasons as for bioprocesses. The two major applications that have been considered so far are the production of low alcohol beers and wines, by the removal of ethanol and the extraction of aroma compounds. In order for the separation of ethanol to become economically viable improved membranes are required as current membranes display selectivities to ethanol only close to that of vapour-liquid equilibrium. It has been reported *(Karlsson and Tragardh, 1993)* that pervaporative enrichment of aroma compounds can be very high, especially for the more volatile compounds.

1.3.4 Separation of Organic Mixtures

The separation of mixtures of organics is of extreme importance throughout the chemical industry. Despite positive laboratory results, the industrial utilisation of pervaporation for

this application does appear a long way off *(Rautenbach et al, 1992)*. It appears that the success of membrane processes such as ultrafiltration, reverse osmosis and dehydration by pervaporation is strongly linked with the fact that one type of membrane can be applied to a whole class of separations. It is likely that a special membrane would have to be developed for almost every different organic-organic separation leading to high membrane costs. This fact will probably limit the use of pervaporation for this application to only a few very important separations.

It should be noted that methanol, being a very polar substance, permeates hydrophilic membranes, developed for dehydration, very well. This fact enables the separation of methanol from organic mixtures utilising existing dehydration membranes. One of the most important applications is for the removal of methanol from methyl or ethyl-tertiobutylether (MTBE, ETBE), which are important gasoline octane enhancing components *(Noezar, Nguyen, Clement and Neel, 1995)*.

1.4 Classification of Pervaporation Membranes

Although only two types of pervaporation membrane have been extensively used commercially (PVA for hydrophilic and PDMS for hydrophobic separations) many other polymer materials have been investigated, as pervaporation membranes, on a laboratory and in a few cases, pilot plant scale. It is useful to classify these polymers into a number of groups. Roughly speaking all polymers can be classed as either glassy or rubbery polymers and a number of sub classes exist within these two groups, as discussed below *(Koops and Smolders, 1991)*.

1.4.1 Glassy Polymers

These have a glass transition temperature above room temperature. Within this group, three types can be distinguished, crystalline, semi-crystalline and amorphous polymers. Generally it is the amorphous and semi crystalline polymers that are most useful as pervaporation membranes. Membranes manufactured from these polymers tend to be hydrophilic and are used primarily for organic dehydrations.

1.4.2 Rubbery Polymers

Rubbery, or elastomeric, polymers have a glass transition temperature below room temperature. They are very flexible, the main chain consisting of C-C, Si-O or C-O bonds. Due to the absence of polar groups in their flexible chains, elastomers preferentially absorb organic liquids with respect to water. This property makes them excellent candidates for being employed in the removal of organics from aqueous solutions.

1.4.3 Copolymers

These are polymers with two or more repeating units, i.e. different monomers that can be coupled together in various ways. Three types of copolymers can be distinguished:-

- Random copolymers - where the structural units are completely randomly distributed
- Block copolymers - where the copolymer is built up of blocks of monomers
- Graft copolymers - where a main chain built up of the same repeating unit has different monomer blocks, as side chains, irregularly distributed along the main chain

1.4.4 Polymer Blends

These are mixtures of two or more polymers that are not covalently bonded to one another. Two kinds of blend are distinguishable, homogeneous blends, in which the polymers are miscible on a molecular scale and heterogeneous blends, in which the polymers are not completely miscible.

1.4.5 Ionic Polymers

These are polymers containing ionic groups which are covalently bonded to the polymer chain. Dependent on the sign of the charge of the ionic groups the membranes made of such materials are classed either anionic or cationic exchange membranes. The charge of the fixed ionic group is neutralised by a counter ion. The counter ion may be either mobile or fixed, but the disadvantage with mobile counter ions is that they are washed out during pervaporation and need to be periodically replaced. All ion exchange membranes are hydrophilic and this makes them very suitable for the dehydration of organics.

1.4.6 Examples of Various Membrane Classes

Table 1.1 lists examples of some of the better performing membranes in each of the above classes, that have been used in Pervaporation investigations and displays sample separation results *(Koops and Smolders, 1991)*.

Polymer	Classification	Component A	Component B	$\alpha_{A/B}$
PP	Amorphous	Benzene	Methanol	2.4
PVC		Water	Formaldehyde	80
PVA	Semi-	Water	Ethanol	140
Nylon-6	Crystalline	Water	Dioxane	45
PE		Benzene	Phenol	9
NBR-51	Elastomeric	Benzene	Water	21000
SBR-27		Benzene	Water	39500
PDMS		Benzene	Water	11000
PE		Benzene	Water	3800
PTFE-PVP	Grafted-	Water	Dioxane	18
PVF-PVP	Copolymer	Water	Ethanol	7
PVA-AAC		Water	Methanol	21
PAA-PAN	Random-	Water	acetic acid	80
PAN-MCR	Copolymer	Water	ethanol	4100
PVP-PAN		cyclo-hexanol	cyclo-hexane	10
Nylon-6/PAA	Polymer Blend	Water	Acetic acid	82
PVA/PHC		Water	Acetic acid	34
PAN/PVP		Water	Dioxane	13
$PE(SO_3^-)$-Na^+	Ion Exchange	Water	Ethanol	671
$PE(SO_3^-)$-Cs^+		Water	i-propanol	>29000
$PSF(SO_3^-)$-H^+		Water	acetic acid	9.4

Table 1.1 - Sample Membranes of Various Classes

Key: PP-Polypropylene PVC-Polyvinylchloride PVA-Polyvinylalcohol
PAA-Polyacrylicacid PAN-Polyacrylonitrile MCR-Methacrylate
PE-Polyethylene PSF-Polysulfone NBR-Nitrile Butadiene Rubber
SBR-Styrene Butadiene Rubber PVF-Polyvinylflouride
PHC-Polyhydoxylcarboxylate PDMS-Polydimethylsiloxane
PTFE-Polytetrafluoroethylene PVP-PolyN-vinylpyrrolidone

The separation factor, $\alpha_{A/B}$, is defined as:-

$$\alpha_{A/B} = \frac{Y_A(1-X_A)}{X_A(1-Y_A)} \qquad (1.1)$$

Where: X_A, Y_A = Mass Frac. of Component A in Feed and Permeate respectively

When choosing a membrane for a specific application it is necessary to select one which displays both a high separation factor and a high flux. Flux is a strong function of process conditions (as can be separation factor) as will be discussed later. It is also necessary to select a membrane that will display stable performance over an extended period of time.

1.5 Removal of Dilute Organics From Aqueous Streams

Pervaporation can be used to treat ground water, leachate and waste waters containing volatile organic compounds (VOC's). About half of the 129 US EPA priority pollutants are VOC's and each is known to be toxic and/or carcinogenic. They are emitted in large quantities, 1600000 to 5000000 tonnes per year in the US, from waste treatment, storage and disposal facilities *(Lipski and Cote, 1990)*. This is a clear indication that conventional waste treatment technologies are inadequate to destroy or remove and contain VOC's.

As well as VOC's, many high boiling (low volatility) organics can be successfully pervaporated from water, provided that the following conditions are met *(Boddeker, Bengtson and Bode, 1990)*:-

- The organics to be separated form non-ideal solutions with water, deviating from Raoult's law in a positive manner, i.e. displaying activity coefficients > 1
- The pure organic species have a low, although not vanishing, vapour pressure
- The membrane polymer exhibits preferential permeability for the organic solution component

The majority of organics considered so far fall into one of three categories *(Boddeker and Bengtson, 1991)*:-

- Alcohols and acids (oxychemicals in biotechnology)
- Aromatic hydrocarbons (organics in chemical processing)
- Chlorinated hydrocarbons (organic solvents of industrial origin)

1.5.1 Alcohols and Acids

As previously mentioned, no hydrophobic membrane has yet been discovered to make the separation of ethanol from water economical. The most widely investigated membrane for this purpose and one of the few to enrich ethanol beyond evaporation enrichment is PDMS. In general, the permeability of alcohols increases with increasing chain length, i.e. decreasing polarity and again PDMS is the standard membrane material. The main rival to PDMS for the enrichment of alcohols is PTMSP (Polytrimethylsilylpropyne) which displays exceptionally high fluxes, but at lower selectivities *(Boddeker and Bengtson, 1991)*.

Acetic acid is a prime example of a high boiling fermentation product which is also a technical water pollutant. Although no longer the primary route for acetic acid manufacture, the fermentation process still accounts for significant quantities, particularly in the production of table vinegar *(Aguilo, Hobbs and Zey, 1986)*. Acetic acid is marginally enriched by PDMS and PEBA (Polyetherblockamide) membranes, but cationic exchange membranes appear to be the most successful *(Boddeker and Bengtson, 1991)*. A potential problem with cationic exchange membranes exists, however, being that the cations may slowly be replaced by the acidic H^+ ions of the feed.

1.5.2 Aromatic Hydrocarbons

Phenol and aromatic derivatives occurring in industrial effluents are characterised by limited water miscibility and high boiling temperatures, ranging to well above 200^{o}C. Again PDMS is the most commonly used membrane material but PEBA membranes have proven particularly successful at enriching phenols *(Boddeker and Bengtson, 1991)*.

1.5.3 Chlorinated Hydrocarbons

On the US EPA list of priority pollutants, 46 of the 129 chemicals listed are chlorinated hydrocarbons *(Boddeker and Bengtson, 1991)*. A substantial number of these can, in theory, be pervaporated. Pervaporability has been demonstrated for a wide range of both aliphatic and aromatic chlorinated hydrocarbons, the recurring species investigated in

most studies being chloroform. The standard membrane is once again PDMS, although SBR and NBR membranes also display good performance.

1.6 Selected Organic Components

The organic components considered, within this study, were chosen to represent different families of industrially important chemicals, which could readily create a water contamination problem. The nature, uses and manufacturing routes of each organic component investigated, along with possible areas of application for pervaporation technology, are discussed below. The majority of the information is summarised from very comprehensive reports, published within encyclopedias, as indicated below.

1.6.1 Phenol

(Jordan, van Barneveld, Gerlich, Kleine-Boymann and Ullrich, 1991)

Most phenol produced is used in the formation of phenol-formaldehyde resins, Caprolactam, Adipic acid, Bisphenol A and Aniline. All of these products have significant economic importance and are used for the production of a wide range of consumer goods and process materials. It is safe to assume that phenol will remain an important chemical for many years to come. The estimated worldwide phenol production for 1989 was 5.0×10^6 tonnes/annum.

The vast majority of phenol is produced by one of two processes, cumene oxidation (the Hock process) or toluene oxidation. The former process is often the most economic as a valuable by-product, acetone, is also produced. One problem with the cumene oxidation process is that wastewater containing 1-3% phenol is produced. Due to the high toxicity of the compound, this phenol must be removed before the water may be discharged into open water. The most commonly used method of removing this phenol is liquid-liquid extraction, using either cumene or acetophenone, both of which are produced within the manufacturing process. Other technologies that have been considered for the removal of phenol from wastewater are steam distillation, adsorption on either activated carbon or ion exchange resins and oxidative decomposition, using oxidising agents such as hydrogen peroxide. Obviously pervaporation may be considered as a competitive technology for this

application. The phenol concentration is typically reduced to 20-500 ppm before being passed to the biological purification stage in a sewage treatment plant

Wastewater streams are also discharged from the phenolic resin production process, containing between 5-10% phenol and it has been suggested that pervaporation may be a more economically viable option than the current extraction methods employed for the removal of the phenol *(Kondo and Sato, 1994)*.

Phenol is also present in coking plant water, produced in the coking of coal and in the wastewater from cracking plants. Again, the phenol has to be removed and is generally sold as a byproduct of these processes. Once again, pervaporation could be employed for this purpose.

It has been suggested that the first commercial application of pervaporation using organophilic membranes may well be a project to be undertaken in Japan, for the removal of 7 % wt. phenol from wastewater to a concentration of 300 ppm *(Asada, 1992)*.

Beyond a temperature of 68.4°C, phenol is totally miscible with water. Miscibility decreases with decreasing temperature and at 20°C is approximately 7.5% w/w, phenol in water.

Phenol is acutely toxic, affecting the central nervous system and the main absorption route is through the skin. The limiting values for occupational health, laid down for work protection, were 5 ppm or 19 mg/m^3 in the USA and Germany.

A comprehensive survey of current literature has been undertaken to compare the efficiency of various membranes for the selective removal of phenol from water, the results of which are presented in table 1.2.

The process parameters, temperature, permeate pressure, feed concentration and membrane thickness all have very significant effects upon flux and selectivity, as discussed later.

Membrane	Temp.	Perm. Pres.	Feed Conc.	Mem. Thickness	Flux	Sep. Factor	Ref.
	^oC	mbar	ppm	μm	kg/m^2hr	α	
Silicone Rubber	25	0.1	11600	200	-	97	1**
PEBA	50	1.9	994	46	0.20	67	2
Polybutadiene	70	10.0	50000	45	0.22	14	3
PEBA (GKSS)	50	-	50000	50	0.88	74	4
PEBA (Pebax)	50	-	50000	45	1.22	44	4
PEBA	50	1.2	15000	100	0.16	42	5
PEBA	60	0.9	547	40	0.58	45	6
PDMS	60	0.9	486	120	0.13	27	6
Raipore	50	-	100000	50	1.70	6	7
PEBA	50	1.3	40000	100	0.48	75	8
Urelan	80	8	50000	-	1.50	21	9

Table 1.2 - Summary of Phenol / Water Separation Results

** See note following table 1.3.

References:-

1 *(Watson and Payne, 1990)*

2 *(Boddeker et al, 1990)*

3 *(Rautenbach and Klatt, 1991)*

4 *(Matsumoto, Kondo and Fujita, 1992)*

5 *(Boddeker, Pingel and Dede, 1992)*

6 *(Raghunath and Hwang, 1992)*

7 *(Beaumelle et al, 1993)*

8 *(Kondo and Sato, 1994)*

9 *(Volkov, Bokarev, Zheleznov, Selinskaya, Rakhimov, Borisov and Zakhovaev, 1995)*

1.6.2 Chloroform

(Rossberg, Lendle, Togel, Dreher, Langer, Rassaerts, Kleinschmidt, Strack, Beck, Lipper, Torkelson, Loser and Beutel, 1986)

Chloroform is broadly used as both an important solvent and chemical intermediate. It has excellent solvent properties for many organic materials, is a good solvent for both iodine and sulphur and is totally miscible with many organic solvents. The principal use for chloroform was in the production of monochlorodifluoromethane (CFC 22), which was widely used as a refrigerant and in turn was a key intermediate in the production of tetrafluoroethene. Following the Montreal convention, in which plans were developed to initiate the phasing out of ozone damaging chemicals, it is likely that CFC 22 production will decline.

Chloroform is produced almost exclusively by the chlorination of methane and the 1981 worldwide production capacity was estimated as being 415 000 tonnes / annum. It is a member of an important family of industrial solvents and intermediates, chlorinated methanes, of which the total 1981 worldwide production was estimated to be in excess of 2×10^6 tonnes / annum. Approximately 58% of the total chlorinated methane usage was for purposes other than CFC manufacture. Even as the production of CFC's declines, chlorinated methanes are anticipated to remain an important family of chemicals, throughout the chemical industry.

Typical chlorinated methane contaminated aqueous streams may result from either contaminated surface water, due mainly to spillage, or chemical plant evaporator condensate. There are very strict limits imposed for the allowable discharge of such solvents and it is anticipated that technology is required to reduce concentrations to a level of below 10 ppm *(Wijmans, Kaschemekat, Davidson and Baker, 1990)*.

For this application pervaporation would have to compete with the proven technologies of vapour stripping, adsorption, distillation, reintroduction into chlorination processes and incineration.

Chloroform is only sparingly soluble in water and displays a minimum solubility at around 35°C of 0.73 % w/w. At 25°C, the solubility is slightly higher, being 0.77 % w/w *(DeForest, 1989)*.

Chloroform is moderately toxic from single exposure, but repeated exposure can lead to severe medical effects. It is a suspected carcinogen and can be readily absorbed through the skin, specifically attacking the liver and kidney organs. The 1985 limiting values for work protection, for chloroform, set by the American Conference of Governmental Industrial Hygienists (ACGIH) are 10 ppm or 50 mg/m^3.

Again, a comprehensive review of published literature for the chloroform / water separation has been undertaken, with the results being tabulated in table 1.3.

Notes for table 1.3:-

* - Results normalised to a membrane thickness of 100μm, by dividing the permeability coefficients reported by 100×10^{-6} m.

** - The separation factors for silicone rubber obtained within the same study *(Watson and Payne, 1990)*, for both phenol and chloroform separation, are substantially higher than those obtained in all other studies of silicone rubber or PDMS. The validity of these results must, therefore, be questioned. It is, however, possible that the silicone rubber used within this study was of substantially different composition to other rubbers, although no indication of this was given.

References:-

1 *(Nguyen and Nobe, 1987)*

2 *(Lee, Bourgeois and Belfort, 1989)*

3 *(Watson and Payne, 1990)*

4 *(Blume, Wijmans and Baker, 1990)*

5 *(Hino, Ohya and Hara, 1991)*

6 *(Goethaert, Dotremont, Kuijpers, Michiels and Vandecasteele, 1993)*

7 *(Yamaguchi, Yamahara, Nakao and Kimura, 1994)*

8 *(Fang, Pham, Mahmud, Santerre, Naraitz and Matsuura, 1995)*

Membrane	Temp.	Perm. Pres.	Feed Conc.	Mem. Thick.	Flux	Sep. Factor	Ref.
	°C	mbar	ppm	μm	kg/m^2hr	α	
Silicone tubing	27	-	470	330	-	9000	1
PVDMS	22	7	100	100*	0.004	11.1	2
PVDF	22	7	100	100*	0.178	8.8	2
PSF/NMP	22	7	100	100*	0.261	1.4	2
PSF/THF	22	7	100	100*	1.236	0.8	2
PDMS	22	7	100	100*	0.028	560	2
ECN	22	7	100	100*	0.016	9.2	2
PVAc	22	7	100	100*	-	0.1	2
SI/imide	22	7	100	100*	0.004	19.4	2
Silicone rubber	25	0.1	100	200	-	15000	3**
PDMS	30	5	10000	3.5	-	540	4
PTFE	25	-	14.8	-	2	5.5	5
Cycrodextrin	25	-	88.8	-	0.05	0.007	5
Silicone rubber	25	-	0.937	200	0.0027	189	5
PTMSP	25	-	0.908	-	0.0313	237	5
PDMS	50	15	250	20	0.40	360	6
PDMS - zeolite Filled	50	15	250	30	0.30	1000	6
Plasma grafted butylacrylate	25	0.3	1000	-	0.15	400	7
Plasma grafted ethylacrylate	25	0.3	1000	-	0.15	85	7
Surface modified PES	23	4	1000	-	0.23	16	8

Table 1.3 - Summary of Chloroform / Water Separation Results

1.6.3 Pyridine

(Shimizu, Watanabe, Kataoka, Shoji, Abe, Morishita and Ichimura, 1993)

Pyridine is an excellent solvent for dehydrochlorination reactions and the extraction of antibiotics. Its primary use is as a starting material for pharmaceuticals and agrochemicals, being used to produce herbicides, insecticides and fungicides. Other pyridine bases, such as alkylpyridines, are also industrially important chemicals, again finding application in the pharmaceutical and agrochemical fields. Owing to the particularly high affinity of pyridine bases to water, contact between the two components is likely to result in a contaminated water stream, of which pervaporation could be considered as a technology for recovering the organic.

Pyridine bases are generally industrially synthesised by the reaction of aldehydes or ketones with ammonia, in the gas phase. During theses reactions either two or three molecules of water are produced for every molecule of pyridine base. This water obviously has to be separated from the product and pervaporation may prove to be a competitive technology for the recovery of pyridine base, before the water stream may be discharged. Separation techniques based upon vapour liquid equilibrium may also be attractive. The problem of an azeotrope, occurring at 41.3 %wt. water, may make such processes unattractive under certain process conditions. The 1989 worldwide production of pyridine was estimated to be 26 000 tonnes / annum and the production of alkylpyridines estimated to be a further 26 500 tonnes / annum.

Pyridine is totally miscible with water at all concentrations.

Pyridine and its common derivatives are acutely toxic. Pyridine is readily absorbed through the skin and attacks the central nervous system, gastrointestinal tract, liver and kidneys. The limit for occupational exposure has been set at 5 ppm, in the USA and Germany.

Very little previous work has been undertaken investigating the pyridine / water separation. That which has is summarised in table 1.4.

Membrane	Temp.	Perm. Pres.	Feed Conc.	Mem. Thickness	Flux	Sep. Factor	Ref.
	^oC	mbar	ppm	μm	kg/m^2hr	α	
PDMS	50	3	20000	-	1.50	31	1
PDMS silicalite filled	50	3	50000	-	0.43	34	2

Table 1.4 - Summary of Pyridine / Water Separation Results

References:-

1 *(Drioli, Zhang and Basile, 1993)*

2 *(Joyce, Devine and Slater, 1995)*

1.6.4 MIBK

(Siegel and Eggersdorfer, 1993)

(Habib, 1989)

MIBK, methyl-isobutylketone, (4-methyl-2-pentanone) is a member of a very industrially important class of chemicals, aliphatic ketones. The major application of MIBK is as a solvent for various resins and nitrocellulose. MIBK is an excellent extracting agent and a rapidly expanding field of application is in the extraction of rare transition complexes, antibiotics or paraffins from mineral oils. When used to extract materials from water, a proportion of the MIBK will dissolve in that water and pervaporation may be considered for its recovery.

MIBK is often industrially produced via a low temperature condensation of acetone to diacetone, which is subsequently dehydrated to form mesityl oxide and hydrogenated to form the final MIBK product. Within this process water is produced during the dehydration stage and it is possible that pervaporation could find application in treating the waste water stream, containing a mixture of ketone and intermediate, particularly mesityl oxide. An alternative manufacturing route is via the direct condensation of acetone in a one step process. In this process an aqueous byproduct stream, potentially containing both MIBK and di-isobutylketone, is produced. MIBK lies third in the list of most produced

aliphatic ketone, behind acetone and 2-butanone. The 1987 worldwide production of MIBK was estimated to be 180 000 tonnes / annum.

MIBK is sparingly soluble in water, displaying a solubility at 25°C of 1.8% w/w. Solubility is found to decrease slightly with an increase in temperature.

MIBK is considered not to be particularly toxic, which helps to explain its popularity as a solvent and extracting agent. The limit for occupational exposure has been set at 50 - 100 ppm or 205 - 400 mg/m^3.

To date, no published work in which MIBK / water separation is attempted, using pervaporation technology, has been found.

1.7 PDMS Membranes

An assessment made by Bruschke *(Bruschke, 1991)* of GFT concluded that PDMS provides the best combination of properties with respect to flux, selectivity and stability for the removal of most organics. An examination of tables 1.2 and 1.3 shows that PDMS is a very competitive material for the pervaporation of phenol and chlorinated hydrocarbons from aqueous streams. For these reasons it has been decided to investigate the use of PDMS membranes within this project and to attempt to further enhance the performance of the membranes by introducing various organofunctional groups into their structure.

1.7.1 Varieties of PDMS Membranes

PDMS membranes are characterised as containing a backbone of repeating dimethylsiloxane, $-Si(CH_2)_2-O-$, units. They are formed by cross-linking long, liquid, chains of PDMS with suitable short chained, silicone based, cross linking agents. Membrane structures, typical of those generally achieved, are displayed pictorially in section 3.1. There may be substantial differences in membrane structure, particularly in the nature of membrane cross-linking, between PDMS membranes used in different studies. Membrane structure and properties may well depend upon PDMS chain length and the nature of the cross-linking agent. It is very uncommon that chain length, cross-linking

density and membrane physical properties are reported and may explain the sometimes substantial differences in performances reported between different studies for essentially the same separation.

PDMS belongs to a family of materials classified as silicone rubber. As can be seen from tables 1.2 & 1.3, several authors have reported pervaporation data for silicone rubber tubing or membranes. It is quite possible that these membranes contain repeating dimethylsiloxane units, but may also contain different or additional units such as diethyl / dipropyl / etc. - methylsiloxane. Care should be taken when comparing the performance of this material with PDMS, unless the structure is known.

Pure PDMS membranes are fairly strong and it is relatively easy to form them into homogeneous films. In order to enhance mechanical rigidity and to allow the production of membranes with very thin active layers, it is common practice, throughout all areas of pervaporation, to form the dense layer on top of a strong microporous support material. The composite, asymmetric membrane so formed may exhibit significantly different performance to an equivalent homogeneous film. The support material itself may create a resistance to material transport through the membrane. Again it is uncommon to find data reporting the influence of the support material and variation between different studies could be partially explained by the use of different materials.

Throughout the pervaporation literature it would appear that the most commonly used PDMS membranes are either commercially available composite membranes supplied by GFT *(e.g. Drioli, Zhang and Basile, 1993)*, membranes obtained from Dow Corning *(e.g. Raghunath and Hwang, 1992)* or membranes produced from the components RTV 615 A&B, supplied by General Electric *(e.g. Vankelecom, Scheppers, Heus and Uytterhoeven, 1994)*. The later components consist of a long chain, vinyl terminated PDMS, *Cl-Si(CH$_2$)$_2$-O-*, (component A) and a cross-linking agent containing several Si-H groups per polymer chain and platinum catalyst (component B). The cross-linking process is achieved by the hydrosilylation reaction, very similar to that described within chapter 3. An alternative, but less common, manufacturing route to hydrosilylation is the sol-gel process, in which dimethyldiethoxysilane is cross-linked with tetramethoxysilane *(Lee, Iwamoto, Sekimoto and Seno, 1989)*.

1.7.2 Zeolite Filled and Modified PDMS

Numerous authors have studied the effect of incorporating zeolites into the PDMS membrane structure, in an attempt to enhance membrane performance. Zeolites are porous alumino-silicates and may be tailored to be either hydrophobic or hydrophilic by adjusting the ratio of aluminium to silicone *(Hennepe, Bargeman, Mulder and Smolders, 1987)*. A decrease in aluminium content leads to increased hydrophobicity. A number of silicate rich zeolites have been investigated for this purpose and the most successful membranes contain either silicalite, of which commercially available membranes are available from GFT, or ZSM-5 *(Vankelecom, Depre, Beukelaer and Uytterhoeven, 1995)*.

Hydrophobic zeolites enhance organic component permeability by increasing the sorption of these component into the membrane structure. At the same time water permeability is reduced as water is excluded from entering the zeolite particles. This leads to both decreased sorption of water and an increased path length for the water molecules, as they have to take a more tortuous path to travel through the membrane *(Hennepe, Smolders, Bargeman and Mulder, 1991)*.

As can be seen from the study of Goethaert et al, ref. 6 in table 1.3, selectivity towards chloroform can be significantly enhanced by the incorporation of zeolite. From table 1.4, it would appear, however, that the zeolite has very little effect upon selectivity towards pyridine. It has been found that the transport of small organic molecules is generally enhanced by the zeolite, but that voluminous molecules may be partly or totally excluded from entering the zeolite pores, due to the molecular sieving effect *(Dotremont, Brabants, Geeroms, Mewis and Vandecasteele, 1995)*.

A few attempts have been made to modify PDMS in other ways, in order to enhance performance, particularly for the industrially important separation of ethanol from water. Segmented polyurethaneurea, containing PDMS as the soft segment and PDMS / polystyrene graft copolymers have been produced for this separation *(Takegami, Yamada and Tsujii, 1992)*. No great improvements in selectivity or permeability were realised, however. Fairly significant enhancements in selectivity, for the same separation, have been achieved by PDMS / PTMSP copolymer blends *(Slater, Hickey and Juricic, 1990)*,

although absolute selectivities are still not very high. The addition of a fluorinated, surface modifying copolymer was found to make the membrane more hydrophobic and led to an enhanced separation factor, towards ethanol, of 16.6 from 12.1 *(Aoki, Yamagiwa, Yoshino and Oikawa, 1993)*.

Replacing the methyl groups with octyl groups has been found to enhance the selectivity of silicone rubber towards certain organics *(Shanley, Ondrey and Moore, 1994)*. It has also been shown that the permselectivities of PDMS membranes towards certain gas molecules can be improved significantly, without appreciable loss of flux, by introducing various organofunctional side chains *(Ashworth, Brisdon, England, Reddy and Zafar, 1991)*. The technique used within this study, to introduce the side chains, was similar to that described within section 3.1.1.

1.8 Closing Remarks

The pre-determined objectives of this project have been set out in the context of industrially important processes and organic / water separation problems. Potential areas of application for pervaporation technology, incorporating both waste water treatment and solvent recovery, have been highlighted for four classes of important chemical families.

An examination of tables 1.3 & 1.4 indicates that large discrepancies often exist between separation performances reported by different authors, using similar membranes, chemical components and process conditions. In many cases, transport resistances external to the membrane itself limit system performance, particularly feed side boundary layer resistance. It is thought that such resistances have often not been sufficiently accounted for and hence overall system and not membrane performance data is often reported. Unless the effect of all external resistances can be calculated out, it is difficult to compare membrane performance measured within different experimental configurations. Such considerations are discussed further within chapters 2 & 4.

Chapter 2

Mass Transport Mechanisms

Scope of Chapter 2

Within this chapter a comprehensive, critical review of mass transport within pervaporation systems is presented. Models are developed to describe component transport through the pervaporation membrane, based upon a solution - diffusion mechanism. A mainly phenomenological approach is employed to account for the effect of flux coupling. The importance of feed side boundary layer resistance is demonstrated and models based upon Ficks first law developed to describe transport in the boundary layer. Once more, the emphasis has been placed upon organophilic pervaporation and PDMS membranes, however, the models developed have general application and in many cases other areas of pervaporation are discussed.

Particular attention has been given to the effect of the, often neglected, convective flow term, that can influence transport in both boundary layer and membrane. It has been demonstrated that this term can be particularly important within the membrane itself.

In section 2.1 an analysis of boundary layer transport is presented, whilst membrane transport is reviewed in sections 2.2 - 2.4. Section 2.5 details an overall transport model, based upon a resistances in series approach.

2.1 Boundary Layer Resistances

In a system where a component of a mixture is selectively removed at an interface, the local concentration of that component will tend to drop. If there is a significant resistance to transport of the component between bulk and interface, a concentration gradient will result. This concentration gradient is assumed to exist across a small, theoretical boundary layer, adjacent to the interface.

Boundary layer resistance, often referred to as concentration polarisation, becomes more significant as the rate of transport and selectivity of component removal increase. Compared with other conventional membrane processes, the fluxes through dense, non-porous, pervaporation membranes are low and it has been noted *(Feng and Huang, 1994)* that many authors have consequently assumed boundary layer resistance to be negligible. This is a very dangerous assumption to make.

Probably the first study displaying the importance of feed side boundary layer resistance in pervaporation *(Psaume, Aptel, Aurelle, Mora and Bersillon, 1988)* showed that for the removal of traces of trichloroethylene, boundary layer resistance actually dominated the transport in their system. In other words, membrane resistance to trichloroethylene transport was found to be negligible compared to resistance in the boundary layer. Subsequently a number of studies have been published showing that boundary layer resistance can generally be of great importance.

2.1.1 Mathematical Treatment

Solute and solvent can migrate through the upstream boundary layer by process of both diffusion and convection. Applying Ficks Law to the diffusive process, the steady state solute flux can be described, at any plane throughout the boundary layer, by:-

$$J_o = -D_{lo}\frac{dC_o}{dx} + uC_o \qquad (2.1)$$

Where: J = Solute Flux, kg/m^{2}s
x = Distance, m
D = Diffusion Coefficient, m^2/s
u = Convective Velocity, m/s
C = Mass Concentration, kg/m^3
l denotes boundary layer
o denotes solute

Although Ficks Law may be described by expressing the concentration driving force in a number of ways, *eq. (2.1)* is the best overall expression for general use *(Cussler, 1984)*.

In a liquid system, D_{lo} cannot always be considered to remain constant, as it is a function of concentration. It has been shown that D_{lo} remains effectively constant across a liquid boundary layer when either $\frac{dC_o}{dx}$ or $C_o \rightarrow 0$ *(Brodkey and Hershey, 1988)*. In the case of

removal of organic pollutants from water, C_o is always low and hence it is safe to assume constant D_{lo}. This may not apply to other areas of Pervaporation where feed concentrations may be high, although it has been reported that D_{lo} will rarely vary by more than 10% *(Feng and Huang, 1994)*.

In a recent paper *(Michaels, 1995)*, it was argued that when solute concentration is very low, as in the case of removal of trace organic solvent from water, convective velocity can be equated to the volume flux of solvent:-

$$u = \frac{J_w}{\rho_w} \qquad (2.2)$$

Where: ρ = Density, kg/m^3 w denotes solvent

This simplification appears unnecessary as solute feed concentration would have to be extremely low for it to apply. A general model can be developed by equating convective velocity to the volume flux of both solvent and solute, without over complicating the subsequent analysis:-

$$u = \frac{J_w}{\rho_w} + \frac{J_o}{\rho_o} \qquad (2.3)$$

In constructing *eq. (2.3)* the assumption is made that solute and solvent densities do not change upon mixing i.e.:-

$$\rho_{av} = \phi_o\rho_o + (1 - \phi_o)\rho_w \qquad (2.4)$$

Where: ϕ = Volume Fraction of Component

av denotes average

Adopting the approach of Michaels and integrating *eq. (2.1)* over the thickness of the boundary layer, assuming D_{lo} to remain constant, yields:-

$$\int_{C_{o(mb)}}^{C_{o(b)}} \frac{dC_o}{-\frac{J_o}{u} + C_o} = \int_0^{\delta_l} \frac{u\,dx}{D_{lo}} \qquad (2.5)$$

$$ln\left(\frac{-\frac{J_o}{u} + C_{o(mb)}}{-\frac{J_o}{u} + C_{o(b)}}\right) = \frac{u\delta_l}{D_{lo}} \qquad (2.6)$$

$$\frac{C_{o(mb)}}{C_{o(b)}} = exp\left(\frac{u\delta_l}{D_{lo}}\right) - \frac{J_o}{C_{o(b)}u}\left(exp\left(\frac{u\delta_l}{D_{lo}}\right) - 1\right) \qquad (2.7)$$

Where: δ_l = Boundary Layer Thickness, m

mb denotes upstream membrane surface

b denotes bulk

The term $\left(\frac{u\delta_l}{D_{lo}}\right)$, the ratio of convective to diffusive velocity, is the Peclet number *(Pe)*. For small *Pe*, $exp(Pe) \approx 1+Pe$ and *eq. (2.7)* reduces to:-

$$C_{o(mb)} = C_{o(b)}(1+Pe) - \left(\frac{J_o\delta_l}{D_{lo}}\right) \qquad (2.8)$$

or:-

$$J_o = \left(\frac{D_{lo}}{\delta_l}\right)(C_{o(b)}(1+Pe) - C_{o(mb)}) \qquad (2.9)$$

and for very small *Pe*:-

$$J_o = \left(\frac{D_{lo}}{\delta_l}\right)(C_{o(b)} - C_{o(mb)}) \qquad (2.10)$$

Eq. (2.10) describes the relationship obtained if only the diffusive term in *eq. (2.1)* is integrated across the boundary layer. This is the case when the magnitude of convective flux is negligible compared to that of diffusive flux.

2.1.2 Mass Transfer Coefficients

2.1.2.1 Sherwood Correlations

The term $\left(\frac{D_{lo}}{\delta_l}\right)$ is the solute mass transfer coefficient across the feed side boundary layer, k_{lo}. It is a function of feed side hydrodynamics and can be predicted by using one of the numerous, semi-empirical, Sherwood correlations that exist for varying flow conditions and geometries. These correlations take the general form *(Gekas and Hallstrom, 1987)*, *(Nijhuis, 1990)*:-

$$Sh = b\,Re^c\,Sc^d\left(\frac{d_c}{L}\right)^e \qquad (2.11)$$

for crossflow configurations and:-

$$Sh = b\, Re^{c}\, Sc^{d} \qquad (2.12)$$

for stirred cells.

Where:-

$$Sh = \text{Sherwood Number} = \frac{k_{lo} d_c}{D_{lo}} \qquad (2.13)$$

$$Re = \text{Reynolds Number} = \frac{v d_c}{\nu} \text{ (Cross flow) or } \frac{\omega d_c}{\nu} \text{ (Stirred Cell)} \qquad (2.14)$$

$$Sc = \text{Schmidt Number} = \frac{\nu}{D_{lo}} \qquad (2.15)$$

b, c, d, e = Coefficients L = Length, m

v = Feed Velocity, m/s ν = Kinematic Viscosity, m^2/s

ω = Rotational Velocity, rad/s

d_c = Characteristic Dimension = Hydraulic Diameter (Cross Flow), m

= Cell Radius (Stirred Cell), m

The coefficients b, c, d and e vary with feed side hydrodynamics. A summary of the values that they take under various flow regimes is given in table 2.1 *(Karlsson and Tragardh, 1993)*.

Flow Regime	***b***	***c***	***d***	***e***	**System**
Laminar	1.62	0.33	0.33	0.33	Crossflow
$Re < 2000$	1.85	0.33	0.33	0.33	Crossflow
$10^4 < Re < 10^5$	0.34	0.75	0.33	0	Crossflow
$Re > 10^5$	0.023	0.8	0.33	0	Crossflow
Laminar	0.29	0.57	0.33	-	Stirred Cell
Turbulent	0.044	0.75	0.33	-	Stirred Cell

Table 2.1 Sherwood Correlation Coefficients

One problem that becomes apparent from the above correlations for stirred cells is that no account is taken of the physical size of the stirrer. It appears obvious that a large stirrer will create more turbulence than a small stirrer, if rotated with equal rotational velocity. The above values for coefficients b, c and d can, therefore, only be used with confidence for systems geometrically similar to that used for their determination. It is postulated here that the effect of stirrer size could be to change the value of coefficient b, whilst c and d

remain constant for all systems. No absolute experimental data has been found to support this theory, although a mathematical analysis displaying the possibility is presented below.

The characteristic dimension required in both the Sherwood and Reynolds numbers, taken above to be the hydraulic diameter of the cell, d_c, could equally be taken to be the stirrer diameter, d_s. It is instructive to examine the influence of substituting d_s for d_c. Define:-

$$\varphi = \frac{d_c}{d_s} \qquad (2.16)$$

Expanding *eq. (2.12)*:-

$$k_{lo} = b\,\omega^{c}\, d_c^{c-1}\, \nu^{d-c}\, D_{lo}^{1-d} \qquad (2.17)$$

Combining *eqs. (2.16) & (2.17)*:-

$$k_{lo} = (b\,\varphi^{c-1})\,\omega^{c}\, d_s^{c-1}\, \nu^{d-c}\, D_{lo}^{1-d} \qquad (2.18)$$

Eq. (2.18) displays that the constant of proportionality, originally *b*, has become $(b\,\varphi^{c-1})$, whereas the coefficients *c* and *d* are unchanged. The implication of this is that the dependency of k_{lo} upon stirrer speed and physical properties is uninfluenced by changes in the size of the stirrer. $(b\,\varphi^{c-1})$ will obviously change in value with changing d_s, which will influence absolute values of k_{lo}. This analysis is speculative but can be expected to hold for geometrically similar stirrers. As the degree of turbulence is a strong function of stirrer type and shape, no simple universal relationship can be easily formulated for stirrers of different geometry.

By considering *eqs. (2.11) & (2.12)* it can be seen that, in the turbulent region, a plot of $1/k_{lo}$ against $1/\omega^{0.75}$ should yield a straight line. This was found to be the case in a study to determine boundary layer resistance in a stirred cell pervaporation rig *(Burslem, Naylor and Field, 1992)* and lends credibility to the value for coefficient c in table 2.1.

2.1.2.2 Diffusion Coefficients

The diffusion process in liquids is complicated and not completely understood. In particular, the concentration dependence of D_{lo} is difficult to predict accurately. Numerous correlations exist for predicting D_{lo} although most are only applicable to specific systems such as non-electrolyte or electrolyte solutions, dilute or concentrated solutions and

aqueous or non aqueous solutions. Probably the most applicable correlation to pervaporation processes is the Wilke-Chang correlation *(Brodkey and Hershey, 1988)*, which is generally applicable to both aqueous and non aqueous, dilute solutions of non-electrolytes:-

$$D_{lo} = 1.17 \times 10^{-16} \frac{T(\phi M_w)^{1/2}}{\mu_w V_o^{0.6}} \qquad (2.19)$$

Where: T = Temperature, K ϕ = Association Parameter

M = Molecular Mass, kg/kmol μ = Viscosity, kg/ms

V = Molar Volume at Normal Boiling Point, m^3/kmol

The term ϕ takes the value of 2.26 for water, 1.9 for methanol, 1.5 for ethanol and 1.0 for other unassociated solvents. D_{lo} values in liquids are generally low, being in the order off $10^{-9} m^2/s$.

2.1.2.3 Typical Values

Experimentally determined k_{lo} values have been reported for both crossflow and stirred cell configurations, using typical laboratory scale equipment and test conditions, employing flat sheet membranes *(Ji, Sikdar and Hwang, 1994)*, *(Raghunath and Hwang, 1992)*, *(Nijhuis, Mulder and Smolders, 1991)*, *(Burslem et al, 1992)*. All k_{lo} values fall in the range 7.4×10^{-6} - 3.3×10^{-5} m/s. It was noted *(Nijhuis et al, 1991)* that a value of 2.5×10^{-5} m/s would be a high, but not unrealistic, value to be reached in practical applications.

The highest reported k_{lo} values are found for hollow fiber membrane configurations *(Lipski and Cote, 1990)*, *(Borges, Mulder and Smolders, 1992)*, *(Gooding, Hickey and Crowder, 1991)*, *(Lipski, Cote and Fleming, 1991)*. Transversal flow configurations are better than those with inside flow and k_{lo} values of 5.0×10^{-5} - 10^{-4} m/s are typically achieved.

Normally u in pervaporation is less than 5×10^{-7} m/s *(Feng and Huang, 1994)* (as may be seen from a study of tables 1.2 - 1.4) and hence typical Pe numbers would be in the range of 0.005 - 0.05, which are small and allow for the use of either *eq. (2.9)* or *(2.10)*.

2.1.3 Applicability of Transport Models

In practice it is desirable to be able to use *eq. (2.10)*, rather than the more rigorous and complicated *eq. (2.7)*, to describe mass transport in the boundary layer. An analysis was performed by Gref et. al. *(Gref, Nguyen and Neel, 1992)* to determine the conditions under which *eq. (2.10)* is applicable. This is presented in a modified form below.

Define:-

$$J_{do} = -D_{lo}\frac{dC_o}{dx} \qquad (2.20)$$

Where: subscript d in J_{do} denotes contribution due to diffusion

Eq. (2.1) may be rewritten, incorporating *eq. (2.3)* as:-

$$J_o = J_{do} + \left(\frac{J_w}{\rho_w} + \frac{J_o}{\rho_o}\right)C_o \qquad (2.21)$$

$$J_o = \frac{J_{do} + \frac{J_w}{\rho_w}C_o}{\left(1 - \frac{C_o}{\rho_o}\right)} \qquad (2.22)$$

From *eq. (2.22)* it should be noted that if the effect of convective flow is not negligible, J_{do} increases throughout the boundary layer as C_o drops.

In the case of the removal of organic pollutants from water, $C_{o(b)}$ and hence C_o throughout the boundary layer, is generally very small. *Eq. (2.22)*, therefore, reduces to:-

$$J_o = J_{do} + \frac{J_w}{\rho_w}C_o \qquad (2.23)$$

Rearranging *eq. (2.23)*, one obtains:-

$$\frac{J_{do}}{J_o} = 1 - \frac{J_w C_o}{J_o \rho_w} \qquad (2.24)$$

From *eq. (2.24)* it can be seen that the contribution of convective flow to the solute flux is negligible when $\frac{J_w C_o}{J_o \rho_w}$ is small.

The terms J_w, J_o and ρ_w are all constant across the boundary layer. The maximum value that C_o can reach is at the boundary layer / bulk fluid interface, i.e. $C_{o(b)}$. As the concentration profile across the boundary layer has yet to be determined it is assumed that $\frac{J_w C_o}{J_o \rho_w}$ is small, compared with unity, when $\frac{J_w}{J_o} << \frac{C_{o(b)}}{\rho_w}$. The right hand side of the inequality is always small for low $C_{o(b)}$ and so the condition will be satisfied when $J_o >> J_w$, i.e. when selectivity to the solute is high.

The condition can be quantified in terms of the selectivity coefficient, β, which is defined as:-

$$\beta = \frac{w_{op}}{w_{ob}} \qquad (2.25)$$

Where: w = Mass Fraction p denotes permeate

w_{op} may be determined from individual component fluxes:-

$$w_{op} = \frac{J_o}{J_o + J_w} \qquad (2.26)$$

For small $C_{o(b)}$:-

$$w_{ob} \approx \frac{C_{o(b)}}{\rho_w} \qquad (2.27)$$

Therefore, from *eqs. (2.25)*, *(2.26)* and *(2.27)*:-

$$\frac{J_w C_{o(b)}}{J_o \rho_w} \beta = \frac{J_w}{J_o + J_w} = 1 - w_{op} \qquad (2.28)$$

$$\frac{J_w C_{o(b)}}{J_o \rho_w} = \frac{1 - w_{op}}{\beta} = \frac{1}{\beta} - w_{ob} \qquad (2.29)$$

If we arbitrarily assume that the contribution of convective flow to solute flux is negligible if $\frac{J_w C_{o(b)}}{J_o \rho_w}$ is less than 5 % (see *eq. (2.24)*), then from *eq. (2.29)* one obtains:-

$$\frac{1}{\beta} < 0.05 + w_{ob} \qquad (2.30)$$

This condition is satisfied, for small w_{ob}, when $\beta > 20$. In the field of removal of organic pollutants from water this is only a very moderate selectivity, unless the pollutant has a very low activity in water.

By combining *eqs. (2.10)* with *(2.25 - 2.27)* it can be easily shown that:-

$$\frac{C_{o(mb)}}{C_{o(b)}} = 1 - \frac{\beta\,(J_o + J_w)}{k_{lo}\,\rho_w} \qquad (2.31)$$

If ρ_o and ρ_w are similar then:-

$$\frac{(J_o + J_w)}{\rho_w} \approx u \qquad (2.32)$$

Hence, *eq. (2.31)* becomes:-

$$\frac{C_{o(mb)}}{C_{o(b)}} = 1 - \frac{\beta\,u}{k_{lo}} \qquad (2.33)$$

Eq. (2.33) displays, concisely, the three factors that influence the extent of boundary layer resistance. Of course *eq. (2.33)* only applies for low C_o and moderate to high selectivity, as discussed above.

2.1.3.1 High Feed Concentrations

It has been noted *(Field and Burslem, 1992)*, *(Feng and Huang, 1994)* that several authors have made the erroneous assumption that boundary layer resistance will only be significant at low feed concentration. Recall *eq. (2.22)*:-

$$J_o = \frac{J_{do} + \frac{J_w}{\rho_w} C_o}{\left(1 - \frac{C_o}{\rho_o}\right)} \qquad (2.22)$$

It can be seen that J_o increases with C_o and hence boundary layer resistance reduces. In general, it may be deduced that the effect of convective flow is to reduce boundary layer resistance and convective flow becomes more significant at higher C_o. Boundary layer resistance could still, however, be very important or even the dominant resistance to transport at higher feed concentrations, when flux and selectivity are high.

2.1.3.2 Summary of Convective Flow Considerations

To summarise, the contribution of convective flow to solute flux is negligible if two conditions are met:-

1. Solute feed concentration is low
2. Selectivity is at least moderately high

For the removal of organic pollutants from water, both of these conditions should generally be met, in the area of technical importance. If both of these conditions are not met, as may be the case in other areas of pervaporation or in special cases where selectivity may be low, the more complicated *eq. (2.7)* must be employed to describe mass transport in the boundary layer. A further complication that may result is that for high feed concentrations D_{lo} could vary significantly across the boundary layer.

2.2 Membrane Sorption

Separation in pervaporation occurs due to preferential sorption and/or diffusion of one of the feed components, in or through the pervaporation membrane. It has been demonstrated *(Bell, Gerner and Strathmann, 1988)* that the overall permeability of a component is determined mainly by preferential sorption in rubbery membranes and preferential diffusivity in glassy membranes. In both types of membranes, component sorption often increases with molecular size, however, an inflexible glassy membrane structure severely inhibits diffusion as molecular size increases, thus leading to the preferential permeation of small molecules. In the far more flexible matrix of a rubbery membrane, containing high free volume, diffusivity decreases only slowly with increasing molecular size.

2.2.1 Solubility Parameter

Sorption is determined by the affinity of a feed component towards the membrane polymer. It is possible to obtain at least a semi-quantitative estimation of the interaction between component and polymer using the solubility parameter theory *(Barton, 1983)*. The solubility parameter, δ_i, contains contributions from dispersion (*d*), polar (*p*) and hydrogen bonding (*h*) character:-

$$\delta_i^2 = \delta_{d,i}^2 + \delta_{p,i}^2 + \delta_{h,i}^2 = \delta_{d,i}^2 + \delta_{p/h,i}^2 \qquad (2.34)$$

Where: δ = Solubility Parameter, $J^{1/2}/cm^{3/2}$

i denotes component *i*

In a binary system (polymer and single penetrant) sorption is likely to be high if δ_i for the polymer and penetrant are similar. If the δ_is are too similar, however, it has been demonstrated *(Zhu, Yang, Fried and Greenberg, 1983)* that penetrant molecules may become immobilised within the polymer, decreasing the effective size of the available transport corridor.

For ternary systems the solubility parameter approach is less successful due to interactions between the components of the liquid feed, although in many cases a good correlation still exists between δ_i difference and preferential sorption *(Nijhuis, Mulder and Smolders, 1993)*.

2.2.2. Sorption Isotherms

Numerous authors have produced sorption isotherms for water and organics, from both liquid and gaseous phases, in typical pervaporation polymers. From the liquid phase a membrane sample, of known mass, is immersed in a solution of known initial concentration. When sorption equilibrium is reached the membrane sample is removed and weighed to determine mass increase. The solution is analysed to determine equilibrium concentration. Sorption of each component, at this concentration, can be determined by mass balance. From the gas phase, the membrane is surrounded by a flowing gas consisting of a carrier, such as nitrogen and a component to be sorbed, of known partial pressure (activity). The mass increase of the membrane is monitored until equilibrium is reached.

2.2.2.1 Flory Huggins Thermodynamics

Flory Huggins thermodynamics appears particularly useful in describing the forms of these isotherms *(Nijhuis, 1990) (Huang and Rhim, 1991) (Mulder, 1991)*. For both glassy and rubbery polymers, sorption isotherms of typical solvents display the characteristic Flory Huggins shape, almost exclusively *(Heintz, Funke, Lichtenthaler and 1991)*. An isotherm typical of that described by Flory Huggins thermodynamics is displayed in fig. 2.1.

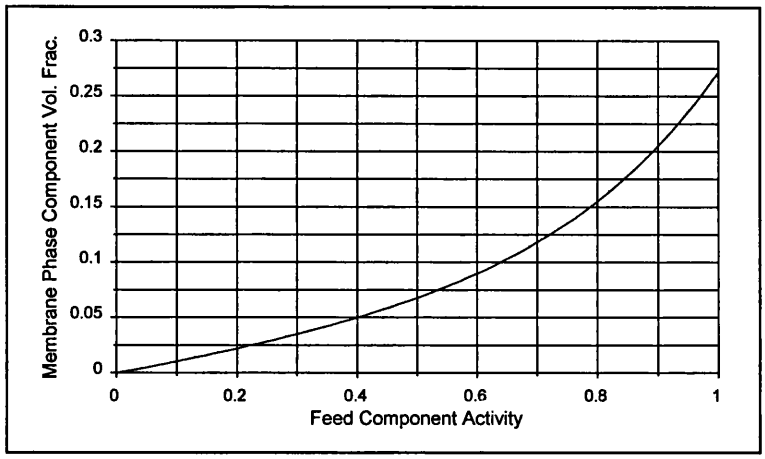

Fig. 2.1 - Typical Flory Huggins Shaped Isotherm

For a binary (polymer and single liquid component) system, the volume fraction of liquid sorbed into the membrane can be related to liquid activity *(Flory, 1953)*:-

$$ln\, a_1 = ln\, \phi_1 + \left(1 - \frac{V_1}{V_3}\right)\phi_3 + \chi_{13}\,\phi_3^{\,2} \qquad (2.35)$$

Where: a = Activity — ϕ = Volume Fraction

V = Molar Volume, m^3/mole — χ = Interaction Parameter

1 denotes liquid — *3* denotes polymer

For a ternary system (organic component *(1)*, water *(2)* and polymer *(3)*) the Flory Huggins equation can easily be extended:-

$$ln\, a_1 = ln\, \phi_1 + (1 - \phi_1) - \phi_2 \frac{V_1}{V_2} - \phi_3 \frac{V_1}{V_3} + (\chi_{12}\,\phi_2 + \chi_{13}\,\phi_3)\,(\phi_2 + \phi_3) - \chi_{23} \frac{V_1}{V_2}\phi_2\,\phi_3 \qquad (2.36)$$

$$ln\, a_2 = ln\, \phi_2 + (1 - \phi_2) - \phi_1 \frac{V_2}{V_1} - \phi_3 \frac{V_2}{V_3} + (\chi_{12}\,\phi_1 \frac{V_2}{V_1} + \chi_{23}\,\phi_3)\,(\phi_1 + \phi_3) - \chi_{13} \frac{V_2}{V_1}\phi_1\,\phi_3 \qquad (2.37)$$

In general the molar volume of the polymer is much larger than that of the penetrants and hence $\frac{V_1}{V_3}$ and $\frac{V_2}{V_3} \rightarrow 0$.

For glassy polymers an additional term has to be added to account for restrictions to chain segment mobility caused by adjacent crystallites. This additional term is the Flory-Rehner modification *(Flory, 1953)* and *eq. (2.35)* becomes:-

$$ln\, a_1 = ln\, \phi_1 + \left(1 - \frac{V_1}{V_3}\right)\phi_3 + \chi_{13}\,\phi_3^{\,2} + \frac{\langle\alpha\rangle_o^{\,2}\,(\upsilon/A)\,V_1\phi_3^{\,2}}{V_{3u}} \qquad (2.38)$$

Where: $\langle\alpha\rangle_o$ = ratio between the mean distance separating the junctions in the unswollen network and the mean end-to-end distance for the corresponding segment if this segment were unrestricted

υ = No. Effective Segments in Sample A = Avogadro Number

u denotes unswollen

For cross linked polymers a term describing the energy change due to elastic strain has to be added to *eq. (2.35) (Nijhuis, 1990)*:-

$$ln\, a_1 = ln\, \phi_1 + \left(1 - \frac{V_1}{V_3}\right)\phi_3 + \chi_{13}\,\phi_3^{\,2} + \frac{V_1\,\rho_3}{M_c}\,(1 - 2M_c/M)\,(\phi_3^{\,1/3} - \frac{1}{2}\phi_3) \qquad (2.39)$$

Where: ρ = Density g/cm^3 M_c = Molecular Mass per Cross Linked Unit

M = Molecular Mass before cross-linking

The factor $(1 - 2M_c / M)$ expresses the correction for network imperfections resulting from chain ends. For a perfect network $M \rightarrow \infty$ and hence it reduces to unity.

The same correction factors can also be added to *eq. (2.36)* describing a ternary system and also to *eq. (2.37)* with the small alteration that all subscripts 1 become 2.

For rubbery pervaporation membranes, in which swelling is low, the elastic strain term is small and can be neglected *(Nijhuis, 1990)*. In addition if water sorption (i.e. ϕ_2) is very low, *eq. (2.36)* reduces to the binary isotherm of *eq. (2.35)*.

It has been demonstrated that the basic form of the Flory Huggins equation, *eq. (2.36)*, gives an excellent fit for good solvents i.e. trichloroethylene, toluene *(Nijhuis, 1990)* and chloroform *(Favre, Nguyen, Schaetzel, Clement and Neel, 1993)*, (*Favre, Nguyen, Schaetzel, Clement and Neel, 1994*), in rubbery membranes. For poorer solvents, the basic Flory Huggins theory must be refined in order to produce an adequate fit. For sorption of alcohols it has been shown *(Favre et al, 1993)*, *(Favre et al, 1994)* that it is necessary to employ a variable interaction parameter, χ_{13}, as proposed by Koningsveld and Kleinjtens *(Koningsveld and Kleinjtens, 1971)*:-

$$\chi_{13} = \alpha + \frac{\beta(1 - w)}{(1 - w\phi_3)^2} \qquad (2.40)$$

α is an empirical correction term, β is linked to mixing enthalpy and w to the coordination number of the network. Unfortunately α, β and w can only be obtained experimentally, by a non linear curve fit of sorption data and hence reduces the usefulness of the Flory Huggins approach.

The basic Flory Huggins theory assumes perfect mobility of polymer chains and no preferential sites in the lattice. It is thought that deviation results from the tendency for solvent to cluster within the polymer matrix. According to Zimm and Lundberg analysis *(Favre et al, 1993)*, *(Favre et al, 1994)* the average cluster size increases as solvent affinity for the membrane decreases.

Where χ_{13} is constant, it may be predicted using the solubility parameter approach *(Zielinski and Duda, 1992)*:-

$$\chi_{13} = \chi_1 + \frac{V_1}{RT}(\delta_1 - \delta_3)^2 \qquad (2.41)$$

Where: R = Gas Constant = 8.314 J/molK

T = temperature, K

Considering *eqs. (2.35) & (2.41)*, ϕ_1 and hence sorption, will tend to increase with increasing temperature, although this dependence is usually not strong. Of course temperature also has a complicated effect upon solvent activity. It has been shown *(Kondo and Sato, 1994)* that both phenol and water sorption in PEBA membranes, from aqueous solution, increase with temperature by almost an order of magnitude between 30 and 70°C. The shapes of the sorption isotherms remain similar over this temperature range.

2.2.2.2. Sorption Coefficient

Whatever form a sorption isotherm may take, in the range of low solvent activity (low feed solvent concentration in the case of ternary systems) the isotherm approximates to that of Henry's law. An activity based sorption coefficient, S^a_1, is defined as:-

$$S^a_1 = \frac{\phi_1}{a_1} \qquad (2.42)$$

Henry's law assumes that S remains constant over the concentration range in which it applies. Also, if the solvent activity coefficient is considered constant across a dilute concentration range, a concentration based sorption coefficient, S^c_1, can be defined:-

$$S^c_1 = \frac{C_{1(ml)}}{C_{1(mb)}} \qquad (2.43)$$

Where: $C_{(mb)}$ = Concentration in feed at membrane/feed interface, kg/m^3

$C_{(ml)}$ = Concentration in membrane at membrane/feed interface, kg/m^3

For PDMS membranes it appears that for both good, including chloroform and poor solvents, S^a remains typically constant up to a component activity of about 0.4 *(Blume, Schwering, Mulder and Smolders, 1991)*, *(Favre et al, 1993)*, *(Favre et al, 1994)*. Hence, S^c will be constant over a much greater $C_{1(mb)}$ range as solute volatility decreases. ϕ_1 reduces with increasing PDMS cross linking density for a good solvent, such as toluene *(Blume, Bos, Schwering, Mulder and Smolders, 1991)*.

For chloroform in NBR and SBR membranes S^c is only constant up to about $C_{1(mb)}$ = 0.8 kg/m^3 at 30°C *(Brun, Larchet, Bulvestre and Auclair, 1985)*, however for isopropylalcohol in PDMS, S^c remains constant up to at least $C_{1(mb)}$ = 100 kg/m^3 at room temperature *(Hennepe, Boswerger, Bargeman, Mulder and Smolders, 1994)*. Constant S^c has been reported for phenol sorption in PEBA membranes up to $C_{1(mb)}$ = 50 kg/m^3 *(Boddeker et al, 1990)*, *(Kondo and Sato, 1994)* at 30, 50 and 70°C.

Water sorption in PDMS membranes is always low, ϕ_2 being reported to be of the order of 0.002 by various studies in temperature ranges of 25-40°C *(Watson and Payne, 1990)*, *(Mulder and Smolders, 1991)*, *(Favre et al, 1993)*, *(Favre et al, 1994)*. It is, therefore, normally appropriate to use the binary isotherm, *eq. (2.35)*, rather than the more complicated ternary isotherm, *eq. (2.36)*, to describe solute sorption, outside of the region of Henry's law. Due to extreme clustering, it is not thought possible to accurately fit water sorption to existing isotherms *(Favre et al, 1994)*.

It is quite possible that the extent of solvent sorption can influence the extent of water sorption. For 5 %wt. alcohol solutions, ϕ_2 was found to increase from 0.0013 to 0.0022 as the alcohol was changed in the series from methanol to butanol, with a corresponding

increase in alcohol sorption *(Mulder and Smolders, 1991)*. Also, for aqueous phenol solutions and PEBA membranes, water sorption was found to be constant up to a phenol concentration of about 1.5 %wt., after which it started to increase *(Boddeker et al, 1990)*, *(Kondo and Sato, 1994)*.

2.3 Membrane Diffusion

2.3.1 Free Volume Arguments

The ability of penetrant molecules to diffuse through polymeric pervaporation membranes, that are essentially completely non porous in structure, can be described according to the free volume theory *(Fujita, 1961)*. In organophilic, rubbery polymers, the polymer segments are in continuous motion, creating free volume (molecular holes) through which transport may occur *(Rhim and Huang, 1989)*. In hydrophilic, glassy polymers there is little segmental motion and the free volume manifests itself as amorphous regions between rigid polymer segments *(Bell et al, 1988)*. These free volume arguments are supported by two separate studies. In partially crystalline polyethylene membranes, permeability was found always to decrease with increasing crystallinity *(Lee, Krovvidi and Greenberg, 1989)* and it was shown that the crystalline phase does not absorb permeating species to any detectable extent. In rubbery PDMS membranes it was shown that both ethanol and water permeability reduced with decreasing dimethylsiloxane monomer length (between 200 and 10 units), thus reducing the distance between cross links *(Takegami et al , 1992)*.

2.3.2 Ficks First Law

Diffusion through a polymeric membrane can be considered to be an example of structure insensitive diffusion, where the solute(s) are dissolved so as to form a homogeneous solution *(Brodkey and Hershey, 1988)*. Structure insensitive diffusion may be described by Ficks first law, as used by numerous authors *(Karlsson and Tragardh, 1993)*. As for transport across a liquid boundary layer, the full form of Ficks law can be written as:-

$$J_i = -D_{mi}\frac{dC_{im}}{dx} + uC_{im} \qquad (2.44)$$

Where: J = Solute Flux, kg/m^{2}s x = Distance, m

D = Diffusion Coefficient, m^2/s u = Convective Velocity, m/s

C = Mass Concentration, kg/m^3 i denotes component i

m denotes in membrane phase

A commonly used variation of eq. *(2.44)*, often used for transport through membranes *(Rautenbach and Albrecht, 1985)* is:-

$$J_i = -\rho_m D_{mi} \frac{dw_{im}}{dx} + \rho_m u w_{im} \qquad (2.45)$$

Where: ρ = density, kg/m^3 w = mass fraction

Eq. (2.45) is perfectly valid for the case where ρ_m remains constant across the specified range of C_{im}. This is obviously the case when sorption is very low. When sorption is high, however, ρ_m cannot be assumed to remain constant for two reasons. Firstly if the membrane and sorbed components have significantly differing densities, ρ_m which is the density of the entire membrane phase, will obviously vary even if the following swelling relationship is valid:-

$$\rho_m = V_{md}\rho_{md} + \Sigma V_i \rho_i \qquad (2.46)$$

Where: V = Volume Fraction *md* denotes dry membrane

Secondly, in many cases *eq. (2.46)* is not valid as when components are sorbed into a membrane structure they tend to fill free volume as well as causing swelling. If the contribution of filling free volume is significant, ρ_m will increase with increasing sorption. When any component that has a high affinity for the membrane is present in the feed at significant concentration, it would appear sensible to use *eq. (2.44)* instead of *eq. (2.45)*.

2.3.3 Convective Flow Term

Even if significant, the convective flow term in *eq. (2.44)* is always neglected *(Geankoplis, 1982)*, yielding:-

$$J_i = -D_{mi} \frac{dC_{im}}{dx} \qquad (2.47)$$

Essentially any contribution to mass transport due to bulk flow is considered to be part of the diffusion coefficient, D_{mi}. No specific reason for this simplification has been found in literature and it would appear to be quite straight forward to use the more rigorous *eq. (2.44)* in order to obtain true D_{mi} values. Applying the same logic as for the liquid boundary layer, if solute concentration of the preferentially permeating component in the membrane is fairly low (i.e. low membrane swelling) and selectivity is at least moderately high, the bulk flow term becomes negligible. Of course these conditions are not always met, especially when feed concentration and sorption are high.

Following a similar approach as for the liquid boundary layer, for a ternary system:-

Define:-

$$J_{do} = -D_{mo}\frac{dC_{om}}{dx} \qquad (2.48)$$

$$u = \frac{J_w}{\rho_w} + \frac{J_o}{\rho_o} \qquad (2.3)$$

Eq. (2.44) may be rewritten, incorporating *eq. (2.3)*:-

$$J_o = J_{do} + \left(\frac{J_w}{\rho_w} + \frac{J_o}{\rho_o}\right)C_{om} \qquad (2.49)$$

$$J_o = \frac{J_{do} + \frac{J_w}{\rho_w}C_{om}}{\left(1 - \frac{C_{om}}{\rho_o}\right)} \qquad (2.50)$$

Eq. (2.50) clearly illustrates the two factors that influence the extent of convective flow, leading to deviation from *eq. (2.47)*. As J_w and/or C_o increase, convective flow increases.

Integrating *eq. (2.44)*, across the thickness of the membrane, in the same manner as across the liquid boundary layer, yields:-

$$\frac{C_{i(m2)}}{C_{i(m1)}} = exp\left(\frac{u\delta_m}{D_{mi}}\right) - \frac{J_i}{C_{i(m1)}u}\left(exp\left(\frac{u\delta_m}{D_{mi}}\right) - 1\right) \qquad (2.51)$$

1 denotes upstream interface *2* denotes downstream interface

Rearranging *eq. (2.51)*:-

$$J_i = \frac{exp\left(\frac{u\delta_m}{D_{mi}}\right) C_{i(m1)}u - C_{i(m2)}u}{exp\left(\frac{u\delta_m}{D_{mi}}\right) - 1} \qquad (2.52)$$

It is suggested that when convective flow is important, *eq. (2.52)* should be used to determine J_i for each component, instead of *eq. (2.47)*. It would usually be necessary to use a numerical technique in order to solve *eq. (2.52)*, however if a few simplifying assumptions can be made the effect of convective flow can be easily illustrated, as described below.

If permeate pressure is low, $C_{i(m2)}$ approaches 0 and hence *eq. (2.52)* reduces, for the solute component, to:-

$$J_o = \frac{C_{o(m1)}u}{1 - \frac{1}{exp\left(\frac{u\delta_m}{D_{mo}}\right)}} \qquad (2.53)$$

When feed concentrations and selectivities are relatively high, solute flux may be much higher than solvent flux, hence:-

$$u \approx \frac{J_o}{\rho_o} \qquad (2.54)$$

In this case *eq. (2.53)* reduces, by simple manipulation, to:-

$$J_o = \rho_o \frac{D_{mo}}{\delta_m} ln\left(\frac{1}{1 - \frac{C_{o(m1)}}{\rho_o}}\right) \qquad (2.55)$$

2.3.3.1 Numerical Examples

From a study of vapour permeation of water and chloroform in PDMS at 40°C *(Favre et al, 1994)*, it was found that $J_o >> J_w$ for all but very low C_{om}. Taking typical parameters from this study:-

$\rho_o = 1500$ kg/m^3 $\qquad$ $D_{mo} = 6.51 \times 10^{-10}$ m^2/s

For a relatively high chloroform feed activity of 0.6, assuming a membrane phase density of just over 1000 kg/m^3:-

$C_{o(m1)} \approx 200$ kg/m^3

Assuming $\delta_m = 100$ μm and low permeate pressure, i.e. $C_{o(m2)} \approx 0$, *eq. (2.55)* gives:-

$J_o = 0.00140$ kg/m^{2}s

Eq. (2.47) gives:-

$J_o = 0.00130$ kg/m^{2}s

Although not large, the discrepancy is noticeable.

An example of a situation where convective flow may have a much greater influence is that in which the non preferentially transported component has a high solubility in the membrane. This is often the case for the dehydration of organic/water mixtures, using glassy membranes.

Using data for a study of sorption and diffusion in PVA membranes at 333 K *(Heintz et al, 1991)*, for a feed concentration of 0.1 mass fraction water and assuming a membrane phase density of 1000 kg/m^3:-

$C_{o(m1)} \approx C_{w(m1)} \approx 70$ kg/m^3

$D_{mw} = 4.2 \times 10^{-13}$ m^2/s

$D_{mo} = 2.0 \times 10^{-14}$ m^2/s

Both D_{mw} and D_{mo} are highly concentration dependent, however for illustrative purposes it will be assumed that they remain constant across the membrane. It is also assumed that bulk flow has a negligible effect on J_w and that permeate pressure is low, hence for a membrane thickness of 0.5 μm:-

$$J_w = -D_{mw}\frac{dC_{wm}}{dx} = 5.88 \times 10^{-5} \text{ kg/m}^2\text{s}$$

If it is assumed that $J_w >> J_o$:-

$$u \approx \frac{J_w}{\rho_w} \approx 6.50 \times 10^{-8} \text{ m/s}$$

Now, J_o can be calculated using *eq. (2.53)* to give:-

$J_o = 5.67 \times 10^{-6}$ kg/m^{2}s

Eq. (2.47) predicts:-

$J_o = 2.80 \times 10^{-6}$ kg/m^{2}s

Although a number of simplifying assumptions have been made, it can be seen that convective flow may significantly affect solvent flux, in this case increasing J_o by about 100%, leading to reduced selectivity. It should be noted that this effect may be even more significant at higher temperatures as u increases significantly with temperature.

2.3.3.2 Discussion

It can be concluded that convective flow is important for a component that displays high S^a, but low D_{mi}. For this reason, it is likely to influence the transport of the non-preferentially transported component (solvent), when S^a is high, or the preferentially transported component (solute), when S^a is high but selectivity low. It is unlikely to be of great importance in rubbery membranes, in which solvent (water) sorption is very low. It may, however, have a significant effect upon solvent (organic) transport in glassy membranes, where S^a_w is often high.

It should be highlighted that although the possible effect of convective flow is clearly demonstrated above, it remains uncertain if such a flow can exist within the restrictive matrix of a polymeric membrane. For example, a very large organic molecule may display a high solubility in the membrane, however its diffusive movement through the membrane may be severely restricted by its large physical size compared to the size of the "free volume channels" available for permeation. It is unclear whether or not these molecules could be convected freely through these same "channels". For this reason, the convective flow of a component may be considerably lower than one would expect in an unconstrained system and it is postulated that this could be accounted for by an efficiency factor, ε, where:-

$$J_i = -D_{mi}\frac{dC_{im}}{dx} + \varepsilon u C_{im} \qquad (2.56)$$

Where $0 \leq \varepsilon \leq 1$.

Unfortunately, it is not possible to test this theory using existing published experimental data. It is recommended that future studies be undertaken to investigate the validity of *eq. (2.56)*. If ε is found to be less than 1 and to vary greatly from system to system, then there is probably justification in adopting the existing approach of ignoring the convective flow term and essentially incorporating it with D_{mi}. If ε is always found to be equal to 1 or equal to a certain value for many different systems, then the convective flow term should surely be incorporated and used to *partially* explain the effect of varying feed component concentrations upon D_{mi}.

2.3.4 Other Membrane Mass Transfer Models

Pervaporation membrane mass transfer can also be successfully described in terms of the thermodynamics of irreversible processes, the driving force for permeation being the chemical potential gradient *(Karlsson and Tragardh, 1993)*. The Maxwell Stefan model, in which all driving forces acting on a component moving through another medium are considered to be balanced by friction with that medium, has also, though less commonly, been used *(Bitter, 1991)*. The resulting transport equations are all of similar form and it does not generally appear to be advantageous to use one approach over the other two. For this reason this study is confined to the Ficks first law approach, which is the most widely used.

2.3.5 Membrane Diffusion Coefficient

D_{mi} is a function of membrane structure and physical properties, the permeating species and process conditions. Although theoretical transport equations have been derived from the free volume theory, it has been suggested *(Rautenbach, Albrecht, 1985)* that the equations are complicated and the parameters required for their use very difficult to measure. A phenomenological approach is generally used to estimate D_{mi} and appears to be of greater practical value.

2.3.5.1 Molecular Size Considerations

As one would expect from free volume considerations, D_{mi} is a strong function of the permeating species molecular size. For both glassy and rubbery membranes, several authors have reported that D_{mi} decreases with increasing molecular size. An exponential dependence of D_{mi} with molecular volume *(Favre et al, 1994)* or molecular mass *(Dotremont et al, 1995)*, *(Watson and Payne, 1990)* has been observed, D_{mi} initially falling sharply as molecular size increases and leveling off at higher molecular size. Molecular orientation can also affect D_{mi}. For isomeric butanols it has been reported *(Favre et. al., 1994)* that D_{mi} for the more elongated molecule, 1-butanol, is slightly higher than for those with a larger cross section, 2-butanol and 2-methyl-2-propanol. Trichloroethylene was found to have a much higher D_{mi} than other similar sized chlorinated hydrocarbons *(Dotremont et al, 1995)*. This was attributed to the double bond, causing trichloroethylene to display a plane geometry.

D_{mi} decreases much more rapidly with increasing molecular size in glassy membranes than in rubbery membranes *(Bell et al, 1988)*. Glassy membranes tend to act almost as molecular sieves, severely inhibiting transport of large molecules through the small gaps between rigid polymer segments. Large molecules can pass much more easily through the flexible rubbery membrane structure. This explains why, from a binary water-organic mixture, glassy membranes preferentially permeate small water molecules, even if it is the least selectively sorbed component, whereas rubbery membranes preferentially permeate the highly sorbed large organic molecules.

2.3.5.2 Chemical Interaction Considerations

D_{mi} is also strongly influenced by the chemical nature of the permeating species. For diffusion through silicone rubber membranes, it has been shown *(Watson and Payne, 1990)*, *(Watson, Zhang and Payne, 1992)* that certain molecules of similar size and similar empirical composition can display widely different D_{mi}. For example, ethanol displays a D_{mi} seven times greater than that of ethylene glycol. These differences are attributed to varying Van der Waals forces that exist between the various functional groups of the permeating molecules and the polymer. The reduction in D_{mi} in the series of alcohols

methanol to decanol is not dramatic (approximately a factor of 4), suggesting that Van der Waals forces are more important than size effects in controlling the diffusion process, for alcohols.

The relative importance of size and Van der Waals factors are very much functions of polymer and permeating species. For silica filled PDMS membranes it was shown *(Lapack, Tou, McGuffin and Enke, 1994)* that for alkanes, D_{mi} is a linear function of molar volume, whereas for alcohols D_{mi} is unaffected by molar volume. In the latter case it is thought that hydrogen bonding between the polar OH group and silica filler totally controls the diffusion process.

2.3.5.3 Effect of Concentration

D_{mi} can be a strong function of permeating species concentration. Several relationships have been proposed, by various authors, to describe this effect. The simplest predict a linear dependence of concentration upon D_{mi} *(Rautenbach and Albrecht, 1985)*:-

$$D_{mi} = D_{mi0}C_{im} \qquad (2.57)$$

or:-

$$D_{mi} = (1 + \gamma_i D_{mi0}C_{im}) \qquad (2.58)$$

Where: D_{mi0} = Diffusion Coefficient at Infinite Dilution in Membrane, m^2/s

γ_i = Placticisation Coefficient, m^3/kg

By far the most popular relationship used for both glassy and rubbery membranes predicts an exponential dependence *(Nguyen, 1987)*, *(Slater et al, 1990)*, *(Mulder and Smolders, 1991)*, *(Karlsson and Tragardh, 1993)*:-

$$D_{mi} = D_{mi0}\exp(\gamma_i C_{im}) \qquad (2.59)$$

or:-

$$D_{mi} = D_{mi0}\exp(\gamma_i \phi_{im}) \qquad (2.60)$$

Where: ϕ = Volume Fraction in Membrane γ_i is dimensionless in the latter case

It should be noted that when *eq. (2.60)* is used, it is often combined with a version of Ficks law expressed in terms of a volume fraction gradient. Neglecting the convective term this may be expressed as:-

$$J_{vi} = -D_{mi} \frac{d\phi_{im}}{dx} \qquad (2.61)$$

Where: J_v = Volumetric Flux, m/s

Following similar arguments to those expressed earlier to question the applicability of *eq. (2.45)*, it can be seen that a combination of *eqs. (2.60) & (2.61)* is not always equivalent to a combination of *eqs. (2.47) & (2.59)*. The two will only be equivalent if ρ_m is considered constant. If it is not, the driving force $\frac{d\phi_{im}}{dx}$ will not vary linearly with $\frac{dC_{im}}{dx}$. From a theoretical point of view it would appear that *eq. (2.61)* is not a true expression of Ficks law and therefore it would be better to use *eqs. (2.47) & (2.59)*. It is recognised, however, that as *eq. (2.60)* is proposed purely upon a phenomenological approach, *eqs. (2.60) & (2.61)* may fit experimental data well, even though the theoretical justification of *eq. (2.61)* can be questioned. Similarly, this phenomenological approach may provide some justification for ignoring the convective flow term in *eq. (2.44)*. It is suggested, however, that a more accurate diffusion model may well be developed if the correct application of as much theory as possible is used.

2.3.6 Determination of Membrane Diffusion Coefficient

Due to the phenomenological approach, no theory exists to enable accurate prediction of either D_{mi0} or γ_i. It is necessary to determine both of these parameters experimentally.

Two methods are commonly used to determine these parameters. Combining *eqs. (2.47) & (2.59)* yields:-

$$J_i = -D_{mi0} \exp(\gamma_i C_{im}) \frac{dC_{im}}{dx} \qquad (2.62)$$

Integrating across the thickness of the membrane gives:-

$$\int_0^{\delta_m} J_i \, dx = -D_{mi0} \int_{C_{i(m1)}}^{C_{i(m2)}} \exp(\gamma_i C_{im}) \, dC_{im} \qquad (2.63)$$

$$J_i = \frac{D_{mi0}}{\delta_m \gamma_i} \left(\exp(\gamma_i C_{i(m1)}) - \exp(\gamma_i C_{i(m2)})\right) \qquad (2.64)$$

If a very low downstream pressure is maintained, $C_{i(m2)}$ can be assumed to be close to zero and *eq. (2.64)* simplifies to become:-

$$J_i = \frac{D_{mi0}}{\delta_m \gamma_i} (exp(\gamma_i C_{i(m1)}) - 1) \qquad (2.65)$$

Sorption isotherms can be determined, as described in the previous section, to give $C_{i(m1)}$ at varying feed concentration, $C_{i(b)}$. D_{mi0} and γ_i can then be determined by fitting *eq. (2.65)* and the sorption data, to data plotting the variation of J_i with $C_{i(b)}$.

This approach has been used for permeation of single components through PDMS membranes from the vapour phase *(Favre et al, 1994)*, in which the feed side concentration (activity) is controlled, at constant temperature, by adjusting the vapour pressure.

2.3.6.1 From Kinetics of Sorption

An alternative approach is to determine D_{mi}, at various feed activities, by measuring the kinetics of sorption, using a gravimetric technique to monitor the mass increase of a membrane sample with time *(Lamer, Rohart, Voilley and Baussart, 1994)*. In this case solutions of Ficks Law were proposed by *Crank (Crank, 1975)* to predict D_{mi}, for various systems, from this kinetic data. Two separate studies, using this approach by measuring the kinetics of sorption from the vapour phase were found to yield curious results *(Blume et al, 1991)*, *(Dotremont et al, 1995)*. In both cases it was reported that D_{mi} appeared to decrease with increasing feed activity for good, non clustering solvents (i.e. chlorinated hydrocarbons) in polydimethylsiloxane, in contradiction to normal theory.

It appears that there may be a problem with this approach. D_{mi} at varying feed activities were calculated using Crank's solutions for a plane sheet, in which the plane sheet is considered to be the membrane sample, surrounded by the sorbing gas at constant activity.

The general diffusion equation takes the from:-

$$\frac{\partial C_{im}}{\partial t} = \frac{\partial}{\partial x}\left(D_{mi}\frac{\partial C_{im}}{\partial x}\right) + \frac{\partial}{\partial y}\left(D_{mi}\frac{\partial C_{im}}{\partial y}\right) + \frac{\partial}{\partial z}\left(D_{mi}\frac{\partial C_{im}}{\partial z}\right) \qquad (2.66)$$

Where: x, y, z denote three dimensional coordinates

In a plane sheet the material is so thin that effectively all diffusing species enter through the plane face and not through the edges. This is obviously the case for a thin membrane and thus *eq. (2.66)* reduces to:-

$$\frac{\partial C_{im}}{\partial t} = \frac{\partial}{\partial x}\left(D_{mi}\frac{\partial C_{im}}{\partial x}\right) \qquad (2.67)$$

If D_{mi} can be considered constant, *eq. (2.67)* reduces to:-

$$\frac{\partial C_{im}}{\partial t} = D_{mi}\left(\frac{\partial^2 C_{im}}{\partial x^2}\right) \qquad (2.68)$$

Eq. (2.68) can be solved for a variety of boundary conditions, using either the separation of variables technique or the Laplace transform.

It is worth noting that no convective flow terms are included in *eqs. (2.66)-(2.68)* and although it is thought that these terms are unlikely to be significant for the experiments described above, care should be taken when applying the equations to other systems.

All the solutions quoted in chapter 4 of Crank's book, for plane sheets, assume constant D_{mi}. It would appear likely that if these solutions are used in a situation where D_{mi} clearly varies significantly with C_{im}, large errors may occur. Of course, for low feed concentration (activity) D_{mi} is effectively constant and equal to D_{mi0}. *Lamer et. al.* maintained low feed concentrations (less than 2 kg/m^3) of relatively high boiling aroma compounds, in aqueous solution. Organic component activities were therefore low and hence $D_{mi} = D_{mi0}$ is a valid assumption. Of course it is necessary, when using aqueous solutions, to maintain an organic concentration sufficiently high so that water sorption is negligible compared to organic sorption.

In the studies of *Blume et. al.* and *Dotremont et. al.*, high gas phase organic activities of up to at least 0.7 were used where obviously $D_{mi} = D_{mi0}$ does not apply. Crank's solution, requiring the assumption that D_{mi} is constant, has actually been used to investigate the effect of changing C_{im} on D_{mi}. It appears that the anomalous results obtained in these studies could be explained by the incorrect use of Crank's solution. The individual D_{mi} values reported are actually complicated integral average values over large C_{im} ranges. It is worth noting that although Crank discusses possibilities, in chapter 7, for determining

concentration dependent D_{mi}, all solutions are based upon infinite or semi infinite media. A membrane sample obviously falls in to the category of a finite medium.

2.3.7 Plasticisation Constant

γ_i is thought of as the coefficient that reflects the increase in free volume of the polymer due to solvent sorption *(Favre et al, 1994)*. Sorbed component(s) can effectively swell the polymer leading to a more open membrane structure, thereby reducing resistance to diffusion. Values of γ_i up to 150, using *eq. (2.60)*, have been reported. For low swelling membranes, or where feed concentrations of the preferentially sorbed component are very low (as is often the case in the removal of pollutants from aqueous streams), D_{mi} can be considered to be constant and equal to D_{mi0}.

It was found *(Favre et al, 1994)* that chloroform, an excellent solvent in PDMS, displays a low but positive γ_i, whereas alcohols and water, poor solvents in PDMS, display negative γ_is. Methanol and water displayed particularly low values of -169 and -2075 respectively, again using *eq. (2.60)*. This behaviour was explained by the polar water and alcohol molecules clustering within the membrane, creating large aggregates that are slow to diffuse, the degree of clustering increasing with increasing local concentration. It is interesting to note that γ_i for chloroform was found to be so low, 0.21, that D_{mi} remained quasi constant over a large concentration range.

For glassy membranes it appears quite possible that the increased clustering effect at increasing water concentration could counteract the effect of swelling and lead to a maximum in D_{mi}. This theory appears to be supported by a study of water and ethanol diffusion in PVA membranes *(Heintz et al, 1991)* where maximum D_{mi} values at particular solvent concentrations were found.

2.3.8 Effect of Temperature and Typical Values

The diffusion process is endothermic and strongly temperature dependent. An Arrhenius expression can be used to describe the variation of D_{mi0} with temperature *(Karlsson and Tragardh, 1993)*:-

$$D_{mi0} = D_{mi0}^{*} exp(-E_d/RT) \qquad (2.69)$$

Where: D_{mi0}^{*} = Pre Exponential Factor, m^2/s E_a = Activation Energy, J/mol

R = Gas Constant, J/molK T = Temperature, K

An increase in temperature results in increased flexibility of the polymer membrane structure.

A small temperature gradient usually exists across the membrane, due to the evaporation of the permeate, however, this is usually considered to be negligible and the diffusion process is modeled as being isothermal.

In a study of ethanol and chloroform diffusion, from aqueous solution, in eight commonly used polymers, PDMS was found to display by far the highest D_{mi} values *(Young, Bourgeois and Belfort, 1989)*. At low feed concentrations D_{mi} (D_{mi0}) values for organic species are typically in the order of 10^{-11} to 10^{-10} m^2/s, at close to ambient temperatures, rising by up to two orders of magnitude as temperature is elevated to 80°C *(Watson and Payne, 1990)*, *(Lamer et al, 1994)*, *(Favre et al, 1994)*.

Being a small molecule, water displays a very high D_{mi0} in PDMS of 1.3×10^{8} m^2/s at 40°C *(Favre et al, 1994)*. γ_{water} is, however, a very large negative value of -2075, due to the clustering effect. This fact helps to explain, in combination with low water sorption, why rubbery membranes preferentially permeate organics from dilute aqueous solutions. Feed water concentrations approach 100% and hence clustering is at its highest.

2.3.9 Physical State of Permeating Components

There is some debate as to the physical state of the permeating components inside of the membrane. When using a phenomenological approach to determine component diffusivities, the state of these permeating components may only be of academic interest. If a more theoretical approach is to be developed, however, it may be important to consider this factor. It is generally assumed that components diffuse through the membrane in the liquid phase and evaporate at the downstream interface of the membrane. In a study of ethanol and water permeation through hydrophobic membranes containing

PDMS, however, it was suggested that both components permeated through the membrane in the gaseous phase *(Takegami et al, 1992)*. This conclusion was reached by comparing experimental permeation data with the free volume theory of both gases and liquids. It was found that the theory for gases could be used to predict trends in the data, whereas that for liquids could not.

2.3.10 Pore Flow Model

It is possible to carry out the process of pervaporation through porous membranes. One would expect to achieve high fluxes but poor selectivity and indeed for any separation selectivity to be realised the pores would have to be very small. The pore flow transport model was developed for permeation through such porous membranes *(Okada and Matsuura, 1991)*. An interesting feature of this model is that both liquid and gaseous phases, separated by a clear boundary, exist within the membrane. The resultant transport equation for a single permeating component is as follows:-

$$J_{mol} = \frac{A}{\delta_m}(P_1 - P_*) + \frac{B}{\delta_m}(P_*^2 - P_2^2) \qquad (2.70)$$

Where: J_{mol} = Molar Flux, mol/m^{2}s P = Pressure, Pa

A = Liquid Transport Parameter, mol/sm^{2}Pa

B = Vapour Transport Parameter, mol/sm^{2}Pa^2

1 denotes upstream * denotes phase boundary

2 denotes downstream

P_* is equal to the saturated vapour pressure of the permeating component. Equations describing the simultaneous transport of two permeating components were also developed from *eq. (2.70)*.

The pore flow model was successfully used, in the same study, to describe the separation of ethyl alcohol/heptane mixtures through cellulose membranes. It was estimated that the pore radii of these membranes were more than 15×10^{-10} m.

The same authors went on to use this model to describe transport through pervaporation membranes that are considered to be non-porous, i.e. PDMS *(Zhang, Fouda and Matsuura, 1992)*, Polyamide *(Tyagi, Fouda and Matsuura, 1995)* and Poly-acrylic-acid *(Okada and*

Matsuura, 1992). There would appear to be a fundamental problem with this approach. As P_2 approaches P_*, the first term in *eq. (2.70)* dominates the transport process. Also, taking typical values of all of the parameters in *eq. (2.70)*, from the examples described in the three above mentioned studies, it appears that even when P_2 is very low, the first term is significant. This suggests that as P_1 is increased J increases significantly, which is in contradiction with the solution diffusion theory and the experimental evidence that supports it. As feed side activities are relatively unaffected by pressure, over a moderate pressure range, the solution diffusion model predicts that increasing feed side pressure has little effect upon sorption. Increasing pressure also has no direct effect upon the diffusion process. It is well known that, practically, feed side pressure has very little effect upon pervaporation performance using non porous membranes *(Neel, 1991)*. From the above three studies it appears that *eq. (2.70)* can describe the affect of changing P_2 upon J reasonably well. No attempt was made, however, to fit the model to experimental data showing the variation of J with P_1 (indeed if there is any variation at all), for non porous membranes and in this case the model would surely have failed.

2.4 Coupling

The previously described relationships for diffusive transport through a membrane are perfectly valid for binary mixtures (i.e. membrane plus one component). They can also be applied to each individual component in a multi-component system, provided that component transport is unaffected by the simultaneous transport of other components. In many situations component interactions are strong and may affect both the solubility and diffusivity of each individual component. This phenomena is known as coupling and in many cases can strongly influence pervaporation performance.

There are generally considered to be two separate elements of coupling. Each component can alter the free volume available in the membrane and may interact with other components on a molecular level *(Brun, Larchet, Melet and Bulvestre, 1985)*. Each element may affect both solubility and/or diffusivity.

2.4.1 Sorption Coupling

Sorption coupling can usually be accounted for by Flory Huggins thermodynamics. Recalling *eqs. (2.36) & (2.37)* for a ternary system:-

$$\ln a_1 = \ln \phi_1 + (1 - \phi_1) - \phi_2 \frac{V_1}{V_2} - \phi_3 \frac{V_1}{V_3} + (\chi_{12}\phi_2 + \chi_{13}\phi_3)(\phi_2 + \phi_3) - \chi_{23}\frac{V_1}{V_2}\phi_2\phi_3 \qquad (2.36)$$

$$\ln a_2 = \ln \phi_2 + (1 - \phi_2) - \phi_1 \frac{V_2}{V_1} - \phi_3 \frac{V_2}{V_3} + (\chi_{12}\phi_1\frac{V_2}{V_1} + \chi_{23}\phi_3)(\phi_1 + \phi_3) - \chi_{13}\frac{V_2}{V_1}\phi_1\phi_3 \qquad (2.37)$$

It can be seen that the interaction parameter χ_{12} can account for coupling between the sorption of components *1 & 2*.

In some cases sorption behaviour can be profoundly altered by the presence of a second component. In polysulphone membranes no sorption of pure water can be detected, however in the presence of ethanol, water is both sorbed and transported preferentially *(Mulder, Franken and Smolders, 1985)*. For aqueous pyridine solutions, pyridine transport is facilitated at low pyridine concentrations and water transport facilitated at high pyridine concentrations, through PDMS membranes *(Drioli et al, 1993)*. This phenomenon was explained by a change in membrane morphology caused by competitive sorption of the two components. In Nitrile Butadiene Rubber membranes, sorption of water from aqueous benzene solutions was found to fall dramatically as benzene activities exceeded 0.7 *(Brun et al, 1985)*. In this case it was thought that the membrane was so swollen by hydrophobic benzene that water was almost totally excluded. In a study of zeolite filled PDMS membranes it was found that the sorption of an organic, from dilute aqueous solution, was always reduced by the presence of a second organic *(Goethaert et al, 1993)*. This was attributed to competitive sorption on the zeolites, each component excluding the other from a number of active sites. In unfilled PDMS much less coupling was observed.

2.4.2 Diffusion Coupling

Diffusion coupling occurs in many cases due to membrane swelling, caused by the sorption of each component. This tends to increase free volume and hence, the diffusivity of a component in a mixture is generally higher than the diffusivity of the pure component.

The diffusion coefficient relationships for binary systems, describing the effect of concentration upon diffusion coefficient, D_{mi}, can be modified in a number of ways *(Karlsson and Tragardh, 1993)*, *(Rautenbach and Albrecht, 1985)*, *(Sferrazza, Escobosa and Gooding, 1988)*. The most generally applicable relationship is a modification of the most popular binary system relationship, described by *eq. (2.59)*:-

$$D_{mi} = D_{mi0} \exp(\gamma_i C_{im}) \qquad (2.59)$$

For a ternary system an extra term is required in the exponential argument to describe the effect of component *j* on the diffusivity of *i* *(Brun et al, 1985)*, *(Mulder and Smolders, 1984)*:-

$$D_{mi} = D_{mi0} \exp(l_i C_{im} + m_{ij} C_{jm}) \qquad (2.71)$$

Where: l, m = interaction parameters

It should be noted that l_i is not always equal to γ_i and that there is no link between l_i, m_{ij} and χ_{ii}, from *eqs. (2.36) & (2.37)*.

In a system of more than two permeating components it seems reasonable, although not reported in literature, to add further interaction parameters and component concentration products into the exponential argument, for each component.

An alternative approach has been described for the transport of ethanol-water mixtures through silicone rubber, the coupling effect being considered to be due to dimerisation of ethanol and water *(Radovanovic, Thiel and Hwang, 1990)*. It is assumed that water clusters break down in the presence of ethanol to form ethanol-water dimers. A fraction of each species is transported both as monomer and dimer. The resulting transport equations are as follows:-

$$J_i = -D_{mi}\frac{dC_{im}}{dx} - D_{mij}\frac{dC_{ijm}}{dx} \qquad (2.72)$$

$$J_j = -D_{mj}\frac{dC_{jm}}{dx} - D_{mij}\frac{dC_{ijm}}{dx} \qquad (2.73)$$

Where: *ij* denotes dimer

Similar relationships, having the same general form as *eqs. (2.72)* and *(2.73)*, have been proposed using chemical potential gradients *(Mulder and Smolders, 1991)* or partial

pressure gradients *(Kedem, 1989)* as the driving force for permeation, instead of concentration. A more complicated approach, based upon the Maxwell Stefan theory has also been used to describe the transport of various aqueous organic mixtures through hydrophilic PVA *(Heintz and Stephan, 1994)*. In this case the fast moving component is assumed to be slowed by frictional interaction with the slow moving component, whereas the slow moving component is accelerated by the same effect.

2.4.2.1 Effect of Process Conditions

An interesting point to note is that it has been demonstrated that when permeate side pressure is high, vapour phase mass transport becomes important and coupling effects may actually occur in the vapour phase *(Ji et al, 1994)*. This may happen in a situation where the diffusive transport of vapour becomes significant with respect to convective transport. Under low permeate pressure, the diffusive component of vapour transport is negligible as all vapour is rapidly convected away from the membrane surface. When diffusion is significant, the resultant vapour phase concentration gradients can be affected by the flow of the other component(s). It could be argued that this phenomenon is not an example of true diffusion coupling, but is just a result of the correct application of Ficks First Law. Individual gas phase component diffusivities are unaffected by the presence of other components.

It has been noted that temperature can have an important effect upon coupling *(Rautenbach and Albrecht, 1985)*. For a series of experiments using Polyethylene membranes to separate benzene and cyclohexane, it was found that coupling of fluxes was negligible at low temperatures, but significant at high temperatures. This was attributed to an increase in sorption as temperature increased. It was suggested that this effect would be less pronounced for more highly cross-linked membranes, in which sorption would generally be lower.

2.4.2.2 Additional Recorded Diffusion Coupling Phenomena

Several studies have reported coupling effects for particular systems. Some of the more interesting phenomena are discussed below.

For the dehydration of organic solvents using hydrophilic membranes, coupling effects are often very important. This is partly due to the high swelling of these membranes, in the presence of water, especially when feed water concentrations are relatively high. Solvent water interactions can also be important, especially when the solvent contains a polar functional group, such as an alcohol. For the dehydration of water/octanol mixtures using cellulose acetate membranes, octanol flux was found to increase to a maximum and then fall again as feed water concentration increased *(Gref et al, 1992)*. The water concentration at which this maximum occurred, as well as its magnitude, were found to vary with stirrer speed. It was postulated that the maximum is a function of both concentration polarisation and possibly temperature polarisation. If temperature polarisation is important, it is likely to increase with decreasing stirrer speed and could partially explain the observed increasing maximum octanol flux with decreasing stirrer speed. This is because, most unusually, the octanol flux was actually found to fall with increasing feed temperature. It should be noted that this type of phenomenon significantly complicates the determination of boundary layer resistance. For the dehydration of pyridine solutions, using polyvinylalcohol (PVA) and ion exchange membranes, coupling was found to accelerate pyridine and slow water permeation, especially at low pyridine feed concentrations *(Drioli et al, 1993)*. It was suggested that as well as an increase in pyridine sorption, due to water swelling of the membrane, the orientation of the pyridine molecules within the membrane could slow the permeation of water molecules. A proportion of the water molecules may have to permeate past the hydrophobic groups of the pyridine ring. For the dehydration of alcohols using PVA membranes it was found that water flux, at a given feed water concentration, declined as the number of different alcohols in the feed increased *(Shaban, 1995)*.

For the removal of organics from aqueous streams, using hydrophobic membranes, coupling effects are often much less important. This can be attributed to the low degree of swelling in cross-linked rubbery membranes, especially as feed organic concentrations tend to be low. Several studies have reported almost negligible coupling effects for good solvents, such as chlorinated organics, in rubbery membranes. Negligible coupling was observed for aqueous mixtures of toluene and/or various chlorinated hydrocarbons, for organic component concentrations of up to 300ppm, in PDMS, PEBA and Polyurethane membranes *(Ji et al, 1994)*. Similar conclusions were drawn from a study using silicone

tubing for aqueous solutions of acetone, ethanol and halogenated hydrocarbons for feed concentrations up to 600 ppm *(Nguyen and Nobe, 1987)*.

A few examples of coupling phenomena occurring in rubbery membranes have been reported. It was shown that in Nitryl Butadiene Rubber and Styrene Butadiene Rubber, water flux increased slightly with increasing chloroform feed concentrations, due to chloroform swelling *(Brun et al, 1985)*. In this study feed concentrations of up to 1700ppm chloroform were used. For permeation of ethanol/water mixtures through PDMS membranes, enhanced transport occurs for both components in the presence of the other *(Slater et al, 1990)*. This was attributed to the weak polar groups of the preferentially dissolved ethanol being directed into the microvoids of the swollen polymer, enhancing the transport of both components.

2.5 Resistances in Series Model

Recalling the equation describing transport in both the liquid boundary layer and membrane, according to Ficks first law:-

$$J_o = -D_o \frac{dC_o}{dx} + uC_o \qquad (2.1)$$

If it can be assumed that the convective flow term is negligible in both the boundary layer and membrane, that D_{lo} and D_{mo} are constant and that permeate pressure is low (i.e. $C_{o(m2)} \approx 0$), then when *eq. (2.1)* is applied to both the boundary layer and membrane the resultant equations are:-

$$J_o = \frac{D_{lo}}{\delta_l} (C_{o(b)} - C_{o(mb)}) \qquad (2.10)$$

$$J_o = \frac{D_{mo}}{\delta_m} C_{o(m1)} \qquad (2.74)$$

If sorption can be described by Henry's law:-

$$S^c_o = \frac{C_{o(m1)}}{C_{o(mb)}} \qquad (2.43)$$

Multiplying both sides of *eq. (2.10)* by S^c_o and combining with *eq. (2.74)* yields:-

$$\frac{J_o \delta_m}{S^c{}_o D_{mo}} + \frac{J_o \delta_l}{D_{lo}} = C_{o(b)} \qquad (2.75)$$

An overall mass transfer coefficient, $k_{(ov)o}$, may now be defined, where:-

$$J_o = k_{(ov)o} C_{o(b)} \qquad (2.76)$$

Where:-

$$\frac{1}{k_{(ov)o}} = \frac{1}{k_{lo}} + \frac{1}{k^c{}_{mo}} \qquad (2.77)$$

$$k_{lo} = \frac{D_{lo}}{\delta_l} \qquad (2.78)$$

$$k^c{}_{mo} = \frac{S^c{}_o D_{mo}}{\delta_m} \qquad (2.79)$$

$S^c{}_o D_{mo}$ is known as the membrane permeability coefficient

$k_{(ov)o}$ can easily be determined by direct measurement from experimental pervaporation data.

If k_{lo} is kept constant (i.e. constant stirrer speed or pumping rate) whilst δ_m is varied, it can be seen from *eqs. (2.77) - (2.79)* that a plot of $\frac{1}{k_{(ov)o}}$ against δ_m will yield a straight line of gradient $\frac{1}{S^c{}_o D_{mo}}$ and y axis intercept of $\frac{1}{k_{lo}}$. A number of authors have used this approach to determine $S^c{}_o D_{mo}$ and/or k_{lo} *(Nijhuis et al, 1991)*, *(Gref et al, 1992)*, *(Raghunath and Hwang, 1992)*, *(Ji et al, 1994)*. Of course this approach is only valid for homogeneous membranes in which D_{mo} and $S^c{}_o$ can be assumed to be constant and independent of δ_m. If composite membranes are used, it is often possible to include the support layer as an additional resistance in series, in which case *eq. (2.77)* becomes:-

$$\frac{1}{k_{(ov)o}} = \frac{1}{k_{lo}} + \frac{1}{k^c{}_{mo}} + \frac{1}{k_{so}} \qquad (2.80)$$

Where:-

k_{so} = Mass Transfer Coefficient of Support, m/s

Eq. (2.80) is only valid if the support layer does not actually affect the chemical and/or physical structure of the dense polymeric membrane layer above it.

An alternative approach to determine $S^c{}_oD_{mo}$ and/or k_{lo}, is to maintain a constant δ_m, but to vary k_{lo}. Recalling the Sherwood correlation for stirred cells:-

$$Sh = b\, Re^c\, Sc^d \qquad (2.12)$$

Expanding *eq. (2.12)* yields:-

$$k_{lo} = b\, \omega^c\, d_c^{c-1}\, \nu^{d-c}\, D_{lo}^{1-d} \qquad (2.17)$$

Hence:-

$$k_{lo} \propto \omega^c \qquad (2.81)$$

Thus, considering eqs. (2.77) and (2.81) it can be seen that a plot of $\frac{1}{k_{(ov)o}}$ against $\frac{1}{\omega^c}$ will yield a straight line with y axis intercept of $\frac{1}{k^c{}_{mo}}$. $\frac{1}{k_{lo}}$ at any ω can be determined by subtracting $\frac{1}{k^c{}_{mo}}$ from $\frac{1}{k_{(ov)o}}$. This approach has also been used *(Burslem et al, 1992)*, *(Field and Burslem, 1992)* and it has the advantage that only a single membrane is required. Of course a similar approach could be adopted for cross flow systems, where $\frac{1}{k_{(ov)o}}$ would be plotted against $\frac{1}{v^c}$.

It should be emphasised that the resistances in series model is only applicable to "ideal" pervaporation systems. Deviations from Henry's law or variation in D_{mo} could lead to significant error. If permeate pressure is not very low, not only will the model be complicated by an additional $C_{o(m2)}$ term, there may also exist an additional resistance to transport in the vapour phase.

Typical concentration profiles obtained for the "ideal" and "non-ideal" case are displayed in fig. (2.2) & (2.3) respectively.

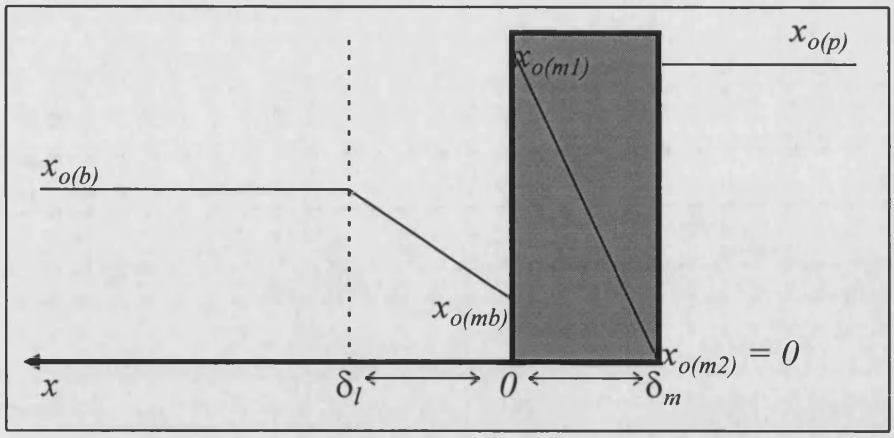

Fig. 2.2 - "Ideal" Pervaporation Concentration Profiles

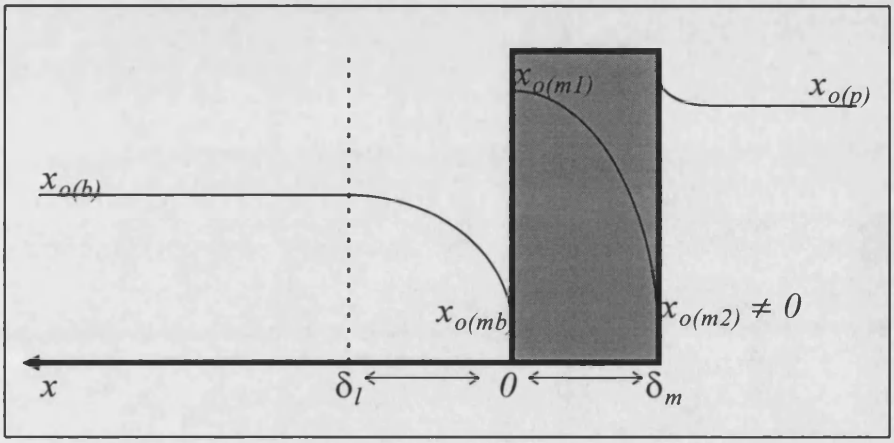

Fig. 2.3 - "Non-ideal" Pervaporation Concentration Profiles

2.6 Closing Remarks

In general, the removal of trace organic contaminants from aqueous streams, using organophilic membranes, can be considered as a case of "ideal" pervaporation, producing concentration profiles similar to those displayed in fig. 2.2. Convective flow terms are usually negligible, owing to the low organic component feed concentration and low water sorption within the membrane. Membrane swelling and flux coupling are also generally very low. Often organic component sorption may be successfully described by Henry's law and membrane diffusion coefficient treated as being quasi constant. This greatly simplifies the mathematical treatment of mass transport and allows for the use of the resistances in series model.

The same conclusions can certainly not be drawn for other areas of pervaporation, particularly when feed concentrations are high and especially for the dehydration of organic solvents using hydrophilic membranes. In these cases, significant departure from ideality may occur at every stage during mass transport.

The models presented within this chapter should provide the basis for describing transport even when such deviations occur.

Chapter 3

Materials and Methods

Scope of Chapter 3

Within this chapter a complete description is given of all experimental and analytical procedures undertaken, in order to both manufacture and test functionalised PDMS membranes. Equations are developed to enable the accurate description of performance in a batch pervaporation rig, in which feed concentration is continuously changing.

3.1 Membrane Manufacture

Essentially two different methodologies (methods 1 & 2 below) were used to enable the incorporation of organofunctional groups into the PDMS membrane structure. In one case a third methodology was employed, although this is basically a simple variation upon method 2.

3.1.1 Method 1

A methodology for synthesising a wide range of organofunctional polysiloxane membranes has been extensively developed at the University of Bath *(Brisdon and Watts, 1985)*, *(Abed-Ali, Brisdon and England, 1989)*. Starting from readily available commercial materials, linear, organofunctional siloxanes are prepared by the platinum catalysed reaction of a substituted 1-alkene with poly-hydrogenmethylsiloxane (PHMS). The reaction involves the addition of an *Si-H* group across a *C=C* double bond:-

$$Me_3SiO(MeSi[H]O)_{40}SiMe_3 + xCH_2{=}CH\text{-}R \rightarrow$$
$$Me_3SiO(MeSi[H]O)_{40-x}(MeSi\{[CH_2]_2R\}O)_xSiMe_3$$

A variety of different functional groups (*R*) may be incorporated into the linear polymer backbone in this manner. *R* generally consists of additional CH_2 unit(s) and an end group representative of one of various chemical families, e.g. ester, ether, amino, benzyl. The chemical structure of the reaction product is more clearly displayed in fig. 3.1.

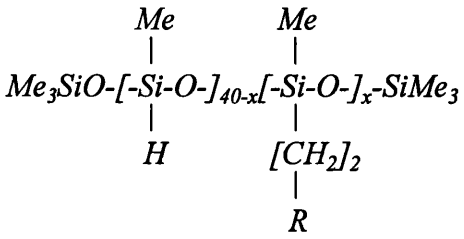

Fig. 3.1 - Chemical Structure of Functionalised Siloxane

The reaction is sensitive to moisture, which may both poison the catalyst and react with the reactive hydride of the PHMS to produce silanol groups which, upon heating, result in cross linking of the polymer chains. All reagents must, therefore, be dried for at least 24 hours with molecular sieves prior to use.

In order to achieve reasonably high functional group loadings within the finished membrane, it is necessary to substitute a large proportion of the hydride with the functional organic chain. It is most important, however, to leave a number of hydrides intact as they are required to cross-link the functionalised siloxane, which is necessary for membrane formation. It was decided in all cases to attempt to substitute 30 hydrides, by control of the stoichiometry of the reaction, leaving 10 available for cross linking purposes.

A measured quantity of PHMS was charged to a reaction flask and a 30 molar excess of substituted 1-alkene added to it. Dry toluene was used as a solvent for the reaction and an approximate toluene to reactant material ratio of 4:1 by volume was added. A molar ratio of approximately 10^{-3} mole Pt / mole *Si-H* is required in order to effectively catalyse the reaction. A catalyst solution was prepared by dissolving 10 mg of hexachloroplatinic acid hydrate, $H_2PtCl_6.xH_2O$, per 1 ml of 2-propanol. Approximately 1 ml of the catalyst solution was charged to the reaction flask per 20 g of PHMS. The flask was fitted with a reflux condenser, placed in an oil bath and heated to a temperature of not more than 100°C, under reflux, utilising a stirrer hot plate. At temperatures in excess of 100°C there is a significant risk that hydrides of neighbouring PHMS molecules may react leading to the liberation of hydrogen gas and PHMS cross-linking. Agitation of the reactants was achieved by means of a magnetic stirrer bar. In order to exclude atmospheric moisture and oxygen, the reaction was carried out under a blanket of dried nitrogen gas.

The progress of the reaction was monitored, in a qualitative manner, using infra red spectrometry. The *Si-H* bond produces a characteristic peak at 2166 wavenumbers. The intensity of this peak decreases as hydride addition occurs, relative to the two peaks produced by the *Si-O* bond, which occur at 1011 and 1082 wavenumbers. Small samples were periodically withdrawn from the reaction flask, pressed between NaCl plates and analysed. The reaction was deemed to have reached completion when no further reduction in the intensity of the Si-H peak could be detected. Typically the end point was reached after a reaction time of between 24 and 120 hours, depending upon the nature of the substituted 1-alkene. After each 24 hour period, if the end point had not been reached, a few additional drops of catalyst solution were added.

When the reaction was complete, the bulk of the solvent was removed using a rotary evaporator. The final traces of volatiles were then removed under high vacuum.

The final product mass was measured and the reaction yield estimated by simple mass balance, assuming that the product consisted solely of functionalised siloxane and that any unreacted alkene was removed along with the toluene solvent. The chemical structure of each product was confirmed by hydrogen NMR spectral analysis, using deuterated chloroform (containing no TMS) as a solvent. A typical ^{1}H NMR trace, together with the associated analysis, is displayed in appendix 1. In most cases the reaction was found to be almost quantitative, with loadings never being below 27 functional chains per PHMS molecule, except for the acetate and diacetate functionalised material. In the later cases it was found that if the reaction was given enough time to reach total completion cross-linking of the polymer chains occurred, yielding a useless product. In order to overcome this problem the reaction was stopped prematurely.

A summary of syntheses and process conditions for all organofunctionalised siloxanes produced via method 1 is displayed in appendix 2.

The organofunctional siloxanes produced by this methodology are generally highly viscous liquids. All products were stored within a freezer in order to reduce the possibility of cross-linking or chemical change in composition. Monitoring was carried out by spectroscopic and NMR techniques and in no case was a change observed.

The formation of the functional, cross-linked membrane is achieved by reacting the remaining *Si-H* units of the linear functionalised siloxane, with appropriate quantities of long chained, silanol terminated, PDMS *(HO-[Si(Me$_2$)-O-]$_m$-H)* in the presence of tetraethoxysilane *(Si[OEt]$_4$)*. The cross-linking process is promoted by an undiluted, dibutyltin dilaurate catalyst *([CH$_3$(CH$_2$)$_{10}$CO$_2$]$_2$Sn[(CH$_2$)$_3$CH$_3$]$_2$)*. *Si[OEt]$_4$* is added to ensure that no residual *Si-H* moieties remain in the finished membrane. After pressing and curing at 80°C for a week, thin polymeric membrane films containing a known mole fraction of organofunctional groups are produced. A schematic representation of the resultant cross-linked membrane is displayed in fig. 3.2.

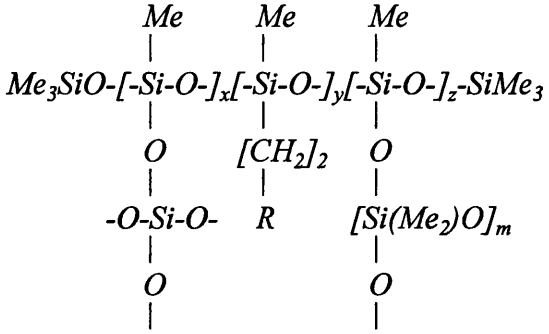

Fig. 3.2 - Cross Linked Organofunctional Siloxane Membrane

3.1.2 Method 2

It is not possible to introduce some functional groups (*R*) into the polysiloxane using the above reaction, particularly highly polar groups containing reactive *O-H* or *N-H* linkages, such as alcohols, acids or primary amines. These groups react with the Si-H group, as well as the double bond and hence addition reactions take place at both ends of the alkene molecule, leading to severe cross-linking. A second methodology for manufacturing a functionalised polysiloxane membrane has been achieved, which involves cross-linking the silanol terminated PDMS with either a trimethoxy- or triethoxy-silane containing the organofunctional group side chain, *([EtO]$_3$Si-(CH$_2$)$_n$-R)* or *([MeO]$_3$Si-(CH$_2$)$_n$-R)*. Many of these compounds are commercially available. Again the cross linking process is promoted by a dibutyltin dilaurate catalyst and the membrane is formed by pressing, after which it is cured. A schematic representation of the resultant cross-linked membrane is shown in fig. 3.3.

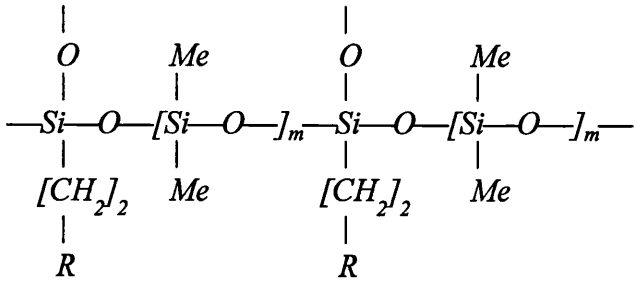

Fig 3.3 - Cross Linked Organofunctional Siloxane Membrane

3.1.3 Method 3

Membranes produced by methods 1 & 2 display significantly differing cross-linking structure. An attempt was made to produce a functionalised membrane from an organofunctional trialkoxysilane, with similar cross-linking to that produced from functionalised PHMS. In this case a quantity of unfunctionalised PHMS was added to the trialkoxysilane / silanol terminated PDMS mixture and the membrane formed by pressing in exactly the same manner as described before. The quantity of PHMS to be added was calculated to provide exactly the same number of cross-linking sites (*Si-H* bonds) as the total number of *C-OH* bonds (of the trialkoxysilane), which are all available for cross-linking purposes. The cross-linking structure of the resultant membrane should be a combination of the structures displayed in figs. 3.2 & 3.3.

3.1.4 Membrane Formation Conditions

The basic unfunctionalised membrane was produced by first mixing together measured quantities of the unfunctionalised PHMS, silanol terminated PDMS and tetraethoxysilane. A measured quantity of the dibutyltin dilaurate catalyst was added and the mixture stirred vigorously. Once the viscosity of the mixture had increased noticeably, the liquid polymer was pressed between cellulose acetate sheets to a force of 20 tonnes, for 1 hour. A thin layer of the microporous polypropylene support, Celgard 2500, was initially positioned on one of the cellulose acetate sheets and the PDMS film formed on top of this layer, producing a composite membrane. The microporous support adds rigidity to the membrane and makes it easier to handle and separate from the acetate sheets. The membrane was then cured at a temperature of 80^{o}C for 1 week before use.

For production of the standard membrane, the silanol terminated PDMS used had a molecular mass of 74000, i.e. each chain contained approximately 1000 dimethylsiloxane units. The ratio of silanol terminated PDMS to PHMS used was 10:1 by mass, with tetraethoxysilane added in excess, the unreacted portion of which was eventually evaporated off during the curing process. The quantity of dibutyltin dilaurate catalyst was set at approximately 3% of the total mass of PDMS + PHMS, which appeared to be the right quantity to produce a successful membrane. The resultant composite membrane proved to be very strong and elastic, without being sticky to touch.

The method 1 functionalised membranes were made in much the same way. The ratio of silanol terminated PDMS to functionalised siloxane was calculated to give the required organofunctionality within the membrane. Functional loading was defined as the percentage of total silicon atoms within the membrane containing an organofunctional chain. Again, tetraethoxysilane was added in excess and the same percentage, 3%, of dibutyltin dilaurate used. It was found that the cross-linking process for the functionalised membranes was generally slower than that for the unfunctionalised membranes and it was often necessary to leave them on the press for longer than 1 hour. In order to accelerate the cross-linking process, the temperature of the press was increased to 40^{o}C. The resultant composite membranes become less elastic and more brittle as functional loading is increased.

In order to produce the method 2 functionalised membranes, the functionalised tri-meth/ethoxy-silane was mixed with silanol terminated PDMS of molecular weight 18000 (approximately 240 dimethylsiloxane units), in a ratio to give the desired functionality. The shorter chained PDMS was chosen in order to provide additional cross-linking sites. This should lead to a more uniform spread of functionality throughout the membrane, as less cross-linking between adjacent oxy-silane molecules is necessary. The dibutyltin dilaurate catalyst was added and the membrane pressed and cured in the same manner as before.

A summary of syntheses for all functionalised membranes produced is displayed in appendix 3.

3.2 Experimental Procedure

Each membrane was tested within a standard, batch pervaporation test rig. A schematic diagram of the test apparatus is shown in fig. 3.4.

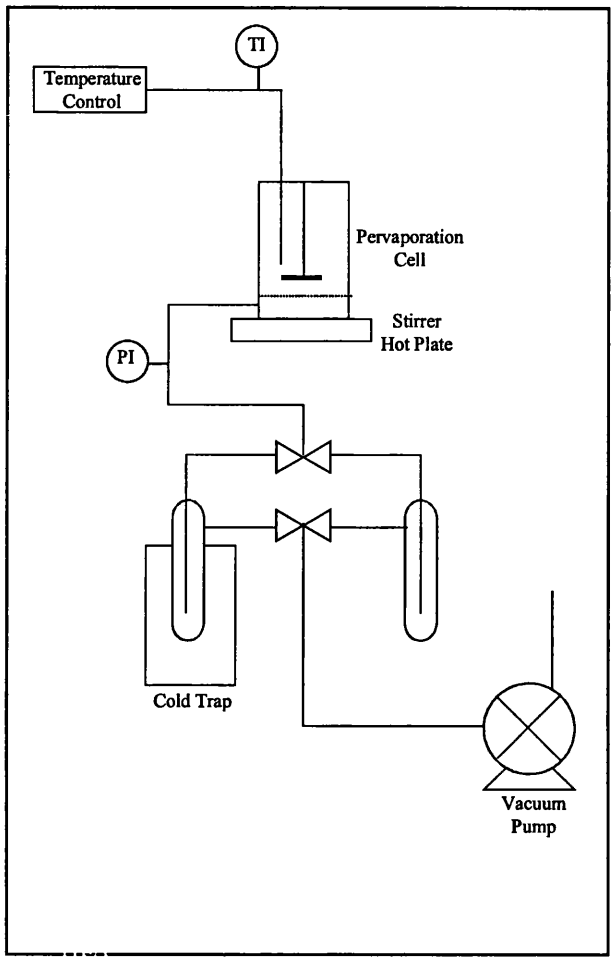

Fig. 3.4 - Pervaporation Apparatus

A circular piece of membrane was cut and its average thickness measured using vernier calipers. As each membrane disc was not always of uniform thickness across its entire cross section, eight separate thickness measurements were taken at equal spacing around the circumference of the membrane. In order to confirm the accuracy of the average value, each membrane disc was weighed. A very good linear correlation was found to exist between average thickness and mass, for all functionalised and unfunctionalised membranes.

The membrane was clamped into a sealed stainless steel test cell above a porous sintered metal support with a viton "o" ring arrangement forming a leak free seal. The cell was filled with the feed solution and placed upon a stirrer/hotplate, the solution being stirred by a magnetic follower. A more detailed schematic diagram of the test cell is displayed in fig. 3.5.

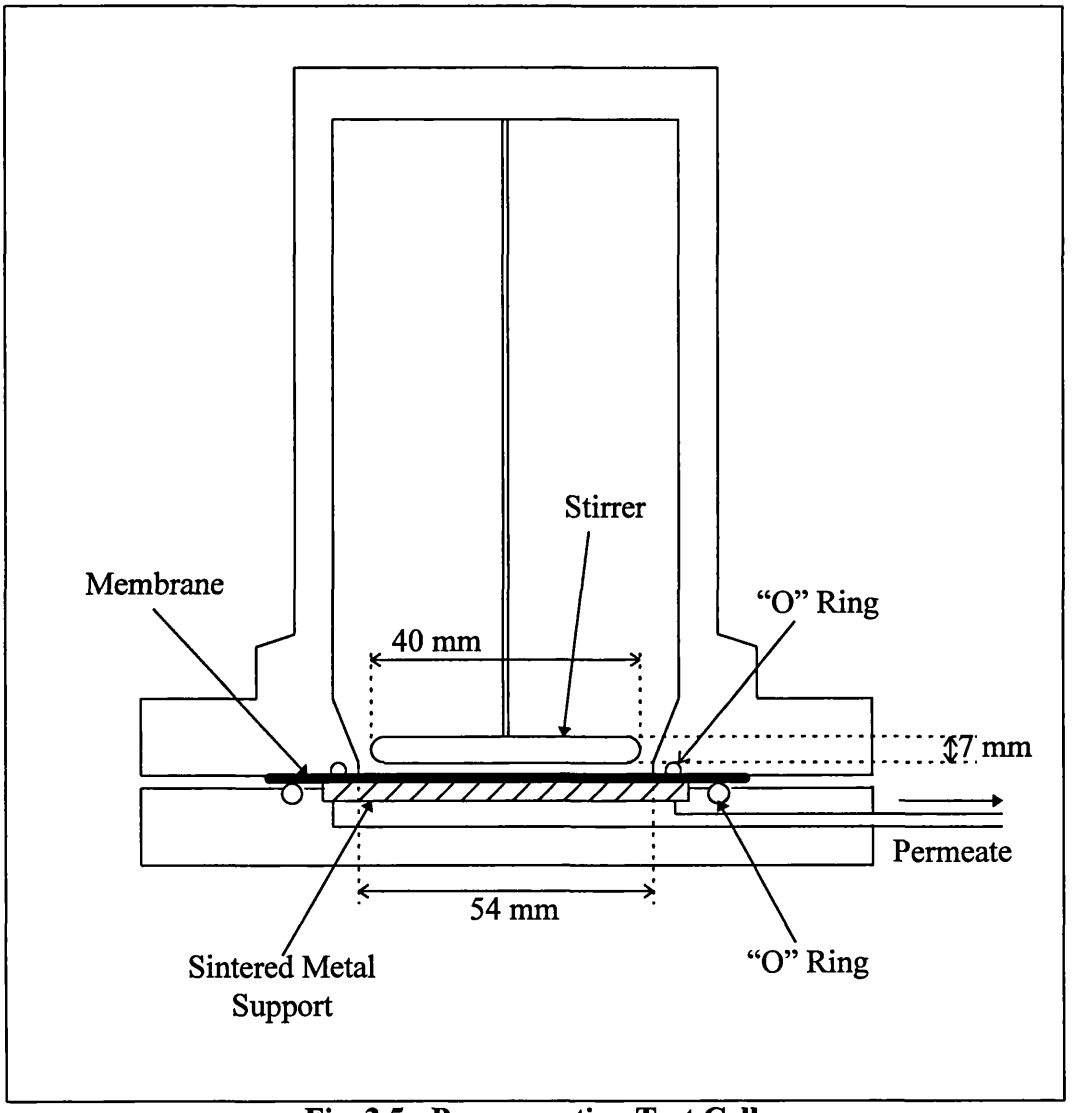

Fig. 3.5 - Pervaporation Test Cell

The cell temperature was controlled and measured with a thermocouple and electronic temperature control system. A vacuum was pulled, by means of a vacuum pump, from the downstream side and the downstream pressure measured between the cell and cold traps. The permeate was condensed and frozen within one of the cold traps, which was cooled with liquid nitrogen.

When phenol solutions were used as feed it was found that phenol often sublimed, crystallising out of the gaseous permeate before reaching the cold trap. To overcome this problem, the section of glass and rubber tubing between the cell and cold trap was fitted with electrical trace heating. During phenol separation experiments, the temperature of this section was maintained at approximately 60°C.

Permeate was collected for a measured length of time, after which it was weighed and analysed for composition, in order to determine flux and selectivity. The results of the first experiment for each new membrane disc were disregarded. During this period the membrane was often found to undergo conditioning, producing results very different to those achieved in later experiments. Subsequent experiments were repeated until consecutive sets of results were closely similar (see section 5.1). Only very rarely did the results of the second and third experiments differ by greater than 5 %.

3.2.1 Mathematics of Batch Pervaporation

As experiments were carried out within a batch test rig, feed concentration was constantly changing throughout the duration of the experiment. For certain separations the feed concentration decreased to half of the initial value. In these cases significant error may be introduced if the concentration, for calculation purposes, is taken to be the simple average of initial and final concentration. If "ideal" pervaporation is assumed and permeate pressure is maintained sufficiently low that $C_{o(m2)} \approx 0$, it may be recalled that:-

$$J_o = k_{(ov)o} C_{o(b)} \qquad (2.76)$$

A simple mass balance upon the organic component within the feed yields:-

$$\frac{-dM_o}{dt} = \frac{M_T}{\rho_b}\frac{dC_{o(b)}}{dt} + \frac{C_{o(b)}}{\rho_b}\frac{dM_T}{dt} \qquad (3.1)$$

Where: M = Mass, kg — t = Time, s

ρ = Density, kg/m^3 — C = Concentration, kg/m^3

T denotes total — o denotes organic component

b denotes bulk

The mass of feed charged at the beginning of each experiment was 470 - 500 g and the total quantity of permeate collected, over the period of an experimental run, was typically 1 - 2 g. $\frac{dM_T}{dt}$ was, therefore, very small and the final term in *eq. (3.1)* may be neglected. It should also be remembered that for low $C_{o(b)}$, $\rho_b \approx \rho_w$. *Eq. (3.1)* may, therefore, be simplified to:-

$$\frac{-dM_o}{dt} = \frac{M_T}{\rho_w}\frac{dC_{o(b)}}{dt} \qquad (3.2)$$

Recalling that flux is defined as the mass flux per unit area, *eqs. (3.2) & (2.76)* may be combined to yield:-

$$\frac{-M_T}{\rho_w}\frac{dC_{o(b)}}{dt} = k_{(ov)o} A\, C_{o(b)} \qquad (3.3)$$

Where: A = Membrane Area Available for Permeation, m^2

Integrating *eq. (3.3)*:-

$$-\int_{C_{o(b)t=0}}^{C_{o(b)t}} \frac{dC_{o(b)}}{C_{o(b)}} = \int_0^t \frac{k_{(ov)o} A\, \rho_w\, dt}{M_T} \qquad (3.4)$$

$$k_{(ov)o} = \frac{M_T}{A\, \rho_w\, t}\, ln\left(\frac{C_{o(b)t=0}}{C_{o(b)t}}\right) \qquad (3.5)$$

$k_{(ov)o}$ may obviously be determined by measuring $C_{o(b)}$ at the end of each experiment and substituting $t = t_{exp}$, into *eq. (3.5)*, where t_{exp} = total time of experiment, s.

In experiments run to determine the effect of feed concentration upon membrane performance, it was necessary to calculate an average feed concentration, $C_{o(b)av}$, given by:-

$$C_{o(b)av} = \frac{1}{t_{exp}} \int_0^{t_{exp}} C_{o(b)t}\, dt \qquad (3.6)$$

Combining *eqs. (3.5) & (3.6)* yields:-

$$C_{o(b)av} = \frac{1}{t_{exp}} \int_0^{t_{exp}} C_{o(b)t=0} \, exp\left(\frac{-\rho_w \, k_{(ov)o} \, A \, t}{M_T}\right) \qquad (3.7)$$

$$C_{o(b)av} = \frac{1}{t_{exp}} \frac{M_T C_{o(b)t=0}}{k_{(ov)o} \, A \, \rho_w} \left(1 - exp\left(\frac{-\rho_w \, k_{(ov)o} \, A \, t_{exp}}{M_T}\right)\right) \qquad (3.8)$$

When using *eq. (3.5)*, care must be taken as when $C_{o(b)t}$ approaches $C_{o(b)t=0}$, the term $ln\left(\frac{C_{o(b)t=0}}{C_{o(b)t}}\right)$ varies to a great extent with only a small change in $C_{o(b)t}$. Thus, unless there is a significant drop in feed concentration over the course of an experiment, a small degree of experimental error in the determination of the final value of $C_{o(b)t}$ could lead to very large error in $k_{o(ov)}$. For chloroform and MIBK separation, $C_{o(b)t}$ dropped to 50 - 75% of $C_{o(b)t=0}$, during the course of an experimental run and it was deemed appropriate to use *eqs. (3.5) & (3.8)*. For phenol separation $C_{o(b)t}$ dropped only to 95 - 98% of $C_{o(b)t=0}$ and for pyridine separation to 90 - 96% of $C_{o(b)t=0}$. In these two cases $C_{o(b)av}$ was taken to be the simple average of initial and final concentration and $k_{(ov)o}$ calculated as being:-

$$k_{(ov)o} = \frac{J_o}{C_{o(b)av}} \qquad (3.9)$$

3.3 Analytical procedure

As relatively high feed concentrations of phenol were employed, the same feed solution was used for a number of experiments, with the addition of both phenol and water equivalent to that removed in the permeate during the previous experimental run. Both feed and retentate were sampled and analysed for phenol concentration using a Cecil 1020 ultra-violet spectrophotometer. As phenol is a weak acid, it dissociates at high pHs and thus the spectrophotometer absorbance reading, at a given concentration, could be pH dependent. To overcome this problem the pH of the solutions to be analysed was adjusted to approximately 3, using dilute sulphuric acid, thus ensuring that all the phenol was in an undissociated state. Initially, the spectrophotometer was calibrated by analysing a series of prepared phenol solutions of known concentration. It was found that phenol absorbed strongly at 240nm and displayed a linear relationship between absorbance and concentration at up to 100 ppm. It was also shown that the absorbance of the pure water blank solution was not affected by the addition of enough acid to adjust the pH to 3.

As the spectrophotometer absorbance reading can be affected by the ambient temperature, the calibration was checked before each use, using a prepared 50 ppm standard. A very consistent absorbance reading at 50 ppm was found of 0.062 ± 0.001, well within the approximate error of ± 5%, as quoted by the manufacturer. The feed or permeate sample was diluted with distilled water and adjusted to pH 3 with a few drops of acid, to give a phenol concentration within the region of 20-100 ppm. The absorbance of the resultant solution was then measured and compared to the 50 ppm standard, using a quartz cuvette with distilled water as a blank.

For chloroform and MIBK separation from water the minor component of the permeate was always water. Maximum accuracy was obtained by analysing for water as opposed to the organic component. If the major component is analysed for, a small percentage error in the determination of its concentration can lead to a large percentage error in minor component concentration. As both chloroform and MIBK are volatile, stoppers were placed at either ends of the permeate collection tubes immediately at the end of each experiment, in order to prevent mass loss.

Due to the low solubility of both organic components in water, the permeate invariably contained two phases, a water saturated organic and organic saturated water phase. A measured quantity of 2-propanol, which is an excellent solvent for both water and organic components, was added to the permeate in order to form a single homogeneous liquid phase. Approximately 9 g of 2-propanol was added to a typical permeate mass of the order of 2 g. A sample was then taken and analysed for water concentration, using a Mettler D18 Karl Fischer Titrator and standard solvents. Each batch of 2-propanol was itself periodically analysed for water content, which was found to be of the order of 0.05% w/w. This was subtracted from the total mass of water calculated within the permeate / 2-propanol solution to give the total water content of the permeate.

As pyridine is totally miscible with water, at room temperature for all concentrations, the permeate was allowed to slowly warm to room temperature before a sample was injected directly into the Karl Fischer Titrator. The permeate typically consisted of about 50% w/w water.

Chapter 4

Experimental Results - Effect of Process Parameters

Scope of Chapter 4

Within this chapter the effect of various process parameters upon pervaporation performance is investigated. The effect of temperature, feed concentration and microporous support material are displayed by fitting experimental data to a relevant mathematical model. A model describing the effect of permeate pressure upon performance is developed, leading to a very useful equation, *eq. (4.7)*, allowing the determination of permeability coefficient, for "ideal" pervaporation, from experimental data. Feed side boundary layer resistance is quantified using the resistances in series approach, described in chapter 2.

Throughout chapter 4, several physical constants such as densities, areas, activity coefficients etc. have been used when applying various equations. The numerical value of each constant used is reported in appendices 4 & 5.

As feed concentration drops throughout the course of a batch pervaporation experimental run, data has been normalised to a single concentration value by first determining $k_{(ov)o}$, using the approach described in chapter 3 and then applying:-

$$J_o = k_{(ov)o} C_{o(b)} \qquad (2.76)$$

$C_{o(b)}$ is generally taken to be very close to the average feed concentration throughout an experimental run.

4.1 Determination of Boundary Layer Mass Transfer Coefficient, k_{lo}

For the separations considered within this study, boundary layer resistance is determined using the resistances in series model, as previously described in chapter 2, using the same membrane and varying stirrer speed. For both phenol and pyridine separation, using 20% acetate functionalised PDMS and unfunctionalised PDMS respectively, it is found that

increasing stirrer speed above 250 rpm makes no measurable difference to component fluxes. As all further permeation experiments are conducted at a stirrer speed of 1000 rpm, it is concluded that boundary layer resistance is negligible for these two separations.

For both chloroform and MIBK separation from water, boundary layer resistance is found to substantially inhibit permeation of the organic component. Recalling, from chapter 2, that membrane resistance may be determined from a plot of $\frac{1}{k_{(ov)o}}$ against $\frac{1}{\omega^c}$, such plots are displayed in figs. 4.1 & 4.2, $k_{(ov)o}$ being calculated using:-

$$k_{(ov)o} = \frac{M_T}{A\,\rho_w\,t}\,ln\left(\frac{C_{o(b)t=0}}{C_{o(b)t}}\right) \qquad (3.5)$$

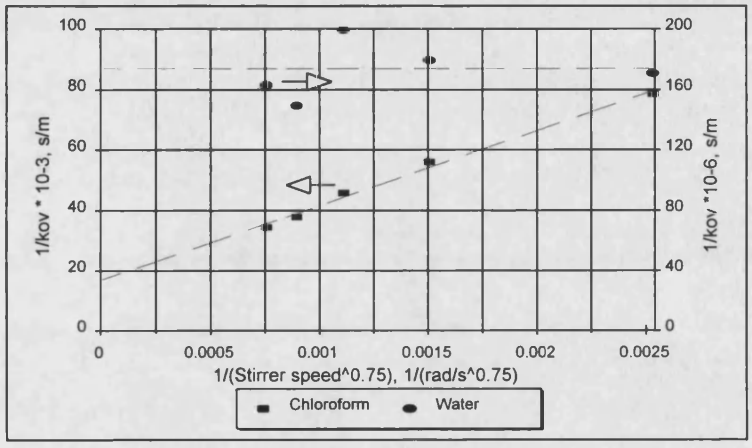

Fig. 4.1 - Chloroform Separation, Plot to Determine k_{lc}

Unfunctionalised PDMS, w_{pf} = 0.003, P_{Tp} < 2 mbar, T = 25°C, δ_m = 106 μm

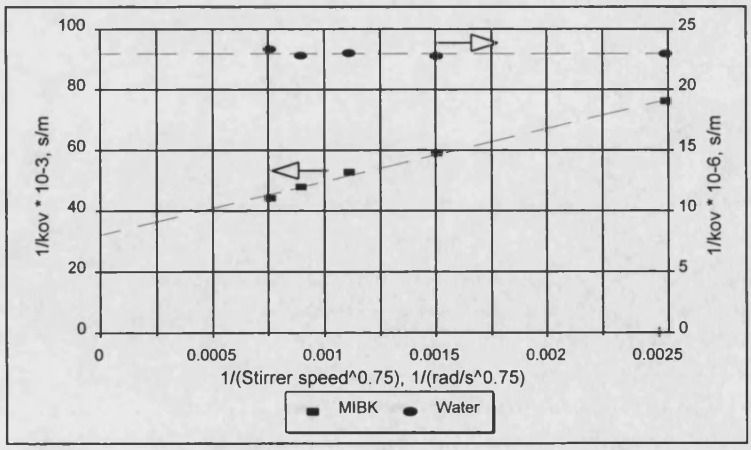

Fig. 4.2 - MIBK Separation, Plot to Determine k_{lm}

Unfunctionalised PDMS, w_{mf} = 0.0075, P_{Tp} < 2 mbar, T = 70°C, δm = 151 μm

In both cases an excellent correlation is achieved for the organic component. As would be expected, $k_{(ov)w}$ remains unaffected by a change in turbulence. The scatter in $k_{(ov)w}$ values for the chloroform separation is probably attributable to experimental error. This is due to the very small mass of water permeating through the membrane in any given experiment, as selectivity towards chloroform is very high.

Recalling that the reciprocal of concentration based membrane mass transfer coefficient, $\frac{1}{k^c_{mo}}$, is given by the intercept with the $\frac{1}{k_{(ov)o}}$ axis, the following values of k^c_{mo} are found from the above plots:-

Chloroform separation: $k^c_{mc} = 5.907 \times 10^{-5}$ m/s

MIBK separation: $k^c_{mm} = 3.115 \times 10^{-5}$ m/s

Again, it should be recalled that:-

$$\frac{1}{k_{(ov)o}} = \frac{1}{k_{lo}} + \frac{1}{k^c_{mo}} \qquad (2.77)$$

From *eq. (2.77)*, k_{lo} may be calculated at any given stirrer speed using the above plots. In all further permeation experiments a stirrer speed of 1000 rpm is used and hence the following values of k_{lo} are found, at this speed:-

Chloroform / Water separation: $k_{lc} = 4.765 \times 10^{-5}$ m/s

MIBK / Water separation: $k_{lm} = 6.344 \times 10^{-5}$ m/s

As one would expect, k_{lm} is somewhat higher than k_{lc}. k_{lo} increases with both increasing temperature and decreasing solvent viscosity. MIBK experiments are carried out at a temperature 45°C higher than that of chloroform. The effect of temperature upon k_{lo} is further discussed in section 4.4.

In all further experimental data, *eq. (2.77)* is used to calculate k^c_{mo} and hence a true indication of the membrane and not system, performance is given. It is found that for both separations boundary layer resistance contributes between 13 and 64 % of the total resistance to organic permeation, depending upon the effectiveness and thickness of the membrane used.

4.2 Effect of Permeate Pressure

4.2.1 Development of Mathematical Model

The effect of permeate pressure upon performance can readily be demonstrated if "ideal" pervaporation is assumed.

The activity of component *i*, in both feed and permeate, at a given temperature is given by:-

$$a_i = \frac{p_i}{P_i^{sat}} \qquad (4.1)$$

Where: p = Partial Pressure, Pa P^{sat} = Saturated Vapour Pressure, Pa

In the liquid feed:-

$$p_{if} = \gamma_i x_{if} P_i^{sat} \qquad (4.2)$$

Where: γ = Activity Coefficient x = Liquid Phase Mole Fraction

In the vapour permeate:-

$$p_{ip} = y_{ip} P_{Tp} \qquad (4.3)$$

Where: T denotes total y = Vapour Phase Mole Fraction

If feed concentrations are such that sorption may be described by Henry's law, at both feed and permeate side, it can be recalled that:-

$$S^a_i = \frac{\phi_{i(m1)}}{a_i} \qquad (2.42)$$

If D_{mi} is assumed constant across the membrane and convective flow may be neglected, Ficks first law becomes:-

$$J_i = \frac{D_{mi}}{\delta_m} (C_{i(m1)} - C_{i(m2)}) \qquad (4.4)$$

The concentration terms may be expressed in terms of molar concentrations, kmol/m^3:-

$$C_{\Phi i(m1)} = \frac{\rho_m \phi_{m(1)}}{MR_i} \qquad (4.5)$$

$$C_{\Phi i(m2)} = \frac{\rho_m \phi_{m(2)}}{MR_i} \qquad (4.6)$$

Where: MR = Molecular Mass Φ denotes molar basis

A combination of *eqs. (4.1)-(4.6) & (2.42)* yields:-

$$J_{\Phi i} = \frac{S^a{}_i D_{mi} \rho_m}{\delta_m MR_i}\left(\gamma_i x_{if} - y_{ip}\frac{P_{Tp}}{P_i^{sat}}\right) \qquad (4.7)$$

Where: $J_{\Phi i}$ = Molar Flux, kmol/m^{2}hr

It should be noted that the permeability coefficient defined by *eq. (4.7)* is not equal to that defined by *eq. (2.79)*, i.e. $S^a{}_i D_{mi} \neq S^c{}_i D_{mi}$. $S^a{}_i D_{mi}$ is an activity based coefficient, whereas $S^c{}_i D_{mi}$ is concentration based (see section 2.2.2.2). It can easily be shown, from *eqs. (2.76), (2.79) & (4.7)*, that:-

$$S^a{}_i D_{mi} = \frac{S^c{}_i D_{mi} C_{of}}{\rho_m\left(\gamma_i x_{if} - y_{ip}\frac{P_{Tp}}{P_i^{sat}}\right)} \qquad (4.8)$$

Define:-

$$A_i = \frac{S^a{}_i D_{mi}}{MR_i} \qquad (4.9)$$

For a ternary system, from *eq. (4.7)* it can be shown that:-

$$\frac{J_{\Phi 1}}{J_{\Phi 2}} = \frac{y_{1p}}{1 - y_{1p}} = \frac{A_1\left(\gamma_1 x_{1f} - y_{1p}\frac{P_{Tp}}{P_1^{sat}}\right)}{A_2\left(\gamma_2 x_{2f} - (1-y_{1p})\frac{P_{Tp}}{P_2^{sat}}\right)} \qquad (4.10)$$

Which reduces to:-

$$y_{1p}^2\left(A_2\frac{P_T}{P_2^{sat}} - A_1\frac{P_T}{P_1^{sat}}\right) + y_{1p}\left(A_2\gamma_2 x_{2f} + A_1\frac{P_T}{P_1^{sat}} + A_1\gamma_1 x_{1f} - A_2\frac{P_T}{P_2^{sat}}\right) - A_1\gamma_1 x_{1f} = 0 \qquad (4.11)$$

Eq. (4.10) describes a quadratic equation in y_{1p} and is valid for the case where feed side boundary layer resistance is negligible. Assuming all other variables are known, y_{1p} can be calculated from *eq. (4.11)*, for any given P_{Tp}. $J_{\Phi 1}$ and $J_{\Phi 2}$ can then be calculated from *eq. (4.7)*. Similar relationships have been derived, starting with different expressions describing component transport in two previous studies *(Watson and Payne, 1990), (Wijmans and Baker, 1993)*. The description of the variation of y_{ip} with P_T being a quadratic equation (*eq. (4.11)*) has not, however, been previously reported.

The activity coefficient, γ_i, is clearly a very important parameter. As data from literature was found to be either inconsistent or incomplete, it was necessary to estimate values of γ_i.

The estimation techniques employed along with the γ_i values obtained, for various process conditions, are comprehensively described in appendix 5.

4.2.2 Examples of Proposed Model and Discussion

The above relationship is displayed graphically in figs. 4.3 & 4.4 for phenol and chloroform separations, using unfunctionalised PDMS membranes. The membrane permeabilities are determined experimentally, using the procedure described in chapter 5, making use of *eq. (4.7)*. The figures display the fluxes that would be obtained in the absence of feed side boundary layer resistance.

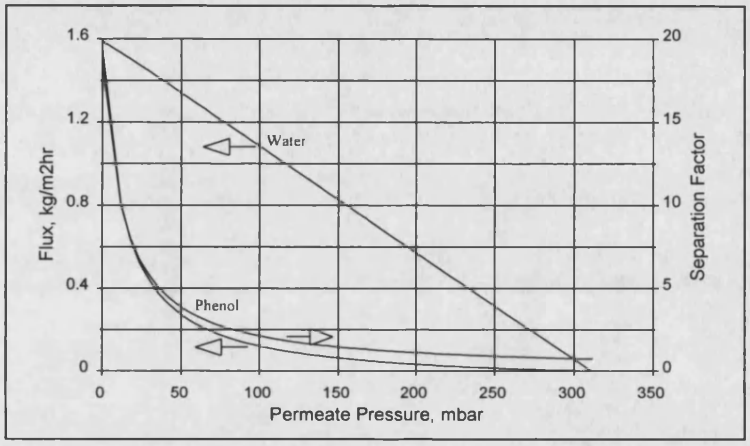

Fig. 4.3 - Phenol Separation, Effect of Permeate Pressure

Unfunc. PDMS, $w_{pf} = 0.05$, $T = 70°C$, $\delta_m = 10\ \mu m$, $S^a{}_p D_{mp} = 2.15 \times 10^{-11}\ m^2/s$, $S^a{}_w D_{mw} = 0.46 \times 10^{-11}\ m^2/s$

Both figures indicate a drop in both water and organic flux as permeate pressure is increased. In both cases the separation factor is found to decrease with increasing permeate pressure. When the permeate pressure becomes equal to the sum of the feed side partial pressures there is no longer a driving force for permeation and the total flux becomes zero. It is interesting to note that at this point the theoretical separation is that achieved purely by vapour-liquid equilibrium. It may be concluded that if the separation achieved by the pervaporation membrane is better than that of vapour-liquid equilibrium, performance will always be increased by decreasing the permeate pressure. If the separation is worse than that of vapour-liquid equilibrium, the separation factor will actually be increased by an

increase in permeate pressure. In both cases, component fluxes will always decrease as permeate pressure is increased.

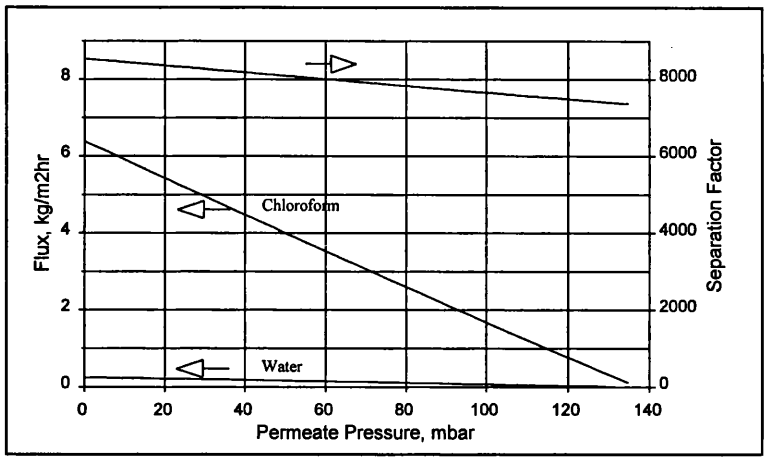

Fig. 4.4 - Effect of Permeate Pressure

Unfunc. PDMS, $w_{cf} = 0.003$, $T = 25°C$, $\delta_m = 10\ \mu m$, $S^a{}_c D_{mc} = 4.68 \times 10^{-11}\ m^2/hr$, $S^a{}_w D_{mw} = 7.17 \times 10^{-13}\ m^2/hr$

Separations that display the greatest enhancement in separation factor over that of vapour-liquid equilibrium will be the most sensitive to increasing permeate pressure. From figs. 4.3 & 4.4 it can be seen that unfunctionalised PDMS displays separation factors far above that of vapour-liquid equilibrium for phenol-water separation, whereas for chloroform-water separation the enhancement is much more modest. Consequently, it can be seen that performance declines dramatically as permeate pressure is increased for phenol / water separation and declines gently for chloroform / water separation. This phenomenon is discussed further in chapters 5 & 6.

In order to take full advantage of the separating potential of PDMS for phenol separation, it would appear crucial to operate at very low permeate pressure.

4.3 Effect of Microporous Support

It has been reported *(Burslem et al, 1992)* that the microporous layer of a composite membrane can significantly affect membrane performance. In order to accurately compare the performance of different functionalised siloxane films, of different thickness, cast upon

the same Celgard 2500 support material, it is necessary to quantify the transport resistance offered by the support.

Celgard 2500 is organophilic by nature and prior to cross-linking the functionalised siloxane / silanol terminated PDMS mixture is a mobile (although viscous) liquid. It is, therefore, thought that the Celgard pores become filled with the rubbery membrane material. This theory is supported by visual examination of the finished composite membranes, for both the functionalised and unfunctionalised PDMS material. As the porosity of Celgard 2500 is 0.45, the permeant has a restricted cross sectional area through which to diffuse, once it reaches the Celgard layer. It is postulated that this reduced cross sectional area is equal to the product of porosity and membrane cross sectional area. The Celgard effectively increases the thickness of the PDMS film by the product of the Celgard thickness and inverse of its porosity.

From *eq. (4.7)* it can be seen that the flux of a component through a membrane is inversely proportional to the membrane thickness:-

$$J_{\Phi i} = \frac{S^a_i D_{mi} \rho_m}{\delta_m MR_i}\left(\gamma_i x_{if} - x_{ip}\frac{P_{Tp}}{P_i^{sat}}\right) \qquad (4.7)$$

This is true for both components and hence for constant process conditions:-

$$J_T = \frac{\eta}{\delta_m}, \; or \; \frac{1}{J_T} = \frac{\delta_m}{\eta} \qquad (4.12)$$

Where: T denotes total $\qquad$ η = Flux Constant, kg/ms

Including the Celgard support layer, the effective PDMS film thickness, δ_m, is given as:-

$$\delta_m = (\delta_T - \delta_C) + \frac{\delta_C}{\psi} \qquad (4.13)$$

Where: δ_C = Celgard 2500 Thickness = 0.025 mm $\quad$ ψ = Celgard 2500 Porosity = 0.45

δ_T = Total Composite Membrane Thickness, mm

Hence:-

$$\frac{1}{J_T} = \frac{\delta_T - \delta_C}{\eta} + \frac{\delta_C}{\eta\psi} \qquad (4.14)$$

Thus a plot of $\frac{1}{J_T}$ against $(\delta_T - \delta_C)$ should yield a straight line of gradient $\frac{1}{\eta}$ and intercept $\frac{\delta_C}{\eta\psi}$.

A study of the plot displayed in fig. 4.5 for phenol / water permeation through unfunctionalised PDMS composite membranes of varying thickness, confirms that this theory is valid. The line shown is that of best fit using the above model and is found to be extremely similar to the line of best fit using linear regression of the data points.

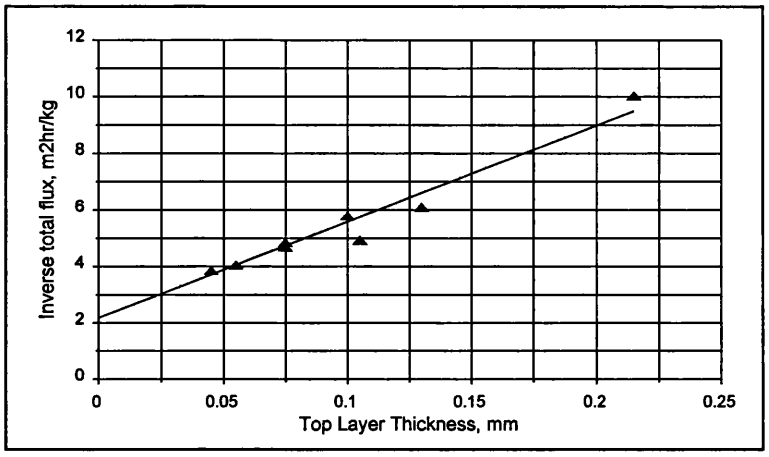

Fig. 4.5 - Effect of Celgard 2500 Microporous Support

Unfunctionalised PDMS, SS = 1000 rpm, P_{Tp} < 2 mbar, T = 70°C, w_{pf} = 0.05

4.3.1 Sintered Metal Support Plate

As mentioned within chapter 3, the composite membrane is supported within the test cell on top of a porous metal plate, produced from sintered stainless steel 316L and of 3 mm thickness. It was thought possible that the plate itself could offer a significant resistance to component transport. In order to test this theory, three different grades of plate were tested, each of the same porosity of 55% but of varying mean pore size, 10, 15 & 30 μm. For phenol separation, it is found that identical pervaporation performance is achieved when using each of the different plates and it is concluded that support plate resistance is negligible. In all further experiments the plate of highest mean pore size is employed.

4.4 Effect of Temperature

It has been found, by numerous authors, that the effect of temperature upon component fluxes can be described by an Arrhenius relationship *(Neel, 1991)*:-

$$J_i = J_i^* \exp\left(\frac{-E_{ai}}{RT}\right) \qquad (4.15)$$

Where: J^* = Pre Exponential Factor, m^2/s E_a = Activation Energy, J/mol

R = Gas Constant, J/molK T = Temperature, K

Hence a plot of $\ln(J_i)$ against $\frac{1}{T}$ should yield a straight line of gradient $\left(\frac{-E_{ai}}{R}\right)$.

4.4.1 Effect upon Boundary Layer Resistance

The feed side boundary layer resistance is also affected by temperature. It can be recalled from section 2.1.2.1 that for a stirred cell in the turbulent region:-

$$Sh = 0.044\, Re^{0.75}\, Sc^{0.33} \qquad (2.12)$$

Also, it can be recalled that D_{lo} may be estimated from the Wilke-Chang correlation:-

$$D_{lo} = 1.17 \times 10^{-16} \frac{T(\phi M_w)^{1/2}}{\mu_w V_o^{0.6}} \qquad (2.19)$$

Eqs. (2.12) & (2.19) can be combined and rearranged to give:-

$$k_{lo} \propto T^{0.67}\, \mu_s^{-1.09} \qquad (4.16)$$

For the two separations where boundary layer resistance is found to be significant within the experimental apparatus, Chloroform and MIBK, effective fluxes (i.e. the fluxes that would occur in the absence of boundary layer resistance) are calculated, using the procedure described in section 4.1. As k_{lo} values are experimentally determined at only one temperature, *eq. (4.16)* is used to estimate k_{lo} at all other temperatures.

4.4.2 Experimental Results

Arrhenius plots for each separation investigated are displayed in figs. 4.6 - 4.9. The E_{ai} values determined from the plots below are displayed in table 4.1.

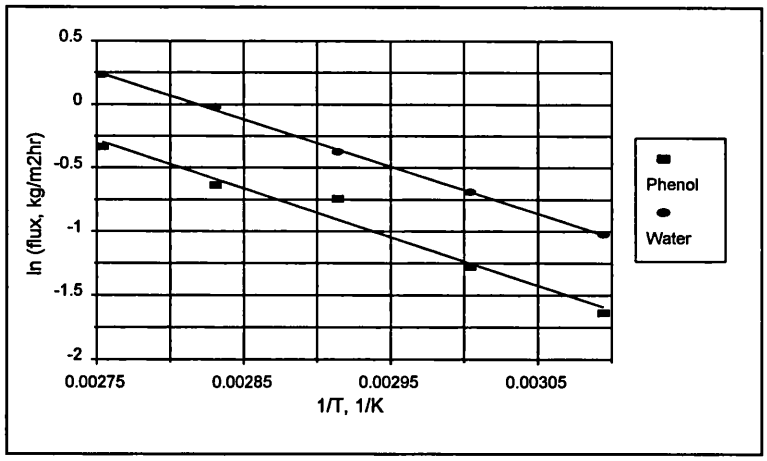

Fig. 4.6 - Phenol Separation, Arrhenius Plot

20% acetate func. PDMS, $w_{pf} = 0.05$, $P_{Tp} < 2$ mbar, $\delta_m = 106$ μm

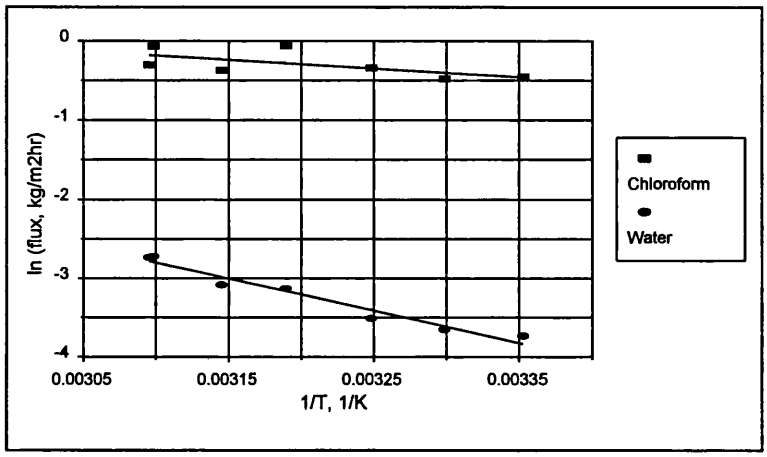

Fig. 4.7 - Chloroform Separation, Arrhenius Plot

Unfunctionalised PDMS, $w_{cf} = 0.003$, $P_{Tp} < 2$ mbar, $\delta m = 106$ μm

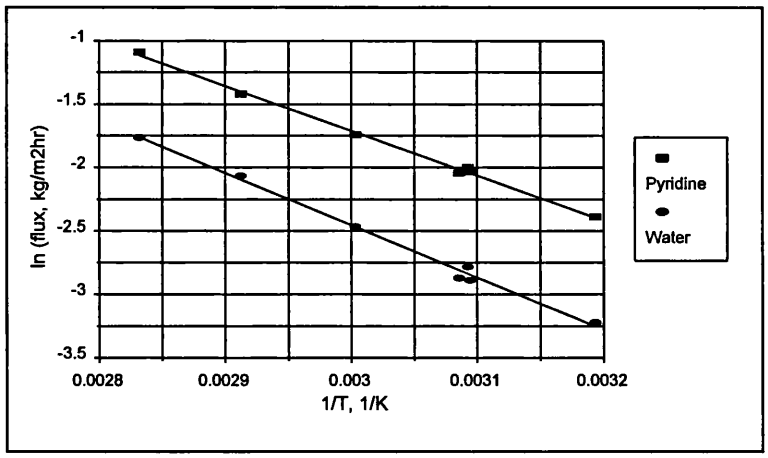

Fig. 4.8 - Pyridine Separation, Arrhenius Plot

Unfunctionalised PDMS, $w_{pf} = 0.04$, $P_{Tp} < 2$ mbar, $\delta m = 161$ μm

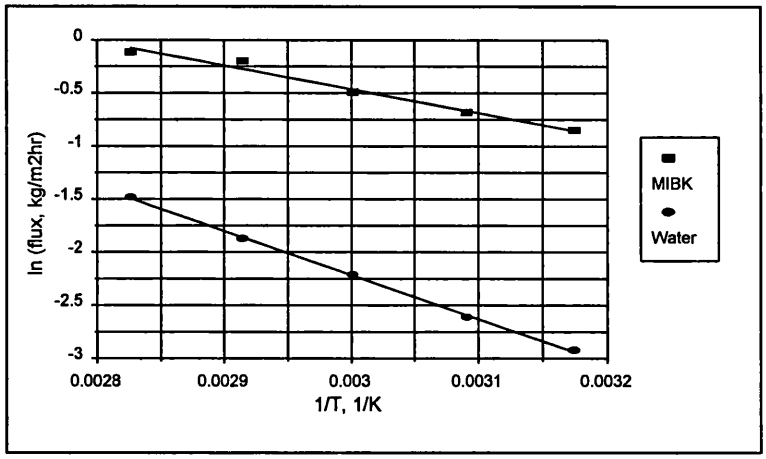

Fig. 4.9 - MIBK Separation, Arrhenius Plot

Unfunctionalised PDMS, $w_{mf} = 0.0075$, $P_{Tp} < 2$ mbar, $\delta m = 151$ μm

Organic	$-E_{ao}$, *kJ/mol*	$-E_{aw}$, *kJ/mol*
Phenol	31.6	30.9
Chloroform	9.15	34.1
Pyridine	29.4	34.3
MIBK	18.6	34.4

Table 4.1 - Activation Energies for Permeation

These values fall towards the lower end of the range of $-E_{ai}$'s for pervaporation systems, reported as generally being 21-92 kJ/mol *(Neel, 1991)*. The main exception is that for chloroform permeation, which is particularly low, indicating that chloroform permeation is not strongly affected by temperature. In a separate study, *(Blume et al, 1991)* $-E_{ai}$ for chloroform of 18.23 kJ/mol was reported. Although significantly higher than the value calculated within this study, two experimental differences existed. Firstly PDMS films produced by a different manufacturing process and of higher cross-linking density were used and secondly only pure component permeation was considered. Within the same study $-E_{ai}$ for acetone permeation was reported as being as low as 7 kJ/mol.

All E_{aw} values are similar suggesting that the temperature dependence of J_w is unaffected by the nature of the permeating organic species. The E_{aw} value for phenol separation is slightly lower than the others and this could be explained by the fact that an acetate functionalised membrane was used, as opposed to an unfunctionalised membrane, for the study of the effect of temperature upon phenol permeation.

As the E_{ao} values are lower than the E_{aw} values for chloroform, pyridine and MIBK separation, selectivity is found to decrease with increasing temperature. This is generally found to be the case in the area of pervaporation as a whole *(Neel, 1991)*. As E_{ao} is almost identical to E_{aw} for phenol / water permeation, changing temperature has very little effect upon selectivity.

4.5 Effect of Feed Concentration

It is possible to calculate membrane component permeability, ${}^{a}_{i}D_{mi}$, at any feed concentration, from *eq. (4.7)*, again using the procedure detailed in section 4.1 to account for feed side boundary layer resistance:-

$$J_i = \frac{{}^{a}_{i}D_{mi}\,\rho_m}{\delta_m\, MR_i}\left(\gamma_i\, x_{if} - x_{ip}\,\frac{P_{Tp}}{P_i^{sat}}\right) \qquad (4.7)$$

Plots displaying the variation of ${}^{a}_{i}D_{mi}$ with mass fraction of the organic present in the feed are displayed in figs. 4.10 - 4.13.

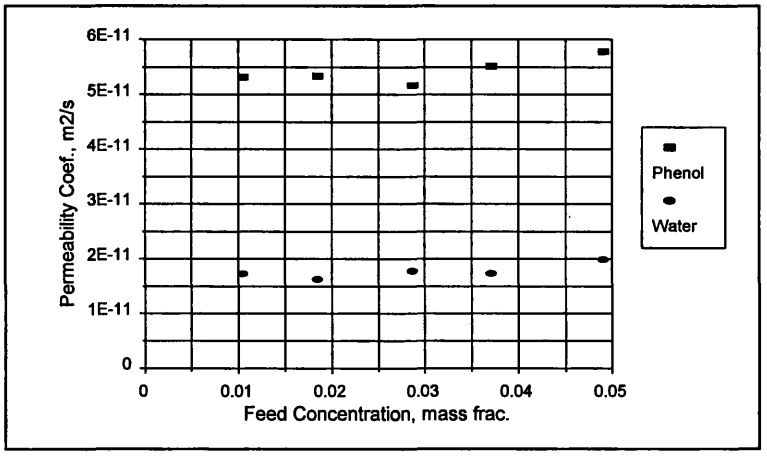

Fig. 4.10 - Phenol Separation, Effect of Feed Concentration

20 % acetate func. PDMS, $P_{Tp} < 2$ mbar, $T = 70°C$, $\delta m = 106$ μm

From figs. 4.10 & 4.11 it can be seen that both phenol and chloroform behave, within the bounds of experimental error, as "ideal" solvents within the membrane. The permeabilities of these two species remain essentially unaffected by changing feed concentration, across the range studied.

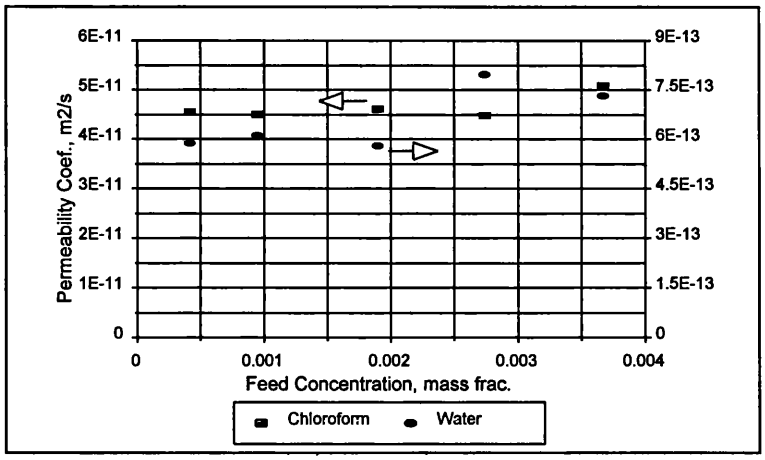

Fig. 4.11 - Chloroform Separation, Effect of Feed Concentration

Unfunctionalised PDMS, $P_{Tp} < 2$ mbar, $T = 25°C$, $\delta m = 106$ μm

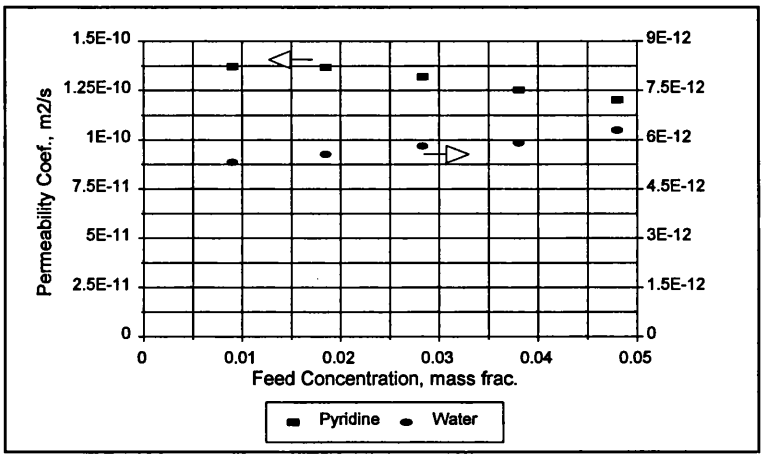

Fig. 4.12 - Pyridine Separation, Effect of Feed Concentration

Unfunctionalised PDMS, $P_{Tp} < 2$ mbar, $T = 70°C$, $\delta m = 161$ μm

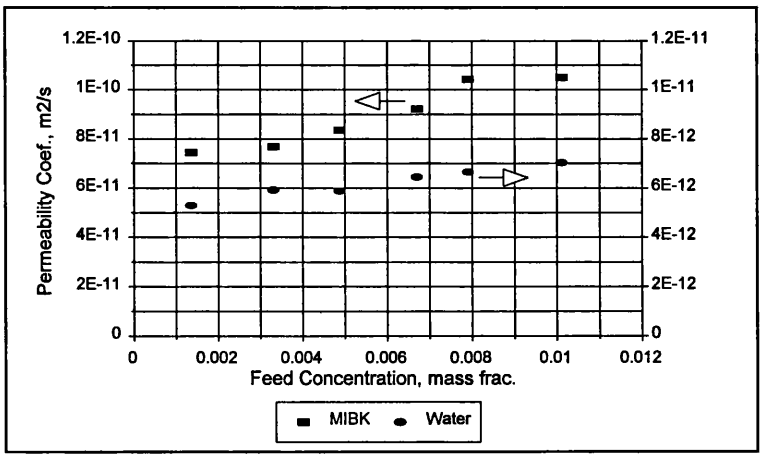

Fig. 4.13 - MIBK Separation, Effect of Feed Concentration

Unfunctionalised PDMS, $P_{Tp} < 2$ mbar, $T = 70°C$, $\delta m = 151$ μm

This behavior for chloroform is totally consistent with data reported in previous studies, as discussed within the sorption and diffusion sections of chapter 2. To recall, it was found *(Favre et al, 1994)* that the sorption isotherm for chloroform showed a linear increase in sorption with activity, up to an activity of 0.4, whereas the diffusion coefficient remained quasi constant. The upper value of feed chloroform mass fraction in fig. 4.11 corresponds to an activity of 0.42. It should also be noted that the absolute values of $S^a_c D_{mc}$ compare well with those obtained from literature. It was reported *(Guo and Kee, 1992)* that for chloroform in silicone rubber at 30°C, $D_{mc0} = 4.4 \times 10^{-10}$ m^2/s. Taking $S^a_c \approx 0.25$ *(Favre et al, 1994)*, measured at 40°C, $S^a_c D_{mc} \approx 1.1 \times 10^{-10}$ m^2/s. This compares with an average value of $S^a_c D_{mc} \approx 0.5 \times 10^{-10}$ m^2/s, measured from fig. 4.11. Of course one would expect the value measured at the higher temperatures to be greater, as D_{mi} and generally S^a_i both increase with increasing temperature. Further discrepancy could be explained by the use of different types of PDMS / silicone rubber membranes.

It appears that water permeability is slightly enhanced by an increase in organic feed concentration, particularly noticeable during chloroform permeation, despite the slightly decreasing driving force for water permeation. This is probably due to the membrane becoming increasingly swollen.

It would appear from figs. 4.12 & 4.13 that the permeation of both pyridine and MIBK are affected by coupling phenomena. It is also interesting to note that coupling has opposite effects upon these two components, pyridine permeability being lowered and MIBK permeability being enhanced by increasing feed concentration. The pyridine / water separation results are totally consistent with a previous study, also employing PDMS membranes *(Drioli, 1993)*. In this study it was concluded that the permeation of pyridine is enhanced, whereas that of water is reduced by decreasing feed pyridine concentration. This phenomenon was explained by a change in membrane morphology caused by the competitive sorption of the two penetrant molecules. An alternative explanation, more consistent with usual coupling theory as discussed in chapter 2 is proposed. As pyridine concentration within the membrane increases, Van der Waals forces could cause neighbouring pyridine rings to cluster, thus reducing D_{mi}. At the same time, as there is a very strong affinity between water and pyridine, water permeation could be enhanced by

similar interactions with the pyridine molecules, which would essentially drag water molecules through with them.

The upper value of MIBK feed concentration in fig. 4.13 corresponds to an activity of 0.34. It is unlikely, therefore, that the enhancement in permeability with increasing concentration can be explained by a non linear increase in S^a_i with increasing concentration. It would appear that MIBK causes the PDMS membrane to swell with increasing concentration, increasing the D_{mi} of both MIBK and water, in agreement with classic coupling theory.

4.6 Closing Remarks

Most of the relationships within chapter 4 are demonstrated for unfunctionalised PDMS, or 20% acetate functionalised PDMS for phenol separation. In further chapters it is assumed that similar relationships and values of measured parameters, for the effect of permeate pressure, microporous support, temperature and concentration apply for all other functionalised membranes. Time pressure has prevented the experimental determination of such parameters for a variety of functionalised membranes to be achieved. It is thought that deviations are likely to be small, although it is recommended that this should be investigated in future work.

It should be stressed that when reporting performance data for pervaporation membranes, it is necessary to quantify and report data displaying the effect of all process parameters discussed within chapter 4. Failure to do so makes it almost impossible to accurately compare membrane performance measured within different studies under varying experimental configurations and process conditions. In many, or even most, studies throughout pervaporation literature, important process parameters are not reported. A study of tables 1.2 - 1.4 shows that key variables such as permeate pressure and membrane thickness are often unreported. It is thought that in many cases feed side boundary layer resistance may contribute a significant or even controlling resistance to permeation, however, numerous papers make no reference to the quantification of this phenomenon. This may explain why greatly different performance may be reported, by different authors, for essentially the same separation using the same type of membrane.

Chapter 5

Experimental Results - Functionalised Membranes

Scope of Chapter 5

Within this chapter the experimentally determined performance of all functionalised membranes produced is presented. For all separations it is demonstrated that selectivities in excess of those achieved solely through vapour liquid equilibrium can be achieved. Enhancements to selectivity are explained by increased organic component and/or reduced water sorption, due to differing affinity of both components with the organofunctional groups. Reductions in permeability are explained by a combination of two factors, each reducing component diffusivity. Firstly, some of the bulky functional groups reduce membrane free volume. Secondly, increased functional loading also tends to have a detrimental effect upon membrane properties, leading to increased brittleness. For chloroform, pyridine and MIBK separation, it is shown that an optimum functional loading exists to enhance selectivity, above which selectivity declines. It is shown that changing membrane cross-linking density, within the range covered by the functionalised membranes, has very little effect upon separation performance.

5.1 Membrane Performance

The performance of each functionalised membrane is compared to that of an unfunctionalised membrane, for each separation, in tables 5.1 - 5.4. $S^a_i D_{mi}$ values are calculated using *eq. (4.7)*, in which effective membrane thickness and the procedure detailed in section 4.1 to account for feed side boundary layer resistance are used. The separation factor and permeability values given are thus the maximum possible values obtainable, which would be reached in the absence of all external resistances to mass transport.

Each value presented in the tables is the average of at least two experiments, after the membrane is suitably conditioned by performing an initial experimental run. In almost all cases the two experiments produce very similar results, well within the bounds of

experimental error and typically within 5% of each other. Further experiments are performed in those rare cases where significantly different results are obtained, until successive experiments give similar results. The initial differences could be attributed to either an error in experimental technique or a long conditioning period being required for certain membranes. For all of the separations studied, separate membrane samples of the same functionalised membrane formulation were compared, for a few select membranes. In all cases the performances of different membrane samples were very similar and within the bounds of the variation typically found by performing two experiments upon the same sample. The base result for the unfunctionalised PDMS membrane is the average of separate experiments performed with at least three separate membrane samples. The methods of preparation referred to as methods 1, 2 & 3 are detailed in section 3.1.

5.1.1 Phenol Separation

5.1.1.1 Effect of Functional Group

For phenol separation, it can be seen from an examination of table 5.1 that the introduction of organofunctional chains into the PDMS membrane generally increases the membrane selectivity. This is believed to be partly due to a reduction in water solubility, caused by the long hydrophobic chains. Introducing very long organic chains appears to greatly reduce the total membrane permeability, as can be seen for the octyl functionalised membrane.

Polar ester groups are particularly effective at increasing phenol permeability, probably due to weak hydrogen bond interaction with the polar -OH group of the phenol molecule. The 20% acetate functionalised membrane displays nearly a four-fold improvement in phenol permeability, over the unfunctionalised membrane, but with a reduced selectivity. Unfortunately the same interaction of polar groups takes place with the water molecules, enhancing water permeation also. It is thought that hydrogen bonding between the ester group and water molecule may be particularly strong. As a water molecule is small, it is probable that each end of the molecule may hydrogen bond to one of the two independent oxygen atoms, within the ester group, as depicted in fig. 5.1. The 20% hexanoate functionalised membrane displays a less dramatic improvement in phenol permeability but

a much enhanced selectivity, owing to the much longer organic chains of the hexanoate molecule.

Functional Group *R*	Chemical Structure	Loading %	$S^a_p D_{mp} \times 10^{11}$ m^2/s	$S^a_w D_{mw} \times 10^{11}$ m^2/s	Sep. Factor
Method 1					
Unfunc. PDMS		0	2.15	0.46	17.7
Acetate	$-CH_2CO_2CH_3$	10	**2.75**	0.76	13.8
		20	**7.58**	2.11	13.1
Di-Acetate	$-CH(CO_2CH_3)_2$	10	**2.46**	0.42	**21.5**
		20	**3.18**	0.73	16.5
		30	**3.41**	1.54	8.6
Hexanoate	$-CH_2CO_2(CH_2)_4CH_3$	10	**3.47**	0.56	**22.1**
		20	**4.88**	0.69	**24.1**
Cyano	$-CH_2CN$	10	**3.55**	0.52	**24.5**
		20	**5.07**	0.87	**21.3**
Octyl	$-(CH_2)_7CH_3$	10	1.23	0.17	**24.1**
Benzyl	$-CH_2Ph$	10	**2.26**	0.39	**20.7**
PentaFluoroBenzyl	$-CH_2C_6F_5$	10	1.30	0.33	15.1
Phenyl Ether	$-CH_2OPh$	10	1.43	0.36	14.8
Ethyl Ether	$-CH_2OC_2H_5$	10	**3.07**	0.41	**27.6**
		20	**4.48**	0.56	**29.0**
Method 2					
Alkenyl	$-CH=CH_2$	10	**4.16**	0.90	16.3
		20	1.03	0.45	8.9
Amino	$-CH_2N(CH_3)_2$	10	**4.39**	0.58	**25.7**
		20	**5.28**	0.58	**29.8**
Amido	$-CONH_2$	10	**2.87**	0.48	**21.8**
Pyridyl	$-(C_5H_4N)$	10	**5.57**	0.62	**31.8**
Cyano	$-CH_2CN$	10	**2.57**	0.48	**19.2**
		20	**2.47**	0.77	12.0
Method 3					
Amino	$-N(CH_3)_2$	10	**2.89**	0.59	**18.1**
		20	**4.36**	0.79	**20.6**

Table 5.1 - Phenol Separation, $T = 70°C$, $w_{pf} = 0.05$

Figures in Bold are Superior to the Unfunctionalised PDMS

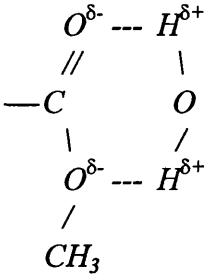

Fig. 5.1 - Hydrogen Bonding of Water and Ester Molecules

The 20% ethyl ether functionalised membrane displays similar performance, with a slightly reduced permeability but enhanced selectivity to that of the 20% hexanoate membrane. Again this may be attributed to polar interaction, however, the ether group is significantly less polar than the ester group, so enhancing both phenol and water permeation to a lesser extent. As there is only one oxygen atom within each ether group, the potential for both ends of a water molecule to be hydrogen bonded to a single ether group does not exist. It would appear that a balance has to be sought between increasing membrane polarity in order to enhance overall permeability and increasing organic content in order to enhance selectivity, but at the penalty of reducing permeability. It is interesting to note that similar performances may be obtained by long organic chains containing highly polar groups (e.g. hexanoate) and shorter organic chains containing less polar groups (e.g. ethyl ether).

Amino, amido, pyridyl and cyano functionalised membranes all display both enhanced phenol permeabilities and selectivities. Each of these groups are basic and interact with the weakly acidic phenol molecules, enhancing phenol permeation significantly. Again the interaction probably involves weak hydrogen bonding. They are the most successful family of groups for phenol separation as water permeation is not greatly enhanced concurrently with phenol permeation. The slight enhancement of water permeability, in each case, is probably attributable to weak polar interaction with the basic polar groups.

Comparing the results of the 10% functionalised membranes produced by method 2, in which all membranes should have a very similar structure, the following sequence describes the performance enhancement achieved by each basic group:-
pyridyl > amino > amido > cyano
The same sequence describes the increase in basicity of the four groups, hence it would appear that performance improves as the basicity of the group increases.

It was thought possible that aromatic groups might facilitate the transport of phenol through π-π interactions with the aromatic phenol ring. The three aromatic functionalised membranes studied display, however, disappointing permeability. It is possible that inflexible aromatic rings greatly constrain the membrane structure, so leading to reduced free volume and low diffusion coefficients. This theory is supported by the fact that for both the phenyl ether and pentafluorobenzyl functionalised membranes, the permeability of

the small water molecule decreases by a much lesser extent than that of the bulkier phenol molecule. This is consistent with the free volume theory describing the diffusion process as discussed in chapter 2. The fact that the benzyl functionalised membrane displays no such decline in phenol permeability is probably due to an increased phenol sorption through favourable π-π interaction between aromatic rings.

5.1.1.2 Functional Loading and Structural Factors

It can be seen that increasing the functional loading from 10 to 20% generally increases overall permeability without greatly affecting selectivity. Anomalous behaviour is produced by the allyl and diacetate functionalised membranes. It is thought that this could be due to membrane structural effects as will be discussed later within this chapter.

A comparison of the performance of the two sets of cyano functionalised membranes, one produced via functionalised PHMS (method 1) and one via functionalised silane (method 2) suggests that the former method is the more successful. For both 10 and 20% functionality, both permeability and selectivity are higher for the method 1 membranes. This may be partially due to structural factors. Also, the functionalised tri-eth/methoxy silane molecules can cross-link to a large extent with themselves, producing areas of very highly localised functionalisation. Membranes produced from functionalised PHMS should display a much more even functional loading throughout the entire membrane.

It would appear that it is not possible to enhance the performance of membranes manufactured using the functionalised silane by simply adding a quantity of PHMS (method 3) in order to produce similar cross linking to method 1 membranes. It can be seen that the amino functionalised membranes produced in this manner are actually out performed by the method 2 membranes. This is probably due to the fact that a method 3 formulation produces a very rigid membrane structure, because of the proximity of a long sequence of *Si-H* moieties.

5.1.2 Chloroform, Pyridine and MIBK Separation

Membranes representative of each family of functional group are tested for chloroform and pyridine separations from water. For MIBK separation, two new membranes with long hydrocarbon chains, tridecyl and branched heptyl, are evaluated.

Functional Group *R*	Chemical Structure	Loading %	$S^a_c D_{mc} \times 10^{11}$ m^2/s	$S^a_w D_{mw} \times 10^{13}$ m^2/s	Sep. Factor
Method 1					
Unfunc. PDMS		0	4.68	7.17	8510
Acetate	$-CH_2CO_2CH_3$	10	2.25	7.37	4040
		20	**4.84**	16.82	3810
Di-Acetate	$-CH(CO_2CH_3)_2$	10	3.17	7.21	5800
Hexanoate	$-CH_2CO_2(CH_2)_4CH_3$	10	**5.63**	6.88	**10760**
		20	2.50	6.21	5280
Cyano	$-CH_2CN$	10	3.43	6.75	6690
		20	1.47	9.04	2160
Octyl	$-(CH_2)_7CH_3$	10	2.77	2.95	**12200**
Benzyl	$-CH_2Ph$	10	3.80	5.06	**9800**
PentaFluroBenzyl	$-CH_2C_6F_5$	10	2.55	3.73	**8930**
		20	1.35	4.19	4240
Phenyl Ether	$-CH_2OPh$	10	2.98	5.71	6830
Ethyl Ether	$-CH_2OC_2H_5$	10	4.10	6.57	8170
		20	4.26	7.48	7440
Method 2					
Alkenyl	$-CH=CH_2$	10	**7.64**	12.36	8160
		20	4.06	7.56	7020
Amino	$-N(CH_3)_2$	20	2.97	13.61	2910
Cyano	$-CH_2CN$	10	3.06	6.18	6490
		20	3.49	8.95	5120

Table 5.2 - Chloroform Separation, $T = 25°C$, $w_{cf} = 0.003$

5.1.2.1 Effect of Functional Group

The various functional groups have similar effects upon the separation from water of chloroform, pyridine and MIBK. Generally the addition of a functional group decreases organic permeability. The major exception is the allyl group, which at 10% functional loading can be seen to enhance organic permeability for each of the three separations. The other anomaly concerns ester groups which at certain functional loadings enhance chloroform permeation. It would appear that chloroform permeability is extremely

sensitive to ester functional loading, displaying over a two fold change in magnitude as both acetate and hexanoate loadings are increased from 10% to 20%. It is curious to note that the change occurs in opposite directions, permeability increasing as acetate loading is increased from 10 to 20%, whilst decreasing as hexanoate loading is increased in the same manner. As for phenol / water separation, there would appear to be an important trade-off in performance between increased membrane polarity and organic content.

Functional Group *R*	**Chemical Structure**	**Loading** %	$S^a_p D_{mp} \times 10^{11}$ **m²/s**	$S^a_w D_{mw} \times 10^{11}$ **m²/s**	**Sep. Factor**
Method 1					
Unfunc. PDMS		0	13.07	0.56	55.7
Acetate	$-CH_2CO_2CH_3$	10	4.44	0.43	25.0
		20	8.59	0.75	27.5
Hexanoate	$-CH_2CO_2(CH_2)_4CH_3$	10	11.06	0.45	**58.0**
		20	5.76	0.41	34.4
Cyano	$-CH_2CN$	10	10.22	0.52	47.1
		20	4.76	0.66	16.9
Octyl	$-(CH_2)_7CH_3$	10	6.66	0.19	**84.1**
Benzyl	$-CH_2Ph$	10	9.23	0.33	**66.0**
PentaFluroBenzyl	$-CH_2C_6F_5$	10	8.56	0.31	**66.0**
		20	3.93	0.17	54.4
Phenyl Ether	$-CH_2OPh$	10	7.35	0.30	**58.7**
Ethyl Ether	$-CH_2OC_2H_5$	10	8.56	0.42	48.9
		20	7.04	0.44	37.8
Method 2					
Alkenyl	$-CH=CH_2$	10	**15.77**	0.69	54.2
		20	**14.89**	0.83	42.6
Pyridyl	$-(C_5H_4N)$	10	5.10	0.47	26.3

Table 5.3 - Pyridine Separation, $T = 70°C$, $w_{pf} = 0.02$

Membranes containing basic groups do not perform well. This is to be expected as chloroform, pyridine and MIBK do not contain the acidic groups necessary for the acid / base interactions that occur with phenol molecules. The pyridyl functionalised membrane strongly inhibits pyridine permeation. It had been thought possible that the sorption of pyridine may be strongly enhanced by pyridyl functional groups following the principle of "like dissolves like". This would appear not to be the case unless the interaction is so strong that permeating pyridine molecules become partially immobilised within the membrane, leading to very low D_{mp}. For each separation some of the aromatic ring

functionalised membranes exhibit slight enhancement in selectivity compared to the unfunctionalised material.

Functional Group *R*	Chemical Structure	Loading %	$S^a_M D_{mM}$ × 10^{11} m^2/s	$S^a_w D_{mw}$ × 10^{11} m^2/s	Sep. Factor
Method 1					
Unfunc. PDMS		0	12.23	0.66	705
Hexanoate	$-CH_2CO_2(CH_2)_4CH_3$	20	6.32	0.79	310
PentaFluroBenzyl	$-CH_2C_6F_5$	10	9.59	0.43	**845**
Ethyl Ether	$-CH_2OC_2H_5$	20	6.68	0.61	468
Octyl	$-(CH_2)_7CH_3$	10	7.80	0.29	**1030**
Tridecyl	$-(CH_2)_{12}CH_3$	6.67 10	10.60 7.05	0.34 0.22	**1190** **1260**
Branched Heptyl *	$-C(CH_3)CH_2C(CH_3)_3$	10 12.5	6.64 6.19	0.27 0.27	**911** **886**
Method 2					
Alkenyl	$-CH=CH_2$	10	**28.73**	2.30	526

Table 5.4 - MIBK Separation, $T = 70°C$, $w_{mf} = 0.0075$

* For the branch heptane functional group there is only one CH_2 unit present between the silicon atom and attached group, as opposed to the usual two CH_2 units. (See fig. 3.1).

Significant enhancement in selectivity is achieved, for all three separations, by the introduction of long chain organic groups. The increased organic content strongly inhibits water permeation, almost certainly due to reduced sorption through interaction with the strongly hydrophobic chains. For MIBK separation, three separate long chain molecules are investigated. The membranes of functional loadings of 10% octyl, 6.67% tridecyl and 12.5% branched heptyl all contain exactly the same total organic content (i.e. the same total number of carbon atoms). It can be seen that the longer, straight chained molecule, tridecyl, out performs the shorter chain, octyl, which in turn out performs the branched chain. It appears likely that the branched molecule effectively fills more free volume than the straight chain, thus inhibiting diffusion, particularly of the larger permeating molecule MIBK. The straight chained molecules probably assume a linear orientation within the membrane structure, effectively producing channels of higher free volume through which larger molecules may diffuse more readily. It is probable that permeating molecules would have to travel a less tortuous path in the latter case. It would appear quite logical that a

smaller quantity of longer, straight chained molecules would produce a greater number of such channels.

5.1.3 Effect of Functional Groups upon Sorption and Diffusion

Where enhancements to organic permeability are made it is likely that the sorption coefficient is enhanced by interaction between the permeating organic and functional group, consistent with the theory that performance in rubbery membranes is controlled by sorption, as discussed in chapter 2. This theory is also consistent with a study performed upon ester functionalised PDMS membranes for CO_2 / CH_4 gas separation *(Ashworth et al, 1991)*. The increase in selectivity towards CO_2 was proved to be as a result of an increase in solubility. As organic content within the membrane is increased, solubility of low polarity organic components is likely to increase, consistent with the principle of "like dissolves like". It is probable that the solubility of water is reduced by an increasing, hydrophobic, organic content within the membrane. Water solubility may be enhanced by the incorporation of polar groups, through hydrogen bonding interaction.

It is difficult to conceive of a mechanism by which diffusion coefficients of either organic or water could be enhanced by the addition of functional groups and indeed it is thought that they are reduced by the addition of the more bulky groups. Following free volume arguments, it is likely that bulky groups will inhibit the diffusion of the larger organic molecules to a greater extent than that of the smaller water molecules.

As well as producing direct effects upon the sorption and diffusion processes, the addition of functional groups may also indirectly affect one or both by causing a change in membrane physical properties. The addition of certain functional groups leads to a resultant membrane that is a lot more brittle than the unfunctionalised membrane. Brittleness tends to increase with increasing functional loading. Eventually a point is reached at which a functionalised film is so brittle that it is impossible to produce defect free membranes from it, using a pressing technique. An attempt was made to produce membranes of all functional groups listed in table 5.1 at a loading of 20%. It was found that it was particularly difficult to produce 20% loading membranes of bulky functional groups, due to the brittleness problem and in several cases this proved impossible, as

indicated by the lack of 20% membranes for certain groups within the table. As brittleness increases, membranes become more glassy and less rubbery in form, leading to rapidly decreasing organic component diffusion coefficients. If taken to extreme it is quite possible that a highly functionalised membrane that preferentially permeated water could be produced.

The performance of the diacetate functionalised membranes for the separation of phenol from water is disappointing when compared to that of the mono-acetate. The diacetate membranes are noticeably very brittle and certainly much more so than those produced containing the mono-acetate group. The fact that permeability increases whilst selectivity decreases dramatically with increasing diacetate loading could be an indication that slight membrane defects occur at the higher loadings.

It seems surprising that alkenyl groups increase organic permeability for all four separations. It is difficult to imagine that molecular interactions between the double bond and organic permeants would be strong, although it is possible that weak interaction could exist with the aromatic phenol ring. It is thought likely, therefore, that the alkenyl groups cause a beneficial change in the physical properties of the membrane, possibly leading to a decrease in brittleness at low to moderate loadings. It is worth noting that alkenyl functionalised membranes produce the most inconsistent results of any functionalised membrane and it is possible that it is difficult to produce them with a consistent membrane structure.

5.2 Comparison of Performance for Different Separations

Table 5.5 compares the water and organic species permeabilities, for various functionalised membranes, for the three different separations carried out at the same temperature, 70°C.

The marked differences in organic permeability can be explained by the chemical nature of the different components. Being a much less polar and consequently much more hydrophobic molecule than either phenol or pyridine, one would expect MIBK to exhibit much higher solubilities within hydrophobic PDMS. It would appear, however, that the permeability coefficients for MIBK are of similar magnitude to those of pyridine, in all

cases. This suggests that the membrane diffusivities of MIBK must be substantially lower than those of pyridine. The pyridine molecule has a lower molecular mass than MIBK and probably more crucially the geometries of the two molecules are very different. Having an aromatic ring, the pyridine molecule is extremely compact and flat, whereas the MIBK molecule is long and branched. It is probable that these geometric differences allow the pyridine molecule to pass more freely through the membrane structure, consistent with free volume arguments. It is also possible that MIBK has such a strong affinity for PDMS that it becomes partially immobilised within the membrane structure.

Func. Group	Loading %	Phenol $S^a_w D_{mw} \times 10^{11}$ m^2/s	Pyridine $S^a_w D_{mw} \times 10^{11}$ m^2/s	MIBK $S^a_w D_{mw} \times 10^{11}$ m^2/s		Phenol $S^a_p D_{mp} \times 10^{11}$ m^2/s	Pyridine $S^a_p D_{mp} \times 10^{11}$ m^2/s	MIBK $S^a_M D_{mM} \times 10^{11}$ m^2/s
Method 1								
Unfunc. PDMS	0	0.46	0.56	0.66		2.15	13.10	12.20
Acetate	10	0.76	0.43			2.75	4.44	
	20	2.11	0.75			7.58	8.59	
Hexanoate	10	0.56	0.45			3.47	11.11	
	20	0.69	0.41	0.79		4.88	5.76	6.32
Cyano	10	0.52	0.52			3.55	10.20	
	20	0.87	0.66			5.07	4.59	
Octyl	10	0.17	0.19	0.29		1.23	6.66	7.80
Benzyl	10	0.39	0.33			2.26	9.23	
PF Benzyl	10	0.33	0.31	0.43		1.30	8.56	9.59
Phenyl Ether	10	0.36	0.30			1.43	7.35	
Ethyl Ether	10	0.41	0.42			3.07	8.56	
	20	0.56	0.44	0.61		4.48	7.04	6.68
Method 2								
Allyl	10	0.90	0.69	2.30		4.16	15.80	28.70
	20	0.45	0.83			1.03	14.90	
Pyridyl	10	0.62	0.47			5.57	5.10	

Table 5.5 - Comparison of Performance for Three Separations, $T = 70°C$

If water transport were unaffected by the transport of the organic species, one would expect that $S^a_w D_{mw}$ for a given membrane would be very similar for all separations. This is obviously not the case and coupling theory needs to be applied to account for the phenomenon. As discussed in chapter 2, membrane solubility and / or diffusivity may be increased by membrane swelling, caused by the sorption of an organic species. In all cases $S^a_w D_{mw}$ is significantly higher in the presence of MIBK rather than phenol or pyridine.

This is to be expected as it has already been stated that the solubility of MIBK is thought to be higher than the other two, leading to greater swelling. For unfunctionalised PDMS, water permeability is greater in the presence of pyridine than phenol. This suggests that phenol has a lower solubility in PDMS than pyridine, probably due to the highly polar -OH group, although it is also possible that water sorption is enhanced by the presence of the highly hydrophilic pyridine, sorbed into the membrane.

Geometric factors are also expected to be of importance in determining the low phenol permeability coefficients. The phenol molecule has a mass nearly 20% greater than that of the pyridine molecule. It is planar, although is not quite as flat as the pyridine molecule, owing to the protruding -OH. Thus phenol membrane diffusivity would be expected to be a little lower than that of pyridine. Also, as has been discussed in chapter 2, it has been found that the diffusivities of alcohols in PDMS are strongly influenced by Van der Waals interactions between the membrane and the polar -OH group. The same interactions could exist with phenol, slowing transport of the molecule, although the bulky aromatic phenol ring would shield the polar group from these interactions to some degree.

It can be seen that $S^a{}_w D_{mw}$, for all functionalised membranes, are broadly similar in the presence of either phenol or pyridine. In the cases where phenol permeability is strongly enhanced by the incorporation of a functional group and pyridine permeability is not, it can be seen that $S^a{}_w D_{mw}$ becomes higher in the presence of phenol. This is totally consistent with the theory that the effect of the beneficial functional group is to increase organic sorption, leading in turn to increased swelling and water permeability. From these observations it would appear sensible to conclude that the large differences between phenol and pyridine permeabilities are mainly due to phenol having a much lower membrane diffusivity.

As discussed in chapter 2, it is well known that chloroform has a high solubility in PDMS. Although it has the highest molecular mass of the four organic components considered, it is a compact molecule and likely to display reasonably high membrane diffusivity. A combination of these two factors explains the exceptionally good performance of PDMS, for the separation of chloroform from water.

5.3 Effect of Functional Loading

From tables 5.2 and 5.3, it can be seen that for both chloroform and pyridine separations, increasing functional loading from 10 to 20% generally leads to a decline in membrane performance. This suggests that an optimum loading may exist at which point the positive influence of the functional group exceeds the negative influence of changing membrane properties to the greatest extent. In order to test this theory, octyl functionalised membranes of varying functional loading are produced and tested for chloroform, pyridine and MIBK separations. The results are displayed in figs. 5.2 - 5.4.

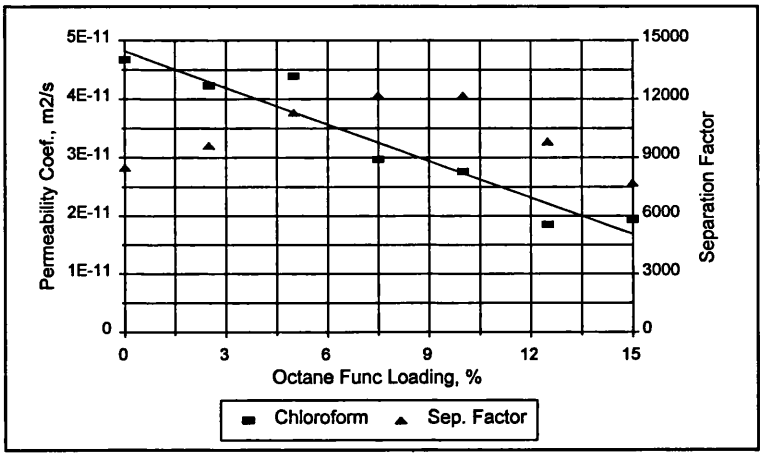

Fig. 5.2 - Chloroform Separation, Effect of Functional Loading

Octyl Functionalised PDMS, $P_{Tp} < 2$ mbar, $T = 25°C$

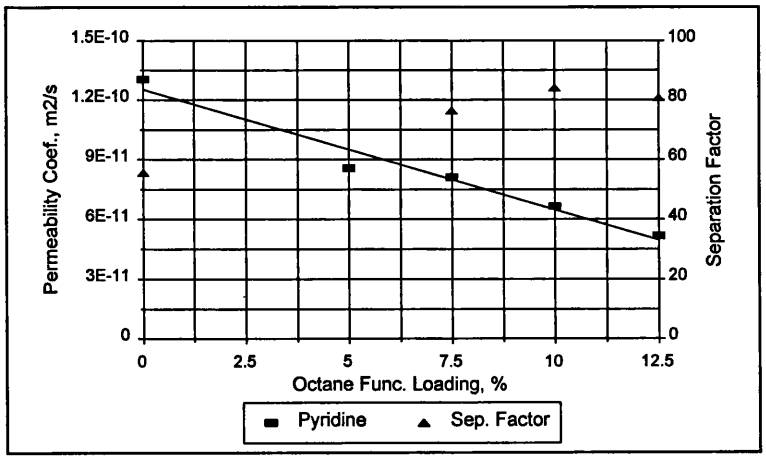

Fig. 5.3 - Pyridine Separation, Effect of Functional Loading

Octyl Functionalised PDMS, $P_{Tp} < 2$ mbar, $T = 70°C$

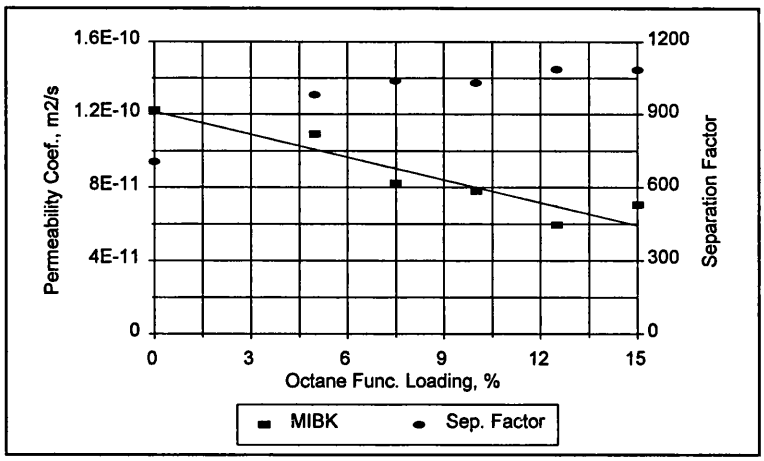

Fig. 5.4 - MIBK Separation, Effect of Functional Loading

Octyl Functionalised PDMS, $P_{Tp} < 2$ mbar, $T = 70°C$

In all three cases a fairly good linear correlation exists between decline in organic permeability and increasing octyl loading. The separation factor initially increases with increasing functional loading and reaches a definite maximum for chloroform and pyridine separations at around 10%. For MIBK separation there is very little change in separation factor between a loading of 7.5 and 15%. Beyond 15% it became impossible to produce defect free membranes, due to the extreme brittleness of the siloxane films.

5.4 Membrane Selection

When assessing which functionalised membrane would give the best overall performance for a given separation, it is worth remembering that component fluxes are inversely proportional to membrane thickness. A high selectivity / low permeability membrane can be produced to give acceptable fluxes by simply making it thinner, to a certain physical limit where the membrane becomes mechanically too weak. Often it is not desirable to use membranes of the minimum possible thickness as organic flux may be controlled by feed side boundary layer resistance and in these cases using a thinner membrane would lead to a large increase in water flux, but only a small increase in organic flux. As it has been shown that both chloroform and MIBK fluxes are strongly affected by feed side boundary resistance, it is probable that the functionalised membrane displaying the highest separation factor would be the most effective for the separation of these two components from water, regardless (within reason) of permeability. For phenol and pyridine separation from water, separation factors are much lower and hence feed side boundary resistance has less

influence upon organic flux. For this reason it would probably be advantageous to use relatively thin membranes and / or membranes of high permeability. The best membrane may, therefore, not necessarily be the one that displays the highest separation factor. These considerations are further discussed in chapters 6 & 7.

When evaluating the effectiveness of a pervaporation membrane, it is interesting to compare the separation factor achieved with that which would be obtained purely by process of evaporation. In a recent study *(Wijmans and Baker, 1993)* it was argued that the transport of a component could be described in a thermodynamically equivalent manner to the classical solution-diffusion model by a two step process. It is assumed that evaporation of the liquid feed occurs to produce a saturated vapour which then permeates through the membrane under a partial pressure gradient driving force. It should be emphasised that the evaporation step does not in reality occur, but that in theory pervaporation from the liquid phase should yield exactly the same performance as vapour permeation from the saturated vapour phase above the liquid feed.

The assumption of this thermodynamically equivalent model allows for the definition of both independent evaporation and membrane separation factors.

$$\alpha_{evap} = \frac{(p_{if}/p_{ip})}{(x_{if}/x_{jf})} \qquad (5.1)$$

$$\alpha_{mem} = \frac{(y_{ip}/y_{jp})}{(p_{if}/p_{jf})} \qquad (5.2)$$

Where p_{if} is given by:-

$$p_{if} = \gamma_i x_{if} P_i^{sat} \qquad (4.2)$$

It can clearly be seen that overall separation factor is the product of the two individual factors:-

$$\alpha = \alpha_{evap} \times \alpha_{mem} \qquad (5.3)$$

In order for the separation to be enhanced, from that achieved purely through vapour-liquid equilibrium, α_{mem} must clearly be of magnitude greater than 1.

Table 5.6 displays the various factors for unfunctionalised PDMS and the membrane displaying the highest selectivity, for each separation.

Organic	α_{evap}	Mem.	α_{mem}	α	Mem.	α_{mem}	α
Phenol	0.74	Unfunc.	23.9	17.7	10% Pyridyl	43.0	31.8
Chloroform	7350	Unfunc.	1.16	8510	10% Octyl	1.66	12200
Pyridine	7.46	Unfunc.	7.47	55.7	10% Octyl	11.3	84.1
MIBK	129	Unfunc.	5.47	705	10% Tridecyl	9.77	1260

Table 5.6 - Comparison of Pervaporation with Evaporation

In all cases enhanced separation, above that achievable purely by evaporation, is realised, although only modest enhancements are achieved for chloroform separation. It is interesting to note that α_{mem} increases dramatically with decreasing α_{evap} and that α_{evap} appears the dominant factor in determining α.

5.5 Effect of Cross-Linking Density

One effect of increasing organofunctional loading is that it changes the cross-linking density of the resultant PDMS film. As functional loading is increased, a higher proportion of the functionalised PHMS or silane material is required and consequently the proportion of the long chained silanol terminated PDMS is reduced. This leads to an increased number of cross-links within the film, which could reduce membrane flexibility and free volume and in itself be an important parameter in determining membrane performance.

In a study of the separation of dioxane from water, using PDMS membranes produced via a sol gel process *(Lee et al, 1989)*, it was found that both permeability and selectivity towards dioxane reduced significantly with increasing cross-linking. It was concluded that the decreasing mobility of the cross-linked chains makes the diffusion process more size dependent, retarding larger molecules to a greater extent than small molecules. It should be noted that cross-linking densities were relatively high as the monomers used in the production of the films were small in chain length. In a separate study *(Takegami et al, 1992)* similar conclusions were drawn in which, for ethanol / water separation, permeability and selectivity towards ethanol increased with decreasing cross-linking density, until the average number of dimethylsiloxane units between cross links exceeded 50. PDMS films were produced using a similar method to that described within this study,

in which cross-linking density was controlled by using vinyl (as opposed to silanol) terminated PDMS monomers of varying chain length. As the molecular mass of the monomer was increased from 1000 to 15000, ethanol permeability was found to double and separation factor found to increase by one third. In a third study *(Blume et al, 1991)* the pure component sorption of three organics, including chloroform, in PDMS was found to decrease quite dramatically with increasing cross linking density. Cross-linking density was controlled by the addition of varying quantities of cross linking agent to a PDMS monomer. Again, all cross-linking densities were relatively high, the number of siloxane units between cross-links being of the order of 16.

5.5.1 Varying PDMS : PHMS Ratio

A number of unfunctionalised PDMS membranes are produced, using silanol terminated PDMS of molecular mass 74000, with varying ratios of PHMS to PDMS starting material. In each case tetraethoxysilane is added in excess to complete the cross linking process. The performance of these membranes for the phenol and chloroform separations is displayed in figs. 5.5 & 5.6.

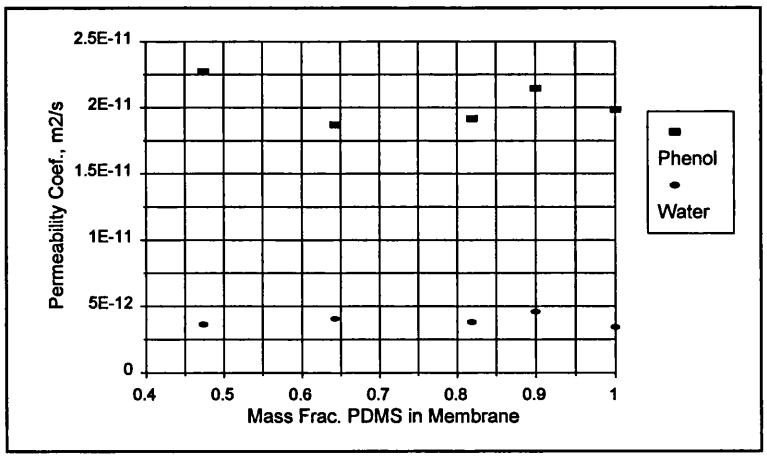

Fig. 5.5 - Phenol Separation, Effect of Cross-Linking Density

Unfunctionalised PDMS, T = 70°C, w_{pf} = 0.05

The cross-linking densities of all functionalised membranes produced fall within the range covered in figs. 5.5 & 5.6. It appears that, within the bounds of experimental error, cross-linking density has very little effect upon separation performance across this range. It should be noted that although a decline in performance with increased cross-linking density

is not observed, the cross-linking densities fall in a much lower range than that covered in the above mentioned studies. The average number of siloxane units between cross-links, for the membranes reported in figs. 5.5 & 5.6, range from approximately 50 - 1000. Also, as the silanol terminated PDMS used has a chain length of 1000 units, even when PHMS content within the completed film is high, there will still be a 1000 unit gap between many cross links.

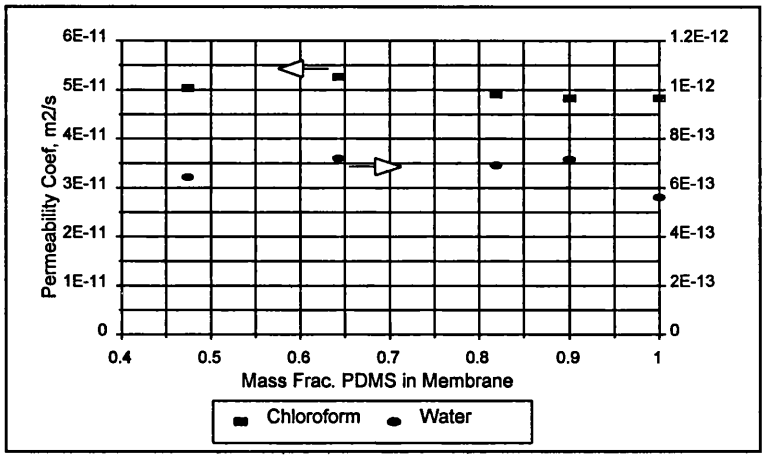

Fig. 5.6 - Chloroform Separation, Effect of Cross-Linking Density

Unfunctionalised PDMS, $T = 25°C$, $w_{cf} = 0.003$

It may be concluded that, within the range investigated, changing cross-linking density has a negligible effect upon membrane performance. Performance differences between different functionalised membranes must, therefore, be attributed to the chemical nature of the various functional groups.

5.5.2 Varying PDMS Chain Length

In addition membranes are produced of a fixed PDMS / PHMS mass ratio of 10:1, but of varying silanol terminated PDMS chain length. The performance of these membranes for phenol separation is displayed in fig. 5.7.

Fig. 5.7 displays a decline in performance with decreasing monomer chain length, consistent with the findings of the study reported above. The drop in performance between a silanol terminated PDMS chain of molecular mass 74000 and 18000 is slight and a significant reduction is only observed at the lowest molecular mass of 4200. It may be

concluded that it is sensible to use a high chain length, of at least molecular mass 18000, for the production of PDMS membranes. This has been the case for all functionalised membranes.

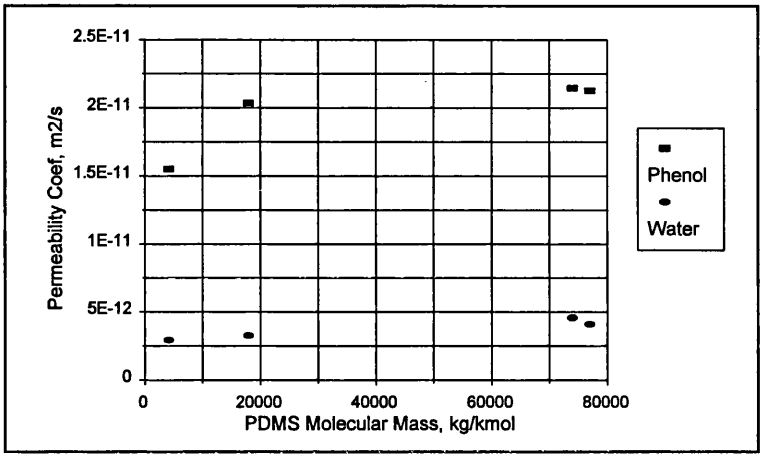

Fig. 5.7 - Phenol Separation, Effect of PDMS Monomer Chain Length

Unfunctionalised PDMS, $T = 70°C$, $w_{pf} = 0.05$

5.6 Closing Remarks

It is clearly demonstrated that separation performance can be significantly enhanced by the incorporation of organofunctional groups into the membrane structure. The greatest benefits may be realised if the organofunctional group has a strong affinity for the permeating organic species. It is suggested that three families of functionalised PDMS membranes could be produced which would each have general application for a variety of separations. For low polarity organic species, membranes containing a long, straight, hydrocarbon chain should display high selectivity, principally by inhibiting water transport. For acidic species, organic component transport may be significantly facilitated by the incorporation of a strongly basic group. Although the production of an acid functionalised membrane is not achieved within this study, it is thought, using the same principle, that the transport of basic species should be facilitated by the incorporation of an acidic group.

The greatest source of "non-ideality", for the separations considered within this study is the coupling effect of organic transport upon water transport. This is emphasised by the fact that water permeability is a strong function of permeating organic species. Although in all

other respects "ideal" behaviour is observed at the feed concentrations used, it is only safe to assume that coupling effects are negligible at very low organic component feed concentrations.

When chemically modifying membrane materials, it is very important to consider the indirect effects upon separation performance, realised through changing the physical properties and structure of the resultant membrane.

Chapter 6

Process Modeling and Operating Considerations

Scope of Chapter 6

The model describing membrane transport, developed within chapter 4, is extended to incorporate the effect of feed side boundary layer resistance, to produce a single, integrated pervaporation model. The model is used to investigate the effect of changing operating variables, for systems likely to be typical of those employed for large scale operations.

The effect of changing condensation temperature is investigated and the problems associated with the production of a solid phase, at low temperatures, discussed. A problem with the existing Arrhenius relationship between flux and temperature is highlighted; it predicts that component transport will occur even when there is no longer a driving force for permeation. A new model suggesting an Arrhenius relationship with permeability coefficient, which successfully predicts zero flux under conditions of zero driving force, is proposed and fitted to experimental data. It is subsequently shown that, for a given feed temperature and composition, a maximum condensation temperature exists, above which no transport will occur.

The benefits of combining phase separation with pervaporation, for the case where permeate composition exceeds the limit of miscibility, is demonstrated. The various options for module configuration are discussed and optimal configurations suggested for each separation investigated.

6.1 Integrated Pervaporation Model

As convective flow of the organic component may be generally neglected within the feed side boundary layer, for most practical organophilic pervaporation applications (see chapter 2), transport of the preferentially permeating component may be described by:-

$$J_o = \left(\frac{D_{lo}}{\delta_l}\right)(C_{o(b)} - C_{o(mb)}) \qquad (2.10)$$

For low C_o, the density of the boundary layer is approximately equal to the density of water, hence expressing *eq. (2.10)* in molar concentration terms yields:-

$$J_{\Phi o} = \left(\frac{D_{lo}}{\delta_l}\right)\left(\frac{\rho_w}{MR_w}\right)(x_{o(b)} - x_{o(mb)}) \qquad (6.1)$$

Where:$J_{\Phi o}$ = Molar Flux, kmol/m^{2}hr

Rearranging *eq. (6.1)* yields:-

$$x_{o(mb)} = x_{o(b)} - \frac{J_{\Phi o}\,\delta_l\,MR_w}{\rho_w\,D_{lo}} \qquad (6.2)$$

It may be recalled, from chapter 4, that the general membrane transport relationship can be expressed as:-

$$J_{\Phi i} = \frac{S^a_{\ i}\,D_{mi}\,\rho_m}{\delta_m\,MR_i}\left(\gamma_i\,x_{if} - y_{ip}\,\frac{P_{Tp}}{P_i^{sat}}\right) \qquad (4.7)$$

Given that in the presence of significant boundary layer resistance, x_{if} should be placed equal to $x_{o(mb)}$, a combination of *eqs. (4.7) & (6.2)* yields:-

$$J_{\Phi o} = \frac{A_o\frac{\rho_m}{\delta_m}}{(1 + A_o\frac{\rho_m}{\delta_m}B_o)}\left(\gamma_o\,x_{o(b)} - y_{op}\,\frac{P_{Tp}}{P_o^{sat}}\right) \qquad (6.3)$$

Where:-

$$A_i = \frac{S^a_{\ i}\,D_{mi}}{MR_i} \qquad (4.9)$$

B_o is defined as:-

$$B_o = \frac{\delta_l\,\gamma_o\,MR_w}{D_{lo}\,\rho_w} \qquad (6.4)$$

A combination of *eq. (6.3)* with *eqs. (4.7) & (4.9)* for the water component yields:-

$$\frac{J_{\Phi o}}{J_{\Phi w}} = \frac{y_{op}}{1 - y_{op}} = \frac{\frac{A_o}{(1 + A_o\frac{\rho_m}{\delta_m}B_o)}\left(\gamma_o\,x_{o(b)} - y_{op}\,\frac{P_{Tp}}{P_o^{sat}}\right)}{A_w\left(\gamma_w\,x_{wf} - (1-y_{op})\,\frac{P_{Tp}}{P_w^{sat}}\right)} \qquad (6.5)$$

Although containing more parameters than *eq. (4.10)*, *eq. (6.5)* again simply reduces to a quadratic equation in y_{op}:-

$$y_{op}^{2}\left(A_w\frac{P_{Tp}}{P_w^{sat}} + A_oB_oA_w\frac{\rho_m}{\delta_m}\frac{P_{Tp}}{P_w^{sat}} - A_o\frac{P_{Tp}}{P_o^{sat}}\right) +$$

$$y_{op}\left(A_w\gamma_w x_{wf} - A_w\frac{P_{Tp}}{P_w^{sat}} + A_oB_oA_w\frac{\rho_m}{\delta_m}\gamma_w x_{wf} - A_oB_oA_w\frac{\rho_m}{\delta_m}\frac{P_{Tp}}{P_w^{sat}} + A_o\frac{P_{Tp}}{P_o^{sat}} + A_o\gamma_o x_{o(b)}\right)$$

$$- A_o\gamma_o x_{o(b)} = 0 \qquad (6.6)$$

6.2 Effect of Operating Variables

Using *eqs. (4.7), (6.3) & (6.6)* to describe the transport of both water and organic components, the effect of varying $x_{o(b)}$, k_{lo}, δ_m and P_{Tp} upon overall performance can be determined. The results presented below are theoretical curves, produced from these equations, using the experimentally determined membrane permeability coefficients for pure PDMS, as reported in tables 5.1 - 5.4. Chloroform and Phenol separations from water are chosen to represent the extremes of separation performance. Similar trends are found for Pyridine and MIBK separation from water, the results lying in between the two extremes.

It should be noted that the model takes no account of coupling effects. As is demonstrated within chapters 4 & 5, it is not always safe to assume that these effects are negligible. For phenol and chloroform separations, however, it is shown that coupling effects are very low. Water transport may be slightly affected, particularly at very low organic concentrations where water permeability would be expected to decline.

6.2.1 Feed Concentration, $x_{o(b)}$

For the given fixed conditions specified, the effect of changing $x_{o(b)}$ upon flux and separation factor is illustrated in figs. 6.1 & 6.2.

In both cases, when $p_{o(b)} >> P_{Tp}$ the organic component flux increases linearly with increasing $x_{o(b)}$. At very low $x_{o(b)}$, the term $y_{op}\frac{P_{Tp}}{P_o^{sat}}$ in *eq. (6.3)* becomes significant and a non-linear increase is observed, particularly apparent in fig. 6.2.

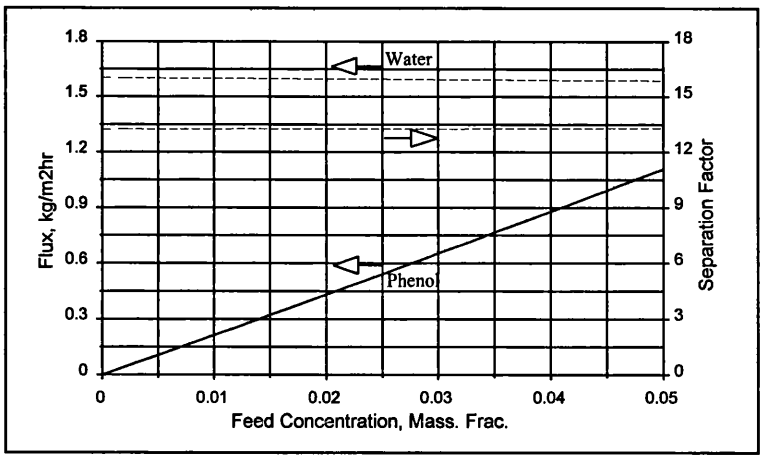

Fig. 6.1 - Phenol Separation, Effect of $x_{o(b)}$.

Unfunc. PDMS, $k_{lo} = 2.5\times10^{-5}$ m/s, $\delta_m = 10$ μm, $P_{Tp} = 1$ mbar, $T = 70$°C

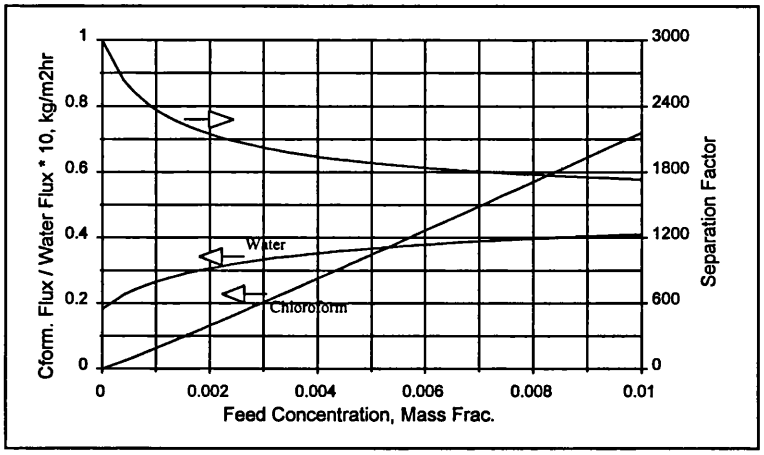

Fig. 6.2 - Chloroform Separation, Effect of $x_{o(b)}$.

Unfunc. PDMS, $k_{lo} = 2.5\times10^{-5}$ m/s, $\delta_m = 50$ μm, $P_{Tp} = 20$ mbar, $T = 25$°C

Water flux is influenced by two competing effects. Considering the driving force for water transport from *eq. (4.7)*, $\left(\gamma_w x_{wf} - y_{wp}\frac{P_{Tp}}{P_w^{sat}}\right)$, it can be seen that as $x_{o(b)}$ increases both x_{wf} and y_{wp} decrease. For the phenol separation it can be seen that water flux remains essentially constant, within the stated feed concentration range. In this case a very low P_{Tp} is required in order to achieve good performance and hence the term $y_{wp}\frac{P_{Tp}}{P_w^{sat}}$ is always very small. For the chloroform separation, $\frac{P_{Tp}}{P_w^{sat}} = 0.63$ and hence the term $y_{wp}\frac{P_{Tp}}{P_w^{sat}}$ becomes significant at low y_{op}. This leads to a reduction in water flux with decreasing organic concentration. Conversely water flux increases significantly, in a non-linear

manner, with increasing chloroform feed concentration, leading to the observed decrease in separation factor.

6.2.2 Liquid Boundary Layer Mass Transfer Coefficient, k_{lo}

The effect of varying k_{lo} is displayed in figs. 6.3 & 6.4.

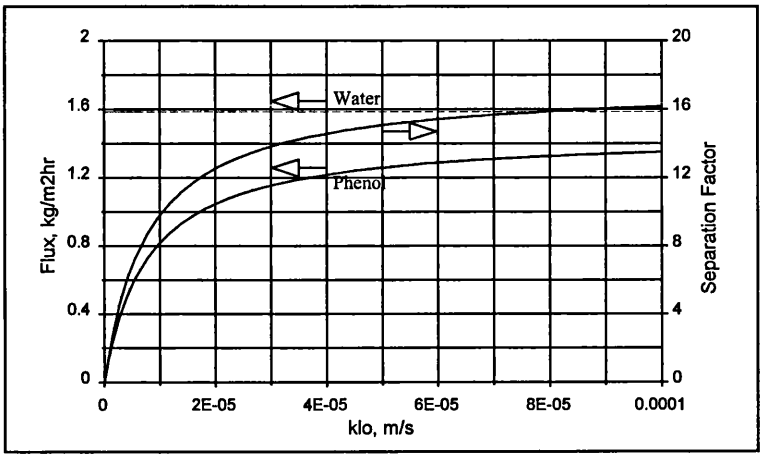

Fig. 6.3 - Phenol Separation, Effect of k_{lo}

Unfunc. PDMS, $x_{o(b)} = 0.05$, $\delta_m = 10$ μm, $P_{Tp} = 1$ mbar, $T = 70°C$

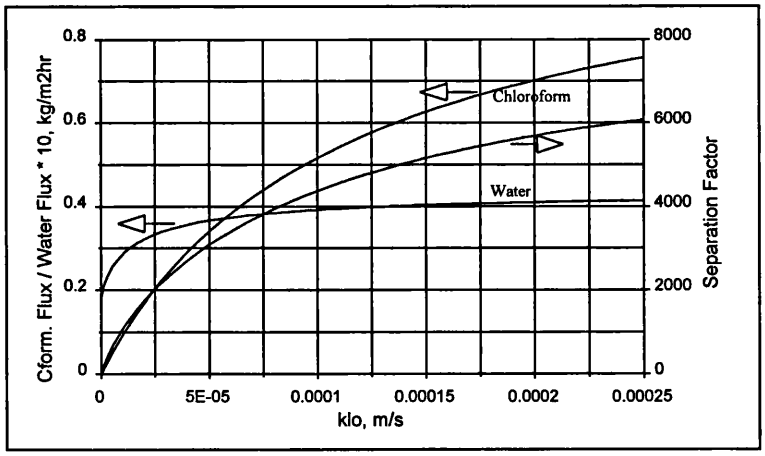

Fig. 6.4 - Chloroform Separation, Effect of k_{lo}

Unfunc. PDMS, $x_{o(b)} = 0.003$, $\delta_m = 50$ μm, $P_{Tp} = 20$ mbar, $T = 25°C$

It can clearly be seen that organic component flux is strongly influenced by k_{lo} and that in the region of technical feasibility, chloroform transport may be seriously inhibited by boundary layer resistance. Although water flux is unaffected directly by boundary layer

resistance, it is once again affected in an indirect manner by the $y_{wp}\frac{P_{Tp}}{P_w^{sat}}$ term. Once more, this effect is particularly apparent for the chloroform separation displayed in fig. 6.4. For the phenol separation, water flux is essentially unaffected by k_{lo}.

6.2.3 Effective Membrane Thickness, δ_m.

The effect of varying δ_m is displayed in figs. 6.5 & 6.6.

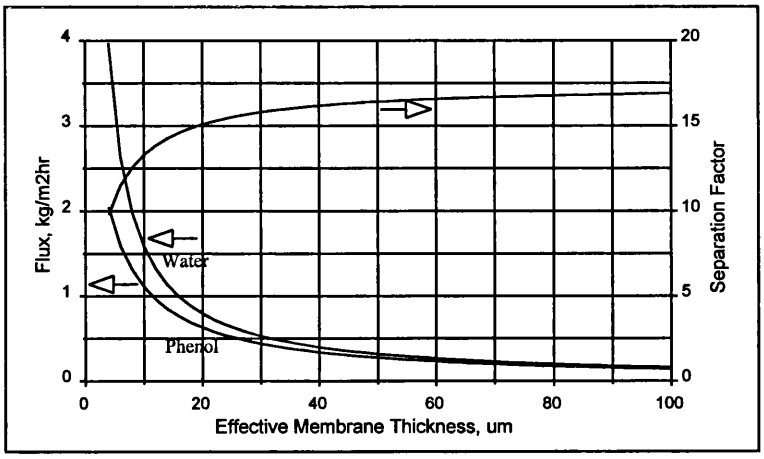

Fig. 6.5 - Phenol Separation, Effect of δ_m

Unfunc. PDMS, $k_{lo} = 2.5\times10^{-5}$ m/s, $x_{o(b)} = 0.05$, $P_{Tp} = 1$ mbar, $T = 70°C$

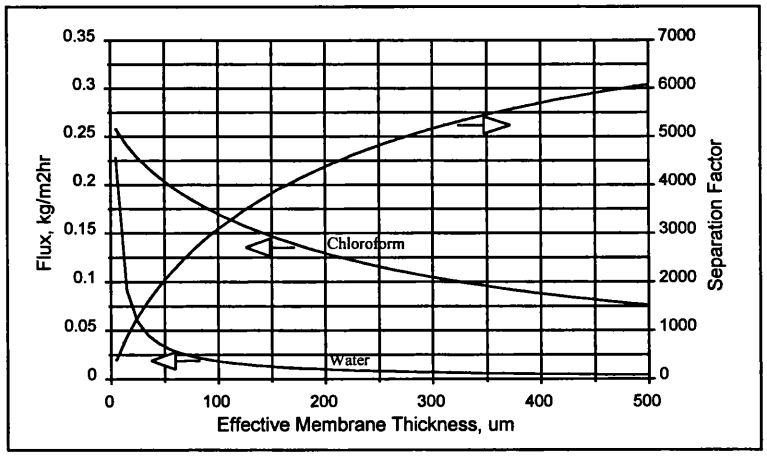

Fig. 6.6 - Chloroform Separation, Effect of δ_m

Unfunc. PDMS, $k_{lo} = 2.5\times10^{-5}$ m/s, $x_{o(b)} = 0.003$, $P_{Tp} = 20$ mbar, $T = 25°C$

In the absence of boundary layer resistance one would expect a direct inverse proportionality between flux and membrane thickness, with unchanging separation factor.

As can be clearly seen from figs. 6.5 & 6.6, at low δ_m boundary resistance can severely limit organic component flux. The effect of reducing δ_m in this region is to cause a dramatic increase in water flux with only a small increase in organic component flux, leading to poor separation factors. For commercial applications it would appear that the production of extremely thin PDMS films of the order of a few micrometers thick is not desirable, even for phenol separation. Indeed for VOC removal, fig. 6.6 indicates that it may well be beneficial to use relatively very thick membranes, in excess of 100 μm. It is logical to conclude that for such applications membrane improvements in separation factor are of much greater importance than improvements in total permeability.

6.2.4 Permeate Pressure, P_{Tp}

The effect of varying P_{Tp} is displayed in figs. 6.7 & 6.8.

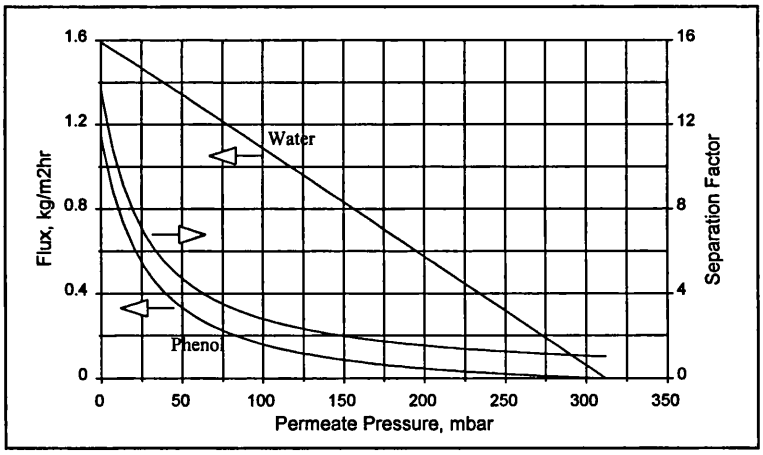

Fig. 6.7 - Phenol Separation, Effect of P_{Tp}

Unfunc. PDMS, $k_{lo} = 2.5\times10^{-5}$ m/s, $x_{o(b)} = 0.05$, $\delta_m = 10$ μm, $T = 70°C$

As feed side boundary layer resistance is low compared to membrane resistance, for the phenol separation, the performance curve of fig. 6.7 is very similar to that in the absence of boundary layer resistance, fig. 4.3. For the chloroform separation, figs. 6.8 & 4.4 display very different trends. As boundary layer resistance is now very significant, chloroform flux is inhibited to such an extent that $\alpha < \alpha_{evap}$. As discussed in chapter 4, this leads to an actual increase in α with increasing P_{Tp}, the ultimate value reached at the point when $P_{Tp} = P_{o(b)} + P_{wf}$ (i.e. at zero flux) being α_{evap}.

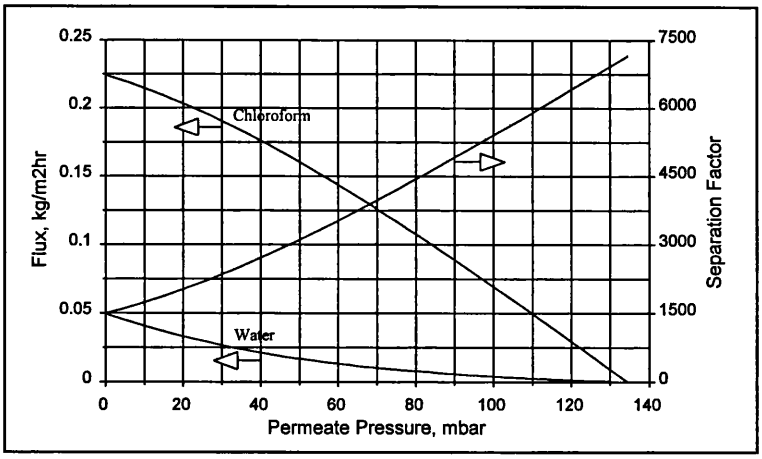

Fig. 6.8 - Chloroform Separation, Effect of P_{Tp}

Unfunc. PDMS, $k_{lo} = 2.5\times10^{-5}$ m/s, $x_{o(b)} = 0.003$, $\delta_m = 50$ μm, $T = 25$°C

It is quite possible to achieve a situation where $\alpha \approx \alpha_{evap}$ and thus α remains relatively independent of P_{Tp}. Such a situation under a set of realistic conditions, for MIBK separation from water, is displayed in fig. 6.9.

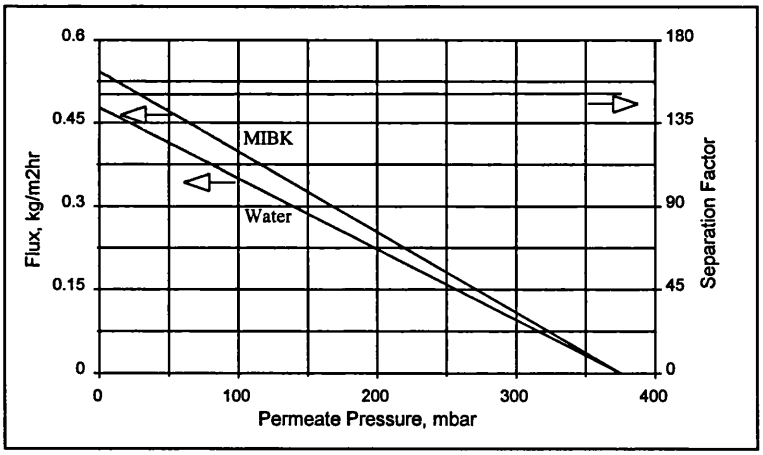

Fig. 6.9 - MIBK Separation, Effect of P_{Tp}

Unfunc. PDMS, $k_{lo} = 2.5\times10^{-5}$ m/s, $x_{o(b)} = 0.0075$, $\delta_m = 48.5$ μm, $T = 70$°C

In all cases component fluxes must still always increase with decreasing P_{Tp}.

6.3 Condensation Temperature Considerations

Maintaining a low permeate pressure solely by means of a vacuum pump is generally considered to be prohibitively expensive. It is usually commercially desirable to maintain the vacuum required through condensation of the permeate. In this case a low temperature

is required in order to both condense the vapour permeate and to reduce the vapour pressure in equilibrium with the condensate.

6.3.1 Solid Permeate Phase

One problem that becomes readily apparent is that in order to reduce the vapour pressure of volatile components to a sufficient level such that a substantial activity gradient for permeation exists, very low condensation temperatures may be required. It would not be desirable to operate at a condensation temperature of below 0°C, as at this temperature the water within the permeate would freeze leading to more complex and expensive module design in order to be able to handle such a solid phase stream. Additional material and energy costs would also be added by the need to use refrigerants to achieve such low temperatures.

Phenol is a solid under ambient temperatures and has a freezing point of 40°C. As displayed in fig. 6.7, low permeate pressures are required if adequate separation performance is to be achieved. At a temperature of 40°C, water has a saturated vapour pressure of 74 mbar and hence it is highly unlikely to be practicable to operate at such a temperature to avoid the problem of a solid phase. In a pilot plant scale investigation of the continuous pervaporation of aqueous phenol *(Boddeker et al, 1992)*, two condensers were operated in parallel using glycol/water mixtures to achieve condensation temperatures as low as -28°C. Whilst one condenser was employed in condensing permeate the other was defrosted at a temperature of 40°C in order to produce a liquid stream. Continuous operation was achieved by periodically alternating the two condensers between condensation and defrosting functions. It would appear that this would generally be the best configuration for achieving the separation of phenol and water.

The other three organics considered within the study all have freezing points well below that of water and in some cases it may well be economically attractive to operate at condensation temperatures in excess of 0°C. In order to increase the activity gradient for permeation it may be more sensible to elevate the feed temperature as opposed to employing very low condenser temperatures. Recall *eq. (4.7)*:-

$$J_{\Phi i} = \frac{S^a{}_i D_{mi} \rho_m}{\delta_m MR_i} \left(\gamma_i x_{if} - y_{ip} \frac{P_{Tp}}{P_i^{sat}} \right) \qquad (4.7)$$

By operating at elevated feed temperatures, P_i^{sat} increases and hence the term $y_{ip} \frac{P_{Tp}}{P_i^{sat}}$ decreases, leading to an increased driving force and allowing for higher P_{Tp} and condensation temperatures. A disadvantage of operating at elevated temperature is that the entire feed stream has to be heated and as water is the major component, large quantities of energy may be required. Sensible application of energy integration, using heat exchange in order to preheat the feed with the hot retentate stream, would limit the energy input required, which could be achieved by either heat exchange or direct steam injection.

6.3.2 Arrhenius Relationships

A problem with the approach described within chapter 4 for predicting the effect of temperature upon performance now becomes apparent. By rearranging *eq. (4.15)*:-

$$J_i = J_i^* \exp\left(\frac{-E_{ai}}{RT}\right) \qquad (4.15)$$

It can be seen that J_i may be predicted at any T by:-

$$J_{iT2} = J_{iT1} \exp\left(\frac{-E_{ai}}{R}\left(\frac{1}{T_1} - \frac{1}{T_2}\right)\right) \qquad (6.7)$$

At a fixed permeate pressure, it can be seen from *eq. (4.7)* that at a certain critical feed temperature the term $\left(\gamma_i x_{if} - y_{ip} \frac{P_{Tp}}{P_i^{sat}} \right)$ will become zero and hence no driving force for permeation will exist. Below this temperature component fluxes will be zero, however, *eq. (6.7)* predicts that flux will occur at any temperature. It may be concluded that *eqs. (4.15)* & *(6.7)* are only truly valid at sufficiently high feed temperatures and / or low permeate pressures such that the term $y_{ip} \frac{P_{Tp}}{P_i^{sat}}$ becomes negligible. If this is not the case, an alternative approach is proposed that separates the effect of temperature upon both membrane permeability and activity driving force. This is an extension of the approach adopted by Wijmans and Baker *(Wijmans and Baker, 1993)* in which separation factor is split into separate evaporation (driving force) and membrane factors, as discussed in chapter 5.

6.3.2.1 Proposed New Relationship

It may be recalled, from chapter 2, that an Arrhenius relationship between membrane diffusion coefficient and temperature has been reported:-

$$D_{mi0} = D_{mi0} * exp\left(\frac{-E_a}{RT}\right) \qquad (2.69)$$

Also, it should be remembered that, according to Flory Huggins thermodynamics, changing temperature has only a moderate effect upon sorption coefficient. It is, therefore, proposed that an Arrhenius relationship may exist between membrane permeability coefficient and temperature:-

$$S^a_i D_{mi} = S^a_i D_{mi} * exp\left(\frac{-E_a}{RT}\right) \qquad (6.8)$$

It should be noted that *eq. (6.8)* describes a relationship similar to that used within gas separation, using dense, polymeric membranes *(Neel, 1991)*. It is thought that it may only be valid for the case where membrane swelling is low, i.e. for low membrane concentrations, as is the case for the removal of trace organics from waste water using pervaporation and for gas separation. At high concentrations, departure from Henrys law for sorption and significant coupling effects may cause large deviation from the relationship described by *eq. (6.8)*.

$S^a_i D_{mi}$ may be determined at various feed temperatures using *eq. (4.7)*. Using the same data as that used to produce figs. 4.6 - 4.9, Arrhenius plots of $S^a_i D_{mi}$ are made and displayed in figs. 6.10 - 6.13.

The calculated activation energy values are displayed in table 6.1.

Organic	$-E_{ao}$, kJ/mol	$-E_{aw}$, kJ/mol
Phenol	15.2	30.6
Chloroform	17.4	33.9
Pyridine	19.9	34.1
MIBK	22.3	34.3

Table 6.1 - Activation Energies for Permeation

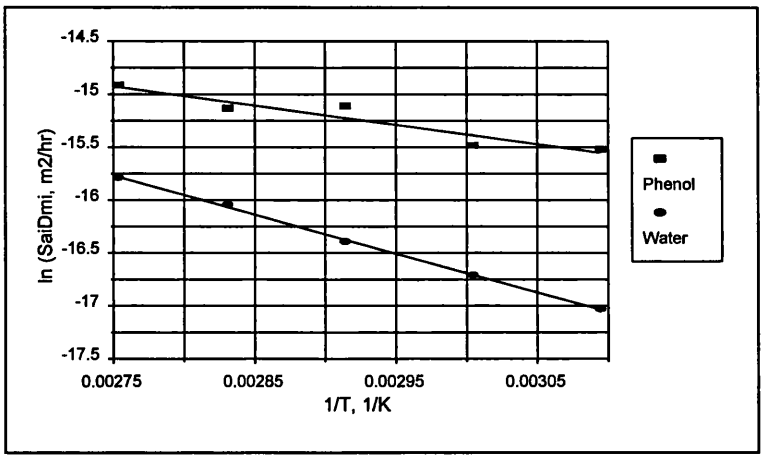

Fig. 6.10 - Phenol Separation, Arrhenius Plot

20% acetate func. PDMS, $w_{pf} = 0.05$, $P_{Tp} < 2$ mbar, $\delta_m = 106$ μm

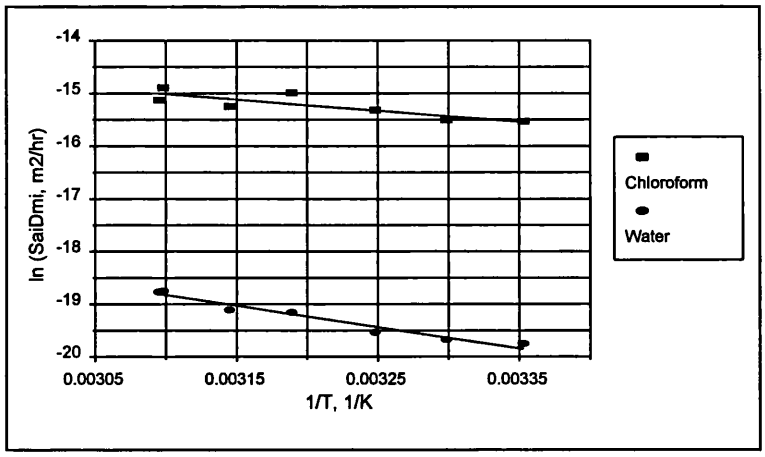

Fig. 6.11 - Chloroform Separation, Arrhenius Plot

Unfunctionalised PDMS, $w_{cf} = 0.003$, $P_{Tp} < 2$ mbar, $\delta_m = 106$ μm

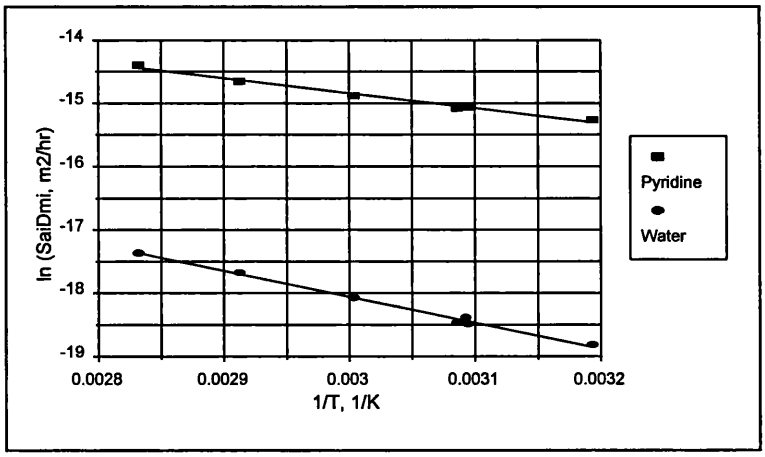

Fig. 6.12 - Pyridine Separation, Arrhenius Plot

Unfunctionalised PDMS, $w_{pf} = 0.04$, $P_{Tp} < 2$ mbar, $\delta_m = 161$ μm

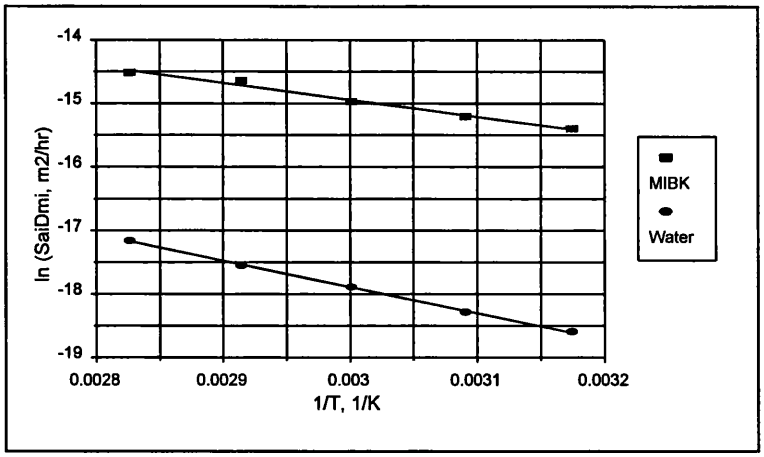

Fig. 6.13 - MIBK Separation, Arrhenius Plot

Unfunctionalised PDMS, $w_{Mf} = 0.0075$, $P_{Tp} < 2$ mbar, $\delta m = 151$ μm

$-E_{aw}$ values are closely similar, for all separations and very close in magnitude to those displayed in table 4.1. It is interesting to note that $-E_{ao}$ values are generally lower than those displayed in table 4.1 and are now more similar to each other in magnitude. This suggests that the true activation energy for sorption and diffusion through the membrane is only slightly dependent upon the nature of the permeating species. The previously reported values of activation energy are based upon *eq. (4.15)*, meaning that the values are a reflection of the temperature dependency of both membrane permeability and driving force.

A cautionary note should be made when considering the conclusions drawn from table 6.1 and figs. 6.9 - 6.13. The magnitude of calculated activation energies is very sensitive to experimental error.

In most cases described above, P_{Tp} is maintained at a low value such that the term $y_{ip} \frac{P_{Tp}}{P_i^{sat}}$ is generally small. For the phenol separation, $y_{pp} \frac{P_{Tp}}{P_i^{sat}}$ ranges from 35% of $\gamma_i x_{if}$ at the lowest temperature, 50°C, to 2.3% at the highest temperature, 90°C. For the pyridine separation the equivalent range is 12 - 1.4%. For the MIBK separation $y_{Mp} \frac{P_{Tp}}{P_i^{sat}} < 0.05\ \gamma_i x_{if}$ in all cases and for the chloroform separation $y_{cp} \frac{P_{Tp}}{P_i^{sat}} < 0.02\ \gamma_i x_{if}$ in all cases. A

thorough test of the new model would require further experiments under a greater number of conditions in which $y_{ip}\frac{P_{Tp}}{P_i^{sat}}$ is significant.

6.3.2.2 Comparison of Models

The results produced using the two different models, *eqs. (4.15) & (6.8)* are displayed for typical phenol and chloroform separations in figs. 6.14 & 6.15. In both cases a condenser temperature of 1°C was chosen. At all times the solubility limit of both phenol and chloroform in water is exceeded, within the condensed permeate. Each component, therefore, independently exerts its own saturated vapour pressure and P_{Tp} may be estimated by:-

$$P_{Tp} = P_1^{sat} + P_2^{sat} \qquad (6.9)$$

Where P_1^{sat} and P_2^{sat} are determined at the condensation temperature.

In both figures feed side boundary layer resistance is assumed to be negligible compared to membrane resistance. The label 1 denotes results obtained by *eq. (4.15)* and the label 2 denotes those obtained by *eq. (6.8)*.

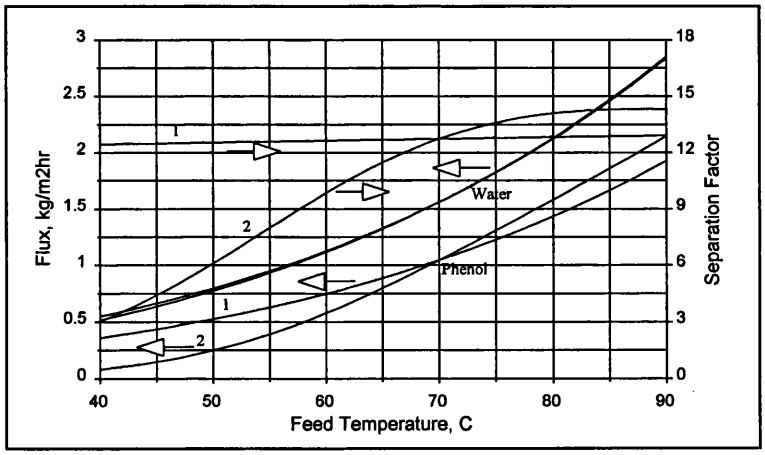

Fig. 6.14 -Phenol Separation, Comparison of Arrhenius Models

Unfunc. PDMS, w_{pf}= 0.05, T_{cond} = 1°C (P_{Tp} = 6.54 mbar), δ_m = 10 μm, $k_{lo} >> k_{mo}$

When the term $y_{ip}\frac{P_{Tp}}{P_i^{sat}}$ is much smaller than $\gamma_i x_{if}$, *eqs. (4.15) & (6.8)* produce similar results. When the former term becomes significant, a large deviation between the two models exists. As can be seen from fig. 6.14, for phenol separation, the water fluxes

predicted by the two different models are almost identical. This is due to the fact that P_w^{sat} >> P_{Tp}. The phenol flux drops more dramatically with feed temperature using model 2, leading to a subsequent decline in separation factor.

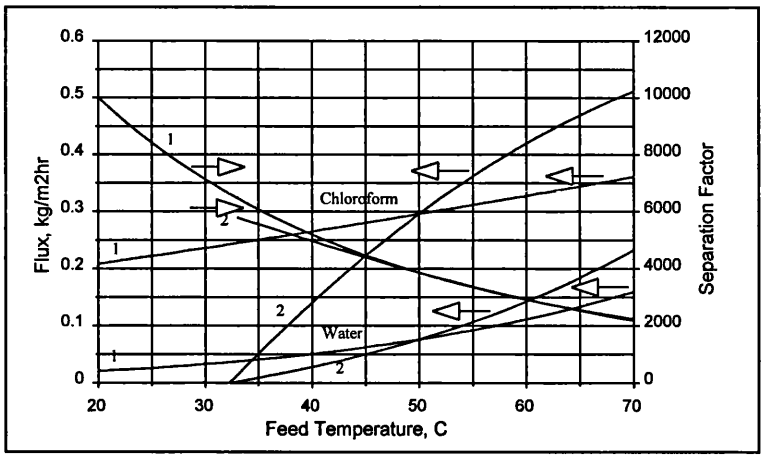

Fig. 6.15 -Chloroform Separation, Comparison of Arrhenius Models

Unfunc. PDMS, w_{cf} = 0.001, T_{cond} = 1°C (P_{Tp} = 90.93 mbar), δ_m = 50 μm, k_{lo} >> k_{mo}

For the chloroform separation, fig. 6.15, much greater declines are observed in both water and chloroform flux when using model 2. In both cases the $y_{ip}\frac{P_{Tp}}{P_i^{sat}}$ term is significant. As discussed before, a great advantage of using model 2 can be observed visually from fig. 6.15. When the feed temperature reaches 32°C an activity gradient for permeation no longer exists as the sum of the component vapour pressures on the feed side become equal to the permeate pressure. Whereas model 2 accurately predicts this behaviour, model 1 predicts that transport will still occur at and below this temperature.

A further advantage of using model 2 is that it allows for the easy incorporation of feed side boundary layer resistance, as the membrane permeability coefficient and not the overall flux is subject to the Arrhenius relationship. One could use model 1 easily only if the term $y_{ip}\frac{P_{Tp}}{P_i^{sat}}$ were negligible. In this case it would be possible to use *eq. (4.15)* to determine component fluxes in the absence of boundary layer resistance and then to use a resistances in series model (as described in chapter 2) to account for the feed side boundary layer. If $y_{ip}\frac{P_{Tp}}{P_i^{sat}}$ were not negligible, this term would vary strongly with temperature and one would expect a decreasing concentration gradient across the membrane with

decreasing temperature, which would neglect the validity of a resistances in series approach. An iterative technique would probably be required in order to simultaneously solve the transport equations in both boundary layer and membrane.

6.3.3 Effect of Condensation Temperature

Assuming model 2 and *eq. (6.9)*, the effect of varying condensation temperature upon both flux and separation factor, at varying feed temperatures, is displayed in figs. 6.16 & 6.17.

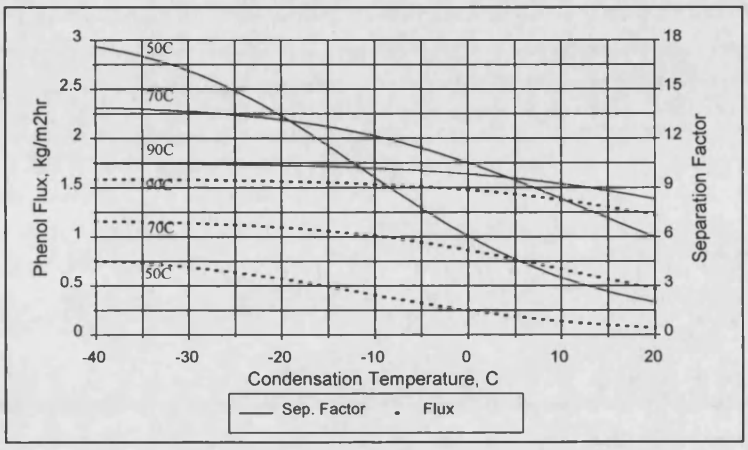

Fig 6.16 - Phenol Separation, Effect of Varying Condensation Temperature

Unfunc. PDMS, $w_{p(b)} = 0.05$, $\delta m = 10$ μm, $k_{lo} = 2.5 \times 10^{-5}$ m/s

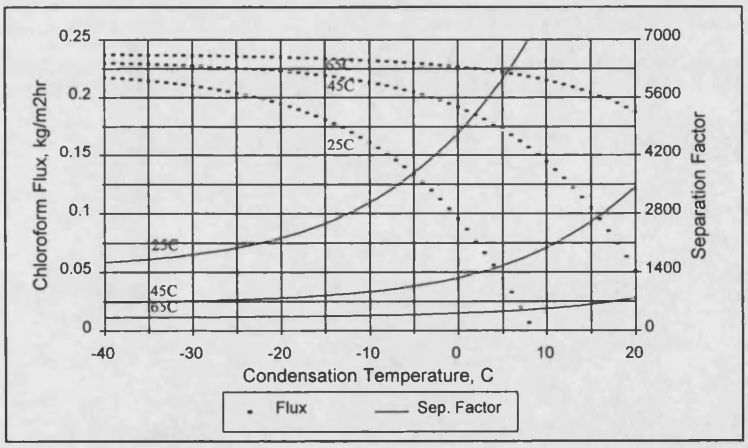

Fig 6.17 - Chloroform Separation, Effect of Varying Condensation Temperature

Unfunc. PDMS, $w_{c(b)} = 0.003$, $\delta m = 50$ μm, $k_{lo} = 2.5 \times 10^{-5}$ m/s

As one would expect, it can be seen from fig. 6.16 that phenol flux and hence separation factor, declines significantly with increasing condensation temperature as the $y_{ip}\frac{P_{Tp}}{P_i^{sat}}$ term becomes of increasing importance. The separation factor at an extremely low condensation temperature is higher for the lower feed temperature, as feed side boundary layer resistance is less important at the lower phenol flux. It should be remembered that under the same degree of turbulence, k_{lo} would increase significantly with increasing temperature, as discussed in chapter 4, leading to better performance at higher temperatures.

Similar effects upon chloroform flux are observed in fig. 6.17. The much larger separation factors observed at the lower temperature is due to a combination of the fact that chloroform permeation increases only slowly with increasing temperature (as displayed in fig. 6.15) and that separation factor increases towards the thermodynamic value as the activity driving force for permeation approaches zero (as indicated in fig. 4.4).

It would appear sensible to operate at a high feed temperature when separating phenol from water. This would allow for reasonable performance at a condensation temperature of above 0°C. It may be necessary to utilise a membrane of increased thickness in order to reduce the effect of feed side boundary layer resistance.

For the chloroform separation the choice of an optimal feed temperature is not at all straight forward. High flux can only be achieved at a condensation temperature of above 0°C if an elevated feed temperature is employed. Separation factor diminishes dramatically with increasing temperature, however and an optimum could only be found by a rigorous economic evaluation of a specifically defined separation problem.

6.3.4 Maximum Possible Condensation Temperature

As water is so much more volatile than phenol, the maximum condensation temperature for permeation to occur is always approximately equal to the feed temperature. This is due to the fact that both the feed side saturated vapour pressure and permeate pressure are approximately equal to the saturated vapour pressure of water, at each respective temperature. As chloroform is much more volatile than water, the permeate pressure is always very close to the saturated vapour pressure of chloroform, as long as the

concentration limit for chloroform solubility in water is exceeded in the permeate. Assuming concentrations well below the solubility limit in the feed, the required maximum condensation temperature will be much below the feed temperature. Fig. 6.18 displays the maximum temperature required, calculated from *eqs. (4.2) & (6.9)*, for varying feed concentration.

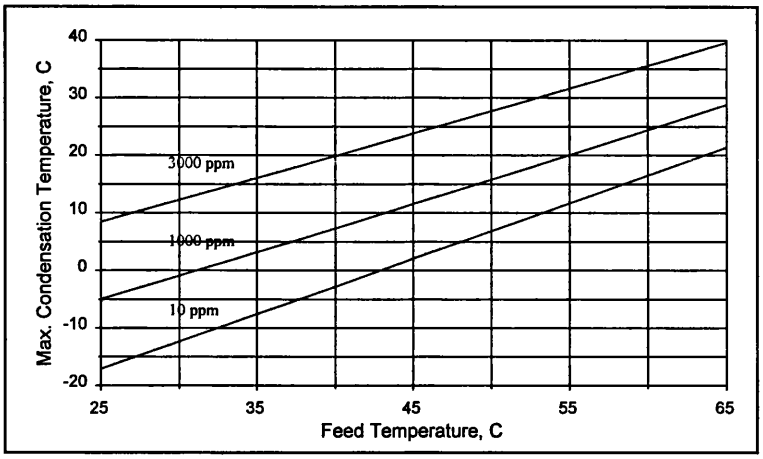

Fig 6.18 - Chloroform Separation, Maximum T_{cond} for Permeation

As can be seen, if a low retentate concentration (e.g. 10 ppm) is required, the feed temperature must be elevated to well above ambient temperature, if a condensation temperature in excess of 0°C is to be employed.

6.4 Permeate Phase Separation

As the majority of organic species have a limited solubility in water, it will often be the case that the permeate will comprise of two phases, a water saturated organic and organic saturated water phase. It is obviously very easy to separate these phases by simple decantation. If the organic solubility in water is sufficiently low, the saturated water phase can be simply recycled by mixing it with the feed stream to the pervaporation module. If the organic solubility is high, further treatment of this phase may be required, possibly within a second pervaporation unit. The water saturated organic stream may be dried if necessary, possibly utilising hydrophilic pervaporation, yielding a valuable recovered product.

Provided that feed concentrations and membrane performance are sufficient to produce two phases, the water saturated organic product stream will always be of the same composition, regardless of feed concentration. The water concentration in the organic phase product will generally be much lower than the overall permeate concentration, leading to significant enhancement in effective separation factors, α_{eff}:-

$$\alpha_{eff} = \frac{w_{osat}(1-w_{of})}{w_{of}(1-w_{osat})} \qquad (6.10)$$

Where: w_{osat} = Mass Frac. Organic in Water Saturated Organic Phase

w_{of} = Mass Frac. Organic in Feed

Assuming that at a given temperature the saturated mass fractions of organic in water, w_{ow}, and water in organic, w_{wo}, are known, the composition of the two product streams, following phase separation of the permeate, may be determined by simple mass balance:-

$$J_w = w_{wo}J_{wp} + (1-w_{ow})J_{op} \qquad (6.11)$$

$$J_o = w_{ow}J_{wp} + (1-w_{wo})J_{op} \qquad (6.12)$$

Where: J_w, J_o = Overall Water and Organic Component Fluxes Respectively, kg/m^{2}hr

J_{wp}, J_{op} = Water Phase and Organic Phase Product Stream Fluxes, kg/m^{2}hr

A combination of *eqs. (6.11) & (6.12)* gives:-

$$J_{op} = \frac{\xi J_w - J_o}{(\xi + 1)w_{wo} - 1} \qquad (6.13)$$

Where:-

$$\xi = \frac{w_{ow}}{1 - w_{ow}} \qquad (6.14)$$

Also:-

$$J_{wp} = J_w + J_p - J_{op} \qquad (6.15)$$

6.4.1 Phenol Separation

For phenol separation, if a condensation temperature of 1°C were chosen, with two condensers operating in condensing and defrosting modes in parallel, additional phase separation equipment would not be required. The liquid, phenol saturated water phase would flow continuously from the condenser, whereas the water saturated phenol phase

would be retained as a solid, within the condenser, until the defrosting process occurred. Assuming that the water phase were to be recycled for further treatment, the performance of the system for various feed concentrations is displayed in fig. 6.19. Please note that throughout section 6.4:-

a. denotes permeate fluxes and separation factor

b. denotes water saturated organic phase product stream fluxes and effective separation factors

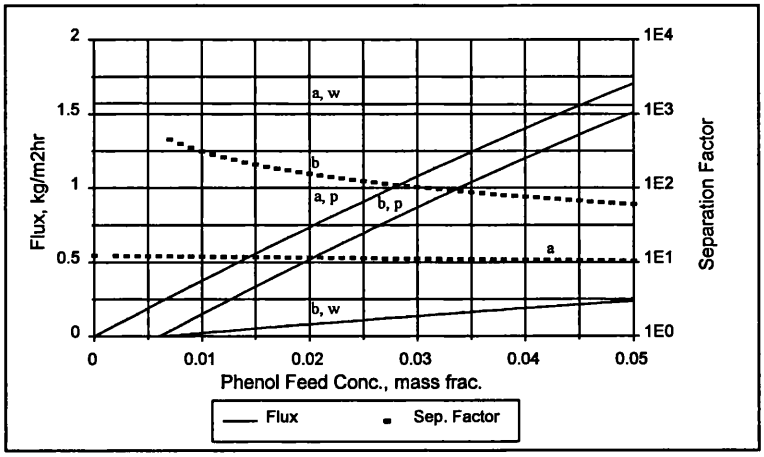

Fig. 6.19 - Phenol Separation, Effect of Permeate Phase Separation

Unfunc. PDMS, $T_{feed} = 70°C$, $T_{cond} = 1°C$ ($P_{Tp} = 6.54$ mbar), $\delta_m = 10$ μm, $k_{lo} = 2.5 \times 10^{-5}$ m/s

From fig. 6.19 it can be seen that effective separation factors of an order of magnitude higher than membrane separation factors may easily be achieved. α_{eff} increases dramatically with decreasing feed concentration as the product stream is always of fixed composition, 76% phenol at 1°C. Under the specified process conditions it can be seen that the product stream, b, phenol and water flux drops to zero at a feed concentration of 6060 ppm. Below this concentration the permeate composition is such that phase separation no longer occurs and a single liquid product stream is produced of the same composition as the permeate, a. In this case, a membrane displaying increased separation factors would be very beneficial as it would allow phase separation to occur at lower feed concentrations. With the above system a large quantity of both water and phenol (the difference between fluxes a and b) would have to be recycled, leading to increased membrane area and energy costs. An increase in membrane separation factor would lead to a reduction in this recycle rate. A membrane of increased permeability would be

beneficial, although not at the cost of reduced separation factor as feed side boundary layer resistance is already significant and would limit improvements in phenol flux.

6.4.1.1 Benefits of Enhanced Membrane Properties for Phenol Separation

To demonstrate the benefits of enhanced membrane properties, results for the same system as described above using the best membrane for phenol separation, 10% pyridyl functionalised, are displayed in fig. 6.20. In order to produce similar permeate phenol fluxes to those of fig. 6.19, an effective membrane thickness of 20 μm is chosen.

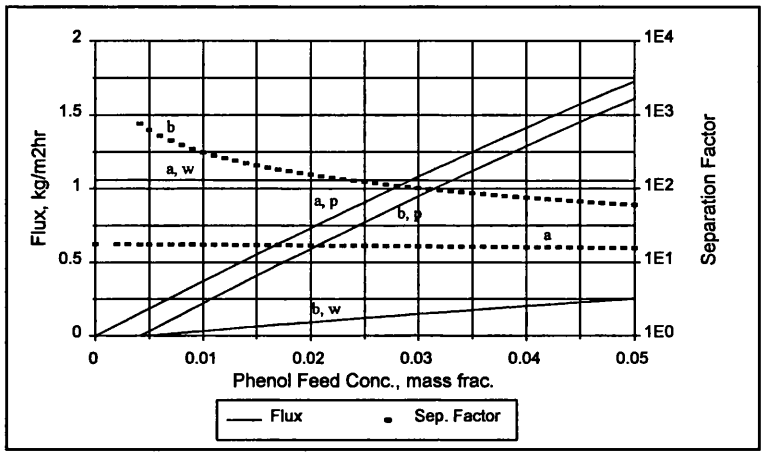

Fig. 6.20 - Enhanced Membrane, Effect of Permeate Phase Separation

10% Pyridyl Func. PDMS, $T_{feed} = 70°C$, $T_{cond} = 1°C$ ($P_{Tp} = 6.54$ mbar), $\delta_m = 20$ μm, $k_{lo} = 2.5 \times 10^{-5}$ m/s

From fig. 6.20 it can be seen that, under the specified process conditions, phase separation can be achieved at a 32% lower feed concentration and that the organic saturated water stream is reduced by 35-40%. Under conditions of higher k_{lo} and lower T_{cond} the enhancements over the unfunctionalised membrane would be greater. Of course, if a lower T_{cond} was employed the entire permeate stream would be frozen. Phase separation could still be achieved by a two stage condenser defrosting, initially at a temperature of 1°C.

6.4.2 Chloroform Separation

For chloroform separation, results for the unfunctionalised membrane, at a feed temperature of 50°C, are displayed in fig. 6.21. *Eq. (6.8)* is used to describe the Arrhenius

relationship in calculating $S^a{}_i D_{mi}$ at 50°C from the experimental data at 25°C, as reported in table 5.2. Due to the extremely low solubility of water in chloroform an organic product stream of just 651 ppm water can be produced at 1°C.

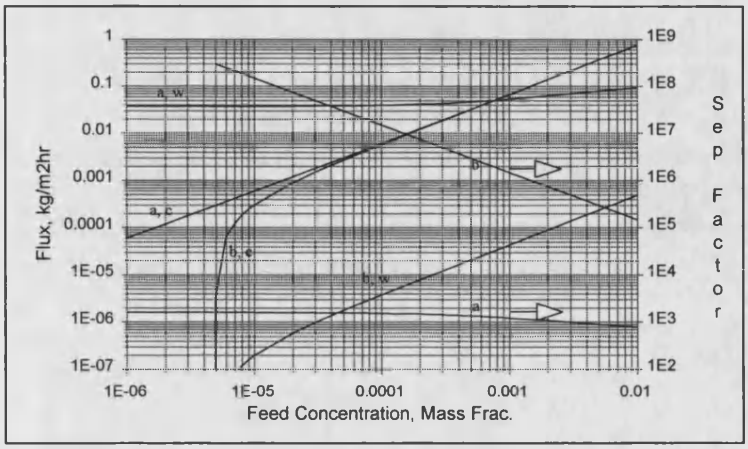

Fig. 6.21 - Chloroform Separation, Effect of Permeate Phase Separation

Unfunc. PDMS, T_{feed} = 50°C, T_{cond} = 1°C (P_{Tp} = 90.9 mbar), δ_m = 50 μm, $k_{lo} = 2.5 \times 10^{-5}$ m/s

A comparison of fig. 6.19 & 6.21 displays that the water phase product flux in the presence of chloroform is at least an order of magnitude lower than in the presence of phenol. Also, due to the low solubility of chloroform in water, the quantity of chloroform within this phase is very low, compared to that removed in the organic phase product stream, down to a feed concentration of approximately 10 ppm. Due to these two factors it is unlikely that a membrane of increased separation factor would greatly reduce energy or membrane area costs, unless it proved necessary to reduce feed concentrations to below 10 ppm. Under the process conditions indicated in fig. 6.21, the chloroform flux is almost totally limited by feed side boundary layer resistance. Unless feed side turbulence could be significantly enhanced, the use of a higher permeability membrane would lead to only a very marginal increase in chloroform flux, but possibly a large increase in water flux.

6.4.2.1 Benefits of Enhanced Membrane Properties for Chloroform Separation

The performance of the high selectivity membrane, 10% octyl functionalised PDMS, is displayed in fig. 6.22.

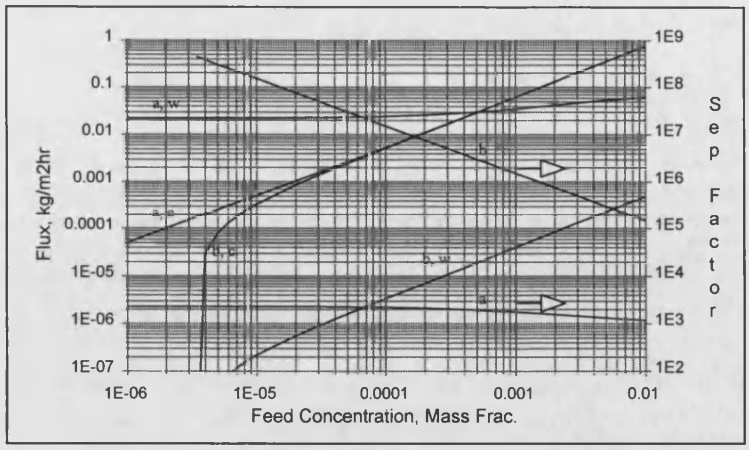

Fig. 6.22 - Enhanced Membrane, Effect of Permeate Phase Separation

10% Octyl Func. PDMS, T_{feed} = 50°C, T_{cond} = 1°C (P_{Tp} = 90.9 mbar), δ_m = 50 μm, $k_{lo} = 2.5 \times 10^{-5}$ m/s

A comparison of figs. 6.21 & 6.22 displays similar performance, for the two different membranes, at feed concentrations above 10 ppm. The water phase product stream for the higher selectivity membrane would indeed be about half the magnitude as that for the unfunctionalised membrane. As discussed above this is unlikely to be of great advantage as the stream is so small. Below 10 ppm it can be seen that performance is definitely enhanced by the high selectivity membrane. The limits of feed concentration below which permeate phase separation will not occur are 4.94 and 3.46 ppm for the unfunctionalised and high selectivity membranes respectively. Again, under conditions of lower T_{cond}, the performance differences between the two membranes would be further exaggerated. Of course at such lower temperatures the problem of ice formation would exist, leading to the requirement of the more expensive two condenser in parallel configuration.

6.4.3 Pyridine and MIBK Separations

Similar conclusions may be drawn for MIBK separation as for chloroform. A water saturated organic product stream containing only 0.02375 mass fraction of water may be produced after phase separation. Under identical process conditions to those detailed in fig. 6.21 and with δ_m = 50μm, phase separation will occur at MIBK feed concentrations in excess of 114 and 45 ppm for the unfunctionalised PDMS and 10% pentadecyl functionalised PDMS membranes respectively.

In order to obtain MIBK fluxes of similar magnitude to those obtained in figs. 6.21 & 6.22, a higher feed side operating temperature is required. This combined with the lower P_{Tp}, obtained at the same condensation temperatures, produces organic saturated water product streams an order of magnitude higher than for chloroform separation. Particularly at the lower feed concentration range, the savings made due to the reduction of the magnitude of this stream when using the higher selectivity membrane may be significant. At a membrane thickness such that the high selectivity membrane displays similar MIBK flux to the unfunctionalised membrane, the water product stream is reduced in magnitude by approximately 50%.

As pyridine and water are miscible at all concentrations, within the liquid phase, the opportunities for achieving permeate phase separation are limited. By operating at a condensation temperature of somewhat below 0°C it may be possible to freeze out some of the water, lowering the water content in the resultant liquid pyridine product stream. Unfortunately the required pyridine / water phase miscibility data at such temperatures is not apparent in current literature and thus no quantitative data is presented.

6.5 Module Configuration

When determining module configuration, consideration should be given to the reduction of those resistances that most limit performance for a particular separation. From the experimental and theoretical data presented in chapters 4 & 5, the following conclusions may be drawn for each of the separations considered within this study.

Phenol: Performance is critically dependent upon permeate pressure, a pressure no higher than a few mbar being generally required. As separation factors are not particularly high, feed side boundary layer resistance is not usually too significant. It would be beneficial to produce membranes of relatively low δ_m to allow for high fluxes, although below a thickness in the order of 10 μm feed side boundary layer resistance may become important.

Chloroform / MIBK: As both permeability and separation factors for both of these components are high, organic transport is critically limited by feed side boundary layer resistance. Configurations that maximise turbulence are, therefore, of great interest. Due

to this limitation, the production of thin membranes is counter productive and indeed relatively thick membranes of upwards of 100 μm might be preferable, as these would limit water flux. Very low permeate pressures are not required unless feed temperatures and concentrations are both very low and indeed for the chloroform separation, relatively high pressures may be desirable, due to the increase in separation factor.

Pyridine: The requirements for this separation fall in between the two categories mentioned above, probably being closer to those for the phenol separation. Relatively low permeate pressures (<25 mbar), moderately low membrane thickness (<25 μm) and reasonably high turbulence would all generally be desirable.

6.5.1 Selection of Module Type

There are five principle types of module configuration suitable for use in pervaporation: capillary, hollow fibre, spiral wound, plate and frame and disc type. Capillary, hollow fibre and spiral wound modules are relatively cheap, having a high membrane area to module size ratio and can display good feed side hydrodynamics. For the hollow fibre modules, shell-side feed would need to be considered in order to maximise turbulence.

Plate and Frame and disc type modules are relatively expensive, having low membrane area to module size ratios and requiring many seals. Feed side hydrodynamics for plate and frame modules tend to be relatively poor giving only moderate turbulence. Greater turbulence may be achieved by disc type modules, although it is thought unlikely that they could match transversal flow hollow fibre modules in this respect. Both types of module are, however, robust and relatively easy to produce and are the only viable option for many applications.

Capillary and hollow fibre membrane materials have to be strong as the membrane strands are unsupported within the module. An extrusion process is used to produce the membrane strands and it is not possible to extrude a composite membrane with a microporous support. As modified PDMS films tend to be fairly brittle by nature, a microporous support material is often necessary to provide rigidity and it might not be possible to produce homogeneous hollow fibres from many of the functionalised materials. It is certainly possible to produce

hollow fibres from unfunctionalised PDMS and it may be possible to produce composite membranes by coating the surface of these fibres with a thin layer of the functionalised material, in order to enhance selectivity.

Capillary and hollow fibre modules display the ideal combinations of properties for chloroform and MIBK separation. As discussed in chapter 2, feed side mass transfer coefficients are very high, particularly when transversal feed flow on the shell side is employed. Membrane thickness is generally high, in order to produce the required mechanical strength and this is often beneficial in reducing water flux. For phenol and pyridine separation, these modules are unlikely to prove practical. Hydrodynamic considerations are less important and membrane thicknesses are generally too large. Shell side feed may be impractical as a large pressure drop may occur on the permeate side if the resultant vapours were to be transported along the inside of the capillaries. Feeding the liquid phase on the inside of the capillaries would lead to high feed pressure drops, necessitating the use of large pumps.

Spiral wound modules are produced from flat sheet membranes and consist of permeate spacers sandwiched between two membranes, several of which are wound spirally around a central tube, together with feed spacers. Permeate side pressure drop is high as the permeate has to travel long distances through the porous spacer. This would certainly exclude this configuration as an option for phenol separation. Feed side hydrodynamics are not as favourable as those for hollow fibres and hence it is unlikely that this configuration would be desirable for chloroform or MIBK separation. The production using flat sheet membranes would certainly allow for the use of thin, composite, functionalised PDMS membranes. If permeate side pressure drop could be kept within acceptable limits, this configuration could certainly be attractive for pyridine separation.

Plate and Frame or Disc type modules also employ flat sheet membranes. Due to the relatively poor feed side hydrodynamics, these configurations would be unattractive for chloroform or MIBK separation. Permeate side pressure drop is always low as the permeate may flow through wide channels. For this reason, combined with the fact that thin, functionalised membranes could easily be employed, this configuration is thought to

be the most appropriate for phenol separation. For similar reasons, it may also prove to be the best configuration for pyridine separation.

A summary of module designs thought most appropriate for each separation is displayed in table 6.2.

Organic Component	Plate and Frame	Disc Type	Spiral Wound	Capillary / Hollow Fibre
Phenol	*	*		
Pyridine	*	*	*	
MIBK				*
Chloroform				*

Table 6.2 - Most Appropriate Module Designs

Note: * denotes most appropriate

6.6 Further Considerations

Celgard 2500 is 25 μm thick and, as is demonstrated in chapter 4, its pores become filled with the functionalised PDMS material. It would, therefore, be difficult to produce a membrane of effective thickness, δ_m, of less than 56 μm using Celgard 2500 as a support, due to its 45% porosity. For phenol and pyridine separations, membranes of $\delta_m < 56$ μm may be desirable. A microporous support material would have to be found that was either thinner or prevented the modified PDMS from filling its pores, during manufacture of the composite membrane. Several alternatives exist, such as polyester and polysulphone, which have both been experimentally used *(Boddeker and Bengtson, 1991)*.

Another important consideration is that it would be necessary to ensure the membranes produced were defect free and did not contain pin holes. It should be relatively easy to test for pin holes by passing a gas across the membrane top surface and measuring the quantity that passes through the membrane. Once discovered, pin holes could easily be filled using a small quantity of additional PDMS material. An alternative would be to dip coat the entire membrane surface.

6.7 Closing Remarks

A study of *eqs. (4.11) & (6.6)* highlights the usefulness of equations of quadratic form for describing the simultaneous transport of two components in a pervaporation system. The importance of the $y_{op} \frac{P_{Tp}}{P_o^{sat}}$ term is demonstrated and when significant can explain deviations from linear trends in flux with concentration. Care should be taken to consider the magnitude of this term when investigating potential coupling effects, so as to distinguish between genuine and apparent coupling.

The importance of separating driving force and membrane effects, by concentrating upon permeability coefficients instead of flux, is demonstrated. It allows for a much more realistic model of the effect of temperature upon pervaporation performance to be realised, by allowing for zero flux under conditions of zero driving force. Again, it also allows for the importance of the $y_{op} \frac{P_{Tp}}{P_o^{sat}}$ term, under conditions of significantly high P_{Tp}, to be shown. When this term is negligibly small the normal model is equally applicable, provided that the effect of feed side boundary resistance is allowed for.

If pervaporation can enhance concentrations to in excess of the limit of component miscibility, it has been shown that in combination with phase separation, pervaporation may lead to reasonable component separation, even if membrane selectivity is relatively low. For separations where selectivities are very high, enhancing module design is shown to be of greater importance than making membrane improvements.

Chapter 7

Process Evaluation and Economic Considerations

Scope of Chapter 7

Within chapter 7, differential mass and energy balance equations are developed based upon the transport models presented within chapters 4 & 6. These equations are solved in order to evaluate pervaporation performance for a number of model separations. This approach allows the evaluation of total membrane area and energy requirement under a variety of process conditions. The results generated are used to demonstrate the benefits that may be realised by employing functionalised PDMS membranes.

A comparison between the separation performance of pervaporation and processes based solely upon vapour-liquid equilibrium as a separating mechanism is made. It is demonstrated that a simple two stage flash process may well compare favourably with pervaporation for chloroform separation.

The economics of pervaporation are discussed with reference to a number of previous studies. In many cases a direct economic comparison between pervaporation and other separation processes is reported. The possibility of combining pervaporation with other processes, within a hybrid system, is also investigated.

7.1 Differential Mass and Energy Balance Equations

In order to determine the membrane area required to perform a specified separation, differential mass and energy balance equations must be derived and solved simultaneously by numerical integration. The development of all equations required to perform such an operation is described below.

Using the integrated model described within chapter 6, y_{op} may be calculated for a given $x_{o(b)}$ using *eq. (6.6)*. J_o and J_w may then be determined using *eqs. (4.7) & (6.3)*:-

$$y_{op}^{2}\left(A_w\frac{P_{Tp}}{P_w^{sat}} + A_oB_oA_w\frac{\rho_m}{\delta_m}\frac{P_{Tp}}{P_w^{sat}} - A_o\frac{P_{Tp}}{P_o^{sat}}\right) +$$

$$y_{op}\left(A_w\gamma_w x_{wf} - A_w\frac{P_{Tp}}{P_w^{sat}} + A_oB_oA_w\frac{\rho_m}{\delta_m}\gamma_w x_{wf} - A_oB_oA_w\frac{\rho_m}{\delta_m}\frac{P_{Tp}}{P_w^{sat}} + A_o\frac{P_{Tp}}{P_o^{sat}} + A_o\gamma_o x_{o(b)}\right)$$

$$- A_o\gamma_o x_{o(b)} = 0 \qquad (6.6)$$

$$J_{\Phi w} = \frac{S^a_w D_{mw}\rho_m}{\delta_m MR_w}\left(\gamma_w x_{wf} - y_{wp}\frac{P_{Tp}}{P_w^{sat}}\right) \qquad (4.7)$$

$$J_{\Phi o} = \frac{A_o\frac{\rho_m}{\delta_m}}{(1 + A_o\frac{\rho_m}{\delta_m}B_o)}\left(\gamma_o x_{o(b)} - y_{op}\frac{P_{Tp}}{P_o^{sat}}\right) \qquad (6.3)$$

$S^a_i D_{mi}$ values are taken from tables 5.1 - 5.4, as all separation case studies are carried out at the same module feed temperatures as used for their determination. Within a module, feed temperature drops as energy is absorbed in order to supply the latent heat for vaporisation of the permeating components. As can be seen from a study of appendix 4, γ_i can be a strong function of temperature. In all case studies, temperature drops are kept relatively low and hence γ_i is assumed to remain constant with temperature. γ_i can also vary significantly with feed concentration. For chloroform and MIBK separations, concentrations are sufficiently low that it may be assumed that γ_i is constant and equal to the activity coefficient at infinite dilution, γ_i^{∞}. For pyridine separation, a study of fig. A8 (appendix 4) displays that γ_i is only a weak function of concentration and a constant value measured at a pyridine mass fraction, w_{ip}, of 0.01 is used. A study of fig. A4 displays that γ_i varies significantly with phenol concentration. In this case, the following equation, given by linear regression of the results presented in fig. A4, is used to estimate γ_i:-

$$\gamma_i = -(106.5\, w_{ip}) + 26.17 \qquad (7.1)$$

As in chapter 6, coupling effects are neglected and hence $S^a_i D_{mi}$ is assumed to remain constant with changing concentration.

The rate of transport of each component through the membrane over an incremental membrane area is given by:-

$$dm_i = J_i dA \qquad (7.2)$$

Where: J = Flux, kg/m^{2}s $\quad$ m = Mass Flow, kg/s

A = Area, m^2

dm_i is equal to rate of removal of component i from the feed, i.e.:-

$$dm_i = -dm_{fi} \tag{7.3}$$

Heat must be absorbed from the feed solution in order to supply the required energy for vaporisation of each component:-

$$-dq = \Delta H^T_{vapo} dm_o + \Delta H^T_{vapw} dm_w \tag{7.4}$$

Where: q = Power, kW $\quad$ ΔH^T_{vap} = Heat of Vaporisation at Temperature T, kJ/kg

ΔH^T_{vapi} is a strong function of temperature. It may be determined at any temperature using a principle, based upon Hess' law of heat summation. This is that the same amount of energy is required to vaporise a liquid at one temperature, T_{ref} and heat the vapour to another temperature, T, as to heat the liquid from T_{ref} to T and then to vaporise at T, i.e.:-

$$\Delta H^{Tref}_{vapi} + \int_{T_{ref}}^{T} Cp^v{}_i \, dT = \int_{T_{ref}}^{T} Cp^L{}_i \, dT + \Delta H^T_{vapi} \tag{7.5}$$

Where: Cp = Specific Heat Capacity, kJ/kgK $\quad$ v denotes vapour

L denotes liquid

Cp^v and Cp^L are only weak functions of temperature and may be assumed to remain constant over the moderate temperature ranges expected to be encountered in pervaporation. *Eq. (7.5)*, therefore, reduces to:-

$$\Delta H^T_{vapi} = \Delta H^{Tref}_{vapi} + (Cp^L{}_i - Cp^v{}_i)(T_{ref} - T) \tag{7.6}$$

The energy absorbed causes the feed temperature to drop:-

$$dT_f = \frac{-dq}{m_{fo} Cp^L{}_o + m_{fw} Cp^L{}_w} \tag{7.7}$$

It should be recalled that component flux varies with temperature according to the Arrhenius relationship:-

$$J_{iT2} = J_i^{Tref} exp\left(\frac{-E_{ai}}{R}\left(\frac{1}{T_{ref}} - \frac{1}{T_2}\right)\right) \qquad (6.7)$$

Note: The reference temperatures used in the calculation of J_i^{Tref} and ΔH^T_{vap} do not necessarily have to be the same.

Although the validity of *eq. (6.7)* under conditions of diminishing driving force for permeation is questioned, within this study, it is used for simplicity. In all cases, feed side temperature drops are kept low (< 15°C) and care is taken to avoid a situation where driving force approaches zero.

The saturated vapour pressure of a pure component, at a given temperature, can be estimated by the Antoine equation:-

$$log_{10}(P_i^{sat}) = A_i - \frac{B_i}{T + C_i} \qquad (7.8)$$

Where: P = Pressure, mmHg T = Temperature, °C

A_i, B_i, C_i = Dimensional Antoine Constants

The above equations were simultaneously solved using Eulers method of numerical integration, utilising a computer spreadsheet. One hundred area increments were used, i.e.:-

$$dA = 0.01A \qquad (7.9)$$

7.1.1 Equation Solving Technique

The following parameters have to be specified in order to solve the above equations:-

$S^a{}_i D_{mi}$, m^2/s - at ref. T	P_i^{sat}, Pa - at same ref. T	δ_m, m
ρ_m, kg/m^3	$\left(\frac{E_{ai}}{R}\right)$, K	$\left(\frac{D_{lo}}{\delta_l}\right)$, m/s
P_{Tp}, Pa	MR_i, kg/kmol	ρ_w, kg/m^3
$\Delta H^{Tref}{}_{vapi}$, kJ/kg	$Cp^L{}_i$, kJ/kgK	$Cp^v{}_i$, kJ/kgK

In addition, inlet process conditions are required:-

m_f, kg/s (total feed flow) x_{if}, dimensionless T_f, K (initial T)
A, m^2

The following computational algorithm is used:-

1. Set $a = 0$
2. Calculate y_{ip} for given x_{if}, using *eq. (6.6)*
3. Calculate J_i for given T_f, using *eqs. (6.7), (4.7) & (6.3)*
4. Calculate dm_i, using *eq. (7.2) & (7.9)*
5. Calculate ΔH^T_{vapi}, using *eq. (7.6)*
6. Calculate dq, using *eq. (7.4)*
7. Calculate dT_f, using *eq. (7.7)*
8. Calculate new m_{fi} and hence new x_{if}, using *eq. (7.3)*
9. Set $a = a + dA$ and $T_f = T_f - dT_f$
10. Goto step 2 and repeat until $a = A$

The permeate mass flow and composition can be calculated from a summation of all individual dm_i's.

7.1.2 Calculation of Condensation Temperature

As P_{Tp} is already specified, it is necessary to calculate the permeate condensation temperature required to give such a total vapour pressure. This condensation temperature will obviously be a function of both P_{Tp} and y_{ip} and an iterative method is required for its determination.

In the case where the permeate composition exceeds the solubility limits of each component in the other, two distinct immiscible phases exist and each component exerts its own saturated vapour pressure, i.e.:-

$$P_{Tp} = P_1^{sat} + P_2^{sat} \qquad (6.9)$$

Where there is total miscibility between the two components:-

$$P_{Tp} = \gamma_1 x_{1p} P_1^{sat} + \gamma_2 x_{2p} P_2^{sat} \qquad (7.10)$$

P_{Tp} is calculated at a guess permeate temperature using either *eqs. (6.9) & (7.8)* or *(7.8) & (7.10)*, as appropriate. The temperature is modified until P_{Tp} is equal to the specified permeate pressure.

7.1.3 Validation of Approach

The computer program pvdesign 3.1 (supplied by Institut fur verfahrens technik, RWTH Aachen) also solves mass and energy balance equations and calculates permeate temperatures. It uses interpolation of experimental membrane performance data and a Runge-Kutta technique in order to numerically solve differential equations. The results of this program, for various input conditions, are compared with those obtained by following the procedure described above. The required membrane performance data is input by assuming that *eqs. (4.7), (6.3) & (6.6)* describe the effect of feed concentration upon flux and selectivity. In all cases agreement is extremely close (± 2-3%) validating the accuracy of the approach and indicating that a method more sophisticated than simple Euler is not required.

7.2 Feed Temperature Drop

If relatively low selectivity membranes are employed, a large quantity of water will pass through the membrane. As water possesses such a high latent heat of vaporisation, feed temperature will drop rapidly, according to *eq. (7.7)*. In order to maintain satisfactory component fluxes, it is necessary to prevent the feed temperature from falling too low. Practically, this is achieved by aligning a number of small membrane modules in series and employing inter-modular heat exchange in order to maintain temperature. Commonly several, or all, of these individual modules are contained within a common vacuum vessel condenser. If a permeate solid phase necessitates the need for a two condenser in parallel system, a common vacuum vessel may not be used, as simultaneous condensing and defrosting cycles could not occur. It would still be possible to connect several modules to the same external condenser systems.

An economic trade off exists between limiting total membrane area, by maintaining high feed temperatures and minimising module equipment and heat exchanger costs. Overall

membrane module cost is a function of both membrane area and number of modules required. If feed temperature is to be allowed to drop only a little, a high number of individual modules will be required. Approximately the same overall inter-modular heating duty will be required whether or not feed temperature is allowed to drop substantially. If only a small drop is allowed, however, a large number of small exchangers will be required, which again will generally be more expensive than a smaller number of larger exchangers.

An optimum feed temperature drop could only be determined by comprehensive economic evaluation and would be very dependent upon the nature of the separation to be achieved.

7.3 Benefits of Functionalised Membranes

In order to demonstrate the benefits of employing functionalised PDMS membranes, some sample separation parameters are defined. The differential equations described in section 7.1 are solved in order to determine required membrane area, number of modules, heating and condensing duties and permeate and retentate stream compositions.

7.3.1 Assumptions

Within these calculations a number of assumptions are made, as discussed below.

Module size: It is highly likely that monetary savings could be made by ordering a number of identical membrane modules, rather than ordering a variety of custom built sizes. It is assumed that each individual module will be identical, i.e. of identical membrane area. The feed side temperature drop across each module will, therefore, vary.

Temperature drop: Each system is designed so that the feed side temperature drop will not exceed a pre-determined maximum value in any of the individual modules. This value is set fairly arbitrarily, but is designed to yield a sensible total number of modules and membrane area.

Effect of temperature: Specific heat capacities, densities and activity coefficients are all assumed to remain constant over the low ranges of feed temperatures specified. Although temperature may have a significant effect upon feed side boundary layer resistance, k_{lo} is assumed to remain constant and hence it is essentially a weighted average value over the temperature range.

Condenser configuration: It is assumed that all permeate from each individual membrane module is simultaneously condensed within a single condenser.

7.3.2 Phenol Separation

It is assumed that a constant process stream of flowrate, q_f, 1000 kg/hr, at 70°C, containing 3% wt. phenol has to be treated to reduce the phenol concentration to 300 ppm, after which it may be passed to a biological treatment facility. As selectivity towards phenol is relatively low, it is determined that the allowable feed temperature drop across any given module should not exceed the fairly high value of 15°C. In between modules the temperature is elevated back up to the initial temperature of 70°C. A T_{cond} of 1°C is chosen and as phase separation of the permeate is achieved, P_{Tp} may be calculated using *eq. (6.9)*. A summary of input conditions is displayed below:-

q_f = 1000 kg/hr

w_{pf} = 0.03

w_{pr} = 0.0003 (retentate concentration)

k_{lo} = 2.5×10^{-5} m/s

T_{cond} = 1°C (P_{Tp} = 6.53 mbar)

T_f = 70°C

$-\Delta T_f$ < 15°C

The performance of an unfunctionalised PDMS membrane, for the above specified separation, of δ_m = 10 μm is determined. Below this membrane thickness, feed side boundary layer resistance begins to greatly influence phenol flux. The performance of the unfunctionalised membrane is compared with that of the best functionalised membrane, 10% pyridyl functionalised PDMS. When making the comparison, membrane thickness

becomes an important parameter, due to the difference in component permeabilities between the two membranes. Three separate cases are studied:-

1. Functionalised δ_m = unfunctionalised δ_m and the area required to produce the desired retentate concentration is calculated.

2. Functionalised δ_m is adjusted to produce the desired retentate concentration using exactly the same number of modules and membrane area as required for the unfunctionalised membrane.

3. Both functionalised δ_m and membrane area are adjusted to produce both retentate and permeate streams exactly identical in concentration to those produced by the unfunctionalised membrane.

The results of each evaluation are presented in table 7.1 and a more comprehensive breakdown for each individual module is displayed in appendix 6. The slight discrepancy in mass balances, <0.3%, between inlet and outlet streams is due to small rounding error in the calculation procedure.

Case	δ_m μm	A_T m^2	*nmod*	Q_{heat} kW	Q_{cond} kW	q_r kg/hr	w_{pr}	q_p kg/hr	w_{pp}
Unfunc	10	263	19	207	250	635	0.0003	368	0.082
Func 1	10	165	15	173	211	688	0.0003	315	0.095
Func 2	20.6	263	19	148	178	734	0.0003	268	0.112
Func 3	6.18	120	19	207	250	635	0.0003	368	0.082

Table 7.1 - Phenol Separation, Case Study Results

A_T = Total Membrane Area, m^2

nmod = Number of Equal Area Modules ($A_T = nmod \times A_{mod}$)

Q_{heat} = Total Heating Duty, kW (required to re-elevate feed temperature)

Q_{cond} = Total Condenser Duty, kW

r denotes retentate p denotes permeate

It can be seen that in all cases w_{pp} exceeds the limit for phase separation to occur.

For the functionalised membrane case 1, a 16% saving in total energy usage and a 37% saving in total membrane area is realised. The permeate stream is modestly both reduced in size and enriched in phenol concentration.

For case 2, a large total energy saving of 29% is realised and the permeate stream is both reduced in size by 27% and enriched in phenol concentration by 37%.

For case 3, identical results are produced as for the unfunctionalised membrane, with a very significant 54% reduction in total membrane area.

7.3.2.1 Two Unit Process

When determining which of the three cases would prove the most beneficial, the relative costs of energy, membrane and modules and further treatment of the permeate stream need to be evaluated. Again this is a complex problem, particularly as numerous options exist for further permeate treatment. As in all cases the concentration of phenol in the permeate is of the order of only 10%, it is highly likely that further treatment would be required. A sensible option would appear to be to remove the water saturated, solid, phenol permeate phase as product and to pass the phenol saturated, liquid, water phase to a second pervaporation unit for further concentration. Both the water permeate phase and retentate, from the second unit, could be recycled and combined with the feed stream to the first unit, whereas the permeate phenol phase could again be removed as product. A schematic diagram displaying this configuration is given in fig. 7.1. It would not be sensible to employ just a one unit process with phase separation and recycling. As overall permeate phenol concentrations from the first unit are so low, the vast majority of the phenol would be recycled within the saturated water stream, leading to the requirement of extremely high membrane areas and energy inputs.

The two unit system is modeled for the unfunctionalised membrane and case 1 & 2 of the functionalised membrane. Exactly the same input conditions, as specified above, are used. The second unit is specified in such a manner that the concentration of the combined recycle stream is equal to the unit 1 feed stream, i.e. 3% phenol. The same δ_m, feed and condensate temperature and feed side boundary layer resistance specifications are set. As a

significant proportion of the unit 1 permeate is recycled, the unit 1 inlet flowrate, q_{in}, is increased. *Eqs. (6.13) - (6.15)* are used to determine the compositions and flowrates of the two permeate phases of each unit. The results of each evaluation are displayed in tables 7.2 & 7.3 and again a more comprehensive performance breakdown is given in appendix 6.

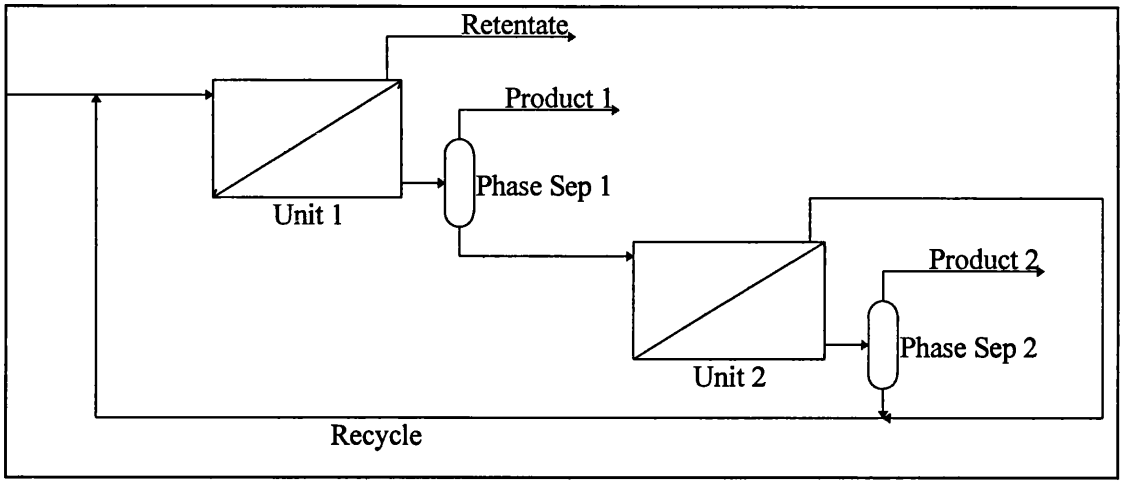

Fig. 7.1 - Two Unit Process

Case	δ_m μm	A_T m^2	*nmod*	Q_{heat} kW	Q_{cond} kW	q_{in} kg/hr
Unfunc	10	404	18	313	380	1520
Func 1	10	231	15	243	297	1402
Func 2	20.6	374	12	188	234	1313

Table 7.2 - Case Studies With Recycle, Unit 1

Case	δ_m μm	A_T m^2	*nmod*	Q_{heat} kW	Q_{cond} kW	q_{in} kg/hr
Unfunc	10	40.1	5	72	42	548
Func 1	10	17.2	4	50	26	424
Func 2	20.6	22.8	3	36	17	330

Table. 7.3 - Case Studies With Recycle, Unit 2

In all cases a simple mass balance and the use of *eqs. (6.13) - (6.15)* yields the unit 1 retentate stream (to be discharged into the biological treatment facility) and combined unit phenol phase product streams (*prod*) as:-

q_r = 961 kg/hr w_{pr} = 0.0003

q_{prod} = 39 kg/hr w_{prod} = 0.76

In both cases, the beneficial savings in total membrane area, number of modules and energy requirements are significantly extenuated when the recycling configuration is employed. For the case 3 option, similar results would be obtained as for the unfunctionalised membrane in tables 7.2 & 7.3, but again at approximately the same reduced total membrane area of 54%. Again, it should be emphasised that it is unlikely that any of these solutions are optimal, but clearly display the benefits that may be realised by the use of enhanced membranes.

7.3.3 Pyridine Separation

A single pervaporation unit is again modeled for a sample separation, in order to reduce the pyridine concentration of a 1000 kg/hr feed stream from 1% to 300 ppm pyridine, for subsequent treatment in a biological process. The following input conditions are specified:-

q_f = 1000 kg/hr

w_{pf} = 0.01

w_{pr} = 0.0003 (retentate concentration)

k_{lo} = 2.5×10^{-5} m/s

T_{cond} = 1°C (P_{Tp} = 7.54 mbar)

T_f = 70°C

$-\Delta T_f$ < 15°C

The performance of an unfunctionalised membrane of δ_m = 25 μm is evaluated and compared to the best performing functionalised membrane, 10% octyl functionalised PDMS. Phase separation of the permeate is not possible, unless an attempt is made to freeze out some water. It is not, therefore, too clear how much additional treatment the permeate stream would require before a useful product could be obtained, using further pervaporation units. For this reason it is decided to concentrate upon a case 3 study, producing identical output streams and energy requirements, in order to demonstrate the

benefits of the functionalised membrane. The results of the evaluations are displayed in table 7.4.

Case	δ_m μm	A_T m^2	*nmod*	Q_{heat} kW	Q_{cond} kW	q_r kg/hr	w_{pr}	q_p kg/hr	w_{pp}
Unfunc	25	154	5	49	69	898	0.0003	103	0.0950
Func 3	5.21	93	5	49	69	898	0.0003	103	0.0950

Table 7.4 - Pyridine Separation, Case Study Results

As can be clearly seen, a reduction in total membrane area requirement of 40% may be realised when using the functionalised membrane.

7.3.4 Chloroform Separation

A similar case 3 study is performed to compare the performance of an unfunctionalised membrane with the best performing membrane for chloroform separation, 7.5% octyl functionalised PDMS. A feed stream at 25°C, of 1000 kg/hr, containing 100 ppm chloroform, is to be treated to reduce the concentration to 1 ppm, suitable for direct discharge into the general water system. As indicated by fig. 6.18, in order for a driving force for permeation to exist at a feed temperature of 25°C, a very low condensation temperature of < -17°C is required. The following input conditions are specified:-

q_f = 1000 kg/hr

w_{pf} = 100×10^{-6}

w_{pr} = 1×10^{-6} (retentate concentration)

k_{lo} = 2.5×10^{-5} m/s

T_{cond} = -20°C (P_{Tp} = 26.44 mbar)

T_f = 25°C

A 50 μm unfunctionalised membrane thickness is chosen. The results of the evaluations are displayed in table 7.5.

Case	δ_m μm	A_T m^2	*nmod*	Q_{heat} kW	Q_{cond} kW	q_r kg/hr	w_{pr}	q_p kg/hr	w_{pp}
Unfunc	50	118	1	0	0.76	998.87	1×10^{-6}	1.13	0.087
Func 3	21.2	114	1	0	0.76	998.87	1×10^{-6}	1.13	0.087

Table 7.5 - Chloroform Separation, Case Study Results

It can be seen that the permeate stream is very small, compared to the retentate stream. Due to this fact, the feed side temperature drop is negligible. Phase separation of this stream would yield a useful chloroform product containing only a very small quantity of water and a small chloroform saturated water stream, which could easily be recycled for further treatment. As discussed previously, an alternative to utilising such a low condensation temperature would be to elevate the feed temperature. As the feed stream is almost three orders of magnitude larger than the permeate stream, a very substantial energy input would be required to achieve this. Even with the use of sensible energy integration, total energy usage due to heat losses would be large. It would generally appear more sensible to use the ambient feed temperature and low condensation temperature. Although operating at such a low temperature is relatively expensive and would necessitate the use of a two condenser in parallel system, the saving in energy is very large and the absolute overall condenser equipment and operating costs would be low, due to the small size of the permeate stream.

Despite the significant enhancement in intrinsic selectivity, between the functionalised and unfunctionalised membrane, it can be seen that under the specified input conditions the benefits of using the functionalised membrane are very small. A saving in total membrane area of only 3.4% may be realised. The reason for this disappointing result is that feed side boundary layer resistance has a very large effect upon chloroform transport and, as discussed in chapter 2, this resistance has a relatively larger effect upon the better performing membrane, severely limiting any improvement in system performance. Thicker membranes could be employed to help reduce this influence, however, as the permeate stream is so small and quality so high, increased thickness would lead to increased required membrane area with very little benefit in reducing further permeate treatment.

If a transversal hollow fibre configuration could be employed, a k_{lo} of up to 10^{-4} m/s could be realistically achieved, as discussed in chapter 2. The case 3 evaluation is repeated with exactly the same input conditions as above, but with $k_{lo} = 10^{-4}$ m/s. The results are presented in table 7.6.

Case	δ_m μm	A_T m^2	*nmod*	Q_{heat} kW	Q_{cond} kW	q_r kg/hr	w_{pr}	q_p kg/hr	w_{pp}
Unfunc	50	78	1	0	0.519	999.20	1×10^{-6}	0.80	0.1228
Func 3	19.3	68.5	1	0	0.519	999.20	1×10^{-6}	0.80	0.1228

Table 7.6 - Chloroform Separation, Case Study Results, $k_{lo} = 10^{-4}$ m/s

Under these conditions a much larger, but still not startling, 12% saving in membrane area may be realised when using the functionalised membrane. Boundary layer resistance is still very significant. With the unfunctionalised membrane, a saving in total area of 34% can be realised by increasing k_{lo} by a factor of 4 (compare tables 7.5 & 7.6). It would appear sensible to conclude that it is more important to optimise hydrodynamic conditions than to enhance membrane performance for chloroform separation. Owing to the high permeate quality, it may be acceptable to operate at low membrane thickness, particularly under good hydrodynamic conditions, in order to reduce membrane area requirement. It should be noted that even for the phenol and pyridine separations detailed above, boundary layer resistance is still reasonably significant and improving hydrodynamics would further extenuate the benefits of using functionalised membranes.

7.3.5 MIBK

It is assumed that an aqueous process stream of 1000 kg/hr, containing 1% MIBK at 70°C requires treatment. Due to the low toxicity of MIBK, it is assumed that the concentration has to be reduced to 10 ppm, before discharge into the general water system is permissible. Again a case 3 study is performed to compare the best functionalised membrane, 10% tridecyl functionalised PDMS, performance with the unfunctionalised membrane. As for chloroform, the study is performed at two different k_{lo} values of (a) 2.5×10^{-5} and (b) 10^{-4} m/s. The following input conditions are specified:-

q_f = 1000 kg/hr

w_{pf} = 0.01

w_{pr} = 1×10^{-5} (retentate concentration)

T_{cond} = 1°C (P_{Tp} = 12.03 mbar)

T_f = 70°C

$-\Delta T_f$ < 15°C

The results are presented in table 7.7.

Case	δ_m μm	A_T m^2	*nmod*	Q_{heat} kW	Q_{cond} kW	q_r kg/hr	w_{pr}	q_p kg/hr	w_{pp}
(a) $k_{lo} = 2.5 \times 10^{-5}$ m/s									
Unfunc	50	111	3	18.99	32.15	947.5	1×10^{-5}	52.8	0.1893
Func 3	14.4	99	3	18.99	32.15	947.5	1×10^{-5}	52.8	0.1893
(b) $k_{lo} = 10^{-4}$ m/s.									
Unfunc	50	49.5	1	0	14.26	972	1×10^{-5}	28.0	0.3564
Func 3	11	33.6	1	0	14.26	972	1×10^{-5}	28.0	0.3564

Table 7.7 - MIBK Separation, Case Study Results

In all cases permeate phase separation would produce a 98.1% pure MIBK product stream, containing the majority of the total MIBK and a water stream containing just 1.7% MIBK, which could readily be recycled to the feed of the pervaporation unit.

As for chloroform separation, the benefits of enhancing feed side hydrodynamics can be seen, leading to a 55% reduction in membrane area for the unfunctionalised membrane. Again, the benefits of utilising the functionalised membrane are extenuated at the higher k_{lo}, leading to a further 32% reduction in total area.

7.3.6 Discussion

As is shown within the above case studies, membrane permeabilities are sufficiently high that acceptable performance may be achieved with reasonably thick and hence mechanically robust, membranes. Except for the phenol separation, enhancing

permeability further becomes counter productive as feed side boundary layer resistance limits organic flux. Enhancing selectivity is more productive, even if this enhancement is made at the expense of reduced permeability. To a certain limit, flux can be maintained by simply using a thinner membrane.

As displayed in the case studies for chloroform separation, enhancing membrane performance in a situation where feed side boundary layer resistance dominates organic flux yields very little benefit. In these cases much greater performance enhancements may be realised by optimising feed side hydrodynamics. For the other three separations where feed side boundary layer resistance, although important, is not dominant, significant benefits may be realised by utilising enhanced membranes.

The performance of the functionalised membranes produced may be compared with that of the various classes of membranes displayed in tables 1.3 - 1.4. It can clearly be seen that for chloroform and pyridine separations, the best functionalised PDMS membranes display significantly higher intrinsic selectivity than any other membrane so far reported, with the exception of the unusual result for chloroform separation using silicone rubber. Although MIBK separation has not been studied before, it is probably fair to assume that the best functionalised membrane would compare very favourably with any other material. It is interesting to note that for each of these three organic components, functionalised PDMS membranes containing long, straight chained, alkyl groups display the best performance. When commercially developing a membrane it is of great advantage to produce a product that has a wide range of application. It may well prove to be commercially attractive to manufacture a long chained, alkyl, functionalised membrane. This would probably demonstrate significant performance enhancements for a wide variety of separations of organics from water, especially where the organic component contains a large, low polarity group.

Although functionalised PDMS membranes containing basic groups display large enhancements in performance over unfunctionalised PDMS membranes, it would appear from a study of table 1.2 that they are still out performed by PEBA membranes. For phenol separation, functionalised PDMS membranes would be of commercial interest only if either they could be made significantly cheaper than PEBA membranes, or if PEBA

membranes contained an intrinsically detrimental property, such as lack of mechanical rigidity or instability in performance over long operating periods. No mention of such problems have been reported in literature to date, although it is interesting to note that it would appear that studies upon PEBA membranes have been confined to relatively large (> 40 μm) membrane thicknesses. The results for phenol separation indicate that the principle of incorporating acidic or basic groups within a membrane structure, be it PDMS or another material, in order to facilitate the transport of basic or acidic organic species, remains of interest. Again it may be possible to produce a single membrane suitable for a family of different separations.

7.3.7 Vapour-Liquid Equilibrium Considerations

In order for pervaporation to be truly competitive with processes based upon vapour-liquid equilibrium, it is thought likely that the overall separation factors achieved must significantly exceed that achieved through simple evaporation, α_{evap}. If this were not the case, pervaporation would probably not compete well with either distillation or even simple flash units. As can be seen from table 5.6, the intrinsic membrane separation factors for the unfunctionalised and best functionalised membranes all exceed α_{evap}, for each separation.

For phenol separation a very definite advantage is achieved as $\alpha_{evap} < 1$, indicating that it would be necessary to evaporate off the major component, water, requiring massive energy input to supply the latent heat for vaporisation. It appears that as the activity of an organic component, within aqueous solution, increases, intrinsic α exceeds α_{evap} by decreasing amounts. It is also important to remember that feed side boundary layer resistance limits organic flux more severely as intrinsic α and, hence, α_{evap} increase. As can be seen by a study of figs. 6.7 - 6.9, this resistance has the effect of reducing overall separation factor. As α_{mem} for chloroform is only slightly greater than 1, if boundary layer resistance is at all important it may easily reduce overall α to a value well below α_{evap}. The same effect may also be apparent for MIBK separation, which is also strongly influenced by boundary layer resistance.

Utilising δ_m = 50 μm and the same process conditions as indicated in the case studies above, plots of overall α for varying k_{lo} are compared against α_{evap}, for both the unfunctionalised and best functionalised membrane, in figs. 7.2 & 7.3.

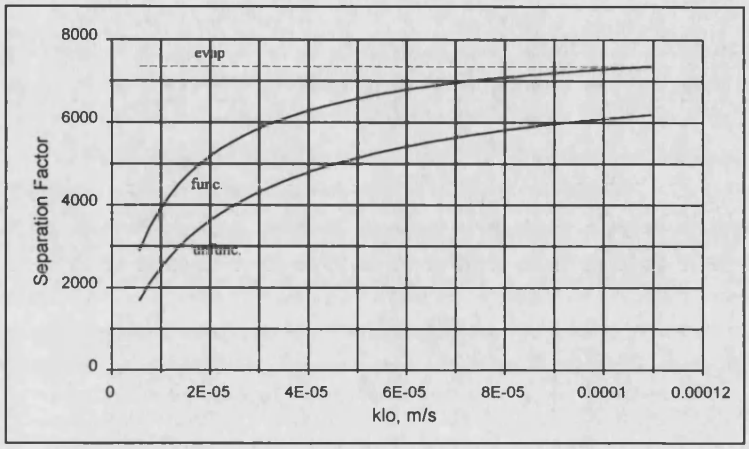

Fig. 7.2 - Chloroform Separation, Effect of k_{lo}

T_{feed} = 25°C, T_{cond} = 1°C (P_{Tp} = 26.44 mbar), δm = 50 μm, w_{cf} = *0.0001*

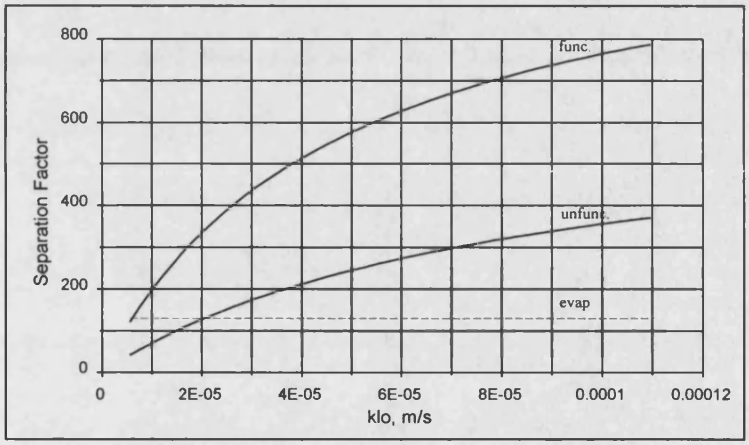

Fig 7.3 - MIBK Separation, Effect of k_{lo}

T_{feed} = 70°C, T_{cond} = 1°C (P_{Tp} = 12.03 mbar), δm = 50 μm, w_{mf} = *0.01*

For chloroform separation it can be seen that even when k_{lo} approaches the limit of practical feasibility, overall α only equals α_{evap} for the best functionalised membrane. The use of a much greater δ_m would lead to separation factors in excess of α_{evap} being achieved. This would lead, however, to a much greater required total membrane area and increased expense. Considering the excellent performance achieved for the above specified separation, as displayed in table 7.6, it would appear counter productive to operate under this condition of increased expense. It may be concluded that although pervaporation

performs extremely well for chloroform separation, it is thermodynamically a very easy separation and it is likely that methods based solely upon vapour-liquid equilibrium would prove economically more viable. Suitable processes might include distillation, membrane distillation or even simple flash systems.

7.3.7.1 Comparison with Two Stage Flash Process

In order to demonstrate this point, the same separation as specified for tables 7.5 & 7.6 may be readily achieved by a simple, isothermal (at 25°C), two stage flash process. It is assumed that total disengagement of vapour, from the liquid phase, is achieved and *eq. (5.1)* is used to describe the vapour composition in equilibrium with the specified liquid composition in both flash units:-

$$\alpha_{evap} = \frac{(p_{cf}/p_{wf})}{(x_{cf}/x_{wf})} \qquad (5.1)$$

Where p_{if} is given by:-

$$p_{if} = \gamma_i x_{if} P_i^{sat} \qquad (4.2)$$

The liquid phase composition from the first unit is specified to be 1 ppm chloroform, i.e. the desired retentate concentration. The equivalent composition for the second unit is set at 100 ppm, i.e. equal to the feed concentration. This stream is recycled and combined with the feed stream to the first unit. A simple mass balance, in combination with *eq. (5.1)*, yields the overall flowrate (q, kg/hr) and chloroform mass fraction (w_c) results, for each process stream. The results are displayed in fig. 7.4.

Although the flash units are not sized, the lack of mechanical parts and very simple design should yield an inexpensive process. Energy requirement would be low as only a small fraction of each unit feed stream is vaporised. The small product stream would require condensation and, following phase separation, a useful chloroform product would again be recovered. It is likely that distillation may prove an even more attractive option for chloroform recovery.

Pervaporation might only be viable for this separation if a multi purpose unit is being used for a number of separations at a particular site. In this case it may prove to be sensible to

use the existing pervaporation equipment rather than to undertake the capital expense in investing in further plant equipment.

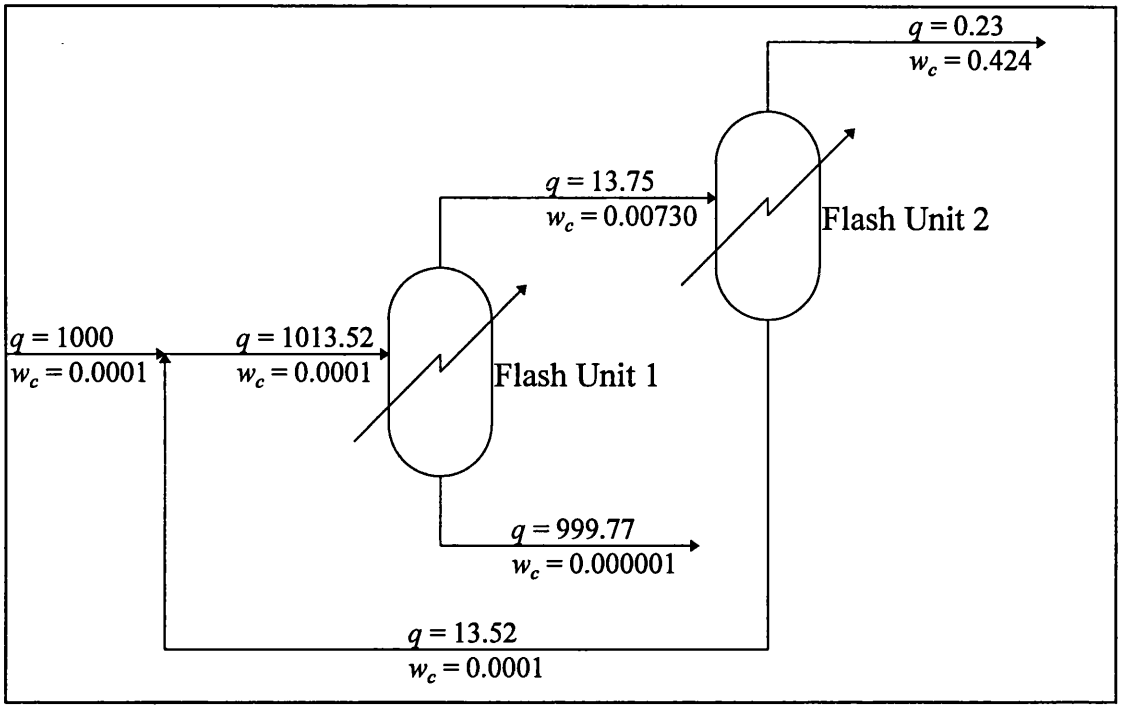

Fig. 7.4 - Two Stage Flash Process

In order for MIBK separation to be competitive, the need to maximise k_{lo} is emphasised by fig. 7.3. Utilising the functionalised membrane offers clear advantages as at $k_{lo} = 10^{-4}$ m/s, $\alpha = 6.0\ \alpha_{evap}$ may be achieved with the functionalised membrane, whereas only $\alpha = 2.8\ \alpha_{evap}$ may be achieved with the unfunctionalised membrane.

As boundary layer resistance has a much smaller effect upon pyridine permeation, overall α values approaching the intrinsic values given in table 5.6 should be readily achieved, which far exceed α_{evap}.

7.4 Further Economic Considerations

In order to undertake a comprehensive economic evaluation of a pervaporation system the separation to be achieved has to be very tightly defined. A change in any operating parameter could entirely change both the physical configuration and economics of the process. For this reason a rigorous quantitative analysis is not attempted, however, further

economic considerations and summaries of studies undertaken by other authors are discussed below.

A number of authors have attempted to cost a pervaporation process for given separations. In order to achieve this it is necessary to estimate the cost of each individual equipment component required and the cost of energy, engineering, construction, labour and maintenance. Equipment cost curves and equations and estimates of the magnitudes of the other costs involved have been comprehensively reported by a number of authors, for typical pervaporation equipment and configurations *(Ji, Hilaly, Sikdar and Hwang, 1994)*, *(Hickey and Gooding, 1994)*, *(Blume et al, 1990)*, *(Lipski and Cote, 1990)*. In all of these studies, most of the cost data is taken from two particularly useful books *(Wood, 1983)*, *(Peters and Timmerhaus, 1990)*. The Marshall & Swift Equipment Cost Index, published monthly within *Chemical Engineering* is very useful in updating costs, initially estimated some time ago, to present day costs.

7.4.1 Economic Case Studies

The overall treatment costs for various separations using organophilic membranes, expressed as $\$/m^3$ of treated feed, are summarised in table 7.8. This cost incorporates both operating and capital costs over the working life of the plant. In each case the Marshall and Swift index is used in order to update overall costs to 1995 values. The overall treatment cost has simply been factored up using:-

$$Cost_{1995} = Cost_{ref\,year} \times \frac{Index_{1995}}{Index_{ref\,year}} \qquad (7.11)$$

Where various operating conditions and configurations have been considered, those which produce the minimum overall cost are reported.

Most of the studies performed above are concerned with the removal of volatile organics, at low concentrations, from contaminated waste water. Two of the studies, 3.2 & 4.2, are representative of typical solvent recovery applications. Although in both cases the treatment costs are relatively high, a substantial credit may be realised due to the recovery of a valuable solvent, which may well make each process profitable. Case 6.2 is representative of a typical offshore water treatment problem.

Ref	Organic	q_f m^3/hr	w_f ppm	w_r ppm	Cost $/m^3	Configuration
1.1	Toluene	16	500	50	0.57	Hollow Fibre
1.2	Methylene Chloride	16	500	50	0.57	Hollow Fibre
1.3	Trichloroethylene	16	500	50	0.57	Hollow Fibre
2.1	Methylene Chloride	10	100	10	0.95	Spiral Wound
2.2	Chloroform	10	100	10	0.83	Spiral Wound
2.3	Trichloroethylene	10	100	10	0.67	Spiral Wound
2.4	1,2-dichloroethane	10	100	10	1.56	Spiral Wound
3.1	VOC	15.8	1000	100	0.65	Spiral Wound
3.2	VOC	15.8	20000	2000	1.51	Spiral Wound
4.1	Benzene	3.16	1000	10	3.46	Spiral Wound
4.2	Ethyl Acetate	3.16	20000	2000	3.49	Spiral Wound
5.1	Trichloroethylene	10	10	0.1	0.63	Hollow Fibre
6.1	VOC	10	10	0.1	0.67	Spiral Wound
6.2	VOC	500	500	5	0.51	Spiral Wound

Table 7.11 - Economic Analysis

References:-

1.1 - 1.3 *(Ji et al, 1994)* 2.1 - 2.4 *(Hickey and Gooding, 1994)*

3.1 - 3.2 *(Blume et al, 1990)* 4.1 - 4.2 *(Wijmans et al, 1990)*

5.1 *(Lipski and Cote, 1990)* 6.1 - 6.2 *(Nijhuis, 1990)*

Although treatment cost is a strong function of separation and process conditions, it can be seen that all the overall costs are of a similar order of magnitude. Although the costs in studies 4.1 & 4.2 seem very high, it was noted that treatment cost reduced with increasing feed flow rate, reaching a minimum of the order of $\$2.00/m^3$. For the hollow fibre configuration studies, 1.1, 1.2 & 1.3, it was noted that when operating in the laminar feed side region, capital costs dominate, whereas in the turbulent region, operating costs dominate overall costs. Treatment costs in studies 6.1 & 6.2 were quoted in the currency Dfl. An approximate conversion rate of 1\$ = 1.8 Dfl is used.

7.4.2 Membrane and Module Cost

A crucial parameter in all of the above studies is the cost of both membranes and modules. Where these actual costs have been reported, the most common values taken are $\$100/m^2$ for the membrane and a further $\$100/m^2$ of membrane for the module, as used in studies 1.1 - 1.4, 3.1 - 3.2 and 5.1. In studies 2.1 - 2.4 the membrane cost was assumed to be $\$150/m^2$ and the module cost taken to be $200 per module. In two of these studies the total membrane and module cost was reported as a proportion of the overall treatment cost. For cases 2.1 - 2.4 membrane and module cost amounted to 49.1 - 60.6% of the total cost and for cases 3.1 - 3.2 amounted to 20 - 26% of the total.

It has been suggested *(Rautenbach et al, 1992)* that a combined membrane and module cost of $\$200/m^2$ is too low. Based upon costs supplied by Bayer AG and GFT, for spiral wound modules, combined membrane and module costs of 5 times this value are thought more realistic. Using this new figure and other revised capital and operating costs a direct cost comparison with case 3.1 was undertaken. Total costs were calculated to be 3.4 times greater than those reported in table 7.11 and membrane and module cost found to represent 52% of the total.

If membrane and module costs really do represent such high proportions of the overall cost, very significant savings may be made by reducing membrane area. If it is assumed that functionalised PDMS membranes may be produced at the same price as unfunctionalised PDMS membranes, the economic benefits of using the former may be approximately quantified. For example, taking data from the case study for pyridine separation presented in table 7.4, it can be seen that a 20% saving in overall cost may be realised if it is assumed that membrane and module cost represents 50% of the overall cost.

7.4.3 Comparison with Competing Technologies

Obviously, when considering the economics of pervaporation it is necessary to make a cost comparison with other competing technologies. For the case 5.1 above, pervaporation was found to display at least a 35% saving in overall costs over a combination of air stripping and activated carbon adsorption. Both cases 6.1 & 6.2 were compared economically with

liquid phase carbon adsorption, air stripping / gas phase adsorption and air stripping / bio filtration. Pervaporation displayed savings of at least 68% for case 6.1 and 38% for case 6.2. It was also determined that the space requirement of a pervaporation plant is significantly lower than that for any of the other processes. This would be of particular advantage in the off shore water treatment case, 6.2, where available space would be limited. Of course, pervaporation may not appear as economically attractive if the membrane and module costs are, in reality, significantly higher than those used within the analysis.

Three further studies have concluded that pervaporation displays significant economic benefits over competing technologies. For the removal of small quantities of methylethylketone and benzene from wastewater, pervaporation was found to display 6% capital and 52% operating cost savings over oxidation and 22% capital and 5% operating cost savings over steam stripping *(Barber and Miller, 1994)*. For the removal of trichloroethylene from contaminated ground water, pervaporation was shown to display high capital costs but a 70% reduction in operating costs, when compared to carbon adsorption. Pervaporation was also shown to be competitive with distillation for the recovery of isopropylalcohol, IPA, from a 7.0 %wt. IPA, aqueous stream *(Athyde, Markiewicz, Miller and Wijmans, 1995)*. A payback period of 2.2 years was found compared with that of 4.1 years for distillation.

7.4.4 Hybrid Systems

Due to the diminishing driving force for permeation, pervaporation technology can become prohibitively expensive if very low organic concentrations are to be required. Conversely, at very high organic feed concentrations, pervaporation technology is unlikely to compare favourably with distillation. In order to achieve a given separation in the most economically attractive manner, the combination of pervaporation with other separation technologies, within hybrid processes, should be considered. The approximate organic concentration range of applicability for a variety of technologies, for the separation of VOC's from water, has been reported *(Schofield et al, 1991)* and is displayed in table 7.12.

Technology	Organic Conc.		Technology	Organic Conc.	
	min	max		min	max
Carbon Adsorption	<1 ppm	500 ppm	Pervaporation	10 ppm	100%
Air Stripping	<1 ppm	1100 ppm	Solvent Extraction	50 ppm	8%
Reverse Osmosis	<1 ppm	3%	Wet Air Oxidation	100 ppm	10%
Liquid Membranes	1 ppm	1000 ppm	Distillation	4%	100%
Steam Stripping	1 ppm	30%	Incineration	10%	100%

Table 7.12 - Range of Applicability for Various Separation Technologies

Hybrid processes combining distillation with hydrophilic pervaporation have been proven to be economically viable, on an industrial scale, for the dehydration of organic solvents *(Fleming, 1990)*. Similar systems could be used, utilising organophilic pervaporation, for the removal of organics from water, when organic feed concentrations are high. Hybrid processes combining pervaporation with carbon adsorption have been evaluated for reducing trichloroethylene concentrations in groundwater to less than 1 ppb *(Barber and Miller, 1994)*, *(Athyde et al, 1995)*. The hybrid process was found to be economically favourable, compared to carbon adsorption alone, provided that the plant were required to operate for more than 3 years. A pervaporation / reverse osmosis hybrid process has been evaluated for the removal of phenol from waste water *(Rautenbach and Klatt, 1991)*. The hybrid process proved economically favourable to adsorption and the costs were similar to that of solvent extraction. It was concluded that if pervaporation membrane performance could be enhanced and / or membrane and module costs reduced, the hybrid process could display significant cost advantages over extraction.

7.5 Closing Remarks

An examination of the case studies presented in tables 7.1 - 7.7 highlights the importance of membrane thickness as an operating parameter. Best advantage of enhanced membrane material can only be realised if a range of different thicknesses are available. This is particularly true when low selectivity / low permeability membranes are employed, where significant performance enhancement can only be achieved if relatively thin membranes are available. Conversely, for membranes of high selectivity and enhanced permeability,

relatively thick membranes may be required in order to reduce the effect of feed side boundary layer resistance. It is unlikely that a given membrane would be commercially available in an extensive range of different thicknesses. When selecting which thicknesses to produce, it is of great importance to consider the types of separations that the membrane is most likely to be employed for and the hydrodynamic conditions achievable within the likely choice of module. A balance between the relative magnitudes of feed side boundary layer and membrane resistances has to be achieved. It may well be instructive to investigate the conditions under which the relative magnitudes are such that economic optimal configurations are achieved, for a number of different separations.

The selection of operating temperatures is also of great importance. Where overall selectivity is low, it would generally appear sensible to operate at high feed temperatures and condensation temperatures of above 0°C. This avoids the problem of expensive refrigeration and large solid phase streams. Where selectivity is high, operating at ambient feed temperatures and low condensation temperatures would appear to be beneficial. As the permeate stream is small in magnitude, the additional costs incurred to deal with the solid phase and operate at a sub 0°C condensation temperature should not be great. Elevating the feed temperature would require a large energy input, especially as the major feed component is water.

A large quantity of work, throughout pervaporation literature, has been undertaken for the removal of very volatile organics from water. Although pervaporation performs well, these separations are generally thermodynamically easy, especially when organic component activity coefficients are high. Particularly as pervaporation performance is severely limited by feed side boundary layer resistance, for these separations, it would appear unlikely that pervaporation could compare favourably with separation process based upon vapour-liquid equilibrium. This point is demonstrated by consideration of the two stage flash process proposed for chloroform separation. It is recommended that, in future, pervaporation research should concentrate upon the recovery of medium activity in water (i.e. no more active than MIBK) to low activity organic components from aqueous solution.

Perhaps the most crucial limiting factor in preventing organophilic pervaporation processes from becoming economically viable is the cost of membranes and modules. As these costs

typically constitute upwards of 50% of the total process cost, the production of cheap membranes and modules is of great priority. It is quite possible that very cheap, but poor performing materials could lead to a more economically attractive process than high performing, expensive materials. This might particularly be the case if energy costs are low and/or advantage may be taken of energy integration.

Chapter 8

Conclusions and Recommendations for Further Work

8.1 Conclusions

The industrial significance of organophilic pervaporation technology, for both wastewater treatment and solvent recovery applications, is discussed. For each of the organic components considered within this study, phenol, chloroform, pyridine and MIBK, potential pervaporation applications are highlighted for the recovery of such components from aqueous streams, produced during both component manufacture and usage.

8.1.1 Functionalised PDMS Membranes

The general applicability of two methodologies for the introduction of organofunctional groups into the PDMS structure is demonstrated, for numerous families of different groups. It is shown that significant separation performance enhancements may be achieved by the use of functionalised membranes, for each of the four separations investigated. It would appear almost certain that enhancements are due to an increase in organic component membrane sorption and/or a reduction in water sorption, due to changed interaction with the functional group. The transport of weakly acidic phenol molecules can be significantly enhanced through weak acid-base interaction with basic groups, leading to significant increases in both permeability and selectivity. Selectivity to the other three organic components can be substantially enhanced by the introduction of long chained alkyl groups. These groups strongly inhibit water transport, whilst only moderately inhibiting organic component transport. Although overall permeability declines, acceptable fluxes may still be maintained by the production of thinner membranes, down to a certain physical limit. A comparison of the functionalised membranes considered to yield the best overall separation performance is made with the unfunctionalised PDMS membranes, for each different separation, in table 8.1.

The introduction of functional groups into the membrane structure has the detrimental effect of increasing membrane brittleness. This phenomenon increases with increasing

functional loading and yields a membrane less rubbery and flexible in structure, leading to a reduction in organic component permeability. An optimal functional loading is shown to exist, at which the positive benefits of the preferential feed component interaction with the functional group outweigh the negative effects of increased brittleness to the greatest extent. For chloroform, pyridine and MIBK separation, a functional loading of approximately 10% octyl groups produces optimum selectivity.

Separation	Mem.	$S^a{}_oD_{mo}$ $\times 10^{11}$ m^2/s	α	Mem.	$S^a{}_oD_{mo}$ $\times 10^{11}$ m^2/s	α
Phenol	Unfunc.	2.15	17.7	10% Pyridyl	5.57	31.8
Chloroform	Unfunc.	4.68	8510	10% Octyl	2.77	12200
Pyridine	Unfunc.	13.07	55.7	10% Octyl	6.66	84.1
MIBK	Unfunc.	12.23	705	10% Tridecyl	7.05	1260

Table 8.1 - Comparison of Membrane Performance

Notes for table 8.1:-

$S^a{}_oD_{mo}$ = Organic Component Membrane Permeability Coefficient, m^2/s

α = Separation Factor

Chloroform results measured at 25°C, all others measured at 70°C

In some cases the cross-linking structure of both functionalised and unfunctionalised membranes is important in determining separation performance. With respect to the same functional group, functionalised membranes produced from functionalised PHMS (method 1) out perform membranes of equivalent functional loading produced from a trialkoxysilane (method 2). This is likely to be as a result of an even distribution of functional group throughout the membrane structure using method 1. Method 2 membranes are likely to exhibit a much less even distribution, with localised areas of very high group loading. Secondly, from a study of unfunctionalised PDMS membranes it is shown that permeability declines with increasing cross-linking density. Using membranes produced by varying the ratios of long chained PDMS to short chained PHMS, this decline is demonstrated to be negligible across the range of cross-linking densities generally employed within this study. Thirdly, the importance of using high PDMS chain lengths

(>240 repeating dimethylsiloxane units) is demonstrated, as below this value permeability declines.

8.1.2 Mass Transport Mechanisms

A comprehensive review of mass transport within pervaporation systems is undertaken and an approach based upon the solution-diffusion mechanism and Ficks first law adopted. Feed side boundary layer resistance is shown to be of generally great importance and in some cases can be the dominant resistance to mass transfer. It is shown that transport by convection is generally negligible compared to diffusive transport, within the boundary layer, for pervaporation processes in general. The same conclusion can certainly not be drawn for transport within the membrane itself. A combination of high membrane concentrations of a particular mobile component with low selectivity towards that component may produce substantial convective flows. This is particularly the case in hydrophilic pervaporation in which membrane solubilities of the non-preferentially transported organic component are often high. It remains unclear whether or not it is possible to achieve a full or partial convective flow within the restrictive matrix of a membrane structure. The potential importance of this phenomenon is, however, numerically demonstrated and it is recommended that further work in this area is required.

In most cases, organophilic pervaporation systems can be considered to behave in an "ideal" manner. This is due to a combination of typically low organic component concentrations and low membrane water sorption. Up to feed side activities of approximately 0.4, organic component sorption coefficients can be considered to be constant, obeying Henry's law. A combination of relatively low membrane concentrations of both water and organic component along with low membrane swelling, generally allows for the assumption of constant membrane diffusion coefficients. This "ideal" behaviour greatly simplifies the subsequent analysis of mass transport and allows for the use of a resistances in series model in order to model the entire process. It is experimentally demonstrated that the most likely source of "non-ideality" in organophilic pervaporation is the coupling effect of the organic component upon the transport of water. Even when the organic component behaves "ideally", water transport can be affected by membrane swelling caused by sorption of the organic. In hydrophilic pervaporation systems "non-

ideal" behaviour generally occurs at every stage of mass transport and the assumption of constant permeability coefficients is inappropriate and the use of a resistances in series approach compromised.

8.1.3 Process Parameters

The experimental and theoretical determination of the effect of various process parameters is investigated. Feed side boundary layer resistance is quantified using the resistances in series approach and indeed is found to be very significant for both chloroform and MIBK separations from water, even when using relatively thick membranes (>100 μm) and high (1000 rpm) stirrer speeds. It is noted that throughout pervaporation literature, performance data for similar separations has been reported by different authors and that widely differing results are often obtained for essentially the same separations using the same membranes. In many cases no mention of the effect or quantification of boundary layer resistance is made. It is thought that this phenomenon has often been overlooked and that published results reflect system performance rather than purely membrane performance. The inconsistencies between different studies are due to the use of differing experimental equipment.

The effect of the microporous Celgard 2500, used as a support material for each membrane in this study, has been quantified. It is found that the PDMS material fills the pores of the organophilic Celgard during membrane production. This causes an increase in effective membrane thickness, quantified as being equal to the thickness of the Celgard (25 μm) divided by its porosity (0.45).

Experimental data is fitted to models describing the effects of temperature and permeate pressure upon pervaporation performance and an examination of the effect of feed concentration made. It is shown that under conditions of zero driving force, i.e. when the sum of the partial pressure of each permeate component equals the sum of the partial pressure exerted by each feed component, fluxes drop to zero and the selectivity achieved is equal to that obtained by simple evaporation. Provided that overall pervaporation selectivities are greater than those achieved purely by a process of evaporation, both selectivity and flux increases with decreasing permeate pressure. If selectivities are below

that achieved by evaporation, selectivities actually decline with decreasing permeate pressure, although fluxes always increase. The greater the enhancement in selectivity above that achieved by evaporation, the more sensitive that selectivity is to an increase in permeate pressure, in some cases dropping dramatically as permeate pressure increases much above a few mbar. This is shown to be particularly the case for phenol / water separation.

A classical Arrhenius relationship between component flux and temperature is obtained, allowing for the calculation of apparent activation energies for component permeation. Coupling effects are found to be important for water transport and are also shown to be of importance for pyridine and MIBK transport. Pyridine permeability is found to decrease with increasing pyridine concentration and conversely MIBK permeability found to increase with increasing MIBK concentration. The former effect is thought likely to be as a result of neighboring pyridine molecules clustering and the later due to an increase in membrane swelling caused by an increase in MIBK concentration, consistent with classical theory.

In order to be able to accurately compare membrane performance data measured in different studies, using differing experimental apparatus and process conditions, it is crucial to have data reporting the effects of boundary layer resistance, microporous support, permeate pressure, concentration and temperature. Procedures for calculating out the effects of all external resistances to mass transfer are detailed within this study, allowing the calculation of true membrane, as opposed to system, performances. It is recommended that membrane permeability coefficients rather than overall flux, which is in itself very much a function of external resistances, should be calculated and reported.

8.1.4 Process Modeling and Evaluation

A new comprehensive integrated model, with due reference to boundary layer resistance, is developed, based upon the assumption of "ideal" pervaporation. It is used to investigate the effect of both membrane properties and process conditions upon overall pervaporation performance.

Differential mass and energy balance equations, based upon the integrated model, are developed and solved in order to determine required membrane areas and energy requirements for model separation problems. In many cases it is shown that very significant savings may be realised if functionalised PDMS membranes are employed as opposed to unfunctionalised membranes. In order to take full advantage of enhanced membrane materials it is shown that membrane thickness is a crucial parameter. Often only moderate savings may be made unless the selection of a membrane approaching optimal thickness is possible. It is clearly demonstrated that in situations where feed side boundary layer resistance dominates mass transport, employing enhanced membranes yields negligible performance enhancements. In this case improving feed side hydrodynamics is of much greater priority.

In industrial applications where it is usual to maintain a low permeate pressure by a process of permeate condensation, the implications of producing a solid permeate phase are discussed. In cases where it is necessary to achieve a low permeate pressure in order to realise sufficient performance, or even to maintain a driving force for permeation, the formation of a solid phase is unavoidable. Many of the problems associated with such a phase may be overcome by operating with a two condenser in parallel configuration, each condenser undergoing a defrosting cycle in turn. It is shown that close attention should be paid to the choice of module design and the optimisation of process configurations. In many cases phase separation of the permeate may be achieved by simple decantation and this can greatly enhance the effective selectivities achieved within a pervaporation system.

A new model describing the effect of temperature upon component transport, in which an Arrhenius relationship is applied to the membrane permeability coefficient as opposed to overall flux, is also developed. The advantage of this new model is that it allows for the separation of driving force effects from membrane properties and accurately predicts zero flux under conditions of zero driving force, unlike the former model. The activation energies for permeation of the organic components predicted by the new model are both lower in value and much more similar in magnitude to each other, compared to the model predicting an Arrhenius relationship with flux. An activation energy range of -15.2 to -22.3 kJ/mol is found, for the four separate organic components, using the new model, as opposed to a range of -9.15 to -31.63 kJ/mol.

It is argued that unless selectivities may be realised that are well in excess of those achieved purely by evaporation, pervaporation may not be competitive with techniques that rely solely upon vapour-liquid equilibrium as a separation mechanism. For very volatile organic components displaying high activity coefficients in aqueous solution, such as chloroform, this will often be the case, particularly as selectivities are so high that feed side boundary layer resistance may severely inhibit pervaporation performance. It is recommended that, for this reason, future pervaporation work should be confined to components displaying moderate to low activities in aqueous solutions. Although absolute pervaporation performance for these separations will not appear as attractive as those for components of high activity, much greater selectivity enhancement above that achieved by evaporation will be realised.

Probably the most crucial factor in improving the economics of organophilic pervaporation is a reduction in both membrane and module costs. It is discussed that these costs constitute a very significant proportion of the overall process cost. For this reason, the production of enhanced membrane materials that lead to an overall reduction in membrane area is usually of great practical benefit.

8.2 Recommendations for Future Work

8.2.1 Membrane Materials

1. Production of a modified PDMS membrane containing an acidic organofunctional group: It is thought likely that the transport of basic organic components would be significantly enhanced by such a membrane. In order to achieve this goal, a more advanced methodology is required to enable the acidic group functionalisation of PHMS. In order to prevent the acidic group, of an allyl-acid reactant, reacting with the *Si-H* group of the PHMS, it may be possible to chemically shield the group prior to reaction and then to treat the resultant product in order to re-expose it, either prior to or after membrane formation.

2. Production of pyridyl functionalised membranes produced from functionalised PHMS (method 1): To date the best membrane for phenol separation, pyridyl functionalised

PDMS, has only been produced by the functionalised trialkoxysilane method (method 2). As it has been demonstrated that method 1 membranes give better performance than method 2 membranes, further enhancements may be realised if such membranes could be produced by method 1. Again a more advanced methodology, similar to that for the production of an acidic functionalised membrane, would be required, in order to prevent reaction of the pyridyl group.

3. Incorporation of most promising functional groups into other membrane polymer materials: This may be of particular benefit for organic / water separations for which PDMS is not considered to be the best available base material. In particular, the introduction of long chained alkyl groups is likely to lead to enhanced selectivities for most materials.

4. Incorporation of zeolite fillers: Functionalised PDMS membranes containing zeolites should display further enhancement in selectivity, towards organic feed components of relatively small molecular size.

5. Further investigation of the effect of functional loading: Membranes containing a greater range of functional loading should be produced and tested in order to further investigate optimal loading, particularly for phenol / water separation.

6. Production of thin membranes: As previously discussed, the production of very thin membranes is counter productive in situations where feed side boundary layer resistance dominates organic component transport. For separations displaying relatively low selectivities, e.g. phenol and pyridine separations from water, the production of thin membranes (<10 μm) may still be desirable. It would be necessary to identify a new microporous support material as it is difficult to produce a composite membrane of effective thickness of less than 56 μm using Celgard 2500, due to pore filling during membrane manufacture. A solvent evaporation technique may be appropriate. The membrane constituents and cross-linking agents could be dissolved in an appropriate solvent, the mixture placed on top of a flat surface and the solvent allowed to slowly evaporate.

8.2.2 Experimental Measurement

7. Independent measurement of membrane sorption and diffusion coefficients: This could be achieved by employing the methods detailed within chapter 2. The separation of overall permeability into these two factors would provide a greater insight into the physical and chemical interactions of feed components with membrane functional groups.

8. Assessment of functionalised membranes for further organic / water separations: Evaluations for further families of industrially important organic components, such as alcohols, ethers etc.

9. Effect of feed temperature for a variety of functionalised PDMS membranes: Within this study, the effect of temperature is quantified for only one membrane type, for each separation considered. It is quite possible that different functionalised membranes could display differing activation energies for component permeation.

10. Effect of feed concentration for a variety of functionalised PDMS membranes: Again, only one type of membrane has been used to investigate this effect for each separation. A greater concentration range should be studied, particularly at very low organic component concentrations. This would allow for the determination of diffusion coefficients at infinite dilution and plasticisation and coupling coefficients.

11. Measurement of membrane properties: The measurement of membrane density, glass transition temperature and water contact angle should again provide a greater insight into the effect of various functional groups.

12. Measurement of activity coefficients: It is highlighted that the activity coefficient is a crucial parameter in determining separation performance. As reported data is often both incomplete and inconsistent, an activity coefficient estimation technique is employed within this study. As the absolute accuracy of such an approach can not be guaranteed, the accurate experimental determination of activity coefficient data should be undertaken.

13. Membrane stability: The stability of functionalised membrane performance over an extended period of time should be determined. This could most effectively be achieved by testing membrane samples within a continuous operation experimental rig.

8.2.3 Verification of Proposed Models

14. Effect of stirrer size and geometry upon boundary layer mass transfer coefficients: Experimental work should be undertaken in order to investigate the validity of the relationship proposed by *eq. (2.18)*, for modifying existing Sherwood correlations:-

$$k_{lo} = (b\,\varphi^{c-1})\,\omega^{c}\,d_s^{c-1}\,\nu^{d-c}\,D_{lo}^{1-d} \qquad (2.18)$$

15. Possibility of convective flow occurring within the membrane: This phenomenon should be investigated by attempting to fit *eq. (2.56)* to experimental data:-

$$J_i = -D_{mi}\frac{dC_{im}}{dx} + \varepsilon u C_{im} \qquad (2.56)$$

Should such a flow be proven to exist, values of factor ε should be tabulated for a variety of membrane materials and separations. It is displayed that convective flow is likely to be of greatest significance within hydrophilic membranes.

16. Validation of new model proposed for the effect of temperature: *Eq. (6.8)* essentially separates the effect of component transport driving force, $\left(\gamma_i x_{if} - y_{ip}\frac{P_{Tp}}{P_i^{sat}}\right)$, from the effect of temperature upon membrane properties:-

$$S^a{}_i\,D_{mi} = S^a{}_i\,D_{mi}^{*}\,exp\left(\frac{-E_a}{RT}\right) \qquad (6.8)$$

Experimental work should be performed under a more extensive range of driving force conditions, particularly under relatively high permeate pressures, in order to validate that the effect of temperature upon the two influences on performance can be separated.

8.2.4 Process Evaluation

17. Membrane module design and configuration: A more comprehensive economic analysis should be performed in order to further investigate optimal designs for various classes of separation.

18. Feed side temperature drop: Within this study, when determining membrane areas and number of individual modules required, fairly arbitrarily set values for allowable feed side temperature drop within a module are employed. This parameter should be the subject of a more rigorous evaluation.

19. Comprehensive quantitative economic evaluation: This should be undertaken for real examples of industrially relevant separation problems. The economics of pervaporation using functionalised PDMS membranes should be compared with competing technologies.

20. Hybrid processes, involving a combination of pervaporation with established processes: Hybrid processes should be evaluated with particular emphasis being placed upon the optimisation of hand over feed concentrations between each unit operation.

21. Comparison of pervaporation with separation processes based solely upon vapour-liquid equilibrium: It is suggested that unless pervaporation selectivity significantly exceeds that achievable by simple evaporation, pervaporation processes may not be competitive with vapour-liquid equilibrium based processes. Careful economic evaluation is required in order to conclusively verify this statement.

22. Determination of optimal membrane thickness: It is highlighted within chapter 7 that if full advantage is to be made of enhanced membrane materials, membrane thickness becomes a crucial parameter. It is unlikely that a very extensive range of thicknesses, for a particular membrane type, would be made commercially available. The determination of sample thicknesses that are likely to prove close to optimal for various groups of separations, within differing membrane modules, should be undertaken.

List of Symbols

a = Activity
A = Avogadro Number, Liquid Transport Parameter, mol/sm^{2}Pa, Area, m^2, Constant, Dimensional Antoine Constant
B = Vapour Transport Parameter, mol/sm^{2}Pa^2, Dimensional Antoine Constant
C = Mass Concentration, kg/m^3, Dimensional Antoine Constant
d = Dimension, m
D = Diffusion Coefficient, m^2/s
E = Energy, J/mol
J = Solute Flux, kg/m^{2}s
k = Mass Transfer Coefficient, m/s
l = Interaction Parameter
L = Length, m
m = Interaction Parameter, Mass Flow, kg/s
M = Molecular Mass, kg/kmol, Mass, kg
P = Pressure, Pa, mmHg
q = Power, kW
Q = Duty, kW
R = Gas Constant
S = Sorption Coefficient
T = Temperature, K, °C
t = Time, s
u = Convective Velocity, m/s
v = Feed Velocity, m/s
V = Molar Volume, m^3/kmol, Volume Fraction
w = Mass Fraction, empirical correction term
x = Distance, m, Liquid Phase Mole Fraction
y = Vapour Phase Mole Fraction

α = Separation Factor, empirical correction term
β = Selectivity Coefficient, empirical correction term
χ = Interaction Parameter
δ = Thickness, m, Solubility Parameter, J$^{1/2}$/cm$^{3/2}$
ε = Efficiency Factor
ϕ = Volume Fraction of Component, Association Parameter
γ = Plasticisation Coefficient, m^3/kg, Activity Coefficient
η = Flux Constant, kg/ms
φ = Characteristic Dimension Parameter
μ = Viscosity, kg/ms
ν = Kinematic Viscosity, m^2/s
ρ = Density, kg/m^3
υ = No. Effective Segments in Sample
ω = Rotational Velocity, rad/s
ψ = Celgard 2500 Porosity

Cp = Specific Heat Capacity, kJ/kgK
ΔH^T_{vap} = Heat of Vaporisation at Temperature T, kJ/kg
$nmod$ = Number of Equal Area Modules

Pe = Peclet Number
Re = Reynolds Number
Sc = Schmidt Number
Sh = Sherwood Number

a denotes activation, activity based
av denotes average
b denotes bulk
c denotes characteristic, cross linked unit, concentration based, chloroform, Celgard
d denotes contribution due to diffusion
exp denotes experiment
f denotes feed
i denotes component i
j denotes component j
L denotes liquid
l denotes boundary layer
m denotes membrane, MIBK
mb denotes upstream membrane surface
md denotes dry membrane
mol denotes molar basis
o denotes solute
ov denotes overall
p denotes permeate, phenol, pyridine, permeate
r denotes retentate
s denotes stirrer, support
T denotes total
u denotes unswollen
v denotes volumetric, vapour
w denotes solvent
x denotes x coordinate
y denotes y coordinate
z denotes z coordinate
0 denotes infinite dilution
1 denotes organic component, upstream interface
2 denotes water, downstream interface
3 denotes polymer
$*$ denotes pre exponential factor, phase boundary
Φ denotes molar basis

References

Abed-Ali, S.S., Brisdon, B.J., England, R. (1989). Poly(Organosiloxanes) Containing Crown Ether Functionalities. *Macromolecules*, 22, 3969-3973.

Aguilo, A., Hobbs, C.C., Zey, E.G. (1986). Acetic Acid. *Ullmans Encyclopedia of Industrial Chemistry*, Vol. A 1 ed. Elves, B., Hawkins, S., Russey, W., Schulz, G. Weinheim: VCH Publishers Inc.

Aoki, T., Yamagiwa, K., Yoshino, E., Oikawa, E. (1993). Temperature Sensitive Ethanol Permselectivity of Poly(dimethylsiloxane) Membrane by the Modification of its Surface with Copoly(N-isopropylacrylamide / 1H, 1H, 2H, 2H-perfluorododecyl acrylate). Polymer, 34(7), 1538-1540.

Asada, T. (1992). Future of Pervaporation. *Proceedings of 6th Conf. on Pervaporation Processes in the Chemical Industry*. ed. R Bakish., pp. 554-558.

Ashworth, A.J., Brisdon, B.J., England, R., Reddy, B.S.R., Zafar, T. (1991). The Permselectivity of Polyorganosiloxanes containing Ester Functionalities. *Journal of Membrane Science*, 56, 217-228.

Aspen Plus. (1988). User Guide. Aspen Plus Technology Inc.

Athyde, A.L., Markiewicz, G., Miller, B., Wijmans, J.G. (1995). Removal and Recovery of Volatile Organic Compounds from Water by Pervaporation - Opportunities and Applications. *Proceedings of 7th Conf. on Pervaporation Processes in the Chemical Industry*. ed. R Bakish., pp. 338-348.

Barber, T.A., Miller, B.D. (1994). Pervaporation Technology: Fundamentals and Environmental Applications. *Chemical Engineering*, 101(9), 88-90.

Barton, A.F.M. (1983). Handbook of Solubility Parameters and Cohesion Parameters. Florida: CRC Press.

Beaumelle, D., Marin, M., Gibert, H. (1993). Pervaporation with Organophilic Membranes: State of the Art. *Trans. IChemE*, 71(Part C), 77-89.

Bell, C.M., Gerner, F.J., Strathmann, H. (1988). Selection of Polymers for Pervaporation Membranes. *Journal of Membrane Science*, 36, 315-329.

Bengtson, G., Pingel, H., Boddeker, K.W. (1991). Recovery of ABE Fermentation Products by Integrated Pervaporation. *Proceedings of 5th Conf. on Pervaporation Processes in the Chemical Industry*. ed. R Bakish., pp. 508-510.

Bitter, J.G.A. (1991). Transport Mechanisms in Membrane Separation Processes. New York: Plenum Press.

Blume, I., Bos, A., Schwering, P.J.F., Mulder, M.H.V., Smolders, C.A. (1991). Transport Phenomena of Vapour and Liquid Permeants in Elastomeric Membranes. *Proceedings of 5th International Conference on Pervaporation Processes in the Chemical Industry*. ed. R.Bakish., pp. 190-204.

Blume, I., Schwering, P.J.F., Mulder, M.H.V., Smolders, C.A. (1991). Vapour Sorption and Permeation Properties of Polydimethylsiloxane Films. *Journal of Membrane Science*, 61, 85-97.

Blume, I., Wijmans, J.G., Baker, R.W. (1990). The Separation of Dissolved Organics from Water by Pervaporation. *Journal of Membrane Science*, 49, 253-286.

Boddeker, K.W., Bengtson, G. (1991). Selective Pervaporation of Organics from Water. In: Pervaporation Membrane Separation Processes. Huang, R.Y.M. ed., pp. 437-460. Amsterdam: Elsevier.

Boddeker, K.W., Bengtson, G., Bode, E. (1990). Pervaporation of Low Volatility Aromatics from Water. *Journal of Membrane Science*, 53, 143-158.

Boddeker, K.W., Pingel, H., Dede, K. (1992). Continuous Pervaporation of Aqueous Phenol on a Pilot Plant Scale. *Proceedings of 6th Conf. on Pervaporation Processes in the Chemical Industry*. ed. R Bakish., pp. 514-519.

Borges, C.P., Mulder, M.H.V., Smolders, C.A. (1992). Composite Hollow Fiber for Removal of VOCs from Water by Pervaporation. *Proceedings of 6th International Conference on Pervaporation Processes in the Chemical Industry.* ed. R.Bakish., pp. 207-222.

Brisdon, B.J., Watts, A.M. (1985). Synthesis of Organofunctional Siloxanes Containing Metal-Ligating Side-Chains. *J. Chem. Soc. Dalton Trans.*, 2191-2194.

Brodkey, R.S., Hershey, H.C. (1988). Transport Phenomena A Unified Approach. New York: McGraw-Hill.

Brun, J.P., Larchet, C., Melet, R., Bulvestre, G. (1985). Modeling of the Pervaporation of Binary Mixtures through Moderately Swelling, Non-Reacting Membranes. *Journal of Membrane Science*, 23, 257-283.

Brun, J.P., Larchet, C., Bulvestre, G., Auclair, B. (1985). Sorption and Pervaporation of Dilute Aqueous Solutions of Organic Compounds through Polymer Membranes. *Journal of Membrane Science*, 25, 55-100.

Bruschke, H.E.A. (1991). State-of-Art of Pervaporation. Proceedings of 5th Conf. on Pervaporation Processes in the Chemical Industry. ed. R Bakish., pp. 2-6.

Burslem, R.H., Naylor, T.D., Field, R.W. (1992). The Performance and Stability of Polyacrylate Membranes. *Proceedings of 6th International Conference on Pervaporation Processes in the Chemical Industry.* ed. R.Bakish., pp. 17-34.

Crank, J. (1975). The Mathematics of Diffusion. Second Edition. Oxford: Clarendon Press.

Cussler, E.L. (1984). Diffusion: Mass Transfer in Fluid Systems. Cambridge: Cambridge University Press.

DeForest, E.M. (1989). Chloromethanes. Encyclopedia of Chemical Processing and Design vol. 8 ed. McKetta, J.J. New York: Marcel Dekker Inc. pp. 214-270.

Dotremont, C., Brabants, B., Geeroms, K., Mewis, J., Vandecasteele, C. (1995). Sorption and Diffusion of Chlorinated Hydrocarbons in Silicalite Filled PDMS Membranes. *Journal of Membrane Science*, 104, 109-117.

Drioli, E., Zhang, S., Basile, A. (1993). On the Coupling Effect in Pervaporation. *Journal of Membrane Science*, 81, 43-55.

Drioli, E., Zhang, S., Basile, A. (1993). Recovery of Pyridine from Aqueous Solution by Membrane Pervaporation. *Journal of Membrane Science*, 80, 309-318.

Fang, Y., Pham, V.A., Mahmud, H., Santerre, J.P., Narbaitz, R.M., Matsuura, T. (1995). Application of Surface Modifying Macromolecules for the Preparation of Membranes with High Surface Hydrophobicity to Extract Organic Molecules from Water by Pervaporation. *Proceedings of 7th International Conference on Pervaporation Processes in the Chemical Industry.* ed. R.Bakish., pp. 349-362.

Favre, E., Nguyen, Q.T., Schaetzel, P., Clement, R., Neel, J. (1993). Sorption of Organic Solvents into Dense Silicone Membranes. *Journal of the Chemical Society Faraday Transactions*, 89(24), 4339-4346.

Favre, E., Nguyen, Q.T., Schaetzel, P., Clement, R., Neel, J. (1994). Sorption, Diffusion and Vapor Permeation of Various Penetrants through Dense Polydimethylsiloxane Membranes: a Transport Analysis. *Journal of Membrane Science*, 92, 169-184.

Feng, X., Huang, R.Y.M. (1994). Concentration Polarisation in Pervaporation Separation Processes. *Journal of Membrane Science*, 92, 201-208.

Feng, X., Huang, R.Y.M. (1992). Separation of Isopropanol from Water by Pervaporation using Silicone Based Membranes. *Journal of Membrane Science*, 74, 171-181.

Field, R.W., Burslem, R. (1992). The Effect of Concentration Polarisation upon the Performance of Pervaporation Membranes. *Proceedings of 6th International Conference on Pervaporation Processes in the Chemical Industry.* ed. R.Bakish., pp. 275-289.

Fleming, H.L. (1990). Membrane Pervaporation: Separation of Organic/Aqueous Mixtures. *Separation Science and Technology*, 25(13-15), 1239-1255.

Flory, P.J. (1953). Principles of Polymer Chemistry. New York: Cornell University Press.

Fujita, H. (1961). Diffusion in Polymer-Diluent Systems. Advanced Polymer Science, 3, 1-23.

Geankoplis, C. J. (1982). Mass Transport Phenomena, 5th Printing. New York: Holt, Rinehart and Winston Inc.

Gekas, V., Hallstrom, B. (1987). Mass Transfer in the Membrane Concentration Polarisation Layer Under Turbulent Crossflow. I. Critical Literature Review and Adaptation of Existing Sherwood Correlations to Membrane Operations. *Journal of Membrane Science*, 30, 153-170.

Gmehling, J., Onken, U., Artt, W. (1978). Vapour-Liquid Equilibrium Data Collection. Frankfurt: Dechema.

Goe, G.L. (1982). Pyridine and Pyridine Derivatives. In: Kirk - Othmer Encyclopedia of Chemical Technology. 3rd ed. vol 19. ed. Mark, H.F., Othmer, D.F., Overberger, C.G., Seaborg, G.T., Greyson, M., Eckroth, D. New York: John Wiley & Sons.

Goethaert, S., Dotremont, C., Kuijpers, M., Michiels, M., Vandecasteele, C. (1993). Coupling Phenomena in the Removal of Chlorinated Hydrocarbons by means of Pervaporation. *Journal of Membrane Science*, 78, 135-145.

Gooding, C.H., Hickey, P.J., Crowder, M.L. (1991). Mass Transfer Characteristics of a New Pervaporation Module for Water Purification. *Proceedings of 5th International Conference on Pervaporation Processes in the Chemical Industry*. ed. R.Bakish., pp. 237-249.

Gref, R., Nguyen, Q.T., Neel, J. (1992). Influence of Membrane Properties on System Performances in Pervaporation under Concentration Polarisation Regime. *Separation Science and Technology*, 27(4), 467-491.

Guo, C.J., Kee, D.D. (1992). Effect of Molecular Structure on Diffusion of Organic Solvents in Rubbers. *Chemical Engineering Science*, 47, 1525-1532.

Habib, A.G. (1989). Methyl Isobutyl Ketone. Encyclopedia of Chemical Processing and Design vol. 21. ed. McKetta, J.J. New York: Marcel Dekker Inc. pp. 50-63.

Heintz, A., Funke, H., Lichtenthaler, R.N. (1991). Sorption and Diffusion in Pervaporation Membranes. *Pervaporation Membrane Separation Processes*. ed. R.Y.M. Huang. Amsterdam: Elsevier pp. 279-320.

Heintz, A., Stephan, W. (1994). A Generalised Solution-Diffusion Model of the Pervaporation Process through Composite Membranes. Part II. Concentration Polarization, Coupled Diffusion and the Influence of the Porous Support Layer. *Journal of Membrane Science*, 89, 153-169.

Hennepe, H.J.C.te, Bargeman, D., Mulder, M.H.V., Smolders, C.A. (1987). Zeolite Filled Silicone Rubber Membranes. Part 1. Membrane Preparation and Pervaporation Results. *Journal of Membrane Science*, 35, 39-55.

Hennepe, H.J.C.te, Boswerger, W.B.F., Bargeman, D., Mulder, M.H.V., Smolders, C.A. (1994). Zeolite Filled Silicon Rubber Membranes Experimental Determination of Concentration Profiles. *Journal of Membrane Science*, 89, 185-196.

Hennepe, H.J.C.te, Smolders, C.A., Bargeman, D., Mulder, M.H.V. (1991). Exclusion and Tortuosity Effects for Alcohol / Water Separation by Zeolite Filled PDMS Membranes. *Separation Science and Technology*, 26(4), 585-596.

Hickey, P.J., Gooding, C.H. (1994). The Economic Optimisation of Spiral Wound Membrane Modules for the Pervaporative Removal of VOC's from Water. *Journal of Membrane Science*, 97, 53-70.

Hino, T., Ohya, H., Hara, T. (1991). Removal of Halogenated Organics from their Aqueous Solutions by Pervaporation. *Proceedings of 5th Conf. on Pervaporation Processes in the Chemical Industry*. ed. R Bakish., pp. 423-436.

Huang, R.Y.M., Rhim, J.W. (1991). Separation Characteristics of Pervaporation Membrane Separation Processes. *Pervaporation Membrane Separation Processes*. ed. R.Y.M. Huang. Amsterdam: Elsevier, pp.111-180.

Ji, W., Hilaly, A., Sikdar, S.K., Hwang, S.T. (1994). Optimisation of Multicomponent Pervaporation for Removal of Volatile Organic Compounds from Water. *Journal of Membrane Science*, 97, 109-125.

Ji, W., Sikdar, S.K., Hwang, S.T. (1994). Modeling of Multicomponent Pervaporation for Removal of Volatile Organic Compounds from Water. *Journal of Membrane Science*, 93, 1-19.

Jordan, W., van Barneveld, H., Gerlich, O., Kleine-Boymann, M., Ullrich, J. (1991). Phenol. *Ullmans Encyclopedia of Industrial Chemistry*, Vol A 19 ed. Elves, B., Hawkins, S., Russey, W., Schulz, G. Weinheim: VCH Publishers Inc, pp. 299-312.

Joyce, P.C., Devine, K.M., Slater, C.S. (1995). Separation of Pyridine / Water Solutions using Pervaporation. *Separation Science and Technology*, 30(10), 2145-2158.

Karlsson, H.O.E., Tragardh, G. (1993). Pervaporation of Dilute Organic-Waters Mixtures. A Literature Review on Modeling Studies and Applications to Aroma Compound Recovery. *Journal of Membrane Science*, 76, 121-146.

Kedem, O. (1989). The Role of Coupling in Pervaporation. *Journal of Membrane Science*, 47, 277-284.

Kondo, M., Sato, H. (1994). Treatment of Wastewater from Phenolic Resin Process by Pervaporation. *Desalination*, 98, 147-154.

Koningsveld, R., Kleinjtens, L.A. (1971). Liquid-Liquid Phase Separation in Multicomponent Polymer Systems. X. Concentration Dependence of the Pair Interaction Parameter in the System Cyclohexane-Polystyrene. *Macromolecules*, 4, 637-641.

Koops, G.H., Smolders, C.A. (1991). Estimation and Evaluation of Polymeric Materials for Pervaporation Membranes. In: Pervaporation Membrane Separation Processes. Huang, R.Y.M. ed., pp. 253-278. Amsterdam: Elsevier.

Lamer, T., Rohart, M.S., Voilley, A., Baussart, H. (1994). Influence of Sorption and Diffusion of Aroma Compounds in Silicone Rubber on their Extraction by Pervaporation. *Journal of Membrane Science*, 90, 251-263.

Lapack, M.A., Tou, J.C., McGuffin, V.L., Enke, C.G. (1994). The Correlation of Membrane Permselectivity with Hildebrand Solubility Parameters. *Journal of Membrane Science*, 86, 263-280.

Lee, Y.M., Bourgeois, D., Belfort, G. (1989). Sorption, Diffusion and Pervaporation of Organics in Polymer Membranes. *Journal of Membrane Science*, 44, 161-181.

Lee, Y.M., Bourgeois, D., Belfort, G. (1989). Sorption, Diffusion and Pervaporation of Organics in Polymer Membranes. *Journal of Membrane Science*, 44, 161-181.

Lee, Y.T., Iwamoto, K., Sekimoto, H., Seno, M. (1989). Pervaporation of Water-Dioxane Mixtures with Poly(Dimethylsiloxane-co-Siloxane) Membranes Prepared by a Sol-Gel Process. *Journal of Membrane Science*, 42, 169-182.

Lee, G.T., Krovvidi, K.R., Greenberg, D.B. (1989). Pervaporation of Trace Chlorinated Organics from Water through Irradiated Polyethylene Membrane. *Journal of Membrane Science*, 47, 183-202.

Lipski, C., Cote, P. (1990). The use of Pervaporation for the Removal of Organic Contaminants from Water. *Environmental Progress*, 9(4), 254-261.

Lipski, C., Cote, P., Fleming, H. (1991). Transverse Feed Flow for Hollow Fibres Significantly Improves Mass Transfer at Low Energy Consumption. *Proceedings of 5th International Conference on Pervaporation Processes in the Chemical Industry.* ed. R.Bakish., pp. 134-142.

Matsumoto, Y., Kondo, M., Fujita, T. (1992). Transport Mechanism in PEBA Membrane. *Proceedings of 6th Conf. on Pervaporation Processes in the Chemical Industry.* ed. R Bakish., pp. 55-65.

Michaels, A.S. (1995). Effects of Feed-Side Solute Polarisation on Pervaporative Stripping of Volatile Organic Solutes from Dilute Aqueous Solution: a Generalised Analytical Treatment. *Journal of Membrane Science*, 101, 117-126.

Mulder, M.H.V. (1991). Thermodynamic Principles of Pervaporation. *Pervaporation Membrane Separation Processes.* ed. R.Y.M. Huang. Amsterdam: Elsevier pp. 225-252.

Mulder, M.H.V., Franken, T., Smolders, C.A. (1985). Preferential Sorption Versus Preferential Permeability in Pervaporation. *Journal of Membrane Science*, 22, 155-173.

Mulder, M.H.V., Smolders, C.A. (1991). Mass Transport in Pervaporation Processes. *Separation Science and Technology*, 26(1), 85-95.

Mulder, M.H.V., Smolders, C.A. (1984). On the Mechanism of Separation of Ethanol/Water Mixtures by Pervaporation. I. Calculations of Concentration Profiles. *Journal of Membrane Science*, 17, 289-307.

Neel, J. (1991). Introduction to Pervaporation. *Pervaporation Membrane Separation Processes.* ed. R.Y.M. Huang. Amsterdam: Elsevier pp. 1-110.

Nguyen, T.Q. (1987). Modeling of the Influence of Downstream Pressure for Highly Selective Pervaporation. *Journal of Membrane Science*, 34, 165-183.

Nguyen, T.Q., Nobe, K. (1987). Extraction of Organic Contaminants in Aqueous Solutions by Pervaporation. *Journal of Membrane Science*, 30, 11-22.

Nijhuis, H.H. (1990). Removal of Trace Organics from Water by Pervaporation. A Technical and Economic Analysis. Ph.D. Thesis, University of Twente, Enshede, The Netherlands.

Nijhuis, H.H., Mulder, M.H.V., Smolders, C.A. (1991). Removal of Trace Organics from Aqueous Solutions. Effect of Membrane Thickness. *Journal of Membrane Science*, 61, 99-111.

Nijhuis, H.H., Mulder, M.H.V., Smolders, C.A. (1993). Selection of Elastomeric Membranes for the Removal of Volatile Organics from Water. *Journal of Applied Polymer Science*, 47, 2227-2243.

Noezar, L., Nguyen, Q.T., Clement, R., Neel, J. (1995). High Performance Polymer Blend Membranes for Alcohol - Ether Separation. *Proceedings of 7th International Conference on Pervaporation Processes in the Chemical Industry.* ed. R.Bakish., pp. 45-51.

Okada, T., Matsuura, T. (1991). A New Transport Model for Pervaporation. *Journal of Membrane Science*, 59, 133-150.

Okada, T., Matsuura, T. (1992). Theoretical and Experimental Study of Pervaporation on the Basis of Pore Flow Mechanism. *Proceedings of 6th International Conference on Pervaporation Processes in the Chemical Industry.* ed. R.Bakish., pp. 137-152.

Perry, R.H., Green, D.W., Maloney, J.O. (1984). Perrys Chemical Engineers Handbook. 6th ed. New York: McGraw-Hill.

Peters, M.S., Timmerhaus, K.D. (1982). Plant Design and Economics for Chemical Engineers, New York: McGraw-Hill.

Psaume, R., Aptel, P., Aurelle, J.C., Mora, J.C., Bersillon, J.L. (1988). Pervaporation: Importance of Concentration Polarisation in the Extraction of Trace Organics from Water. *Journal of Membrane Science*, 36, 373-384.

Radovanovic, P., Thiel, S.W., Hwang, S.T. (1990). Transport of Ethanol-Water Dimers in Pervaporation through a Silicone Rubber Membrane. *Journal of Membrane Science*, 48, 55-65.

Raghunath, B., Hwang, S.T. (1992). Effect of Boundary Layer Mass Transfer Resistances in the Pervaporation of Dilute Organics. *Journal of Membrane Science*, 65, 147-161.

Rautenbach, R., Albrecht, R. (1985). The Separation Potential of Pervaporation Part 1. Discussion of Transport Equations and Comparison with Reverse Osmosis. *Journal of Membrane Science*, 25, 1-23.

Rautenbach, R., Klatt, S. (1991). Treatment of Phenol Contaminated Waste water by a RO-PV Hybrid Process. *Proceedings of 5th Conf. on Pervaporation Processes in the Chemical Industry*. ed. R Bakish., pp. 392-408.

Rautenbach, R., Klatt, S., Vier, J. (1992). State of the Art of Pervaporation, 10 Years of Industrial PV. *Proceedings of 6th Conf. on Pervaporation Processes in the Chemical Industry*. ed. R Bakish., pp. 2-15.

Reid, R.C., Prausnitz, J.M., Poling, B.E. (1987). The Properties of Gases and Liquids. 4th ed. New York: McGraw-Hill.

Rhim, J.W., Huang, R.Y.M. (1989). On the Prediction of Separation Factor and Permeability in the Separation of Binary Mixtures by Pervaporation. *Journal of Membrane Science*, 46, 335-348.

Rossberg, M., Lendle, W., Togel, A., Dreher, E.L., Langer, E., Rassaerts, H., Kleinschmidt, P., Strack, H., Beck, U., Lipper, K.A., Torkelson, T.R., Loser, E., Beutel, K.K. (1986). Chlorinated Hydrocarbons. *Ullmans Encyclopedia of Industrial Chemistry*, Vol A 6 ed. Elves, B., Hawkins, S., Russey, W., Schulz, G. Weinheim: VCH Publishers Inc, pp. 233-379.

Schofield, W., McCray, B., Ray, R.J., Newbold, D.D. (1991). Opportunities for Pervaporation in the Water Treatment Industry. *Proceedings of 5th Conf. on Pervaporation Processes in the Chemical Industry*. ed. R Bakish., pp. 409-420.

Sferrazza, R.A., Escobosa, R., Gooding, C.H. (1988). Estimation of Parameters in a Sorption-Diffusion Model of Pervaporation. *Journal of Membrane Science*, 35, 125-136.

Shaban, H.I. (1995). Separation of Binary, Ternary and Multicomponent Organic/Water Mixtures. *Gas Separation and Purification*, 9(2), 75-79.

Shanley, A., Ondrey, G., Moore, S. (1994). Pervaporation finds its Niche. Chemical Engineering, 101(9), 34-37.

Shimizu, S., Watanabe, N., Kataoka, T., Shoji, T., Abe, N., Morishita, S., Ichimura, H. (1993). Pyridine and Pyridine Derivatives. *Ullmans Encyclopedia of Industrial Chemistry*, Vol A 22 ed. Elves, B., Hawkins, S., Russey, W., Schulz, G. Weinheim: VCH Publishers Inc, pp. 399-430.

Siegel, H., Eggersdorfer, M. (1993). Ketones. *Ullmans Encyclopedia of Industrial Chemistry*, Vol A 15 ed. Elves, B., Hawkins, S., Russey, W., Schulz, G. Weinheim: VCH Publishers Inc, pp. 77-94.

Slater, C.S., Hickey, P.J., Juricic, F.P. (1990). Pervaporation of Aqueous Ethanol Mixtures through Polydimethylsiloxane Membranes. *Separation Science and Technology*, 25(9&10), 1063-1077.

Takegami, S., Yamada, H., Tsujii, S. (1992). Pervaporation of Ethanol/Water Mixture using Novel Hydrophobic Membranes containing Polydimethylsiloxane. *Journal of Membrane Science*, 75, 93-105.

Tyagi, R.K., Fouda, A.E., Matsuura, T. (1995). A Pervaporation Model: Membrane Design. *Chemical Engineering Science*, 50(19), 3105-3114.

Vankelecom, I.F.J., Depre, D., Beukelaer, S.D., Uytterhoeven, J.B. (1995). Influence of Zeolites in PDMS Membranes: Pervaporation of Water / Alcohol Mixtures. *Journal of Physical Chemistry*, 99, 13193-13197.

Vankelecom, I.F.J., Scheppers, E., Heus, R., Uytterhoeven, J.B. (1994). Parameters Influencing Zeolite Incorporation in PDMS Membranes. *Journal of Physical Chemistry*, 98, 12390-12396.

Volkov, V.V., Bokarev, A.K., Zheleznov, A.V., Selinskaya, Y.A., Rakhimov, V.M., Borisov, M.Y., Zakhovaev, I.R. (1995). Removal of High Boiling Organic Compounds from their Aqueous Solutions by Pervaporation. *Proceedings of 7th Conf. on Pervaporation Processes in the Chemical Industry.* ed. R Bakish., pp. 397-407.

Watson, J.M., Payne, P.A. (1990). A Study of Organic Compound Pervaporation through Silicone Rubber. *Journal of Membrane Science*, 49, 171-205.

Watson, J.M., Zhang, G.S., Payne, P.A. (1992). The Diffusion Mechanism in Silicone Rubber. *Journal of Membrane Science*, 73, 55-71.

Wijmans, J.G., Baker, R.W. (1993). A Simple Predictive Treatment of the Permeation Process in Pervaporation. *Journal of Membrane Science*, 79, 101-113.

Wijmans, J.G., Kaschemekat, J., Davidson, J.E., Baker, R.W. (1990). Treatment of Organic Contaminated Wastewater Streams by Pervaporation. Environmental Progress, 9(4), 262-268.

Wood, D.R. (1983). Cost Estimation for the Process Industry. Hamilton, Ontario: McMaster University.

Xie, H.A., Ping, Z.H., Nguyen, Q.T., Neel, J. (1992). Dehydration of Highly Corrosive Liquids by Pervaporation. *Proceedings of 6th Conf. on Pervaporation Processes in the Chemical Industry.* ed. R Bakish., pp. 361-367.

Yamaguchi, T., Yamahara, S., Nakao, S., Kimura, S. (1994). Preparation of Pervaporation Membranes for Removal of Dissolved Organics from Water by Plasma-Graft Filling Polymerization. *Journal of Membrane Science*, 95, 39-49.

Young, M.L., Bourgeois, D., Belfort, G. (1989). Sorption, Diffusion and Pervaporation of Organics in Polymer Membranes. *Journal of Membrane Science*, 44, 161-181.

Zhu, C.L., Yang, C.W., Fried, J.R., Greenberg, D.B. (1983). Pervaporation Membranes - A Novel Separation Technique for Trace Organics. *Environmental Progress*, 2, 132-138.

Zhang, S.Q., Fouda, A.E., Matsuura, T. (1992). A Study on Pervaporation of Aqueous Benzyl Alcohol Solution by Polydimethylsiloxane Membrane. *Journal of Membrane Science*, 70, 249-255.

Zielinski, J.M., Duda, J.L. (1992). Predicting Polymer-Solvent Diffusion Coefficients using Free Volume Theory. *Journal of the American Institute of Chemical Engineering*, 38, 405-415.

Appendix 1

NMR Analysis

A sample NMR analysis is presented below for PHMS functionalised with a pendant benzyl substituent. A mass balance carried out upon products and reactants suggests that the reaction has reached almost total completion, yielding a functionality of 29.9 (target = 30). A schematic diagram of the anticipated chemical structure of the product is displayed in fig. A1. The carbon atoms of the functional chain are numbered by the superscripts 1, 2 & 3.

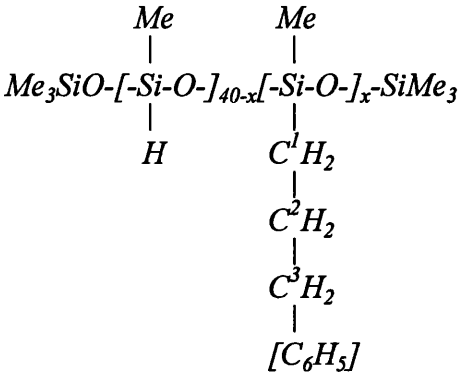

Fig. A1 - Benzyl Functionalised PHMS, Anticipated Product

The ^{1}H NMR spectrum of the product is shown in fig. A2. One would expect the spectrum to contain 6 signals, corresponding to the $Si\text{-}CH_3$, $Si\text{-}H$, C^1H_2, C^2H_2, C^3H_2 and C_6H_5 hydrogen species. A study of fig. A2 shows that 8 signals are detected. It is thought that a small percentage of allyl benzene undergoes anti-Markovnikov addition across the double bond, yielding a slightly different product, as displayed in fig. A3, where x = y + z.

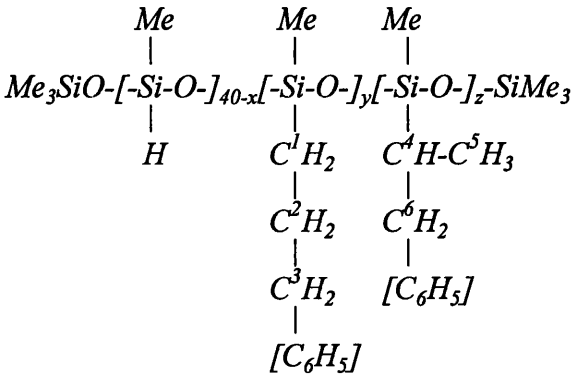

Fig. A3 - Benzyl Functionalised PHMS, Actual Product

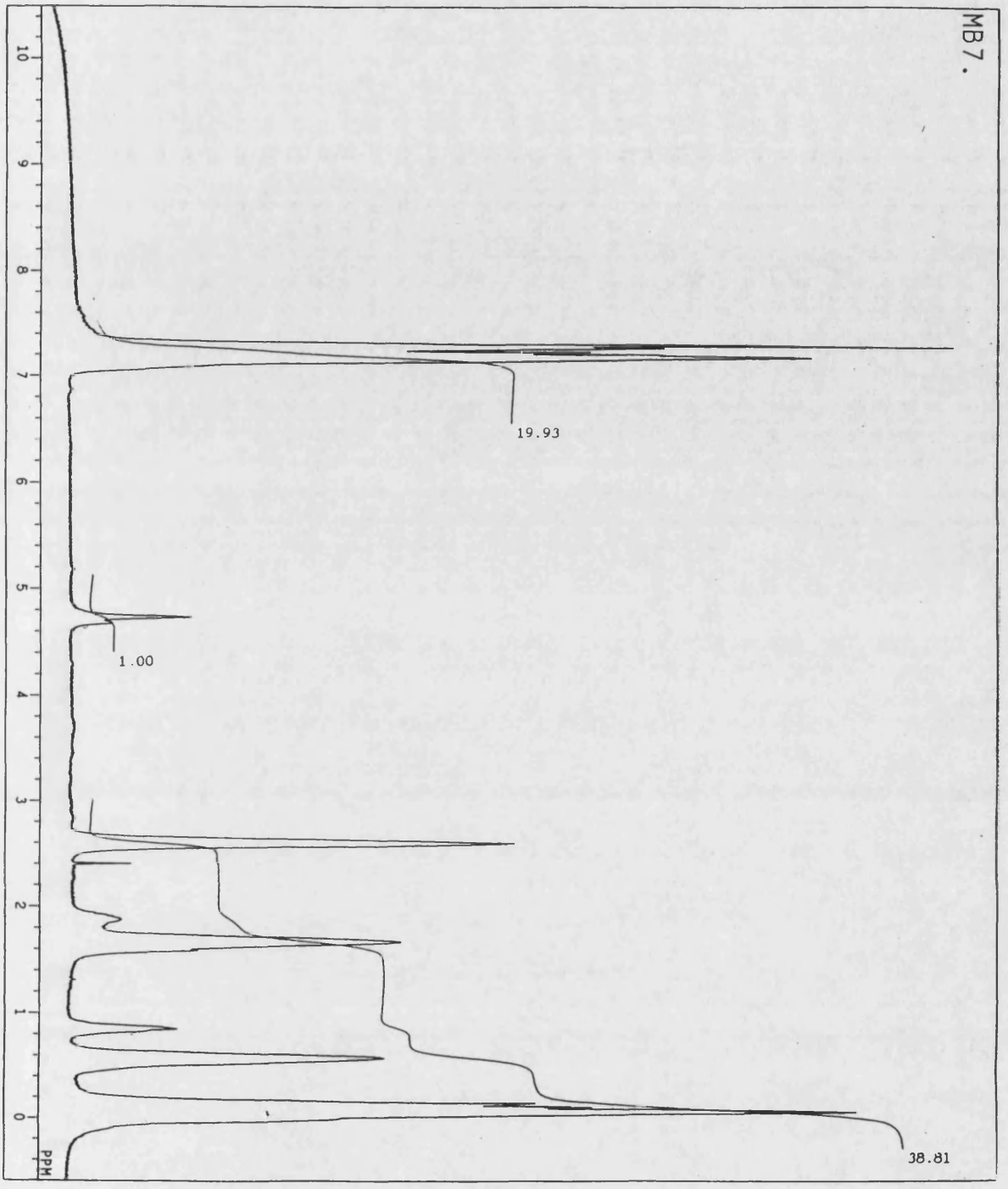

Fig. A2 - ^{1}H NMR Spectrum

The number of hydrogen atoms corresponding to each peak are determined by comparing the vertical increase in baseline height, produced by the peak integrated area. The peak occurring at 0 ppm corresponds to the *Si-CH_3* bonded hydrogen species. There are an average of 138 such hydrogen atoms in oligomeric functionalised PHMS, irrespective of the functional loading. Table A1 displays the results of the NMR evaluation.

Peak Position ppm	Peak Height mm	Number H Atoms	H Atom Bonding
0.00	53	138	$Si\text{-}CH_3$
0.55	20	52	C^1H_2
0.85	4	10	?
1.65	21	55	C^2H_2
1.85	4	10	?
2.60	20	52	C^3H_2
4.75	3.7	10	$Si\text{-}H$
7.20	65	170	C_6H_5

Table A1 - ^{1}H NMR Evaluation

A study of fig. A3 suggests that one would expect to obtain 9 peaks, including one for each of the C^1 - C^6 bonded hydrogen atoms. As only 8 peaks are apparent, it is suspected that an amount of superposition of one of the smaller peaks occurs. This makes it difficult to precisely determine which hydrogen species correspond to the peaks occurring at 0.85 and 1.85 ppm and suggests that one of the larger peaks may be a combination of two species.

Under these conditions, in order to most accurately determine functionality, x, the total number of C^1 - C^6 bonded hydrogen atoms is calculated by summing the individual totals of the peaks at 0.55 - 2.60 ppm. This yields 179 atoms, corresponding to a functionality of 29.8. This figure is in very close agreement with that obtained by mass balance. The peak apparent at 4.75 ppm indicates that a sufficient number of *Si-H* groups remain intact. These are required for subsequent cross-linking purposes during membrane formation.

The large number of C_6H_5 bonded hydrogen species (170), apparent at 7.20 ppm, suggests that a functional loading of 34 is achieved. It is probable that a small quantity of toluene solvent remains dissolved in the final product. The aromatic resonances from the toluene, are also likely to occur very close to 7.20 ppm. The high apparent functionality, given at 7.20 ppm, is almost certainly due to the superposition of the two aromatic peaks.

Appendix 2

Reaction Syntheses

A summary of reaction syntheses, reaction times and final product functionality of all functionalised PHMS material is given in table A2.

No.	Reactant Structure	Quantities Charged				Time	Func
		Reac g	PH g	Tol ml	Cat ml	hr	%
1	$CH_2=CHCH_2CO_2CH_3$	25.00	29.28	150	1.30	25	20.7
2	$CH_2=CHCH(CO_2CH_3)_2$	18.88	10.00	60	0.75	39	24.9
3	$CH_2=CHCH_2CO_2(CH_2)_4CH_3$	18.20	10.00	60	0.75	47	28.2
4	$CH_2=CHCH_2CN$	9.62	12.01	60	0.75	112	29.3
5	$CH_2=CH(CH_2)_7CH_3$	17.46	10.01	60	0.75	48	30.0
6	$CH_2=CHCH_2Ph$	14.12	10.00	60	0.75	46	29.9
7	$CH_2=CHCH_2C_6F_5$	23.33	10.00	60	0.50	37	28.6
8	$CH_2=CHCH_2OPh$	9.00	5.67	60	0.30	161	27.1
9	$CH_2=CHCH_2OC_2H_5$	8.84	8.00	50	0.30	66	28.0
10	$CH_2=CH(CH_2)_{12}CH_3$	7.01	2.79	30	0.20	49	30.0
11	$CH_2=C(CH_3)CH_2C(CH_3)_3$	9.28	7.00	50	0.30	71	29.6

Table A2 - Reaction Syntheses

Key:-

Reac = Reactant PH = PHMS Tol = Toluene Cat = 1 mg/ml Catalyst Soln.

Reactant Names:-

1 Allyl acetate
2 1,1-Diacetoxy-2-propene
3 Allyl hexanoate
4 Allyl cyanide
5 1-Decene
6 Allyl benzene
7 Allyl pentafluorobenzene
8 Allyl phenyl ether
9 Allyl ethyl ether
10 1-Pentadecene
11 2,4,4-Trimethyl-1-pentene

Appendix 3

Membrane Formulations

The formulations of starting materials for the production of all functionalised and unfunctionalised PDMS membranes are given in tables A3 - A7. In each case the range of effective membrane thickness' of the samples used in experimental work are shown.

Mass Frac. PDMS	Mass of Material, g				δ_m μm
	PHMS	PDMS, MR 74000	$Si(OEt)_4$	Dibutyltin Dilaurate	
1.000	-	4.70	0.02	0.08	81-86
0.900*	0.40	4.00	0.40	0.08	106-161
0.819	0.35	1.75	0.35	0.04	96-131
0.643	1.25	2.50	1.25	0.08	106-141
0.474	1.60	1.60	1.60	0.08	81-86

Table A3 - Unfunctionalised Membranes

Func. Group	Load %	Mass of Material, g				δ_m μm
		Func. PHMS	PDMS, MR 74000	$Si(OEt)_4$	Dibutyltin Dilaurate	
Acetate	10	1.30	3.33	0.40	0.17	101-121
	20	9.00	8.15	2.50	0.44	81-106
Di-Acetate	10	1.31	3.00	0.50	0.08	96-100
	20	2.00	1.76	0.40	0.08	121
	30	3.00	1.23	0.50	0.08	81
Hexanoate	10	1.20	3.02	0.20	0.14	101-106
	20	6.99	7.06	0.75	0.40	91-111
Cyano	10	0.80	3.24	0.15	0.14	86-101
	20	1.50	2.49	0.25	0.14	96-101
Octyl	10	1.00	2.80	0.12	0.14	76-81
Benzyl	10	1.20	3.71	0.15	0.17	106
P.F.Benzyl	10	1.30	2.72	0.15	0.14	86-101
	20	4.03	3.43	0.50	0.30	191
Phenyl Ether	10	1.10	2.96	0.23	0.14	91-101
Ethyl Ether	10	0.85	2.97	0.20	0.14	76-81
	20	1.30	1.84	0.32	0.14	71-76
Tridecyl	6.67	1.00	3.38	0.15	0.14	91
	10	1.40	2.98	0.15	0.14	76
Branch Hept.	10	1.00	3.16	0.15	0.14	76
	12.5	1.20	2.90	0.15	0.14	76

Table A4 - Method 1 Functionalised Membranes

* - This is the usual recipe for unfunctionalised PDMS, used in the production of all

unfunctionalised membranes except when investigating the effect of changing cross linking density. The same mass ratio of components is used when producing membranes of varying PDMS chain length.

The functionalised PHMS used for the production of method 1 membranes is that displayed in table A2.

Func. Group	Load %	Mass of Material, g			δ_m μm
		Func. Silane	PDMS, MR 18000	Dibutyltin Dilaurate	
Alkenyl	10	0.80	3.28	0.14	161-171
	20	1.50	2.73	0.14	111-121
Amino	10	1.00	3.21	0.14	111
	20	1.70	2.43	0.14	71-91
Amido	10	1.00	3.71	0.14	71
Pyridyl	10	1.00	2.93	0.14	111-131
Cyano	10	1.10	3.18	0.14	71-81
	20	1.80	2.30	0.14	76-86

Table A5 - Method 2 Functionalised Membranes

The following functionalised silane materials are used for the production of the method 2 membranes displayed in table A5:-

- Alkenyl: Allyltrimethoxysilane
  $[MeO]_3Si\text{-}CH_2CH{=}CH_2$
- Amino: (N,N-dimethyl-3-amino)-propyltrimethoxysilane
  $[MeO]_3Si\text{-}(CH_2)_3\text{-}N(CH_3)_2$
- Amido: 3-Amidopropyltrimethoxysilane
  $[MeO]_3Si\text{-}(CH_2)_2\text{-}CONH_2$
- Pyridyl: 2-Trimethoxysilylethyl-2-pyridine
  $[EtO]_3Si\text{-}(CH_2)_2\text{-}(C_5H_4N)$
- Cyano: 3-Cyanopropyltriethoxysilane
  $[EtO]_3Si\text{-}(CH_2)_2\text{-}CH_2CN$

The same amino functionalised silane, (N,N-dimethyl-3-amino)-propyltrimethoxysilane, was used for the production of the method 3 membranes displayed in table A6.

Func. Group	Load %	Mass of Material, g				δ_m μm
		Func. Silane	PDMS, MR 74000	PHMS	Dibutyltin Dilaurate	
Amino	10	1.00	2.09	0.93	0.14	91
	20	2.00	1.40	1.20	0.14	96

Table A6 - Method 3 Functionalised Membranes

Func. Group	Load %	Mass of Material, g				δ_m μm
		Func. PHMS	PDMS, MR 74000	$Si(OEt)_4$	Dibutyltin Dilaurate	
Octyl	2.5	0.35	4.41	0.18	0.12	76
	5.0	0.40	2.43	0.09	0.09	76
	7.5	0.60	2.33	0.09	0.09	76-81
	10.0	1.00	2.80	0.12	0.14	76-81
	12.5	0.92	1.96	0.09	0.09	65-71
	15.0	1.10	1.87	0.09	0.09	81

Table A7 - Method 1, Octyl Functionalised Membranes

Appendix 4

Activity Coefficients

As already discussed, in order to be able to accurately describe component transport, using relationships derived from *eq. (4.7)*, it is necessary to have accurate activity coefficient, γ_i, data. γ_i is a strong function of both temperature and composition. A comprehensive study of literature yielded inadequate data for each of the four organic components, within aqueous solution, studied. For MIBK no appropriate data was found and for chloroform only a single γ_i value under one specified set of conditions was apparent. More data was available for both phenol and pyridine, however, only a small number of different temperatures were investigated. The data also proved to be inconsistent, as demonstrated by the analysis presented below.

For a given temperature, the effect of composition may be described by the Margules (*eqs. (A.1) & (A.2)*) or Van Laar (*eqs. (A.3) & (A.4)*) equations *(Gmehling, Onken and Artt, 1978)*:-

$$ln\,\gamma_1 = [A_{12} + 2(A_{21}-A_{12})x_1]x_2^2 \qquad (A.1)$$

$$ln\,\gamma_2 = [A_{21} + 2(A_{12}-A_{21})x_2]x_1^2 \qquad (A.2)$$

$$ln\,\gamma_1 = A_{12}\left(\frac{A_{21}x_2}{A_{12}x_1 + A_{21}x_2}\right)^2 \qquad (A.3)$$

$$ln\,\gamma_2 = A_{21}\left(\frac{A_{12}x_1}{A_{12}x_1 + A_{21}x_2}\right)^2 \qquad (A.4)$$

Where: A_{12}, A_{21} = Margules or Van Laar Adjustable Parameters

x = Mole Fraction

1, *2* denotes components 1 & 2

If it is assumed that the organic species is component 2, the activity coefficients at infinite dilution, γ_i^{∞}, may be determined by placing $x_2 = 0$ and $x_1 = 1$. *Eqs. (A.1) - (A.4)* reduce, in both cases, to:-

$$\gamma_1^{\infty} = 1 \qquad (A.5)$$

$$\gamma_2^{\infty} = exp(A_{21}) \qquad (A.6)$$

$$ln\,\gamma_i^C = ln\frac{\Phi_i}{x_i} + \frac{z}{2}q_i ln\frac{\theta_i}{\Phi_i} + l_i - \frac{\Phi_i}{x_i}\Sigma_j x_j l_j \qquad (A.8)$$

$$l_i = \frac{z}{2}(r_i - q_i) - (r_i - 1) \qquad (A.9)$$

$$\theta_i = \frac{q_i x_i}{\Sigma_j q_j x_j} \qquad (A.10)$$

$$\Phi_i = \frac{r_i x_i}{\Sigma_j r_j x_j} \qquad (A.11)$$

Where: x = Mole Fraction

θ = Area Fraction

Φ = Segment Fraction

z = Coordination Number, generally taken to be 10

Parameters r_i & q_i are measures of molecular Van der Waals volumes and molecular surface areas, respectively. They are calculated as the sum of the group volume and area parameters R_k & Q_k:-

$$r_i = \Sigma_k v_k^{(i)} R_k \qquad (A.12)$$

$$q_i = \Sigma_k v_k^{(i)} Q_k \qquad (A.13)$$

$v_k^{(i)}$ is equal to the number of groups of type k in molecule i and hence is always an integer. R_k & Q_k are obtained from the Van der Waals group volume and surface areas, V_{wk} & A_{wk} respectively:-

$$R_k = \frac{V_{wk}}{15.17} \qquad (A.14)$$

$$Q_k = \frac{A_{wk}}{2.5 \times 10^9} \qquad (A.15)$$

The residual contribution is estimated from additional size and group interaction parameters:-

$$ln\,\gamma_i^R = \Sigma_{k\,all\,groups} v_k^{(i)}(ln\,\Gamma_k - ln\Gamma_k^{(i)}) \qquad (A.16)$$

Γ_k is the residual activity coefficient of group k and $\Gamma_k^{(i)}$ is the residual activity coefficient in a reference solution containing only molecules of type i, where:-

$$ln\,\Gamma_k = Q_k\left(1 - ln\,\Sigma_m\theta_m\Psi_{mk} - \Sigma_m\frac{\theta_m\Psi_{km}}{\Sigma_n\theta_n\Psi_{nm}}\right) \qquad (A.17)$$

Eq. (A.17) may also be used for the determination of $\Gamma_k^{(i)}$. m, n & k all denote different functional groups and the summations (Σ_m) are completed for all groups, taking each as species m in turn. It can be seen that Γ_k is a function of interactions between both pairs of groups k & m and m & n.

θ is the group area fraction and is given, for species m, by:-

$$\theta_m = \frac{Q_m X_m}{\Sigma_n Q_n X_n} \qquad (A.18)$$

Where: X_m = Mole Fraction of Group m in the mixture

Ψ is the group interaction parameter and is given, for interaction between groups m and n, by:-

$$\Psi_{mn} = exp\left(-\frac{U_{mn} - U_{nn}}{RT}\right) = exp\left(-\frac{a_{mn}}{T}\right) \qquad (A.19)$$

Where: R = Gas Constant, J/molK

T = Temperature, K

U_{mn} = Interaction Energy Between Groups m and n, J/mol

a_{mn} = Interaction Parameter Between Groups m and n, K

The group interaction parameters, a, must be evaluated from experimental phase equilibrium data. It should be noted that $a_{mn} \neq a_{nm}$.

From *eqs. (A.7) - (A.19)* it can be seen that γ_i may be determined, at any composition and temperature, solely from a number of molecular group size and empirically measured group interaction parameters. Values of all necessary parameters are stored within the Aspen Plus process simulation package database. This package is used to evaluate γ_2 for all components, for a variety of temperatures and compositions, using UNIFAC. The results are displayed graphically in figs. A4 - A9.

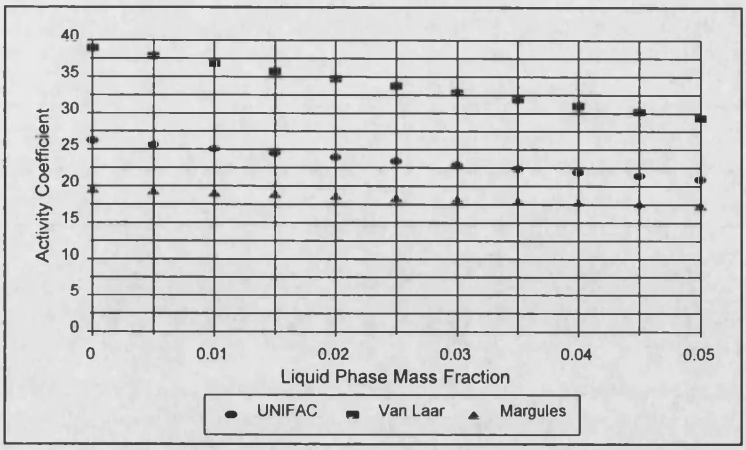

Fig. A4 - Phenol in Water, Variation of γ_p with x_p

Temperature = 70°C (UNIFAC), 75°C (Van Laar and Margules)

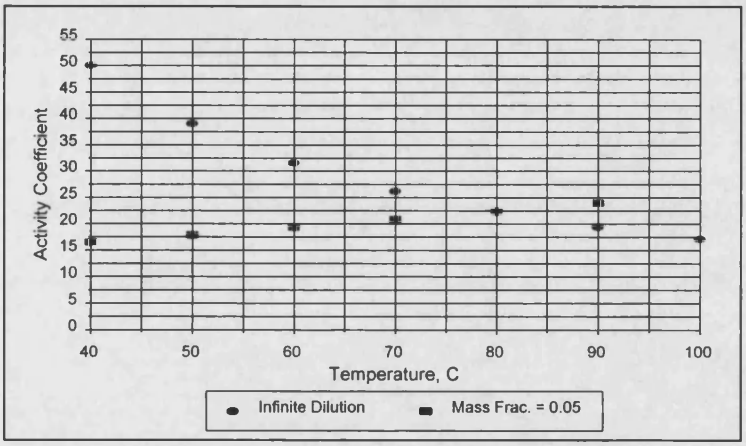

Fig. A5 - Phenol in Water, Variation of γ_p with Temperature

Two different x_p

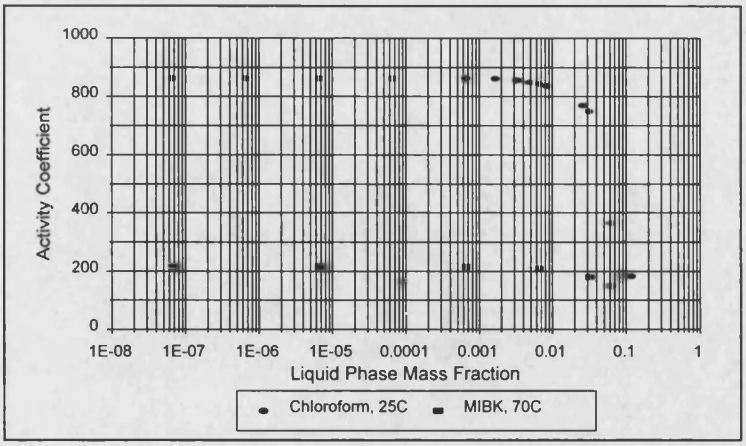

Fig. A6 - Chloroform / MIBK in Water, Variation of γ_2 with x_i

Temperature = 25°C (Chloroform), 70°C (MIBK)

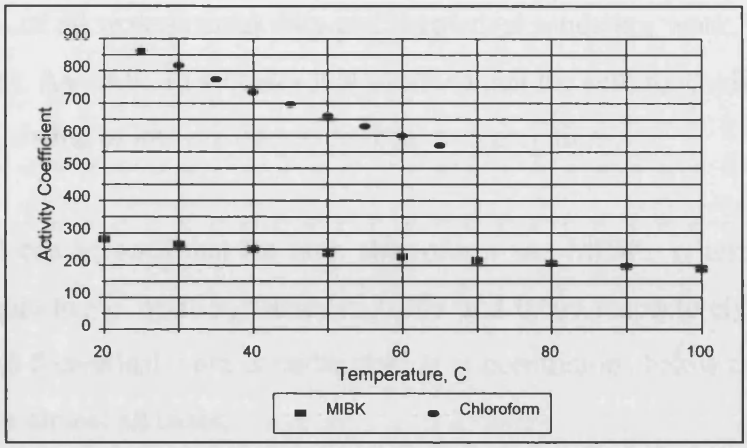

Fig. A7 - Chloroform / MIBK in Water, Variation of γ_2 with Temperature

x_i = infinite dilution

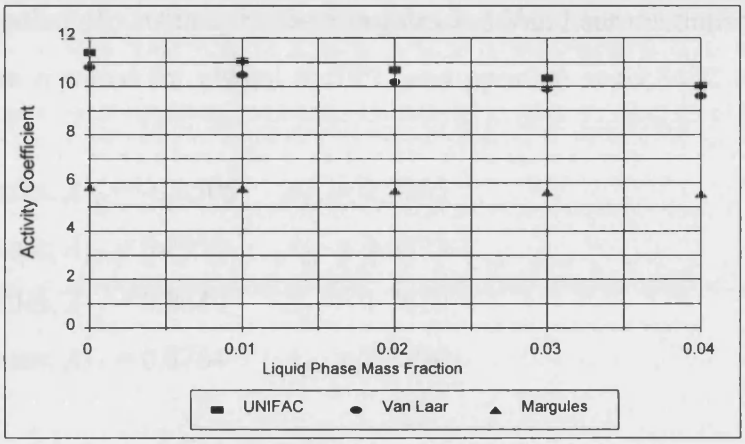

Fig. A8 - Pyridine in Water, Variation of γ_p with x_p

Temperature = 70°C

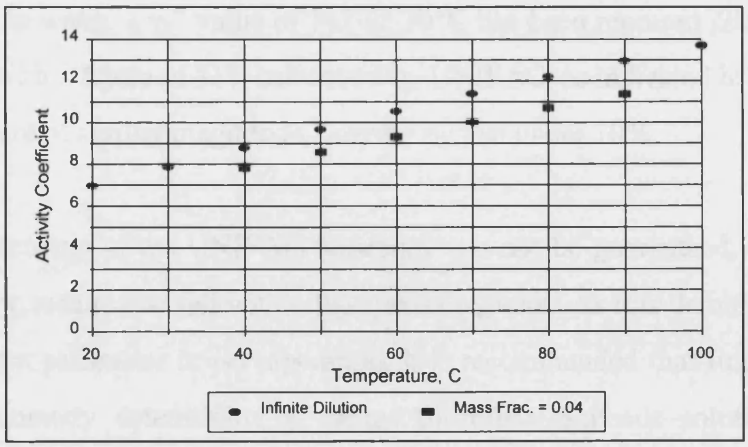

Fig. A9 - Pyridine in Water, Variation of γ_p with Temperature

Two different x_p

For the analysis of all experimental data and theoretical modeling work, γ_2 data is taken directly from figs. A4 - A9. In all cases it is assumed that the activity coefficient for water, γ_w, is equal to 1, owing to low organic component concentrations.

From fig. A6 it can be seen that for both chloroform and MIBK, γ_2 remains essentially constant and equal to γ_2^∞ up to x_2 values of 0.003 and 0.008 respectively. As almost all experimental and theoretical work is undertaken at concentrations below these values, $\gamma_2 = \gamma_2^\infty$ is assumed in almost all cases.

In order to test the validity of the results produced by UNIFAC, the data obtained is compared with that reported in literature in figs. A4 & A8. *Eqs. (A.2) & (A.4)* are used to describe the variation of γ_2 with x_2 by the Margules and Van Laar relationships. The values of A_{12} & A_{21} are reported for phenol at 75°C and pyridine at 69.86°C *(Gmehling et al, 1978)* as:-

Phenol:	Margules, A_{12} = -0.0506	A_{21} = 2.9745
	Van Laar, A_{12} = 0.8959	A_{21} = 3.6623
Pyridine:	Margules, A_{12} = 0.8649	A_{21} = 1.7619
	Van Laar, A_{12} = 0.8764	A_{21} = 2.3796

In both cases the trends given by UNIFAC are similar to those displayed by Van Laar and Margules. The absolute values of γ_2 are also of similar magnitude.

For chloroform in water, a γ_2^∞ value of 747 @ 30°C has been reported *(Brun et al, 1985)*. This compares with a figure of 818, calculated by UNIFAC, as indicated in fig. A8. Again, the two figures are of similar magnitude, varying by just under 10%.

Although the accuracy of the UNIFAC technique can not be guaranteed, it would appear that it produces γ_i results that fall within the correct regions. As it is demonstrated that γ_i is such an important parameter in pervaporation, it is recommended that future work should focus upon accurately determining γ_i values for dilute aqueous solutions of organic components.

Appendix 5

Values of Physical Constants

The values of all physical constants necessary to complete all calculation procedures described within chapters 4-7 are listed below.

A5.1 Water Density and Viscosity, ρ_w & μ_w

The density and viscosity of water, measured at 1 atm, are given by the following empirical equations *(Weast, 1980)*:-

$$\rho_w \ kg/m^3 = (999.83952 + 16.945176\ T - 7.9870401\times10^{-3}\ T^2 - 46.170461\times10^{-6}\ T^3 + 105.56302\times10^{-9}\ T^4 - 280.54253\times10^{-12}\ T^5) / (1 + 16.879850\times10^{-3}\ T) \qquad (A.20)$$

$$0 - 20°C: \log_{10}\mu_w = \frac{1301}{998.333 + 8.1855\ (T - 20) + 0.00585\ (T - 20)^2} - 3.30233 \qquad (A.21)*$$

$$20 - 100°C: \log_{10}\frac{\mu_w}{\mu_{wT=20}} = \frac{1.3272\ (20 - T) - 0.001053\ (T - 20)^2}{T + 105} \qquad (A.22)*$$

Where: T = Temperature, C

* Units of μ_w in *eqs. (A.21) & (A.22)* = Centipoise. To convert to kg/ms, multiply by 0.001.

A5.2 Saturated Vapour Pressure, P_i^{sat}

Component saturated vapour pressures are evaluated using the Antoine equation:-

$$\log_{10}(P_i^{sat}) = A_i - \frac{B_i}{T + C_i} \qquad (7.8)$$

Where: P = Pressure, mmHg $\qquad$ T = Temperature, °C

A_i, B_i, C_i = Dimensional Antoine Constants

Values of A_i, B_i and C_i for all components are displayed in table A.8 *(Gmehling et al, 1978)*.

Component	A_i	B_i	C_i
Water	8.07131	1730.630	233.426
Phenol	6.93051	1382.650	159.493
Chloroform	6.95465	1170.966	226.232
Pyridine	7.01328	1356.930	212.655
MIBK	6.67272	1168.408	191.944

Table A.8 - Antoine Coefficients

To convert from mmHg to Pa, multiply by 133.32237.

A5.3 Component Solubilities, w_{ow} & w_{wo}

The saturated solubilities of organic component in water, w_{ow}, and water in organic component, w_{wo}, for phenol is given in table A.9 *(Jordan et al, 1993)*. The equivalent data for Chloroform *(DeForest, 1989)* and MIBK *(Habib, 1989)* is given in table A.10.

Temp., C	w_{ow}	w_{wo}
1.3	0.068	0.240
2.6	0.069	0.244
23.9	0.078	0.288
29.6	0.075	0.293
32.5	0.080	0.310
38.8	0.078	0.334
45.7	0.097	0.356
50.0	0.115	0.380

Table A.9 - Phenol / Water Phase Solubilities

A5.4 Specific Heat Capacity and Heat of Vaporisation, Cp_i & $\Delta H_i^T{}_{vap}$

The vapour and liquid phase specific heat capacity, Cp and heat of vaporisation, ΔH_{vap}, for each component at reference temperature, T, are given in table A.11. It is assumed that Cp remains constant across the moderate range of temperatures employed within this study.

Temp, C	Chloroform		MIBK	
	w_{ow}	w_{wo}	w_{ow}	w_{wo}
-5	0.0130	-	-	-
0	0.0110	-	-	-
5	0.0100	-	-	-
10	0.0090	-	-	0.013
15	0.0083	-	-	0.014
20	0.0079	-	0.019	0.015
25	0.0077	0.00097	0.018	0.016
30	0.0075	-	0.017	0.018

Table A.10 - Chloroform / MIBK / Water Phase Solubilities

Component	$\Delta H_{i\ vap}^{I}$ kJ/kg	*Ref. T* C	Cp_i^L kJ/kgK	Cp_i^V kJ/kgK	*Ref. T* C	Ref
Water	2260	100	4.19	1.94	70	1
Phenol	511	182	2.24	1.11	50	2
Chloroform	248	20	0.979	0.594	20	3
Pyridine	508	25	1.70	0.989	25	4, 5
MIBK	363	20	1.92	1.08	20	6

Table A.11 - ΔH_{vap} & *Cp*

Refs: 1. *(Brodkey and Hershey, 1988)* 2. *(Jordan et al, 1993)*
3. *(DeForest, 1989)* 4. *(Goe, 1982)*
5. *(Perry, Green and Maloney, 1984)* 6. *(Habib, 1989)*

A5.5 Temperature Independent Properties

The following values for temperature independent properties are used:-

Component molecular mass, MR_i, *(Weast, 1980)*:-

Water: 18.02

Phenol: 94.11

Chloroform: 119.39

Pyridine: 79.10

MIBK: 100.16

Gas Constant, R, = 8.314 kJ/kmolK *(Brodkey and Hershey, 1988)*

PDMS density, ρ_m, = 0.97 kg/m^3 *(Nijhuis, 1990)*

This value for ρ_m is used for all functionalised and unfunctionalised PDMS membranes at all temperatures.

Appendix 6

Individual Module Performance

The performance of each individual module for each of the case studies undertaken, within section 7.3, is detailed in tables A.12 - A. 22, where:-

q = Flowrate, kg/hr

w = Concentration, mass frac.

T = Temperature, C

Q_{heat} = Heating Duty, kW

Q_{cond} = Condensing Duty, kW

A_{mod} = Module Area, m^2

k_{lo} = Mass Transfer Coefficient, m/s

f denotes feed

r denotes retentate

i denotes module i

mod. no.	q_{fi} kg/hr	w_{pfi}	T_{ri} C	Q_{heati} kW	Q_{condi} kW
1	1000.0	0.03000	58.9	0.00	14.36
2	976.3	0.02489	58.8	12.55	14.15
3	953.5	0.02050	58.7	12.37	13.95
4	931.5	0.01677	58.6	12.22	13.78
5	910.3	0.01362	58.4	12.08	13.62
6	889.8	0.01099	58.3	11.51	13.48
7	869.8	0.00881	58.1	11.84	13.36
8	850.2	0.00703	58.0	11.73	13.24
9	831.0	0.00557	57.8	11.64	13.14
10	812.2	0.00439	57.6	11.56	13.05
11	793.6	0.00344	57.4	10.83	12.96
12	775.3	0.00269	57.2	11.41	12.88
13	757.2	0.00208	56.9	11.34	12.80
14	739.3	0.00161	56.7	11.27	12.73
15	721.6	0.00123	56.4	11.21	12.66
16	704.0	0.00094	56.2	10.37	12.58
17	686.5	0.00071	55.9	11.08	12.51
18	669.2	0.00054	55.6	11.02	12.44
19	652.0	0.00040	55.3	10.96	12.37

Table A.12 - Phenol Separation, Unfunc. PDMS, No Recycle

T_{fi} = 70°C, A_{mod} = 13.84 m^2, w_{pr19} = 0.0003

mod. no.	q_{fi} kg/hr	w_{pfi}	T_{ri} C	Q_{heati} kW	Q_{condi} kW
1	1000.0	0.03000	58.0	0.00	15.46
2	973.7	0.02339	58.0	13.48	15.11
3	948.9	0.01804	57.9	13.21	14.82
4	925.5	0.01378	57.8	12.98	14.58
5	903.1	0.01044	57.7	12.78	14.38
6	881.5	0.00784	57.5	12.29	14.21
7	860.7	0.00584	57.4	12.48	14.06
8	840.3	0.00432	57.2	12.36	13.94
9	820.4	0.00317	57.0	12.26	13.83
10	800.9	0.00232	56.7	12.17	13.73
11	781.6	0.00168	56.5	11.36	13.64
12	762.5	0.00121	56.2	12.01	13.55
13	743.6	0.00086	56.0	11.93	13.47
14	724.9	0.00061	55.7	11.86	13.39
15	706.4	0.00043	55.4	11.79	13.31

Table A.13 - Phenol Separation, Func. 1, No Recycle

$T_{fi} = 70°C$, $A_{mod} = 11.00\ m^2$, $w_{pr15} = 0.0003$

mod. no.	q_{fi} kg/hr	w_{pfi}	T_{ri} C	Q_{heati} kW	Q_{condi} kW
1	1000.0	0.03000	62.0	0.00	10.37
2	981.7	0.02459	62.1	9.03	10.16
3	964.4	0.02003	62.1	8.85	9.97
4	947.9	0.01621	62.1	8.71	9.81
5	932.2	0.01304	62.0	8.58	9.67
6	917.1	0.01044	62.0	8.49	9.56
7	902.6	0.00832	62.0	8.38	9.46
8	888.4	0.00660	61.9	8.30	9.38
9	874.6	0.00521	61.8	8.23	9.31
10	861.1	0.00410	61.8	8.18	9.25
11	847.9	0.00321	61.7	7.89	9.20
12	834.8	0.00251	61.6	8.09	9.15
13	821.9	0.00195	61.5	8.05	9.11
14	809.1	0.00151	61.4	8.02	9.08
15	796.4	0.00116	61.3	7.99	9.05
16	783.8	0.00089	61.2	7.60	9.02
17	771.3	0.00068	61.1	7.94	8.99
18	758.8	0.00052	60.9	7.92	8.97
19	746.5	0.00040	60.8	7.89	8.94

Table A.14 - Phenol Separation, Func. 2, No Recycle

$T_{fi} = 70°C$, $A_{mod} = 13.84\ m^2$, $w_{pr19} = 0.0003$

mod. no.	q_{fi} kg/hr	w_{pfi}	T_{ri} C	Q_{heati} kW	Q_{condi} kW
1	1000.0	0.03000	58.8	0.00	14.38
2	976.2	0.02478	58.8	12.56	14.15
3	953.3	0.02033	58.7	12.38	13.95
4	931.4	0.01658	58.6	12.21	13.77
5	910.2	0.01344	58.4	12.07	13.61
6	889.7	0.01083	58.3	11.52	13.47
7	869.7	0.00868	58.1	11.83	13.35
8	850.1	0.00692	58.0	11.73	13.24
9	831.0	0.00549	57.8	11.63	13.14
10	812.2	0.00433	57.6	11.55	13.04
11	793.7	0.00340	57.4	10.82	12.96
12	775.4	0.00265	57.2	11.40	12.88
13	757.3	0.00206	56.9	11.33	12.80
14	739.4	0.00159	56.7	11.27	12.72
15	721.7	0.00122	56.4	11.20	12.65
16	704.1	0.00093	56.2	10.36	12.58
17	686.6	0.00071	55.9	11.08	12.51
18	669.3	0.00054	55.6	11.02	12.44
19	652.1	0.00040	55.3	10.96	12.36

Table A.15 - Phenol Separation, Func. 3, No Recycle

T_{fi} = 70°C, A_{mod} = 6.32 m^2, w_{pr19} = 0.0003

mod. no.	q_{fi} kg/hr	w_{pfi}	T_{ri} C	Q_{heati} kW	Q_{condi} kW
1	1520.0	0.03000	58.2	0.00	23.06
2	1481.9	0.02463	58.1	20.14	22.69
3	1445.4	0.02005	58.0	19.85	22.36
4	1410.4	0.01619	57.9	19.58	22.07
5	1376.5	0.01298	57.7	19.35	21.81
6	1343.7	0.01033	57.6	18.39	21.57
7	1311.8	0.00817	57.4	18.95	21.37
8	1280.7	0.00642	57.2	18.78	21.18
9	1250.1	0.00501	57.0	18.62	21.01
10	1220.1	0.00389	56.8	18.48	20.86
11	1190.6	0.00300	56.5	17.24	20.71
12	1161.4	0.00230	56.3	18.23	20.57
13	1132.6	0.00175	56.0	18.11	20.44
14	1104.1	0.00133	55.7	18.00	20.31
15	1075.8	0.00100	55.5	17.89	20.19
16	1047.8	0.00075	55.1	16.46	20.06
17	1020.0	0.00055	54.8	17.67	19.93
18	992.4	0.00041	54.5	17.56	19.80

Table A.16a - Phenol Separation, Unfunc. PDMS, Recycle, Unit 1

T_{fi} = 70°C, A_{mod} = 22.44 m^2, w_{pr18} = 0.0003

mod. no.	q_{fi} kg/hr	w_{pfi}	T_{ri} C	Q_{heati} kW	Q_{condi} kW
1	548.5	0.06800	57.3	42.75	8.82
2	531.7	0.05761	57.3	7.65	8.63
3	515.7	0.04817	57.2	7.50	8.45
4	500.7	0.03978	57.1	7.35	8.27
5	486.4	0.03246	57.0	7.21	8.11

Table A.16b - Phenol Separation, Unfunc. PDMS, Recycle, Unit 2

T_{fi} = 70°C, A_{mod} = 8.02 m^2, w_{pr5} = 0.02620

mod. no.	q_{fi} kg/hr	w_{pfi}	T_{ri} C	Q_{heati} kW	Q_{condi} kW
1	1402.0	0.03000	58.0	0.00	21.68
2	1365.1	0.02338	58.0	18.91	21.20
3	1330.4	0.01803	57.9	18.53	20.79
4	1297.5	0.01378	57.8	18.20	20.45
5	1266.1	0.01043	57.7	17.93	20.17
6	1235.9	0.00783	57.5	17.24	19.93
7	1206.6	0.00584	57.4	17.51	19.73
8	1178.1	0.00432	57.2	17.34	19.55
9	1150.1	0.00317	57.0	17.20	19.39
10	1122.7	0.00231	56.7	17.07	19.26
11	1095.6	0.00167	56.5	15.93	19.13
12	1068.9	0.00120	56.2	16.84	19.01
13	1042.4	0.00086	56.0	16.74	18.89
14	1016.2	0.00061	55.7	16.64	18.78
15	990.2	0.00043	55.4	16.54	18.66

Table A.17a - Phenol Separation, Func. 1, Recycle, Unit 1

T_{fi} = 70°C, A_{mod} = 15.40 m^2, w_{pr15} = 0.0003

mod. no.	q_{fi} kg/hr	w_{pfi}	T_{ri} C	Q_{heati} kW	Q_{condi} kW
1	423.7	0.06800	57.6	33.03	6.69
2	410.2	0.05541	57.7	5.78	6.48
3	397.8	0.04445	57.7	5.61	6.28
4	386.3	0.03515	57.7	5.46	6.11

Table A.17b - Phenol Separation, Func. 1, Recycle, Unit 2

T_{fi} = 70°C, A_{mod} = 4.30 m^2, w_{pr4} = 0.02744

mod. no.	q_{fi} kg/hr	w_{pfi}	T_{ri} C	Q_{heati} kW	Q_{condi} kW
1	1313.0	0.03000	57.3	0.00	21.47
2	1275.4	0.02181	57.3	18.70	20.82
3	1240.8	0.01561	57.3	18.19	20.31
4	1208.6	0.01101	57.3	17.78	19.90
5	1178.2	0.00767	57.1	17.45	19.59
6	1149.2	0.00529	57.0	16.98	19.33
7	1121.2	0.00361	56.8	17.00	19.13
8	1093.8	0.00244	56.6	16.83	18.96
9	1067.1	0.00163	56.3	16.69	18.82
10	1040.7	0.00108	56.1	16.57	18.69
11	1014.7	0.00071	55.8	15.40	18.57
12	988.9	0.00046	55.5	16.35	18.45

Table A.18a - Phenol Separation, Func. 2, Recycle, Unit 1

T_{fi} = 70°C, A_{mod} = 31.17 m^2, w_{pr12} = 0.0003

mod. no.	q_{fi} kg/hr	w_{pfi}	T_{ri} C	Q_{heati} kW	Q_{condi} kW
1	330.1	0.06800	56.2	25.73	5.80
2	318.0	0.05192	56.4	5.00	5.55
3	307.1	0.03858	56.5	4.80	5.32

Table A.18b - Phenol Separation, Func. 2, Recycle, Unit 2

T_{fi} = 70°C, A_{mod} = 7.60 m^2, w_{pr3} = 0.02800

mod. no.	q_{fi} kg/hr	w_{pfi}	T_{ri} C	Q_{heati} kW	Q_{condi} kW
1	1000.0	0.01000	58.9	0.00	14.34
2	976.5	0.00510	59.0	12.57	13.92
3	955.4	0.00256	59.0	12.24	13.69
4	935.6	0.00127	58.8	12.04	13.55
5	916.5	0.00062	58.7	11.93	13.45

Table A.19 - Pyridine Separation, Unfunc. PDMS, No Recycle

T_{fi} = 70°C, A_{mod} = 30.80 m^2, w_{pr5} = 0.0003

mod. no.	q_{fi} kg/hr	w_{pfi}	T_{ri} C	Q_{heati} kW	Q_{condi} kW
1	1000.0	0.01000	58.9	0.00	14.33
2	976.5	0.00510	59.0	12.57	13.92
3	955.4	0.00256	59.0	12.23	13.68
4	935.7	0.00127	58.8	12.04	13.54
5	916.6	0.00062	58.7	11.92	13.44

Table A.20 - Pyridine Separation, Func. 3, No Recycle

T_{fi} = 70°C, A_{mod} = 18.60 m^2, w_{pr5} = 0.0003

mod. no.	q_{fi} kg/hr	w_{Mfi}	T_{ri} C	Q_{heati} kW	Q_{condi} kW
1	1000.0	0.01000	61.4	0.00	11.36
2	977.0	0.00105	61.8	9.81	10.45
3	961.8	0.00011	61.8	9.18	10.34

Table A.21 - MIBK Separation, Unfunc. PDMS, No Recycle

k_{lo} = 2.5×10^{-5} m/s, T_{fi} = 70°C, A_{mod} = 37.00 m^2, w_{Mr3} = 1×10^{-5}

mod. no.	q_{fi} kg/hr	w_{Mfi}	T_{ri} C	Q_{heati} kW	Q_{condi} kW
1	1000.0	0.01000	61.4	58.02	11.38
2	976.9	0.00106	61.8	9.82	10.47
3	961.8	0.00011	61.8	9.20	10.35

Table A.22 - MIBK Separation, Func. 3, No Recycle

k_{lo} = 2.5×10^{-5} m/s, T_{fi} = 70°C, A_{mod} = 33.00 m^2, w_{Mr3} = 1×10^{-5}